

**THE FLORIDA STATE UNIVERSITY
COLLEGE OF ARTS AND SCIENCES**

**DISSOLVED IRON(II) IN THE PACIFIC OCEAN:
MEASUREMENTS FROM THE PO2 AND P16N CLIVAR/CO₂
REPEAT HYDROGRAPHY EXPEDITIONS**

by

STUART PAUL HANSARD

**A Dissertation submitted to the
Department of Oceanography
in partial fulfillment of the
requirements for the degree of
Doctor of Philosophy**

Degree Awarded:
Summer Semester, 2007

The members of the Committee approve the dissertation of Stuart Paul Hansard,
defended on March 16, 2007.

William M. Landing
Professor Directing Dissertation

William C. Cooper
Outside Committee Member

William Burnett
Committee Member

Philip Froelich
Committee Member

Richard Iverson
Committee Member

Approved:

William K. Dewar, Chair
Department of Oceanography

The Office of Graduate Studies has verified and approved the above named committee members.

for Pamela,
with love and thanks

ACKNOWLEDGEMENTS

I am grateful for the advice and assistance I received from several individuals, including Whitney and Jan King, Martin Roeder, Kathy Barbeau, Daniel O’Sullivan, and Matt Young. Tina Voelker has been extremely understanding during my (insert adjective) transition from student to post-doc. The strong words of encouragement I received from Ben Barnes came to me when I needed them most, and in a language I could understand. Through it all, Donald Hansard has been a good friend and father, and I was extremely fortunate to have benefited from his soft advice and hard currency.

My work was made possible by the CLIVAR Research Program, which provided the means to go to sea and collect samples. The captains and the crews of the R.V. Melville and T.G. Thompson helped to make life at sea safe and productive. The CLIVAR data repository provided several of the oceanographic datasets that were used to produce supporting figures.

The trace metal teams of Florida State University and the University of Hawaii brought clean seawater to the surface where I could analyze it. The dissolved iron measurements made by Chris Measures (UH) were invaluable for interpreting my own data. Cliff Buck (FSU) provided data regarding aerosol deposition and was a great shipmate (though his ping pong could use some work). Bill Jenkins (WHOI) very kindly provided helium isotope data and advice.

The faculty of the FSU Oceanography Department provided a stimulating educational environment and it is with pride that I claim it as my alma mater. The enthusiasm of Jack Winchester served as a model for all students, and his presence and excitement during weekly seminars made each speaker feel his or her topic was uniquely important and interesting. The members of my committee, in particular Bill Burnett and Flip Froelich, provided careful reviews of this paper, which vastly improved its quality.

Finally, I would like to extend sincerest appreciation to Bill Landing, who accepted me as his student and with nearly infinite patience and diligence did his best to develop and guide my understanding of marine chemistry. Now, though I am excited that the long years of tutelage are coming to a close, I feel strangely akin to der Zauberlehrling, who with horrific hubris proclaimed: “Hat der alte Hexenmeister sich doch einmal wegbegeben! Und nun sollen seine Geister auch nach meinem Willen leben! Seine Wort’ und Werke merkt’ich, und den Brauch, und mit Geistesstärke tu ich Wunder auch! “ Who knows, maybe it isn’t over yet...

TABLE OF CONTENTS

List of Tables	vii
List of Figures	viii
Abstract	xi
1. INTRODUCTION	1
1.1 Background	1
1.2 Previous Studies of Iron(II) in Aquatic Environments	7
1.3 Goals of this Work	10
Figures and Tables.....	12
2. MATERIALS AND METHODS	14
2.1 Sampling Collection	14
2.1.1 Sampling Locations.....	14
2.1.2 Sample Collection	14
2.1.3 Sub-sampling from GO-FLO Bottles.....	15
2.1.4 Sample Acidification.....	15
2.2 Sample Analysis	16
2.2.1 Reagents	16
2.2.2 Measurement Apparatus.....	17
2.2.3 Standards and Calibration	18
2.2.4 Data Reporting	18
2.3 Potential Interferences	19
2.3.1 Effect of Sample Acidification on System Response	20
2.3.2 Effect of Sample Acidification on Sample Stability	22
2.3.3 Reduced Species other than Iron(II).....	25
2.3.4 Hydrogen Peroxide.....	27
2.3.5 Dissolved Organic Matter	28
2.3.6 Light	30
2.3.7 Summary of Interference Studies.....	31
Figures and Tables.....	32
3. RESULTS AND DISCUSSION	53
3.1 Spatial Distribution of Iron(II)	53

3.1.1 Cruise PO2	53
3.1.2 Cruise P16N	54
3.1.3 Cross-over Stations	54
3.2 Vertical Profiles and Sources of Iron(II)	55
3.2.1 Iron(II) in Surface Water.....	56
3.2.2 Iron(II) in Deep Water	60
3.2.3 Iron(II) in the West Pacific	61
3.3 Summary of Results.....	63
Figures and Tables.....	66
4. CONCLUSIONS	84
APPENDIX A: Sampling Station Information.....	87
APPENDIX B: Calculation of Iron(II) Oxidation Rates	90
APPENDIX C: Calculation of CO ₂ System Variables	93
APPENDIX D: PMT Control Program	94
APPENDIX E: Calibration Data	102
APPENDIX F: Detailed Method Descriptions	110
APPENDIX G: Raw Data for Cruises PO2 and P16N.....	113
APPENDIX H: Oceanographic Sections for PO2 Transect.....	158
APPENDIX I: Oceanographic Sections for P16N Transect.....	163
REFERENCES	168
BIOGRAPHICAL SKETCH	177

LIST OF TABLES

1. Important biomolecular iron compounds.....	12
2. Sample collection target depths	51
3. Output from CO2SYS program	52
4. PO2 station information	87
5. P16N station information.....	89
6. PO2 calibration information	102
7. P16N calibration information	106
8. Duplicate results for PO2 and P16N.....	108
9. Data table for cruise PO2.....	113
10. Data table for cruise P16N.....	143

LIST OF FIGURES

1. Vertical profile of $[\text{Fe}_{\text{DISS}}]$ during SAFE intercalibration study	13
2. Location map of sampling stations	32
3. Example of raw data output	33
4. Example of typical calibration curve	34
5. Sample stability over time	35
6. Generalized mechanism for luminol oxidation.....	36
7. Structure of peroxy carbonate radical	37
8. Effect of acidification on system response	38
9. Effect of acidification versus $[\text{Fe}_{\text{DISS}}]$	39
10. Aqueous $[\text{CO}_2]$ versus sample depth before and after acidification	40
11. Effect of acidification versus sample collection depth	41
12. System sensitivity for samples collected at different depths	42
13. System response of spiked samples over time	43
14. Box plots of sample stability grouped by sample collection depth.....	44
15. Concentrations calculated with and without drift correction	45
16. System response to additions of potentially interfering trace metals.....	46
17. System response to added H_2O_2	47
18. Structures of ligands used in interference tests.....	48
19. System response to Fe(II) complexed with various organic ligands.....	49
20. System response during a seawater irradiation experiment	50
21. Fe(II) concentrations - PO2 section	66
22. $[\text{Fe(II)}]/[\text{Fe}_{\text{DISS}}]$ ratios - PO2 section	67
23. $[\text{Fe(II)}]$ versus $[\text{Fe}_{\text{DISS}}]$ - PO2 section	68

24. Fe(II) concentrations - P16N section	69
25. [Fe(II)]/[Fe _{DISS}] ratios – P16N section	70
26. [Fe(II)] versus [Fe _{DISS}] - P16N section	71
27. Fe(II) profiles at cross-over stations	72
28. Box plots of [Fe(II)] grouped by depth for PO2W, PO2E, and P16N.....	73
29. Box plots of [Fe(II)]/[Fe _{DISS}] grouped by depth for PO2W, PO2E, and P16N.....	74
30. Fe(II) profiles from study of Hong and Kester (1986).....	75
31. Fe(II) profiles from study of O’Sullivan et al. (1991)	75
32. Fe(II) profiles from study of Boye et al. (2006)	76
33. Fe(II) profiles from study of Hopkinson and Barbeau (2007)	76
34. Chlorophyll fluorescence – PO2 section.....	77
35. Box plots of [Fe(II)]/[Fe _{DISS}] for day and night samples	78
36. Plot of [Fe(II)]/[Fe _{DISS}] versus sample collection time	79
37. Oceanographic sections of CFC-11 for cruises PO2 and P16N.....	80
38. Depth of wind mixed layer plotted on PO2 [Fe(II)] section	81
39. Bathymetry of western PO2 section	82
40. Locations of active volcanoes within the Izu-Bonin arc system	83
41. Fe(II) half-life –PO2 section.....	92
42. Fe(II) half-life – P16N section.....	92
43. PO2 temperature section	158
44. PO2 salinity section	158
45. PO2 dissolved oxygen section	159
46. PO2 pH section	159
47. PO2 total alkalinity section	160
48. PO2 DIC section	160
49. PO2 nitrate section	161

50. PO2 nitrite section	161
51. PO2 phosphate section	162
52. PO2 silicate section	162
53. P16N temperature section	163
54. P16N salinity section	163
55. P16N dissolved oxygen section	164
56. P16N pH section	164
57. P16N total alkalinity section	165
58. P16N DIC section	165
59. P16N nitrate section	166
60. P16N nitrite section	166
61. P16N phosphate section	167
62. P16N silicate section	167

ABSTRACT

The redox speciation of dissolved iron in open ocean seawater was evaluated during two Pacific Ocean research cruises. Using a highly sensitive flow injection method based on luminol chemiluminescence, vertical profiles of reduced iron concentration (Fe(II)) were obtained at 134 stations. In this paper, sampling and analytical methods are discussed and values obtained for Fe(II) are compared to shipboard measurements of total dissolved iron (Fe_{DISS}). Concentration profiles are evaluated within the context of various proposed source mechanisms and experimental models of Fe(II) oxidation kinetics.

Samples were collected from rosette-mounted GO-FLO bottles using trace metal clean equipment and techniques. While this allowed sample collection to depths of 1000 m, the length of time required for rosette retrieval coupled with the potential for rapid oxidative loss of Fe(II) complicates the detection of photochemical production processes that are expected to be operative in the upper water column. Acidification of seawater samples retards oxidation until sample analyses can be completed, but for undetermined reasons it contributes both to the blank response, and to minor instabilities in system response over time that are depth-specific, effects which must be considered and corrected for.

Analysis by luminol chemiluminescence is fast and inexpensive, and typically yielded detection limits of 10-15 pM. A requirement of the method is that Fe(II) present in samples be uniquely oxidized in the reaction cell at the same rate as the Fe(II) used for standard preparation. By changing reaction kinetics, strong organic complexes like EDTA can produce false negatives. Also, reduced species other than iron can be oxidized at the high system pH, leading to positive interferences. Vanadium (IV) and vanadium (V) were found to significantly interfere. Because Fe(II) is believed to form weak complexes in seawater, and reduced vanadium has not been detected in oxic seawater, interferences were believed to be minimal.

The results from the two cruises suggest a relatively consistent pattern of Fe(II) occurrence and distribution in the Pacific Ocean. Surface water maxima are present in most profiles, with median concentrations of 25-30 pM, accounting for approximately 12% of the total dissolved iron. Concentrations decline with depth to undetectable levels in the upper 100 meters. Below this depth, Fe(II) remains low. However, deepest samples (700-1000 m) frequently contained detectable Fe(II), though at a very low percentage of the total dissolved iron. The concentration profile for the upper water column is consistent with a photochemical production

mechanism. However, this production should cease upon sample collection, and the rapid oxidative loss predicted for surface waters should remove these higher Fe(II) concentrations prior to sub-sample collection from the GO-FLO bottles. Fe(II) in deep samples was found in association with the oxygen minimum of the profile, possibly due to the remineralization of sinking biogenic particles. In the northern Philippine Sea, between the Japanese coast and the Izu-Bonin volcanic arc system, Fe(II) concentrations were found to be atypically high. Median surface water concentrations were 150 pM, accounting for approximately 27% of Fe_{DISS}. In the upper 200 meters, concentrations decreased with depth. However, in deeper samples near the submarine arc system (700 - 1000 m), Fe(II) was detected at concentrations up to 370 pM. The high surface water concentrations were found in an area of high measured dust flux. The high concentrations at depth were likely sediment-derived.

1. INTRODUCTION

1.1 Background

Iron is an essential trace element for all organisms, yet its aqueous concentration in the modern open ocean is very low due to its strong affinity for the solid phase (Landing and Bruland, 1987; Johnson et al., 1997; Waite, 2001). For this reason, it has been estimated that primary production is iron-limited in 15-40% of the world ocean (Martin et al., 1991; de Baar and de Jong, 2001). This discovery has led to research into the sources of iron to the open ocean, the chemical forms in which it occurs and is biologically utilized, and its potential role as a key determinant in global carbon cycling (Cooper et al., 1996).

In living organisms, iron is found in a number of organic compounds that participate in fundamental metabolic processes, including respiration, photosynthesis, and growth. [Table 1](#) lists several of these compounds, which are commonly grouped into three classes. The hemoprotein class consists of proteins conjugated with iron protoporphyrins and comprises numerous molecules with diverse functions, including oxygen transport (e.g. hemoglobins, myoglobins), oxygen activation (e.g. catalases, peroxidases, oxidases), and electron transfer (e.g. cytochromes). A second class consists of proteins containing iron bound to sulfide. These so-called iron-sulfur (Fe-S) proteins function as electron transport molecules (e.g. ferredoxins), as catalysts of redox reactions (e.g. nitrogenases, dehydrogenases), and as other important non-redox catalysts (e.g. aconitase). A third class includes various non-heme, non-Fe-S molecules that participate in several important metabolic processes, including oxygen regulation, superoxide dismutation, and DNA synthesis (Crichton, 1991; Weinberg, 1989; Merchant, 2006).

The extensive use of iron as a metal cofactor in biological systems results in large part from its tendency to form inorganic and organic complexes, enabling it to undergo electron transfer and acid-base reactions over a wide range of pE and pH conditions (Crichton, 1991; Stumm and Morgan, 1996). Iron is the fourth most abundant element in the earth's crust, and in the suboxic to mildly reducing conditions in which many biochemical processes likely evolved, the highly soluble ferrous iron species would have been readily available for uptake (Holland, 1973). Thus, the chemical versatility of iron combined with its natural abundance early in Earth's history account for its prominent role as an essential trace metal in evolving biological systems. The subsequent oxidation of the earth's biosphere greatly decreased the availability of iron to biota because ferric iron, the oxidized species, is far less soluble in most oxic environments. The

finding that the biological use of iron has increased over geological time even as its availability to organisms has diminished underscores both the unique suitability of iron for the biological functions in which it participates and the extent to which organisms depend on it (Zerkle et al., 2005).

Early trace metal surveys failed to recognize the low oceanic abundance of iron, due to the difficulty of obtaining contaminant-free measurements. With the advent of clean sampling and analysis techniques it was discovered that, in contrast its high crustal abundance, the concentration of iron in the modern ocean is very low (Landing and Bruland, 1987). A vertical profile from a well-studied site in the North Pacific is shown in Fig. 1. At this site, measurements of dissolved iron (Fe_{DISS}) in the surface waters (0-100 m) ranged from 0.05 – 0.09 nM. Below 100 m, the concentration increased with depth, to approximately 0.75 nM at 1000 m. The observed vertical distribution is characteristic of a nutrient-type profile, in which a biologically important element is depleted at the surface due to uptake by phytoplankton and replenished at depth as sinking biogenic particles are remineralized (Broecker, 1974). The recognition of high metabolic requirements, low oceanic abundance, and a nutrient-type profile led John Martin to propose the so-called “iron hypothesis.”

The central tenet of the iron hypothesis was that in some parts of the ocean phytoplankton growth is limited by the availability of iron. As a result of limited iron availability, other nutrients including nitrogen, phosphorus, and silicon are underutilized, giving rise to high-nutrient, low-chlorophyll (HNLC) regions (Martin, 1988). The existence of HNLC areas in the subarctic Pacific, the equatorial Pacific, and the Southern Ocean had long been recognized (Cullen, 1991), and the hypothesis predicted that primary production could be stimulated by increasing the supply of iron to these areas. It was further hypothesized that during glacial periods, enhanced dust deposition to the Southern Ocean increased the supply of iron, which in turn stimulated primary production to the extent that significant quantities of atmospheric carbon dioxide (CO_2) were removed to the deep oceans in the form of organic carbon (Martin, 1990). Extension of this hypothesis to the present day provided conceptual feasibility for the mitigation of anthropogenic CO_2 emissions by large-scale additions of iron to HNLC regions. Though the idea was highly controversial from a geoengineering standpoint (Chishom and Morel, 1991), the scientific community, along with environmental policy-makers, endorsed conducting small-scale “iron fertilization” experiments for the purpose of advancing scientific knowledge (Roberts, 1991).

As a result, the iron hypothesis has been tested in several mesoscale iron fertilization experiments, described in detail by de Baar et al. (2005). In these experiments, patches of ocean

within HNLC regions were amended with iron by systematically dumping large quantities of iron sulfate into the sea, along with sulfur hexafluoride as a water mass tracer. The patches were then tracked for several days/weeks and numerous response indicators were monitored both inside and outside of the patches, including nutrient levels, phytoplankton abundance and diversity, chlorophyll abundance, photosynthetic quantum efficiency, and inorganic carbon species. The first of these large-scale experiments, IronEx-I and IronEx-II, took place in the eastern equatorial Pacific. Subsequent fertilization experiments have been done in the Southern Ocean (SOIREE, CARUSO/EisenEx, SOFeX, and EIFEX) and in the subarctic Pacific (SEEDS and SERIES). Although the magnitudes of the responses to iron addition varied for each of the experiments, each of the enrichment experiments resulted in significant increases in primary productivity, chlorophyll, and photosynthetic quantum efficiency, and most showed decreases in macronutrient levels and carbon dioxide fugacity (de Baar et al., 2005). While other factors, such as light limitation, grazing pressure, and silicate abundance have been proposed to play a role in the maintenance of HNLC regions (Watson, 2001), these mesoscale fertilization experiments have led to a general consensus that iron is an important limiting nutrient in large areas of the ocean (Hunter et al., 2001).

The manner in and extent to which iron is partitioned into various chemical species are subjects of fundamental importance, as the distribution of these species may further limit or enhance its bioavailability. In particular, processes that maintain the pool of dissolved iron species are of special importance, because colloidal and particulate fractions are not thought to be directly available to marine phytoplankton (Rich and Morel, 1990). In seawater, iron has been observed to occur in two oxidation states, Fe(II) and Fe(III) (Waite and Morel, 1984). In the presence of oxygen, Fe(III) is thermodynamically favored. However, the solubility of $\text{Fe}(\text{OH})_3^\circ$, the hydrolysis species that is predicted to form under seawater conditions, is extremely low, resulting in an overall Fe(III) solubility of 0.2-0.4 nM (Liu and Millero, 2002). Several studies have now shown that most of the Fe(III) present in seawater is bound to organic ligands, which form strong complexes with Fe(III), thereby keeping it in solution (Gledhill and van den Berg, 1994; Rue and Bruland, 1995; Wu and Luther III, 1995). Though organic complexation serves to maintain the pool of dissolved iron, most research suggests that these organometallic complexes are not directly available to marine phytoplankton. Instead, uptake rates appear to be more closely related to the concentration of dissolved inorganic iron species (Hudson and Morel, 1990; Sunda and Huntsman, 1995; Hutchins et al., 1999; Maldonado and Price, 1999). Thus, most models of phytoplankton iron uptake invoke some mechanism by which the organometallic

complex, Fe(III)L, is dissociated prior to uptake, a process that nearly always involves the reduction of Fe(III) to Fe(II).

In contrast to Fe(III), Fe(II) is highly soluble and forms much weaker complexes. Several production mechanisms have been proposed and are reviewed by Sunda (2001). These include reduction of dissolved Fe(III) hydroxides by photochemically-produced superoxide (Voelker and Sedlak, 1995), photoreduction of dissolved Fe(III) hydroxides (King et al., 1993), photoreduction of dissolved Fe(III) organic complexes (Kuma et al., 1992; Miller et al., 1995; Barbeau et al., 2001; Rijkenberg et al., 2006), photoreductive dissolution of colloidal and particulate Fe(III) (Rich and Morel, 1990; Wells et al., 1991), bioreduction of Fe(III)L at cell surfaces (Maldonado and Price, 1999; Maldonado and Price, 2001), extracellular reduction of Fe(III)L by biogenic superoxide (Kustka et al., 2005; Rose and Waite, 2005), viral lysis of cells (Gobler et al., 1997), grazing (Hutchins and Bruland, 1994), recycling of particulate organic matter containing Fe(II) (Hopkinson and Barbeau, 2007), and microbial reduction in isolated suboxic and anoxic micro-environments, such as settling fecal pellets and settling aggregates (Alldredge and Cohen, 1987).

In addition to *in situ* processes, Fe(II) can be physically transported into a parcel of water, in association with particulate matter, or via diffusive flux from an adjacent source. Aerosols contain photochemically-produced Fe(II) that can be readily solubilized upon deposition (Buck et al., 2006). Fe(II) produced in sediments by anaerobic bacteria can be transported elsewhere by advective and diffusive processes (Elrod et al., 2004). Fe(II) can also be supplied to seawater via submarine ground-water discharge (Charette and Sholkovitz, 2003; Windom et al., 2006), and via hydrothermal activity (Coale et al., 1991; Chin et al., 1994; Statham et al., 2005).

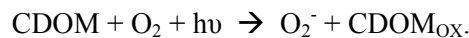
Regardless of the manner in which it is introduced into a parcel of water, Fe(II) is unstable in oxic seawater. Once formed, it will eventually be oxidized to Fe(III), the thermodynamically stable state. The oxidation rate of Fe(II) in seawater has been studied extensively (Millero et al., 1987; Millero and Sotolongo, 1989; King et al., 1995; King, 1998; King and Farlow, 2000; Gonzalez-Davila et al., 2005; Santana-Casiano et al., 2005). The rate has been shown to exhibit first-order dependency on oxygen and hydrogen peroxide (H₂O₂), the chief oxidants present in seawater. In surface seawater, both oxygen and H₂O₂ are present in significant quantities, as oxygen is in equilibrium with the atmosphere and H₂O₂ is produced primarily by photolysis of dissolved organic matter. In deeper water, oxygen is depleted by the respiration of organic matter, and hydrogen peroxide concentrations are negligible (Yuan and Shiller, 1999). Consequently, oxidation rates are predicted to be higher in surface water than in deep water, as the concentration of available oxidants decreases with depth.

Because individual species of Fe(II) are oxidized at different rates, the overall oxidation rate is governed by factors that influence the distribution of Fe(II) species in solution, primarily pH, temperature, and ionic strength (Millero et al., 1987). Equilibrium speciation models predict increased concentrations of readily oxidizable hydroxo ($\text{Fe}(\text{OH})^+$, $\text{Fe}(\text{OH})_2^\circ$) and carbonato complexes ($\text{Fe}(\text{CO}_3)^\circ$, $\text{Fe}(\text{CO}_3)_2^{2-}$) at the upper end of the pH range (8.2), while at lower pH, the concentrations of these species are decreased, slowing the overall rate of oxidation (Millero et al., 1995). The formation of hydroxo complexes is also a function of temperature. Because the water dissociation constant (K_w) decreases with decreasing temperature, for a given pH the concentration of free OH^- will be lower in colder water. Finally, the oxidation rate has also been shown to vary inversely with ionic strength due to the faster reaction of oxygen with Fe(II)-chloro and Fe(II)-sulfato complexes than with Fe(II) hydrolysis species.

Both pH and temperature typically decrease with depth, shifting the Fe(II) speciation towards species that are much less readily oxidized (e.g. Fe^{2+}). Coupled with the decrease in oxidant concentration, the half-life with respect to oxidation for Fe(II) in deep water can be on the order of days. Conversely, at the surface, in warm, oxygenated seawater of $\text{pH} > 8$, with 100 nM H_2O_2 , Fe(II) is predicted to have a half-life of less than one minute (Gonzalez-Davila et al., 2005; Santana-Casiano et al., 2005).

Given the potential for rapid oxidation of Fe(II), steady-state concentrations in surface seawater must be sustained by equally rapid production and supply. This diminishes the importance of allochthonous Fe(II), because transport rates must be slow relative to the rate of oxidation (Charette and Sholkovitz, 2002; Statham et al., 2005; Hopkinson and Barbeau, 2007). Therefore, *in situ* production processes are required if Fe(II) is to have any significant role in biogeochemical processes of the surface ocean. Of the various mechanisms mentioned above, photoreduction and bioreduction have been the most-cited potential sources of Fe(II).

Indirect photoreduction of Fe(III) by superoxide (O_2^-) has been proposed to occur when chromophoric dissolved organic matter absorbs light of sufficient energy (i.e. $\lambda < 400$ nm) to excite an electron, which is subsequently transferred to molecular oxygen:



Due to differences in the rate constants, superoxide can theoretically reduce Fe(III) more rapidly than it oxidizes Fe(II), thus it was hypothesized that significant quantities of Fe(II) could accumulate in sunlit surface seawater (Voelker and Sedlak, 1995). Experiments to determine the relative rates of iron reduction and oxidation by O_2^- using inorganic Fe(III) solutions led to predicted Fe(II) percentages of 30-75% for O_2^- concentrations of 0.1 -1.0 nM (Voelker and Sedlak, 1995). However, the overall importance of this pathway has been debated after the

discovery that most Fe(III) in seawater is organically complexed. Subsequent experiments to determine if Fe(III) organic complexes are reduced by O_2^- have been inconclusive (Barbeau, 2006).

Instead, direct photoreduction of organic complexes has been suggested to proceed by a ligand-to-metal charge transfer, in which the light energy absorbed by the Fe(III) complex promotes an electron to an excited state, initiating the charge transfer (Rue and Bruland, 1997). Using marine siderophores (extracellular biogenic iron chelates) as representative organic complexes, Barbeau et al. (2001) demonstrated that photolysis of these complexes can occur under natural sunlight conditions, resulting in Fe(II) production, and is accompanied by destruction of the organic ligand via cleavage of a carbon-carbon bond. Uptake experiments using isotopically-tagged siderophores indicated that uptake was correlated with photolysis of the Fe(III)-ligand complexes, demonstrating that photoreduction of siderophore-bound iron increased the bioavailability of Fe.

Recent uptake experiments support a biological role for iron redox cycling in the upper ocean. Several studies have demonstrated that for several marine phytoplankton species, uptake of iron is mediated by membrane-bound transport proteins, which bind and internalize only inorganic forms of iron (Fe^{2+}) (Anderson and Morel, 1982; Sunda, 2001 and references cited therein). In iron uptake experiments, Maldonado and Price (2001) grew cultures of *Thalassiosira oceanica*, a marine diatom, in low-iron seawater augmented with a variety of Fe(III) organic complexes, including desferrioxamine B, a strong Fe(III)-binding siderophore. The high uptake rates they observed could not be explained by uptake of $[Fe^{2+}]$ predicted by thermal dissociation of the Fe(III) ligands. Instead, they concluded that membrane-bound ferric reductases reduce the Fe(III) bound to organic ligands to Fe(II), facilitating dissociation of the complex, and increasing $[Fe^{2+}]$. Reduction of Fe(III) was confirmed by measurements of Fe(II) in the growth medium. The degree to which this mechanism will affect the $[Fe^{2+}]$ of the bulk medium will depend upon the rate at which Fe^{2+} can diffuse away from the site of reduction (i.e. at or near the cell surface), versus the rate of uptake (i.e. binding to the membrane transport protein) and the rate of re-complexation with dissolved organic ligands (Sunda, 2001).

Recent studies have demonstrated the extracellular production of superoxide by marine diatoms and cyanobacteria either by reduction of O_2 at the cell surface by reductase enzymes or by the release of cellular reductants such as glutathione into the growth media (Rose et al., 2005; Rose and Waite, 2005; Kustka et al. 2005). In association with O_2^- production, production of Fe(II) in the surrounding medium was also detected, suggesting that phytoplankton may be able to indirectly reduce Fe(III), thus increasing its availability for uptake. As mentioned above,

reduction of inorganic Fe(III) by O_2^- has been documented. Whether organic complexes of Fe(III) are reduced by this mechanism to any significant degree has not been resolved.

All of these production modes are potential sources of aqueous Fe(II), yet their significance to actual open ocean redox cycling is difficult to evaluate due to the lack of open ocean Fe(II) measurements. The predominance of any particular mode over the other should be reflected in vertical profile measurements of Fe(II) and Fe(III) concentrations. For example, photochemical cycling of dissolved iron should be constrained to the upper 30-100 m of the water column, the maximum depth range of ultraviolet light penetration (Garrison, 2002), because only light of sufficient energy can break bonds or photolyze CDOM (Cooper et al., 1988). Due to the attenuation of UV light with depth, an Fe(II) surface maximum is predicted (Moffett and Zika, 1988). Bioreduction would also be expected to produce a characteristic Fe(II) profile, with a subsurface maximum correlated to the chlorophyll maximum, and presumably lower concentrations above and below this level. The shapes of these predicted profiles would also be influenced by uptake and oxidation, with the rate of uptake greatest at the chlorophyll maximum, and the rate of oxidation greatest at the surface, as discussed above.

1.2 Previous Studies of Fe(II) In Aquatic Environments

The first studies of Fe(II) in natural oxic aquatic environments were in freshwater lakes. McMahon (1967, 1969) documented the occurrence of reduced iron in a Canadian lake and measured temporal variations in Fe(II) concentrations on hourly and weekly timescales using spectrophotometric analyses of solvent-extracted bathophenanthroline, which when added to an Fe(II)-bearing sample forms a colored complex. From these studies it was concluded that diurnal and seasonal fluctuations of Fe(II) were the result of photochemical reactions and/or microbial activity. Other studies of freshwater systems have made similar observations and have provided added support for photoreduction of Fe(III) (Collienne, 1983; Mcknight et al., 1988).

There is evidence to suggest that mechanisms of Fe(II) production in lake water might be less important in seawater, due to much lower concentrations of total iron and chromophoric organic compounds necessary for ligand-to-metal charge transfer. In one of the first seawater studies, Hong and Kester (1986) measured Fe(II) concentrations off the west coast of Peru along a transect that included both shelf and open-ocean seawater. Their analytical method included pre-concentration of iron on an 8-hydroxyquinoline (8-HQ) column, followed by colorimetric analysis of Fe(II) after ferrozine complexation. They found high Fe(II) (0-22 nM) in shelf samples taken close to the surface (1-20 m), lower concentrations at depth, and very high concentrations (47 nM) near the sediment-water interface. At Station 72, the only open ocean site

(11°S, 79°W; depth 2500 m), [Fe(II)] of 1 nM was detected at a depth of 21 meters ($Fe_{DISS} = 4$ nM), with no Fe(II) detected in adjacent samples collected at 1, 48, 74, and 100 meters. They attributed the elevated surface concentrations found at the shelf stations to photochemical reduction reactions and the high concentration in the bottom waters to bacterial reduction of Fe(III) solids in suboxic and/or anoxic sediments.

Kuma et al. (1992) measured Fe(II) concentrations in Funka Bay (Japan) using spectrophotometric analysis of Fe(II) complexed with either bathophenanthroline or nitroso-5-(N-propyl-N-sulfopropylamino) phenol after first pre-concentrating Fe(II) on 8-hydroxyquinoline (8-HQ), an iron chelating resin. They observed concentrations of Fe(II) of 40 nM (21% of the total iron) in oxic surface seawater during spring blooms and speculated these high concentrations were the result of photoreduction of sediment-derived iron supplied to the surface layer by vertical mixing. In a similar study, Waite et al. (1995) measured diurnal variations in ferrozine-reactive iron present in surface shelf waters of northern Australia, and found only a small fraction (< 5%) of the total iron present to be ferrozine-reactive (i.e. Fe(II)). Their sampling followed a storm-related re-suspension event, and the total dissolved iron reported ranged from 37 – 323 nM. They noted a close correlation between ferrozine-reactive iron and light intensity, and presented evidence that the soluble pool was most influenced by light.

At equatorial stations located along 140°W longitude, O' Sullivan et al. (1991) applied the ferrozine technique to open-ocean measurements at four stations in the equatorial Pacific (140°W) using a novel approach that deployed ferrozine-impregnated cartridges deployed in a vertical sampling array. This allowed pre-concentration of ferrozine-complexed Fe(II), and enabled Fe(II) to be sequestered in a form that is not easily oxidized. Fe(II) concentrations of 400-450 pM were reported for near-surface samples (1-5 m), with concentrations in deeper samples (5-100 m) ranging from <120 pM to 450 pM.

Methods of Fe(II) analysis that rely on strong complexing agents have been faulted for their tendency to reduce Fe(III) to Fe(II), leading to overestimates of actual Fe(II) concentrations (Shapiro, 1966; Hudson and Morel, 1990). As a result, other techniques have been developed to measure low levels of Fe(II). An alternative technique based on cathodic stripping voltametry was employed by Gledhill and van den Berg (1995). The technique relies upon adsorptive pre-concentration of Fe(III) complexed with 1-nitroso-2-naphthol onto a hanging mercury drop electrode. Fe(II) is calculated by difference, after equilibration of the sample with 2,2-dipyridyl, which inhibits adsorption of reduced iron onto the electrode. The technique was employed in shelf waters of the North Sea, where Fe(II) concentrations were found to range from below detection (0.120 nM) to 1.2 nM. In some surface water samples, these concentrations represented

50-60% of the total dissolved iron. Recently this technique was used in the North Atlantic to measure iron speciation at three stations (Boye et al., 2006). Detectable Fe(II) (0.1 – 0.3 nM) was found for the near surface waters and at deeper levels in association with the chlorophyll maximum. Fe(II) was also detected at depth (0.1 – 0.55 nM) where oxygen levels were low, but not absent. The authors speculated this deeper Fe(II) presence was associated with the destruction of organic matter.

Driven by the need for lower detection limits and the desire to overcome some of the problems presented by spectrophotometric analysis, Seitz and Hercules (1972), developed a flow injection analytical method for Fe(II) in water. The method relied upon the detection of chemiluminescence generated by the reaction of Fe(II) with oxygen in the presence of 5-amino-2,3-dihydro-1,4-phthalazinedione (luminol). This method had several advantages over previous methods. It did not require pre-concentration or other extensive sample preparation. Thus the likelihood of speciation shifts leading to measurement artifacts was minimized. The use of high-speed photomultipliers as light detectors enabled measurements to be made very rapidly with great sensitivity, and was therefore ideal for oxidation rate studies (King et al., 1995; Emmenegger et al., 1998; King, 1998; Rose and Waite, 2002). It has since been used with modifications to measure the concentration and behavior of Fe(II) in lake water (Emmenegger et al., 2001) and in laboratory studies using a seawater matrix (O'Sullivan et al., 1995).

Bowie et al. (2002) analyzed Fe(II) in the South Atlantic (~24°S, 9°E) and Southern Ocean (~51°S, 143°E) using luminol chemiluminescence coupled with pre-concentration on 8-HQ. Continuous underway measurements of Fe(II) and Fe_{DISS} were made during 10-hour and 5-hour towed-fish deployments, sampling at a depth of 1-2 m. Fe(II) concentrations of 5-45 pM were detected in this manner, representing as much as 37% of the total dissolved iron (Bowie et al., 2002). Using a similar method but omitting the pre-concentration step, Hopkinson and Barbeau (2007) found high concentrations of Fe(II) (150-175 pM) in the suboxic zone (150-300 m) at a station in the eastern tropical Pacific (15°N, 115°W), approximately 600 nm off the coast of Mexico. However, the samples they took from the upper 100 m contained no detectable Fe(II).

In spite of numerous theoretical Fe(II) production mechanisms and direct measurements of significant Fe(II) concentrations in oceanic environments, there is a general perception that Fe(II) constitutes a minor or even insignificant fraction of the total dissolved iron. The reasons are possibly four-fold. First, because Fe(II) oxidation rates can be very fast, on the order of seconds, there is perhaps an inclination to regard its occurrence as transient, and thus insignificant. Second, the studies of Fe(II) to date have been geographically restricted (coastal or low O₂ environments), such that reported concentrations might be regarded as unrepresentative of

typical ocean conditions. Third, as mentioned above, the integrity of measurements from previous studies has been questioned. In a workshop summary, it was stated that “the reported concentrations of iron in these studies were often higher than expected for open-ocean environments” (Wells et al., 1995). Finally, the important finding that >99% of the dissolved Fe(III) in seawater is chelated by natural organic ligands (Gledhill and van den Berg, 1994; Rue and Bruland, 1995; Wu and Luther, 1995) has been repeatedly misstated in much of the literature to the effect that >99% of dissolved iron is organically-complexed, either implicitly or explicitly referring to the entire dissolved iron pool as organically-complexed Fe(III) (Gledhill and van den Berg, 1994; Wells et al., 1995; Hutchins et al., 1999; Maldonado and Price, 1999; Archer and Johnson, 2000; Bruland and Rue, 2001; Sunda, 2001; Ussher et al., 2005). This confuses the speciation issue, and highlights the need for both more precise terminology and more definitive studies of the oceanographic distribution and relative abundance of reduced iron.

1.3 Goals of This Work

The CLIVAR/CO₂ Repeat Hydrography Project provided a unique opportunity to study the occurrence of Fe(II) in oceanic waters. CLIVAR, or Climate Variability and Predictability, is one of the chief components of the World Climate Research Program, a consortium of nations dedicated to advancing knowledge of climate determining-processes. A central focus of CLIVAR is to better understand the role of the coupled ocean/atmosphere system within the overall climate system, over time-scales of months to decades. In support of this goal, the Repeat Hydrography Project systematically monitors key ocean sections, integrating hydrographic, ocean tracer, and carbon system data acquisition efforts. Acknowledging the role of iron in the global carbon cycle, and recognizing the need to further elucidate the sources and distribution of iron in the open ocean, the National Science Foundation agreed to provide funding for a global ocean survey of dissolved iron in conjunction with the on-going Repeat Hydrography cruises (Landing et al., 2003). At the time this research was begun, the iron survey was already underway, greatly facilitating data collection and eliminating most logistical concerns. Furthermore, most of the equipment needed for chemiluminescent measurement of reduced iron was already on-hand. This, combined with the need to make rapid, low-level measurements with minimal sample alteration, determined the choice of method.

The chief objective of this dissertation is to present and discuss Fe(II) measurements from two cruises in the North Pacific. Details of the sampling and analytical methods will be presented in the second chapter, along with a discussion of possible analytical interferences. The data will be presented in the third chapter, and will be interpreted within the context of previous

and on-going research. The distributional patterns and their relationship to possible source mechanisms will also be discussed.

Table 1: Some important biochemical iron compounds are listed below.

	Compound	Description	Source
Heme Proteins	Cytochromes	Membrane-bound electron transport protein	1
	Hemoglobin	Oxygen transport; NO transport (plants)	1
	Myoglobin	Oxygen transport; NO transport (plants)	1
	Catalase	Oxygen metabolism (H ₂ O ₂ dismutation)	2
	Peroxidase	Oxygen metabolism (H ₂ O ₂ dismutation)	2
	Oxidases	Molecular oxygen reduction	2
Iron-Sulfur Proteins	Ferredoxin	Electron transport protein	1
	Rubredoxin	Electron transport protein	1
	Aconitase	Respiration, amino acid synthesis	1
	Hydrogenases	Molecular hydrogen oxidation	2
	Nitrogenase	Nitrogen fixation	2
	Nitrate reductase	Dissimilatory nitrate reduction	1
	Nitrite reductase	Dissimilatory nitrite reduction	1
	Dioxygenases	O ₂ cleavage, biodegradation of aromatic compounds	1
Non-Heme, Non-Fe-S Proteins	Amino acid hydroxylases	Protein synthesis	1
	Superoxide dismutases	Oxygen metabolism (superoxide dismutation)	2
	Ribonucleotide reductase	DNA synthesis	2
	Cyclase CHL27	Chlorophyll synthesis	3
	Purple acid phosphatase	Dephosphorylation, enzyme regulation	1

(1) Crichton (1991) (2) Weinberg (1989) (3) Merchant (2006)

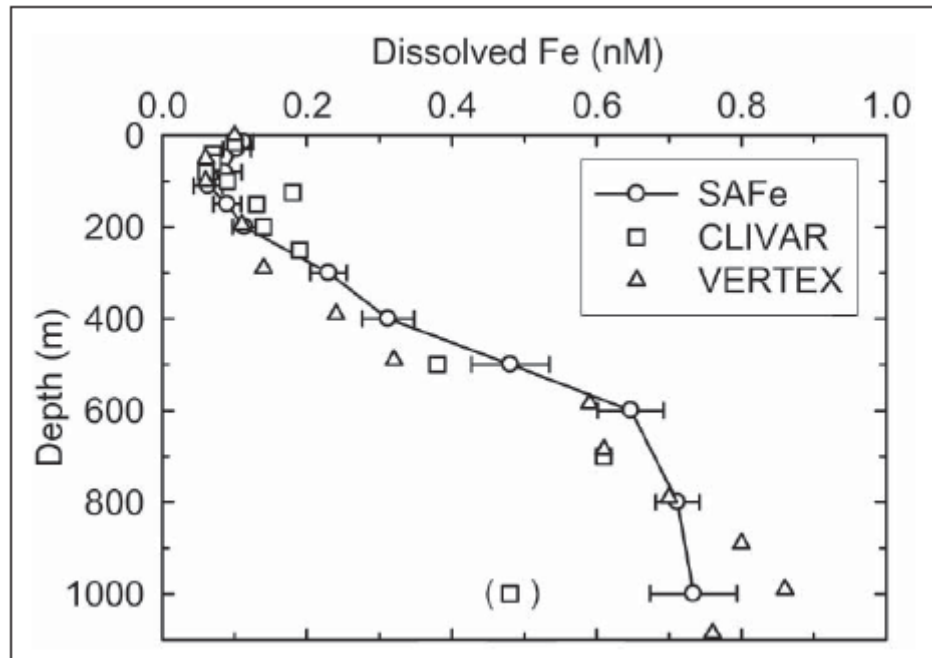


Fig. 1: Dissolved iron profile obtained during the recent SAFe cruise, an intercomparison study of Fe_{DISS} analytical methods (Johnson et al., 2007). Shipboard measurements from the intercomparison study are shown in open circles, open triangles represent data collected during the Vertical Transport and Exchange (VERTEX) program during 1986, and open squares represent data collected on the CLIVAR PO2 cruise. *Figure reproduced with open permission from the American Geophysical Union.*

2. MATERIALS AND METHODS

2.1 Sample Collection

2.1.1. Sampling Locations

Seawater samples were collected on two Pacific research cruises in association with the CLIVAR/CO₂ Repeat Hydrography Program. The first cruise, PO2, occurred June-August, 2004, and consisted of a latitudinal transect from Yokohama, Japan, to San Diego, California aboard the R/V Melville (Scripps Institute of Oceanography). The second cruise, P16N, occurred February-March, 2006, and consisted of a S-N transect from Papeete, Tahiti, to Kodiak, Alaska aboard the R/V Thomas G. Thomson (University of Washington). Sample station locations on both cruises were selected by the main hydrography program, and due to ship-time limitations, trace metal sampling was conducted only at alternating stations. On PO2, 87 stations were sampled for trace metals, with a nominal spacing of 60 nautical miles. On P16N, 37 stations were sampled for trace metals, situated at 120-mile intervals, except for a 60-mile interval in the vicinity of the equator. The cruise tracks and trace metal sampling locations are shown in [Fig. 2](#), and details regarding sample stations are given in [Appendix A](#).

2.1.2 Collecting Seawater Samples using GO-FLO Bottles

On both cruises, samples for trace metal analyses were collected using 12-L Teflon-coated GO-FLO bottles (Model 1080 Series, General Oceanics). The bottles were mounted on a powder-coated aluminum rosette frame equipped with a Seabird SBE-911 CTD, an SBE-43 dissolved oxygen sensor, and a Wet-Labs ECO-AFL fluorometer. When not in use, the GO-FLO bottles were stored inside a Class 100 clean van, with small plastic bags covering the tops, and plastic gloves over the spigots. On station, the bottles were transferred to the sampling deck and attached to the rosette, where they were cocked in the open position. Immediately prior to deployment, the plastic coverings were removed from the bottles. The rosette was lowered through the water column using a dedicated winch spooled with polyurethane-coated Kevlar hydrowire to approximately 10 meters below the deepest target depth (950-1000 m). The rosette was then slowly raised upwards through the water column until reaching the first (deepest) target depth, at which time the first bottle was electronically tripped into the closed position. The remaining samples were similarly collected at predetermined depths, chosen to coincide with the

main hydrography program (Table 2). Once on board and secure, plastic coverings were applied to the GO-FLO bottles, and they were immediately transferred to the clean van for sub-sampling.

2.1.3. Sub-sampling from GO_FLO Bottles

Sub-samples for Fe(II) analysis were collected by filling clean 125 mL HDPE Nalgene containers with gravity-fed filtered seawater. Samples were filtered using a Gelman AcroPak-200 in-line capsule 0.2 μm filter, with a hydrophilic polyethersulfone filter membrane housed in a polypropylene capsule. The filter was connected directly to the GO-FLO spigot outlet using a short length of semi-flexible polyethylene-lined ethyl-vinyl-acetate tubing (0.375" o.d.). Before collecting the first sample, the cartridge filter was flushed with approximately 5 cartridge volumes of sample water. Subsequent samples were rinsed with 3 cartridge volumes. Sub-samples were collected from shallowest to deepest, as fast oxidation rates were anticipated in warm, oxygenated, high pH surface samples. Sub-sampling for Fe(II) was typically complete within 25 minutes of the rosette arriving on deck. Analyses for Fe(II) commenced immediately after sample collection, using the procedures described below.

After the sub-samples for Fe(II) were collected, and while they were being analyzed, sub-samples for total dissolved iron (Fe_{diss}) were collected by members of the trace metals team. These samples were filtered using acid-rinsed Nuclepore PCTE filters with a 0.4 μm pore diameter and analyzed shipboard using spectrophotometric flow injection analysis (Measures et al., 1995) after pre-concentration on 8-hydroxyquinoline resin (Landing et al., 1986). A recent intercomparison study of analytical techniques for measuring Fe_{DISS} has shown that results obtained by this method are comparable with results obtained by other methods (Fig. 1) (Johnson et al., 2007).

2.1.4 Sample Acidification

Fe(II) undergoes rapid oxidation in warm, oxic seawater at pH 8, with a predicted half-life on the order of minutes (Millero et al., 1987; Millero and Sotolongo, 1989; Gonzalez-Davila et al., 2005; Santana-Casiano et al., 2005). The short half-life presented a logistical concern because approximately 20 minutes were required to sub-sample all 12 GO-FLO bottles and begin sample analysis. The rate of oxidation of Fe(II) by oxygen has been shown to a function of pH (Stumm and Lee, 1961; Millero et al. 1987) and adjustment of sample pH to 6.0 was predicted to increase the half-life to > 100 min (see Appendix B for oxidation rate calculations). In the laboratory it was determined that addition of 21 μL 6M HCl to 100 mL of stored surface seawater, initially at pH 8.1, would yield a final pH of 6.0. In the field, adjustment of pH was

accomplished by pre-loading each sample container with 29 μL of 6M quartz-distilled hydrochloric acid (q-HCl) (Fisher trace-metal grade). Each container was filled to the shoulder (138 mL) with filtered seawater, equivalent to the addition of 21 μL 6M q-HCl per 100 mL seawater.

The effect of acidifying samples of differing initial pH with a fixed quantity of q-HCl is considered for Station P16N/49 (27°N, 152°W), taken to represent a typical vertical profile. The *in situ* pH was calculated for each sample using the CO2SYS program (Lewis and Wallace, 1998) (refer to [Appendix C](#) for further details on pH calculations using CO2SYS). The program output is shown in [Table 3](#). Within this profile the calculated pH varied from approximately 8.1 near the surface to approximately 7.6 at a depth of 1000 m. The effect of adding a fixed amount of HCl to samples of varying pH was evaluated by recalculating the pH values after reducing the measured sample alkalinities by 1225 $\mu\text{mol/kg}$, an amount equivalent to the added HCl. The calculated pH of samples after acidification ranged from 5.96 - 6.03. Thus, addition of a fixed aliquot of HCl to the samples resulted in pHs that were very close to the target pH of 6.0, in spite of the *in situ* differences in initial pH and carbonate speciation. Sample acidification is considered further in sections 2.3.1 and 2.3.2.

2.2 Sample Analysis

2.2.1 Reagents

All solutions were prepared in 18 M Ω EPure water (EPW) (Barnstead), unless stated otherwise. A 10 mM stock Fe(II) solution was prepared by dissolving 3.92 g of ferrous ammonium sulfate hexahydrate ($\text{Fe}(\text{NH}_4)_2(\text{SO}_4)_2 \cdot 6\text{H}_2\text{O}$) (Fisher) in 0.1M q-HCl. This stock was prepared every 30 days, and stored in the dark at 4°C when not in use. A 50 μM intermediate stock solution was prepared daily in 0.024M q-HCl by adding 500 μL of 10 mM stock to 100 mL EPW with 400 μL 6M Q-HCl. A 50 nM Fe(II) working stock in 0.024 M q-HCl was also prepared daily by addition of 100 μL intermediate stock to 100 mL EPW with 400 μL 6M q-HCl.

Reagent-grade hydrogen peroxide (30%) was purchased from Fisher Scientific and Sigma-Aldrich, and was stored in the dark at 4°C when not in use. The concentration was calculated to be 8.8 M, and was not independently verified. A 10 mM intermediate stock solution was prepared by addition of 111 μL of the reagent stock to 100 mL EPW. A 50 μM working stock solution was prepared by adding 500 μL of 10 mM intermediate to 100 mL EPW. Intermediate and working stock solutions were prepared immediately prior to use.

Luminol reagent (0.001M) was prepared by dissolving 5-amino-2,3 dihydro-1,4-phthalazinedione in 1 M NH_4OH . After storing for 12-24 hours in the dark to ensure complete

dissolution, the pH was adjusted to 10.3 by addition of 6M q-HCl. The reagent was heated for 15 hours at 60°C to enhance sensitivity (W.M. Landing, pers. comm.). After heating, the reagent was cooled to room temperature prior to use. Luminol reagent was kept in opaque amber containers, and all tubing was light-shielded. Adequate shielding was confirmed by observing no change in the blank signal when lights were extinguished.

2.2.2 Measurement Apparatus

The acidified seawater samples were analyzed for Fe(II) using the chemiluminescent method developed by Seitz and Hercules (1972), adapted for use in seawater (King et al., 1995; O'Sullivan et al., 1995), with modifications (Emmenegger et al., 1998; Rose and Waite, 2001). A description of the method follows.

Using a Rainin Dynamax RP1 peristaltic pump, both sample and reagent are pumped continuously at equal rates (4 mL/min) to a transparent mixing/reaction flow cell, consisting of a 26 cm length of coiled Tygon tubing (nominal i.d. 1.14 mm). When mixed with luminol reagent at pH 10.3, Fe(II) in the sample is rapidly oxidized, forming reaction intermediates that initiate the step-wise oxidization of luminol, culminating with the production of light. To measure the light signal, the coiled Tygon reaction cell is taped directly to the face of a light detector contained within a lightproof film bag. The light detector used on the PO2 cruise was a Hamamatsu HC124-06 PMT operating with a high-voltage of 900 mV. The PMT signal was processed using an external analog/digital conversion card (ELAB) interfaced to a laptop computer. The detector response (mV) was recorded at two-second intervals by ELAB software, and averaged over a one-minute measurement period to obtain the response for an individual sample. Subsequent measurements, including those made on the P16N cruise, were made using a Hamamatsu HC135-11 photon-counting PMT consistently using the default high voltage (400 mV and a counting period of 100 ms. A/D conversion is done internally, and the detector delivers digital output (in counts) directly to the laptop through a serial interface. A Visual Basic application running under Microsoft Excel was written to control the PMT and read incoming data directly into a spreadsheet ([Appendix D](#)). The PMT response (in counts) was recorded for 50 consecutive counting intervals. The average of these was then considered to represent the sample ([Fig. 3](#)). Regardless of the detector used, the consecutive responses for an individual sample were visually monitored to ensure the signal was stable (non-trending) for the duration of the measurement interval.

2.2.3 Standards and Calibration

Fe(II) calibration curves in seawater were obtained 30-60 minutes prior to every analysis run (an analysis run consisted of the 12 samples constituting the depth profile, plus 0-3 duplicate samples, all analyzed in triplicate). Calibration standards were prepared in low-iron seawater that had been allowed to sit in the dark for a minimum of 24 hours. To minimize oxidative loss of added Fe(II), the seawater used for calibration was amended with 21 μL of 6M q-HCl per 100 mL to a pH of 6. Generally, the calibration range was from 0-200 pM Fe(II), with the acidified seawater (no added Fe(II)) serving as the blank. Other authors (Rose and Waite, 2001; Hopkinson and Barbeau, 2007) have observed non-linear calibration curves and used polynomial curve-fitting techniques to quantify results. In this study, non-linear calibration curves were infrequently observed, and usually when calibrating over a large concentration range (0-10 nM). Most calibrations in this study were well-approximated by a linear fit (Fig. 4), perhaps due to the narrow calibration range (typically 0-200 pM Fe(II)), or possibly due to pH adjustment of samples prior to analyses. For ease of computation, linear methods were therefore used to model all concentration/response data, and two-point calibrations were often used to derive calibration slopes. The detection limit for this method was 12 ± 6 pM determined as three times the standard deviation of the calibration intercept divided by the slope (Long and Winefordner, 1983). Calibration data are given in Appendix E. Detailed method descriptions and detection limit calculations are shown in Appendix F.

2.2.4 Data Reporting

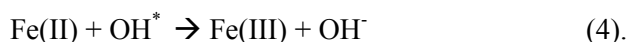
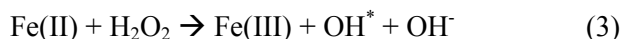
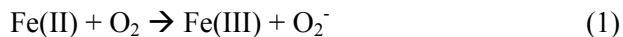
The detector responses for samples were recorded in mV when samples were measured in analog mode (cruise PO2), or in counts when measured in digital mode (cruise P16N). These responses were converted to concentration units by dividing the difference between the sample response and the blank response by the calibration slope, which was expressed in units of mV/pM or counts/pM for the two modes, respectively.

Sample measurements were typically obtained 20 minutes after sub-sampling and pH adjustment. The pH adjustment was intended to slow the rate of oxidation so that loss of Fe(II) during this time was minimized, and that the concentration measured after 20 minutes accurately reflected the concentration of Fe(II) in the GO-FLO bottle at the time of sub-sampling. However, consecutive measurements made at 20-minute intervals often indicated analytical responses that trended with time (Fig. 5). Therefore, an estimate of the initial concentration (i.e. the concentration of Fe(II) present in the GO-FLO bottle at the time of sub-sampling) was obtained by calculating the intercept ($t=0$) of the response-time relationship, assuming a simple linear

model. The calculation is detailed in [Appendix F](#), and the subject is considered further in section 2.3.2.

2.3 Potential Interferences

When the sample reaches the flow cell and mixes with the buffered luminol solution at pH 10.3, Fe(II) is rapidly oxidized. The so-called Haber-Weiss oxidation mechanism has been described by King et al. (1995) to involve the following steps:

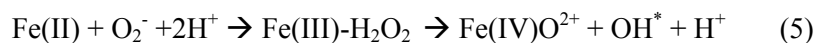


The overall oxidation rate is determined by the relative abundances of Fe(II) species, each of which reacts with molecular oxygen at a unique rate. In particular, Fe(OH)_2° and $\text{Fe(CO}_3)_2^{2-}$ oxidize very rapidly. Their abundance is pH-dependent and accounts for the oxidation rate dependency. At pH 10.3 oxidation occurs on a timescale of milliseconds (Rose and Waite, 2001).

The mechanism of luminol chemiluminescence is not well understood. Various reaction paths have been proposed in which luminol is oxidized by the reaction intermediates formed in reactions 1-4 (Merenyi et al., 1990; Xiao et al., 2000; Rose and Waite, 2001; Xiao et al., 2002). A generalized reaction path can be described that involves three fundamental steps ([Fig. 6](#)). In the primary oxidation step, luminol is oxidized to form a radical intermediate, a one-electron transfer that can be initiated by a variety of highly reactive free-radical species. A secondary oxidation occurs when the luminol radical is oxidized by superoxide, producing the α -hydroxy hydroperoxyl anion (α -HHP). Once formed, α -HHP decomposes to form 3-aminophthalate and nitrogen gas, with emission of light.

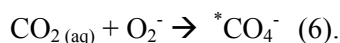
Debate over the mechanism seems to center mostly around the identity/origin of the primary oxidant and the validity of the Haber-Weiss iron oxidation mechanism as applied to conditions in the flow cell. In the Merenyi mechanism for luminol oxidation (Rose and Waite, 2001), the primary oxidation is carried out by the hydroxyl radical produced during the oxidation of Fe(II) by hydrogen peroxide (reaction 3).

Rose and Waite suggested modifications to this model, stating that the formation of the complex required for reaction 3 is too slow. Instead, they proposed an alternative Fe(II) oxidation scheme:



which produces the reactive ferryl ion (Fe(IV)) and the hydroxyl radical, both of which can serve as primary luminol oxidants. They note that in seawater, the hydroxyl radical will react indiscriminately with carbonate, bromide, and bicarbonate, producing a suite of “hydroxyl-like” radicals which are also capable of oxidizing luminol.

Laboratory studies of luminol chemiluminescence by Xiao and others (2002) favor an alternative mechanism in which the primary oxidation of luminol is most effectively carried out by peroxy carbonate radical (Fig. 7), produced when aqueous CO₂ (CO₂(aq)) present in both reagent and sample reacts with superoxide:



According to these researchers, the peroxy carbonate radical is more selective in its reaction with luminol than the hydroxyl radical, resulting in more efficient production of the luminol radical. Their experiments in pure water showed that elimination of CO₂(aq) from the flow cell resulted in strong signal suppression, providing good evidence for their proposed mechanism.

Regardless of the exact mechanism, the method ultimately relies upon a well-characterized relationship between the concentration of Fe(II) present in a sample and the detected light flux. This relationship requires that 1) the concentrations of primary and secondary luminol oxidants in the flow cell be produced quantitatively in exclusive response to Fe(II) oxidation in the flow cell, 2) α -HHP be produced quantitatively only by reactions of luminol with these oxidants, and 3) the flux of light to the detector change only in direct response to the decomposition of α -HHP. Analytical interferences arise when these criteria aren't met. Potential interferences considered here include carbon dioxide, reduced aqueous species other than Fe(II), hydrogen peroxide, dissolved organic matter, and light. The effect of sample acidification on measurements is also considered.

2.3.1 Effect of Sample Acidification on System Response

When a seawater sample is acidified to pH 6, a measurable increase in analytical response is observed (Fig. 8). This response enhancement due to sample acidification was evaluated for 56 samples collected at different locations and depths by collecting an unacidified sample from one of the GO-FLO bottles and measuring the system response before and after sample acidification. The mean difference in system response, expressed as equivalent Fe(II), was 12 ± 6 pM Fe(II). Seawater collected from Gulf of Mexico shelf waters ($\text{Fe}_{\text{DISS}} = 0.7$ nM) shelf gave similar responses to acidification ($\bar{x}_{\text{ave}} = 11 \pm 5$ pM, $n=13$, data not shown). It is important to note that the aged seawater used as the blank and the calibration matrix was acidified

to pH 6 prior to calibration, incorporating the response bias into all calibration curves. Therefore, all reported Fe(II) concentrations have been corrected for this effect.

Several possible explanations for the signal enhancement have been considered. The chemiluminescent yield from the luminol reaction has been observed to be pH-dependent. However, the luminol reagent is highly buffered and the pH does not measurably change in a 1:1 mixture of reagent and acidified seawater. Furthermore, luminol chemiluminescence should decrease with decreasing reaction pH, because protonated α -HHP does not emit light during decomposition (Rose & Waite, 2001). For these reasons, the observed enhancement is not believed to be related to changes in the reaction pH.

An obvious explanation for the increase in analytical response is the presence of trace amounts of Fe(II) in the HCl used to acidify the samples. However, the total concentration of iron in the quartz-distilled HCl used to acidify the samples was less than 2 nM (W.M. Landing, pers. comm.). If it is assumed that all iron in the q-HCl is reduced, addition of 21 μ L HCl to 100 mL samples would contribute no more than 0.4 pM Fe(II) to the samples, and therefore cannot be the sole source of the enhanced response.

Reduction of Fe(III) in response to HCl addition could also cause the observed effect. However, equilibrium modeling of seawater Fe speciation in the presence of oxygen predicts an Fe(II) concentration of < 0.01 pM for seawater at pH 6 and $Fe_{DISS} = 1$ nM. A plot of the signal enhancement against Fe_{DISS} reveals no apparent relationship, providing further evidence that the enhancement is not the result of Fe(III) reduction (Fig. 9).

An alternative explanation for the signal enhancement might lie in the experimental work of Xiao and others (2002), who found that Fe(II)-luminol chemiluminescence only occurred when aqueous carbon dioxide was present in the flow cell. Although they did not establish a quantitative relationship between $CO_2(aq)$ and analytical sensitivity, their findings suggest the possibility that system response is to some extent dependent upon the presence of aqueous CO_2 . Sample acidification has a profound effect on the concentration of aqueous CO_2 because at lower pH, the carbonic acid equilibrium is shifted, converting CO_3^{2-} and HCO_3^- to $CO_2(aq)$. For example, acidification of the uppermost sample at P16N/49 resulted in a predicted aqueous CO_2 concentration of 918 μ mol/kg (Table 3). This represents an 80-fold increase over the estimated *in situ* concentration. Fig. 10 shows the vertical profiles of predicted aqueous CO_2 concentrations for this station before and after acidification, calculated as described above. The figures show that the predicted concentration of $CO_2(aq)$ is greatly increased by acidification, and the relative difference between shallow and deep samples is greatly reduced.

These calculations are based on the assumption of a closed system. Aboard ship, the samples must begin to degas immediately upon acidification, as the partial pressure of CO₂ in the acidified samples is much greater than the partial pressure of CO₂ in the atmosphere. Thus, the actual concentration of CO₂ in the samples at the time of analysis is not known. Nonetheless, Fig. 10 can be used qualitatively to make three (perhaps debatable) points. First, the concentration of aqueous CO₂ in acidified samples should be much greater than the concentration in unacidified samples. This could account for the observed enhancement. Second, the concentration gradient of CO₂(aq) with depth that is present in the water column may persist to some extent after samples are acidified, though the relative difference between surface and deep samples should be much reduced. Third, if the concentration gradient does persist, and if CO₂ does have an effect on system sensitivity, the system response could also vary with depth. However, a plot of the acidification response versus depth shows no obvious relationship (Fig. 11). Previous workers have not reported depth-related changes in analytical sensitivity (W.M. Landing, pers.comm; Hopkinson & Barbeau, 2007). Although it was not considered to be a concern in this study, tests were made at one station to assess system sensitivity for samples collected at different depths. Standard additions of Fe(II) made to seawater samples from Station PO2/018 collected at 15, 135, and 970 m, and yielded response/concentration slopes of 0.070 mV/pM, 0.058 mV/pM, and 0.076 mV/pM, respectively (Fig. 12). Although the limited sample sizes make it difficult to determine whether or not the differences in these slopes are statistically significant, the depth dependency that would be expected from a CO₂ interference is not present. Unfortunately, standard additions to seawater samples of varying depths were not routinely made, and future work should include evaluation of the potential for depth-related matrix effects.

2.3.2 Effect of Sample Acidification on Sample Stability

Preservation of Fe(II) at pH 6 was verified by spiking aged low-iron seawater at pH 6.0 with 100 pM inorganic Fe(II). Continuous monitoring over a 20-minute interval yielded a stable chemiluminescent response (Fig. 13).

In contrast to the stability observed in spiked seawater samples, sequential measurements of natural samples at pH 6 often indicated a slowly increasing or decreasing trend in the response, suggesting a gain or loss of Fe(II) in the sample over time (Fig. 5). To monitor the stability of actual samples, each analysis run was repeated three times, so that each sub-sample was analyzed thrice at approximately 15-20 minute intervals. The stability of each sub-sample was quantified as the slope of the relationship between apparent concentration and the age of the sample (time elapsed between acidification and measurement), using a simple linear model. A negative slope

indicated an apparent loss of Fe(II) over time, a positive slope indicated an apparent gain in the concentration over time, while a slope of zero indicated no change in the concentration over time.

Box plots of trend magnitudes (i.e. the regression slopes in pM/min) grouped by sample collection depth are shown in Fig. 14. The magnitudes of these trends are typically within a range of ± 1 pM [Fe(II)]/min, with the majority of shallow samples having slightly negative slopes (median slope = -0.17 pM/min). Mid-depth samples, which typically contain very little Fe(II), generally show little change in analytical response over time. Deeper samples, however, showed a bias towards positive slopes (median slope = 0.32 pM/min) suggesting a net production of Fe(II) during the period of analysis.

The bias towards signal attenuation in shallow samples could arise from the slow oxidation of Fe(II) by H_2O_2 . H_2O_2 is a strong oxidant and has been found to be present in surface seawater at concentrations of 0-100 nM (Yuan and Shiller, 2005). Unlike oxidation of Fe(II) by O_2 , Fe(II) oxidation by H_2O_2 is first-order with respect to the hydroxide concentration. Lowering the pH slows, but does not eliminate oxidation by H_2O_2 . An estimate of the rate of Fe(II) oxidation by H_2O_2 in seawater is given by:

$$d[\text{Fe(II)}]/dt = -k_{\text{H}_2\text{O}_2}[\text{Fe(II)}][\text{H}_2\text{O}_2].$$

Estimates of $\log k_{\text{H}_2\text{O}_2}$ for seawater at pH 6 and $T=25^\circ\text{C}$ range from 3.0 (Gonzalez-Davila et al. 2005) to 3.3 (Millero and Sotolongo, 1987). For hypothetical Fe(II) and H_2O_2 surface water concentrations of 50 pM and 50 nM, respectively, decay rates of 0.15 – 0.3 pM/min are predicted. Thus, the observed decay of Fe(II) with time in shallow seawater samples at pH 6 is consistent with slow oxidation by H_2O_2 .

It is more difficult to account for the signal increases, which were observed primarily in deep samples. An obvious explanation is that Fe(III) in the sample is slowly being reduced in response to pH adjustment. Another possibility is that slow changes occurring in the sample during analysis enhance system sensitivity to Fe(II).

Thermodynamic equilibrium models predict reduction of Fe(III) only under conditions of low pH and low redox potential. Using MINEQL equilibrium modeling software, it was determined that seawater with 0.7 nM total iron at pH 6 would require a pE of < 9 to thermally reduce enough Fe(II) to be detected using this analytical system (~ 10 pM). Such low redox intensities are found only in suboxic or anoxic environments, environments that were not sampled in this study. Therefore, reduction of inorganic Fe(III) is considered to be unlikely under these conditions.

Deep samples were characterized by low temperatures ($\sim 2.7 - 4.7^\circ\text{C}$). Although some warming occurred in between the time the sample was collected and analyzed, these samples

were the coldest in the profile at the time of analysis. If the oxidation reaction rate in the flow cell is temperature-dependent, then a cold sample could produce diminished chemiluminescent response that increases as it warms. The temperature-dependence was tested in the laboratory by placing seawater in an ice-bath until a temperature of 4°C was reached. The sample was then removed from the ice-bath, acidified to pH 6, and spiked with 50 pM Fe(II) and monitored for a period of 30 minutes. The sample showed no initial or subsequent difference in response than an acidified 50 pM Fe(II) seawater solution at room temperature, suggesting that slow warming of the sample doesn't affect system response.

Deep samples typically had low oxygen levels (5-20 $\mu\text{mol/kg}$). Because O_2 is required for oxidation of Fe(II) in the flow cell, slow oxygenation of a sample might lead to enhanced system sensitivity. Laboratory tests were conducted to determine the effect of low O_2 on chemiluminescent response. Samples were degassed by bubbling with filtered argon for 1 hour, then acidified and spiked with 50 pM Fe(II). Sample degassing had no apparent effect on chemiluminescent response, presumably because the luminol reagent was sufficiently oxygenated to carry out the oxidation reaction in the flow cell.

Changes in the inorganic speciation of Fe(II) are predicted to occur when the pH is adjusted, shifting the equilibrium concentrations away from species that are rapidly oxidized ($\text{Fe}(\text{OH})_2^\circ$, $\text{Fe}(\text{CO}_3)_2^{2-}$), towards species that oxidize more slowly (FeOH , Fe^{2+} , FeCl^- , FeSO_4°) (Millero, 1987; Millero, 1995). These changes occur rapidly in response to pH adjustment, rather than slowly, as observed. When the sample enters the flow cell and reacts with luminol, the speciation rapidly shifts in the opposite direction, towards hydroxyo and carbonato complexes that are oxidized very rapidly. Thus, fast equilibration kinetics in response to changes in pH changes during acidification and analysis allow the analytical system to work with relative disregard for the Fe(II) speciation.

This may not be the case in natural waters, where available complexing ligands include a variety of organic molecules. Currently, little is known about the extent to which Fe(II) forms natural organic complexes. However, limited laboratory studies of oxidation kinetics of artificial Fe(II) organic complexes Fe(II) suggest that some complexes react more slowly with oxygen than the predicted inorganic assemblage (ligands with carboxyl functional groups), while others react much more quickly (Theiss and Singer, 1974; Santana-Casiano et al., 2000; Santana-Casiano et al., 2004). If reactions in the flow cell are dependent upon the manner in which Fe(II) is speciated, then the system response could vary in response to factors other than the total Fe(II) concentration, which will have some important consequences for measurement validity and system behavior.

As discussed previously, the work of Ussher et al. (2006) showed that for several organic Fe(II) complexes, oxidation in the flow cell is slower than for inorganic Fe(II) species, producing diminished chemiluminescence. Hypothetically speaking, if sample acidification causes a slow shift in the ratio of organically complexed Fe(II) to inorganic Fe(II), then a similar shift in system response is expected. Sample acidification increases the proton concentration to $\sim 1 \mu\text{M}$, increases competition for ligand sites, and possibly promotes the dissociation of organometallic complexes. The overall effect on system response will then depend on the relative rates of oxidation and re-complexation under the high pH conditions present in the flow cell.

As mentioned above, the measured concentrations were corrected for post-acidification directional changes in analytical response by linear extrapolation back to the time of acidification. The median correction for shallow samples was +3 pM. The median correction for deep samples was -6 pM. Because samples collected from intermediate depths were typically stable, correction for trending analytical responses was not necessary. A vertical profile of Fe(II) concentration calculated with and without the correction is shown in [Fig. 15](#) for Station P16N/10.

2.3.3 Reduced Species other than Iron (II)

Primary and secondary luminol oxidants can also be produced in the flow cell by reactions other than 1-4. The potential for such interferences was systematically tested for several seawater constituents with redox transitions occurring in oxic ($\text{pE}_{\text{cond}} = 8 - 12.6$) to suboxic ($\text{pE}_{\text{cond}} = 6 - 8$) to anoxic conditions ($\text{pE}_{\text{cond}} < 6$) (Hopkinson and Barbeau, 2007). Of the redox couples occurring within the range of oxic and suboxic seawater (IO_3^-/I^- , $\text{HCrO}_4^-/\text{Cr}^{3+}$, $\text{SeO}_4^{2-}/\text{SeO}_3^{2-}$, $\text{NO}_3^-/\text{NO}_2^-$, $\text{MnO}_2/\text{Mn}^{2+}$, and $\text{Cu}^{2+}/\text{Cu}^+$), only Cu(I) was found to be an interferant. Of the redox couples predicted to occur under anoxic conditions ($\text{CoOOH}_{(s)}/\text{Co}^{2+}$, $\text{Sb(V)}/\text{Sb(III)}$, $\text{H}_3\text{AsO}_4/\text{HAsO}_2$, $\text{VO}_2^+/\text{V}^{3+}$, $\text{VO}_2^+/\text{VO}^{2+}$, $\text{MoO}_4^{2-}/\text{Mo(V)}$), only Co(I), V(III), and V(IV) were found to interfere. The relevancy of these latter species to this study is doubtful, because macroscale anoxic conditions were not encountered on either of the cruises. However, the existence of anoxic microenvironments in open ocean seawater has been documented (Alldredge and Cohen, 1987). Thus these species are considered here to include the possibility of interferences arising from such sources.

To determine if these species were potential interferences under the experimental conditions of this study, 50 pM additions of each were made to Gulf of Mexico seawater at pH 6 ([Fig. 16](#)). Positive results of varying magnitude were observed for all the trace metal species tested. The potential of each metal to significantly interfere with the analysis is discussed below.

The addition of 50 pM Co(II) to acidified seawater resulted in a positive response equivalent to approximately 1 pM Fe(II). In the open ocean, cobalt exhibits a scavenging-type profile, with maximum concentrations in the upper water column that diminish with depth. In the North Pacific, cobalt concentrations are 50 pM at the surface, declining to 4 pM at depth (Donat and Bruland, 1995). Due to the low concentrations and low analytical response relative to Fe(II), Co(II) is not considered to be a significant interference.

Cu(I) also showed a positive response, with a 50 pM addition yielded a signal equivalent to 1.7 pM Fe(III). In the N. Pacific, copper exhibits a modified nutrient profile, with low surface concentrations (0.4 nM) that increase to 2 nM at a depth of 1000 m (Bruland, 1980). Studies in the North Atlantic and Gulf of Mexico have shown that within the mixed layer, 5-10% of the total dissolved copper is Cu(I), with undetectable concentrations below (Moffett and Zika, 1988). Such low concentrations coupled with low chemiluminescent yield make Cu(I) an unlikely source of interference.

V(III) showed the strongest chemiluminescent response of all the species tested, with 50 pM V(III) equivalent to ~6 pM Fe(II). Although V(IV) was not tested in this study, Hopkinson and Barbeau (2007) found V(IV) to provide a signal equivalent to 3% of that produced by Fe(II), i.e. 50 pM V(IV) would be equivalent to 1.5 pM Fe(II). Concentrations of dissolved V in the N. Pacific range from 32 nM in the surface water, to 36 nM by a depth of 500 m. At such high concentrations, even a small fraction present as V(III) or V(IV) could cause significant analytical interferences. However, Hopkinson and Barbeau raised several considerations that argue against the presence of reduced V in seawater. They noted that neither species is thermodynamically predicted under oxic conditions, and with conditional pEs of -2.7 and -3.1 reduction should not occur until sulfidic conditions are reached. They also noted that V(III) is both highly insoluble and rapidly oxidized in the presence of oxygen. Their measurements of the chemiluminescent response decay that occurred upon oxygenation of samples collected from the suboxic zone of the eastern tropical Pacific closely matched the decay rates predicted for Fe(II), while laboratory measurements of V(III) oxidation occurred at rates that were 10 times faster. Although they were able to rule out V(III) as a likely interference, they acknowledged that interference by V(IV) could not be ruled out. Yet recent vanadium speciation measurements on Indian Ocean seawater samples by Okamura et al. (2001) found no V(IV) at levels above 50 pM, their analytical detection limit.

2.3.4 Hydrogen Peroxide

Hydrogen peroxide (H_2O_2), a strong oxidant, has been found to be present in upper-most surface seawater at concentrations of 10-250 nM, rapidly attenuating with depth (Yuan and Shiller, 2005). It has a relatively long lifetime in seawater (3-7 days). When present it will be introduced into the flow cell along with the sample. H_2O_2 is a strong oxidant, and could cause an analytical interference by directly oxidizing luminol. Depending on reaction kinetics, it could also compete with oxygen in the flow cell (reactions 1 and 3), leading to a different suite of oxidation products. Finally, it can react with other flow cell constituents to produce luminol oxidants that would otherwise not be produced. In spite of this potential, the role of H_2O_2 as a potential interference has not been established.

The ability of H_2O_2 to directly oxidize luminol was tested by additions of H_2O_2 to acidified seawater in the absence of added Fe(II). Additions of 0, 60, and 120 nM H_2O_2 resulted in no significant changes in system response (Fig. 17A). Others have found the system to be insensitive to H_2O_2 at levels up to 1 μM , in the absence of Fe(II) (King et al. 1995; Rose and Waite 2001).

The second possibility, competition with oxygen, is unlikely given the observation that at pH 10.3, the reaction of Fe(II) with oxygen is extremely rapid, with nearly all Fe(II) quantitatively converted to Fe(III) plus superoxide (Rose and Waite, 2001). They observed no signal enhancement after addition of 100 nM H_2O_2 to unacidified seawater containing 8 nM Fe(II), and suggest that oxidation of Fe(II) by H_2O_2 at high pH is slow. They also suggest that formation of an intermediate complex (required for an inner-sphere electron transfer) is rate-limiting. They note, however, that at lower pH, the reaction of Fe(II) with oxygen is slower, and suggest that interference by H_2O_2 should increase as pH decreases. In contrast to these findings, O'Sullivan and others (1995), found that the addition of 100 nM H_2O_2 to seawater at pH 6.3 containing 5 nM Fe(II) resulted in a two-fold signal enhancement. In the latter study, a stopped-flow analytical method was used with a lower reaction pH (9.9); the conflicting observations could result from the different protocols.

To assess the potential for interference, two experiments were performed in which H_2O_2 was added to samples containing known concentrations of Fe(II). Reported concentrations of H_2O_2 in the North Pacific at depths of 16-20 meters (the shallowest samples collected in this study) range from 40-120 nM (Yuan and Shiller, 2005), with concentrations attenuating to undetectable levels (<1 nM) by depths of 150-200 meters. Thus, two experiments were performed in this concentration range.

In the first experiment, additions of 0, 60, and 120 nM H₂O₂ were made to seawater samples at pH 6 containing differing Fe(II) concentrations (Fig. 17A). Addition of H₂O₂ to samples containing no added Fe(II) had little effect on the system response, indicating that H₂O₂ did not directly oxidize luminol, and that other constituents, including carbon dioxide and trace metals (e.g. Co(II)), were unaffected by the presence of H₂O₂ at these levels. However, in the presence of Fe(II), added H₂O₂ resulted in an enhanced signal of approximately 15-20% for additions of 60 and 120 nM, respectively.

In the second experiment, additions of 0, 60, and 120 nM H₂O₂ were made to seawater at natural pH (~8). Following addition of H₂O₂, the samples were then acidified to pH 6 and spiked with Fe(II). When the experiment was done in this manner (i.e. addition of H₂O₂ prior to sample acidification and Fe(II) addition), the system responses were equivalent to samples with no added H₂O₂ (Fig. 17B).

The third possibility is that H₂O₂ could react with other species present in the flow cell, producing primary oxidants capable of luminol oxidation. One suggested pathway involves the reaction of hydroperoxide anion with carbon dioxide to produce peroxycarbonate, which decomposes to form carbonate radicals (Xiao et al., 2000). This reaction should not result in chemiluminescence, however, until a secondary oxidant becomes available (e.g. superoxide). Also, in seawater this interference should be pH-sensitive, as the carbonate speciation at low pH favors formation of aqueous CO₂.

2.3.5 Dissolved Organic Matter

Dissolved organic matter (DOM) is present in upper-most open ocean seawater at concentrations ranging from 75-150 μM, while in deep water concentrations range from 4-75 μM (Millero, 2002). The major types of organic compounds present in DOM include carbohydrates, amino acids, hydrocarbons, steroids, carboxylic acids, and humic substances. These last two categories of DOM are known to possess multiple carboxyl, alcohol, and phenol functional groups, which coordinate with iron to form polydentate complexes. In addition to these organic compounds, recent studies of open ocean seawater have discovered the presence of strong metal-binding organic ligands with high affinity for iron (Gledhill and van den Berg, 1994; Rue and Bruland, 1995; Wu and Luther III, 1995). These compounds are believed to include siderophores (low molecular weight compounds of bacterial origin) (Rue and Bruland, 1997; Barbeau, 2001) and porphyrins (intracellular iron-binding prosthetic groups present in a variety of biomolecules), which are released to seawater by grazing, cell lysis, and remineralization of biogenic particles

(Hutchins, 1999). Siderophores and porphyrins possess three pairs of hydroxamate and/or catecholate functional groups and can therefore form strong hexadentate complexes. Collectively these compounds represent a small fraction (1-2 nM) of DOM in the open ocean.

The presence of DOM in the sample matrix has the potential to cause analytical interference in three ways. Significant quantities of DOM in the flow cell can compete with luminol for the necessary reactive oxidants, resulting in diminished production of α -HHP, and the associated chemiluminescent response. DOM can also absorb the light emitted by α -HHP, thus preventing the light from reaching the detector. Finally, Fe(II) that is organically complexed may be less reactive with dissolved oxygen in the flow cell.

These interferences are expected to present analytical difficulties in eutrophic fresh-water or coastal environments, where millimolar DOM concentrations can be present (Millero, 2001). This is supported by the work of Rose and Waite (2001), who examined the effects of Suwannee River fulvic acid (SRFA) on chemiluminescent Fe(II) measurements. Experimenting with SRFA levels of 0.5-1.0 mg/L, they found evidence of strong signal quenching, which they attributed to complexation of Fe(II) with SRFA, occurring external to the flow cell during pre-complexation, or within the flow cell, which is expected to occur very rapidly at high pH due to the deprotonation of the SRFA.

While conceptually useful, interference studies using SRFA are perhaps more relevant to coastal systems than to open ocean conditions, where strong iron-binding ligands, including siderophores and porphyrins, dominate iron speciation. To see how these kinds of ligands might affect the Fe(II) measurements made in this study, three solutions of “model” marine ligands (Fig. 18) were prepared and added to acidified seawater, with and without added Fe(II). Desferrioxamine B, a terrestrial siderophore, was purchased from Fisher and prepared by dissolving in EPW. Ethylenediaminetetraacetic acid (EDTA), a chelating agent, was purchased from Fisher and dissolved in EPW. Protoporphyrin IX, an iron-binding tetrapyrrole closely similar in structure to prosthetic groups found in hemes, cytochromes, chlorophyll, and other biomolecules, was purchased from Frontier Science and prepared by first dissolving in methanol and 0.01 M HCl followed by dilution in EPW to the desired concentration. “Pre-complexed” Fe-L solutions were prepared in EPW that had been bubbled with argon for 1 hour to remove oxygen. In the absence of oxygen, Fe(II) oxidation will be slow to occur. Solutions were allowed to equilibrate for a period of 30 minutes prior to measurement.

The effects of these organic ligands on system sensitivity are shown in Fig. 19. In the absence of added Fe(II), ligands added directly to acidified seawater in concentrations of 50 -500 pM showed no effect on blank response, suggesting that interference by light absorption or

luminol competition does not occur. For both DFB and PPIX, addition of “pre-complexed” Fe-L solutions at Fe-L ratios of 1:1 and 1:10 yielded system responses that were equivalent to those with no added ligand (i.e. Fe(II) only). However, solutions containing 1:1 Fe(II)-EDTA showed system responses equivalent to solutions with no added Fe(II), suggesting that Fe(II)-EDTA complexes are unreactive in the flow cell. EDTA is a synthetic chelating compound with slow metal-exchange kinetics (Stumm and Morgan, 1996) and was chosen to represent the extreme case in a spectrum of iron-binding ligand strengths. Though it bears little resemblance to naturally occurring marine compounds, the results suggest that any Fe(II) in seawater bound to such strong, kinetically sluggish ligands would probably not be detected by luminol chemiluminescence.

Ussher et al. (2006) studied the effects of several different ligands on chemiluminescent measurement of Fe(II). Their experiments were done in pure water, with high iron concentrations (2 nM) and relatively low Fe:L ratios (1:50). Comparison of Fe:L responses to controls showed that in most cases, the effect of additional ligand was to diminish response, either by accelerating oxidation of Fe(II) during equilibration or by retarding oxidation in the flow cell. However, they found that humic acid and PPIX resulted in higher responses than control samples, either by slowing oxidation of Fe(II) in the sample containers or by reduction of Fe(III).

2.3.6 Light

Primary and secondary luminol oxidants that are unrelated to the concentration of Fe(II) can be introduced into the flow cell, either via the sample or the luminol reagent. In the case of the reagent, exposure of luminol to light results in photoproduction of the luminol radical, which can then react with oxygen to produce superoxide (Rose and Waite 2001). The light sensitivity was confirmed in this study. Direct exposure even to diffuse laboratory light resulted in an increase in baseline signals. Luminol reagent was therefore stored in brown, opaque containers, and all reagent tubing was light-shielded. To verify luminol stability during an analytical run, frequent reference checks were made of the calibration blanks and standards.

Exposure of samples to UV light can affect system response by reducing Fe(III) present in the sample and by producing free radicals that can potentially be transported into the flow cell. Although the luminol reagent was found to be light sensitive, exposure of samples to the low-level UV light present in the laboratory did not cause any observable interference. However, in photoreduction experiments, seawater samples exposed to very short wavelength UV light (256 nm) were found to generate high analytical responses (Fig. 20). While some of this response is probably due to the photoreduction of Fe(III), the analytical responses were often higher than

would be expected even assuming complete reduction of all Fe(III). This is attributed to the photoproduction of free radicals that are capable of luminol oxidation (Rose and Waite, 2001).

In the open ocean, light of wavelengths less than 400 nm can penetrate to depths of ~100 m (Garrison, 2002). Some photochemical reactions (including the reduction of Fe(III)) are therefore expected to occur. Superoxide, produced by the oxidation of DOM, is expected to be present in surface seawater at levels of 0.1-2 nM (Voelker and Sedlak, 1995). Estimates of steady-state hydroxyl radical concentrations are at sub-attomolar levels (Qian et al., 2001). Extremely low concentrations coupled with very short lifetimes of microseconds to seconds suggest that the effect of these interferences on the analytical method should be negligible, given the time interval required to retrieve the rosette and sub-sample the GO-FLO bottles (~25 minutes for the shallowest sample).

2.3.7 Summary of Interference Studies

Sample acidification adds to the seawater blank response for undetermined reasons, but results are corrected for this effect. Minor time-dependent instabilities in system response, presumably associated with sample acidification, were observed and corrected for.

Of the redox couples expected in oxic seawater that might cause interferences, literature and experimental data showed that none were significant. V(III) and V(IV), expected under anoxic conditions, were both found to cause elevated system response. V(III) produced the greatest interference, though is least likely to be present. V(IV) produces a minor interference at low levels. However, the few documented measurements of V(IV) in oxic seawater suggest that its concentration in oxic seawater is too low to result in significant interference.

Theoretical reasons suggest that hydrogen peroxide could cause interferences, yet when interference experiments were conducted in the manner that most represented field conditions, no interference by hydrogen peroxide was observed.

Studies have found that the presence of high concentrations of organic matter in samples results in decreased analytical sensitivity. Laboratory experiments using model ligands suggest that ligands most likely to be associated with iron (i.e. siderophores) do not cause noticeable interferences. However, complete signal loss was observed with EDTA, a synthetic ligand, indicating that ligands with slow-exchange kinetics have the potential to affect system response.

Light interference was noted when luminol reagent was exposed to laboratory light. As a result, reagent containers and tubing was light-shielded. Exposure of samples to diffuse lab lighting showed no observable affect on analytical response.

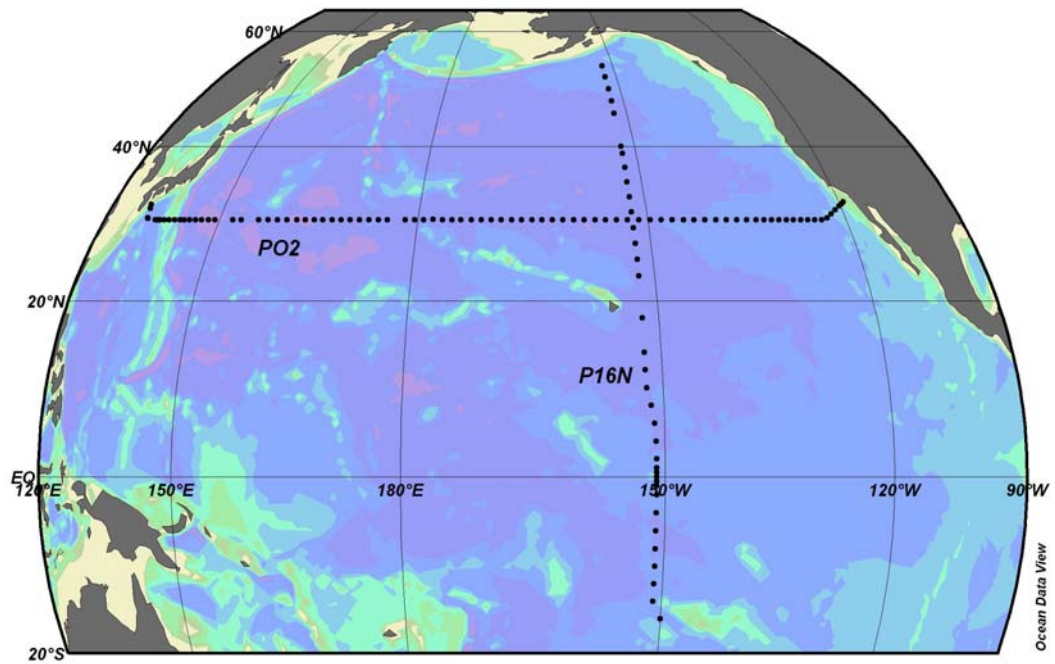


Fig. 2: This map shows the trace metal sampling stations for cruises PO2 and P16N. Cruise PO2 was a latitudinal transect along 30°N from Yokohama, Japan to San Diego, California, during June-August, 2004. Cruise P16N was a meridional transect along 152°W, from Tahiti to Alaska, during February-March, 2006.

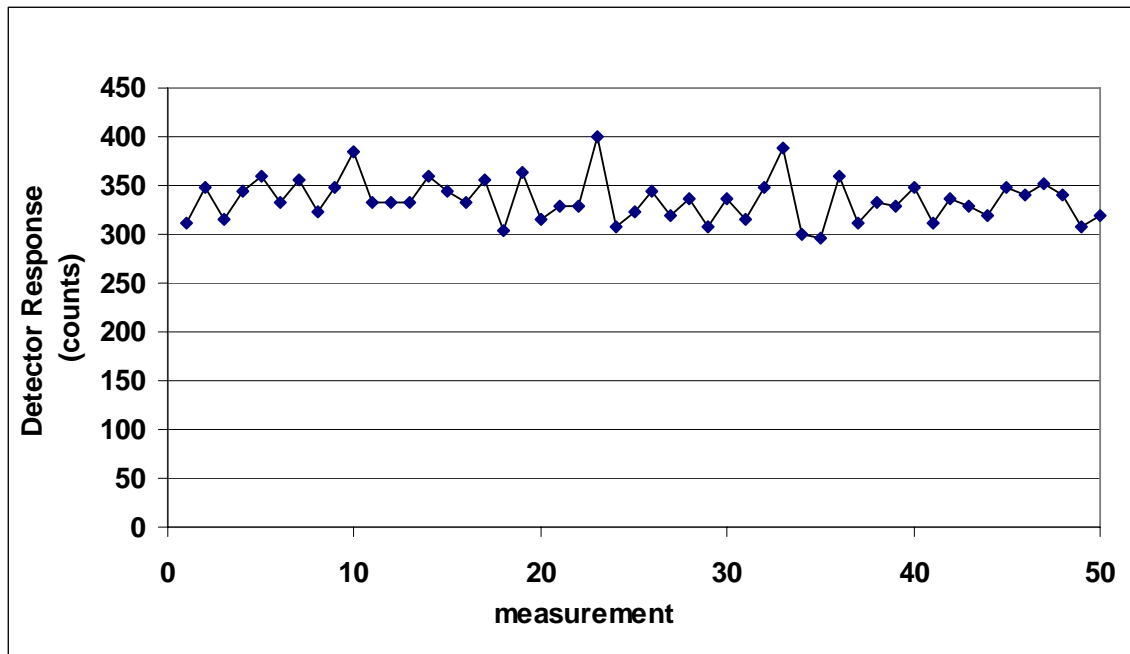


Fig. 3: An example of raw data output from the HC135-11 detector is shown here. System response is shown on the y-axis in counts. Each data point represents the number of light pulses counted using a counting period of 100 ms. The categorical x-axis is used to separate the 50 consecutive measurements. Shown here are 50 consecutive measurements made over a period of 5 seconds.

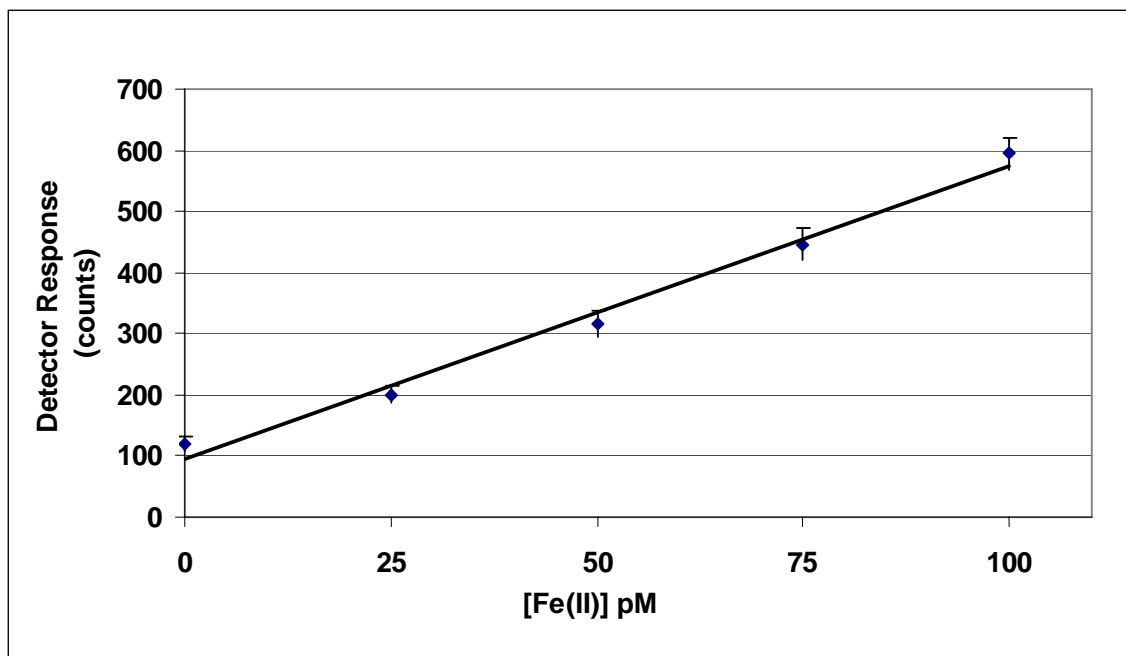


Fig. 4: This figure illustrates a typical calibration curve from cruise P16N produced by spiking 5 acidified seawater samples (pH 6.0) with different amounts of Fe(II). The y-axis shows the average number of counts for 50 consecutive counting periods (counting period is 100 ms) with error bars representing ± 1 standard deviation. The spike concentration is on the x-axis in pM Fe(II) .

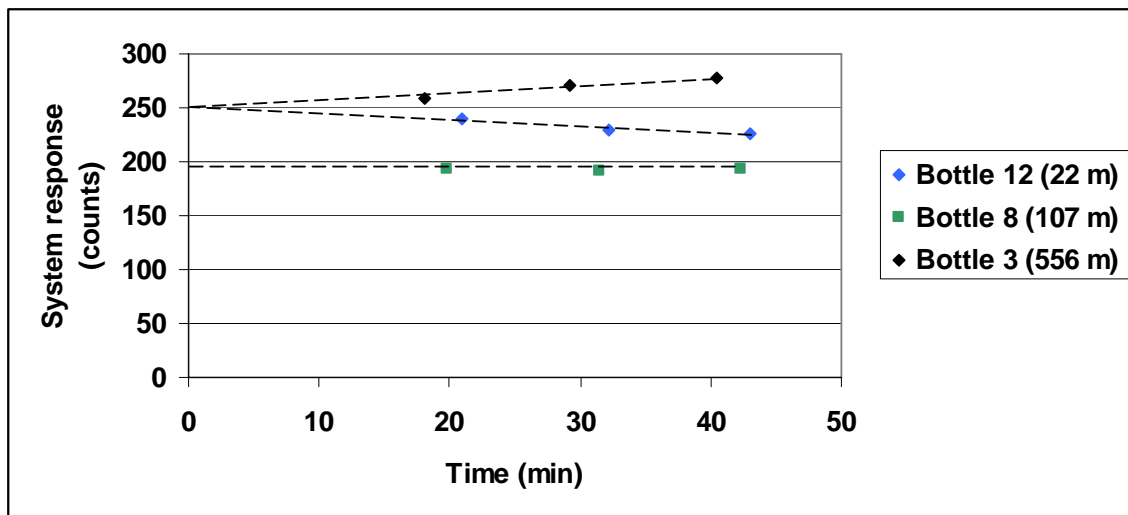


Fig. 5: Sequential measurements of samples from Station P16N/14 plotted against the time elapsed between sample acidification and measurement. The dashed line represents a linear fit of the sequential measurements back to the time of acidification ($t=0$). The sample from bottle 12 showed a decreasing trend with time, the sample from bottle 3 showed an increasing trend with time, and the sample from bottle 8 showed no trend over time. For this study, the estimated response at $t=0$ was used to determine the Fe(II) concentration, determined by linear extrapolation as shown in the figure.

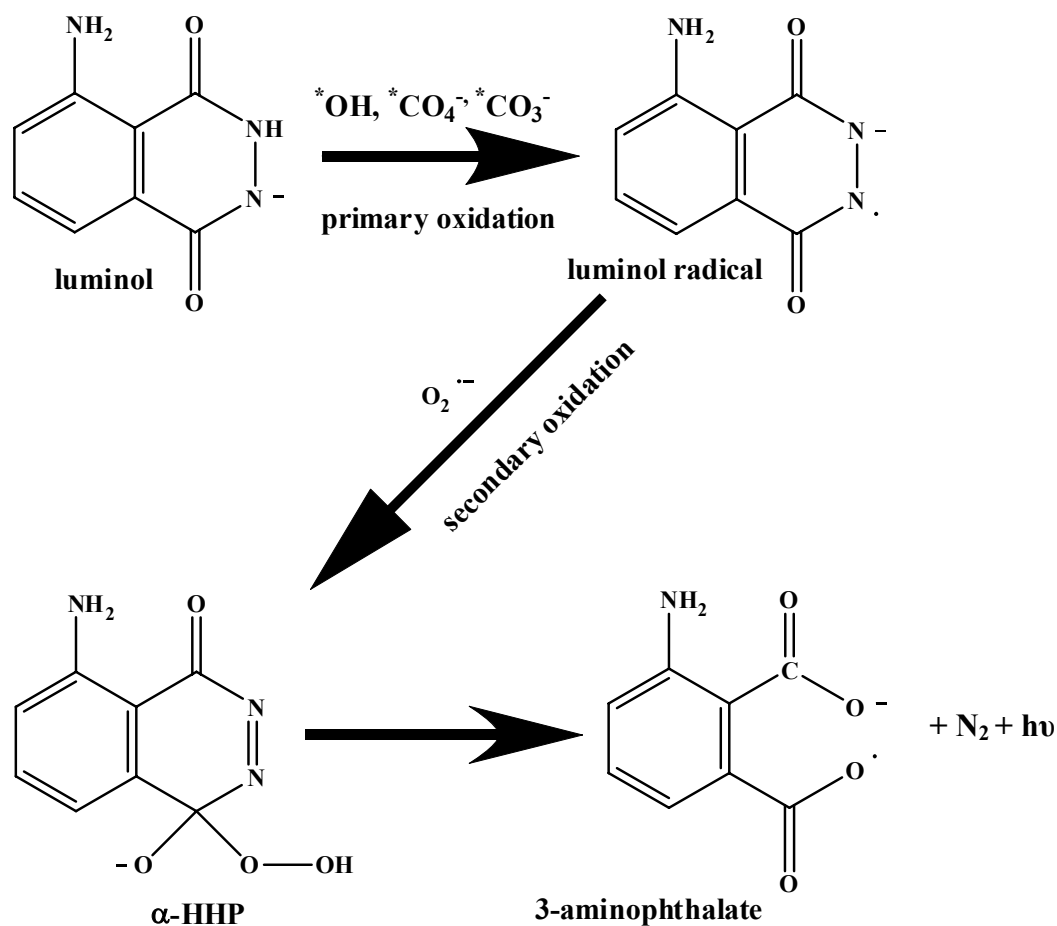


Fig. 6: This is a generalized mechanism for the oxidation of luminol at high pH (after Rose and Waite 2001; Xiao et al. 2002). The primary oxidant has been proposed to be hydroxyl radical, peroxy carbonate radical, or carbonate radical. The secondary oxidant is superoxide. Once formed, HHP spontaneously decomposes to 3-aminophthalate, producing nitrogen gas and emitting light.

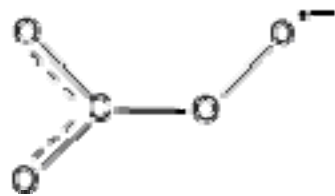


Fig. 7: Structure of the peroxy carbonate radical, after Xiao et al.(2005).

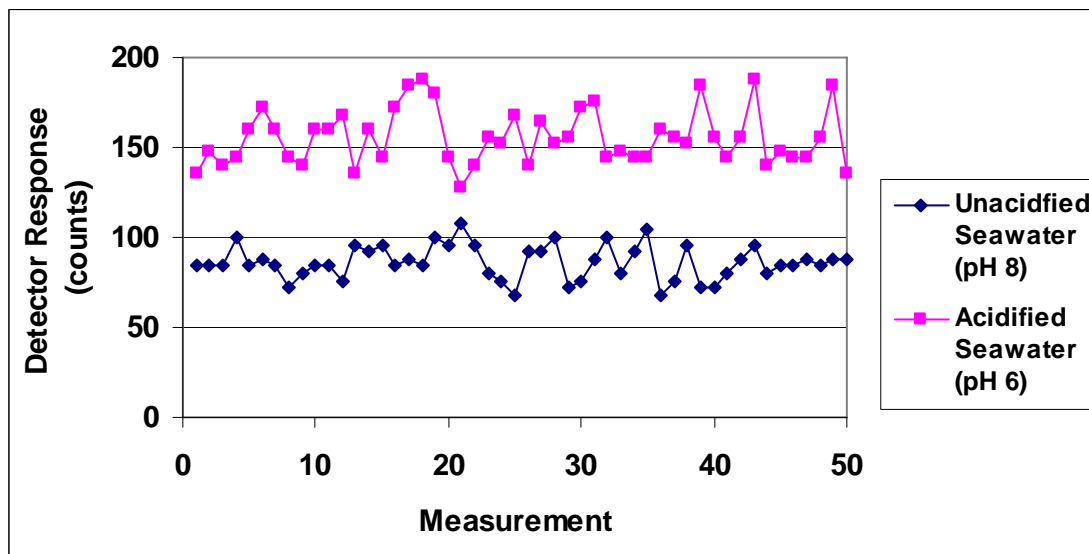


Fig. 8: This figure illustrates the increase in signal response that occurs when seawater samples are acidified to pH 6.0 by addition of q-HCl. System response is shown on the y-axis in counts (counting interval is 100 ms). The categorical x-axis is used to separate the 50 consecutive measurements. The blue series represents system response for unacidified seawater (mean response is 86 ± 10 counts). The pink series represents the response for acidified seawater at pH 6 (mean response is 155 ± 15 counts). For this sample, the increase in response due to acidification is equivalent to 10.5 pM Fe(II), obtained by dividing the response difference by a calibration slope of 6.6 counts/pM.

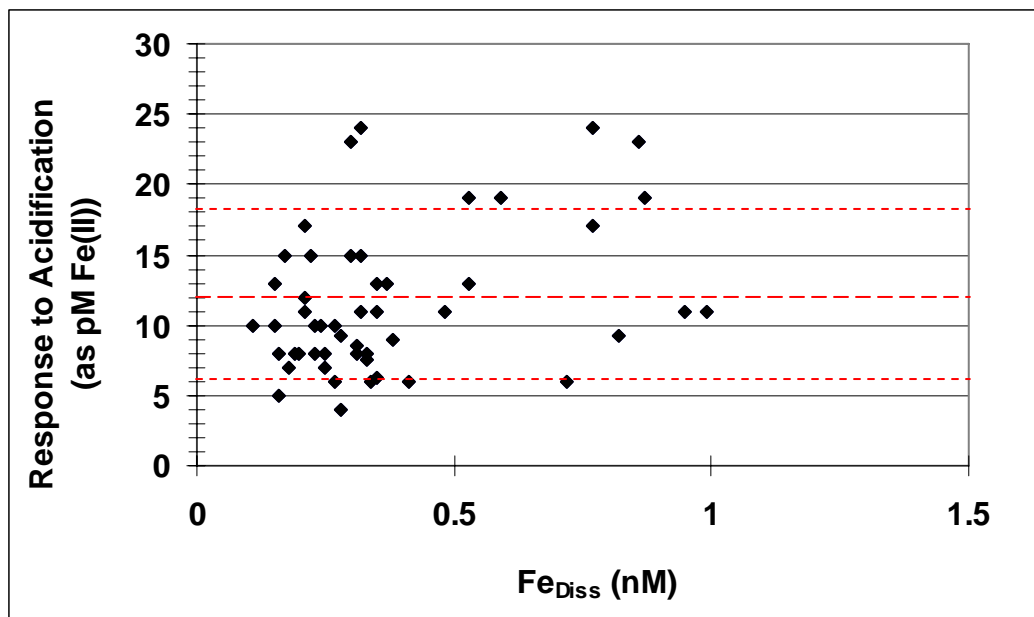


Fig. 9: This figure shows the increase in system response due to acidification on the y-axis, plotted against dissolved iron (nM) on the x-axis, measured for 56 samples collected on cruise PO2. The increase in system response is expressed as equivalent Fe(II) and is calculated by dividing the difference between the acidified response and the unacidified response by the analytical sensitivity (calibration slope) determined at the time of measurement. The mean increase in response was 12 ± 6 pM (indicated by red dashed lines).

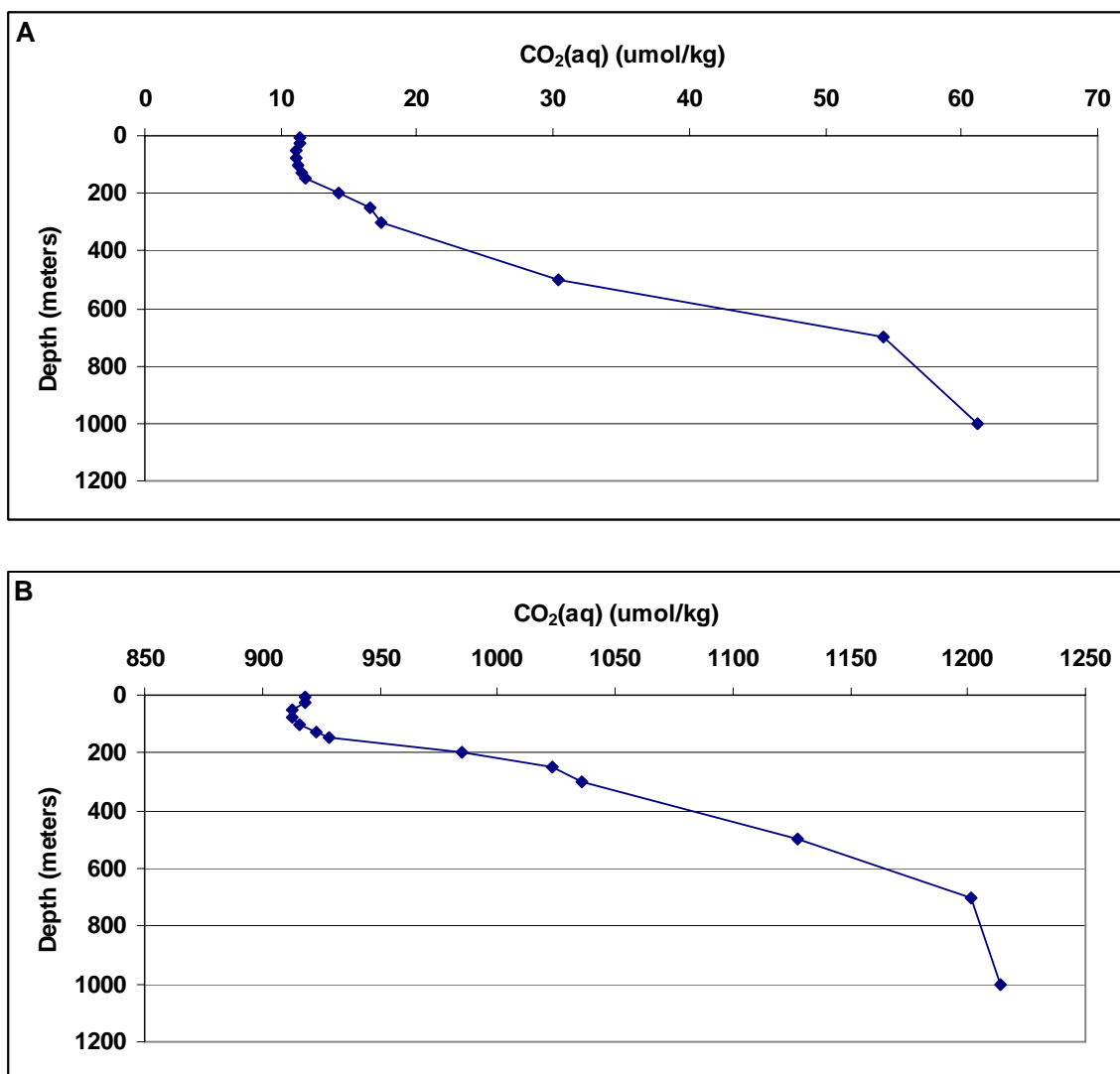


Fig. 10: The vertical profiles for of CO₂(aq) at station P16N/49 (27°N, 152°W) calculated for on-deck conditions (1 atm pressure assuming no temperature change prior to acidification **(A)** and after acidification to pH 6.0 **(B)**. CO₂(aq) was calculated using the CO2SYS program as described in the text and in Appendix C, data shown in Table 3.

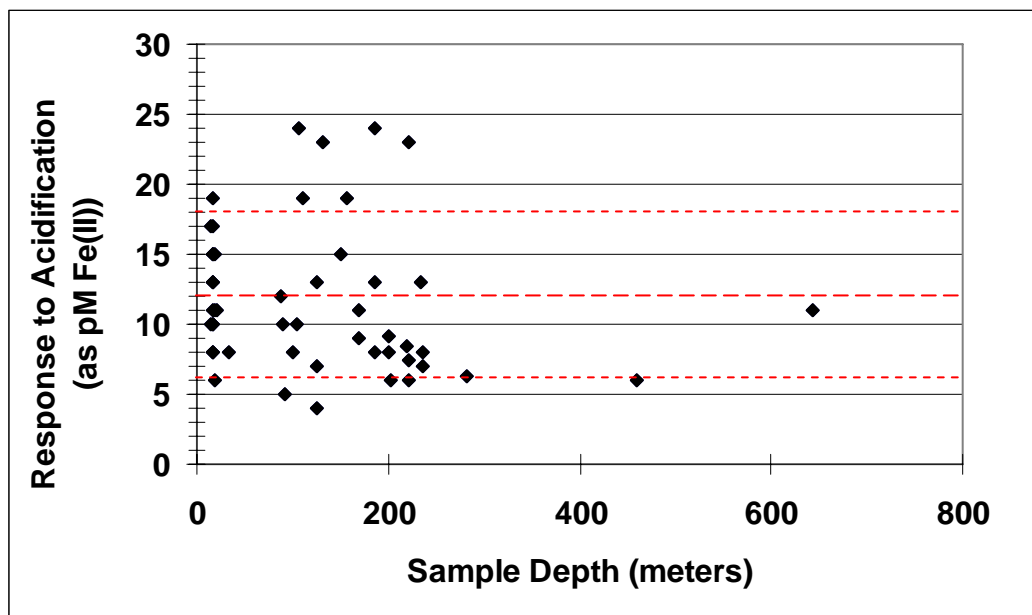


Fig. 11: This figure shows the increase in system response due to acidification on the y-axis, plotted against sample collection depth (meters) on the x-axis, measured for 56 samples collected on cruise PO2. The increase in system response is expressed as equivalent Fe(II) and is calculated by dividing the difference between the acidified response and the unacidified response by the analytical sensitivity (calibration slope) determined at the time of measurement. The mean increase in response was 12 ± 6 pM (indicated by red dashed lines).

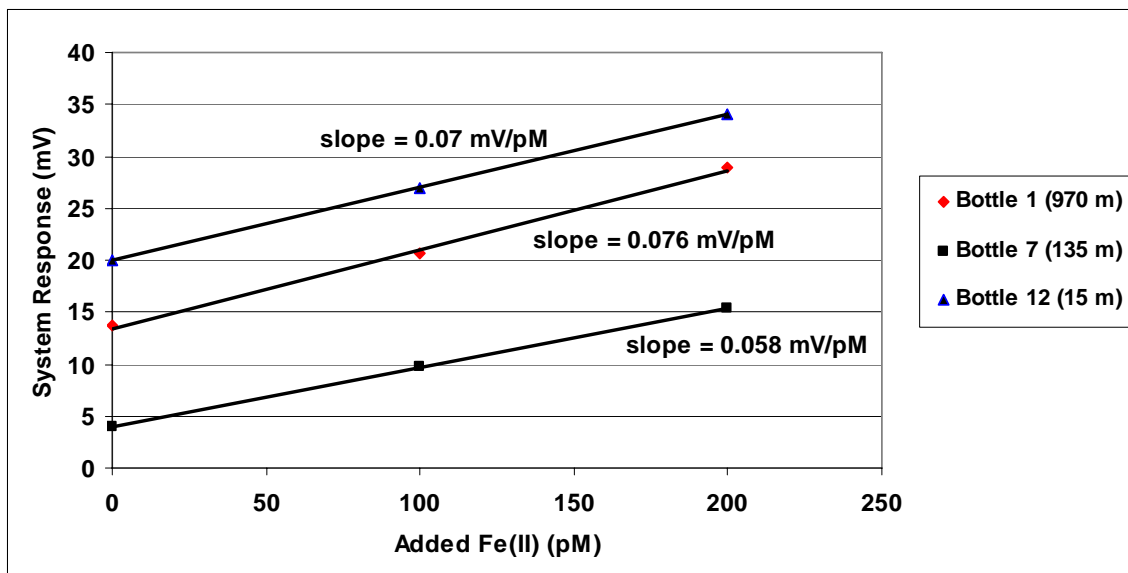


Fig. 12: System response (mV) is plotted on the y-axis versus added Fe(II) (pM) on the x-axis for acidified seawater samples collected from different depths at Station PO2/018 (30°N, 137°W). Fe(II) was added in 100 pM increments immediately after the initial measurements.

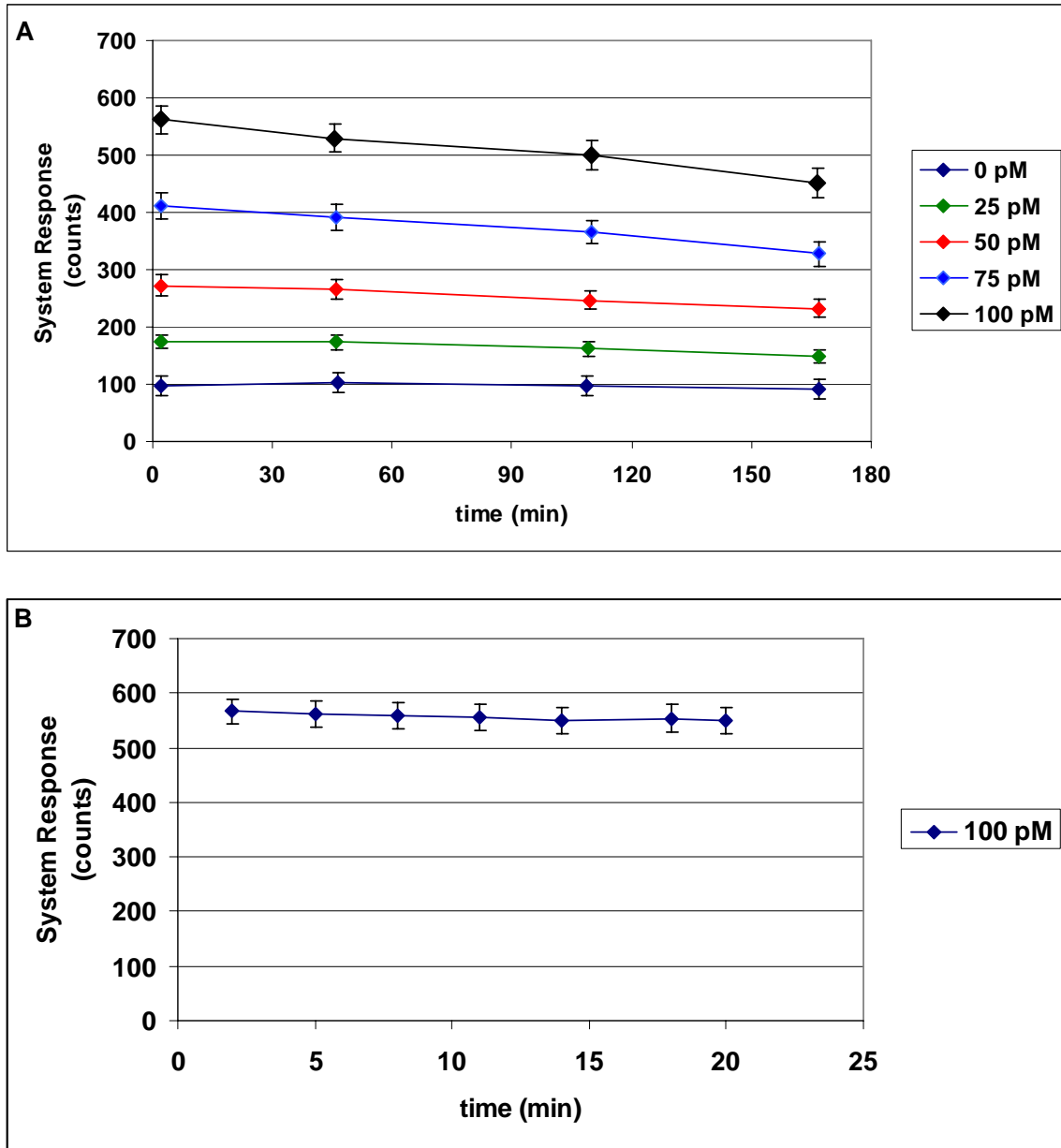


Fig 13: System response for spiked seawater samples is shown on the y-axis plotted against the interval of time between spike preparation and measurement for two different analytical runs. In the first run (A), the long-term stability of calibration standards was evaluated. In the second run (B), the stability of a standard was measured at 3 min intervals for a period of 20 min.

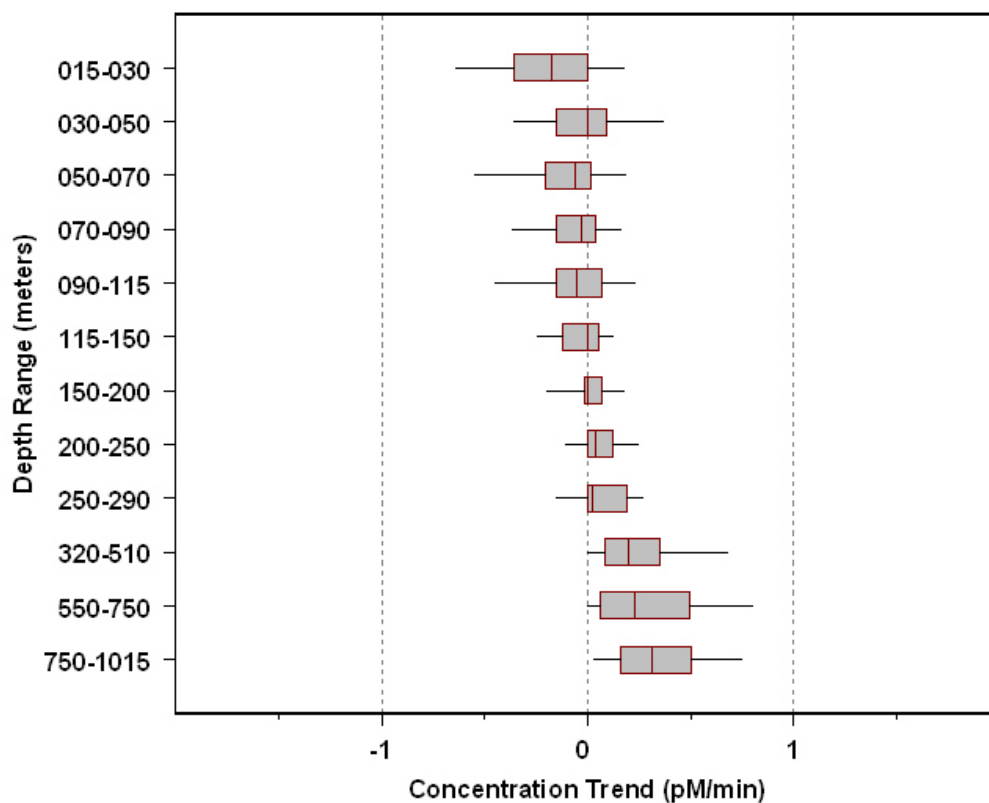


Fig. 14: Box and whisker plots are shown of sample stability grouped by depth range. The sample stability (on the x-axis) is expressed as the linear slope of the time-related trend in Fe(II) concentration after sample acidification. Samples are from stations PO2/111-187 and P16N, n=66. The vertical sides of each box represent the 25th and 75 percentiles and the vertical segment represents the median value (50th percentile). Whiskers on the left terminate at the 10th percentile and whiskers on the right terminate at the 90th percentile.

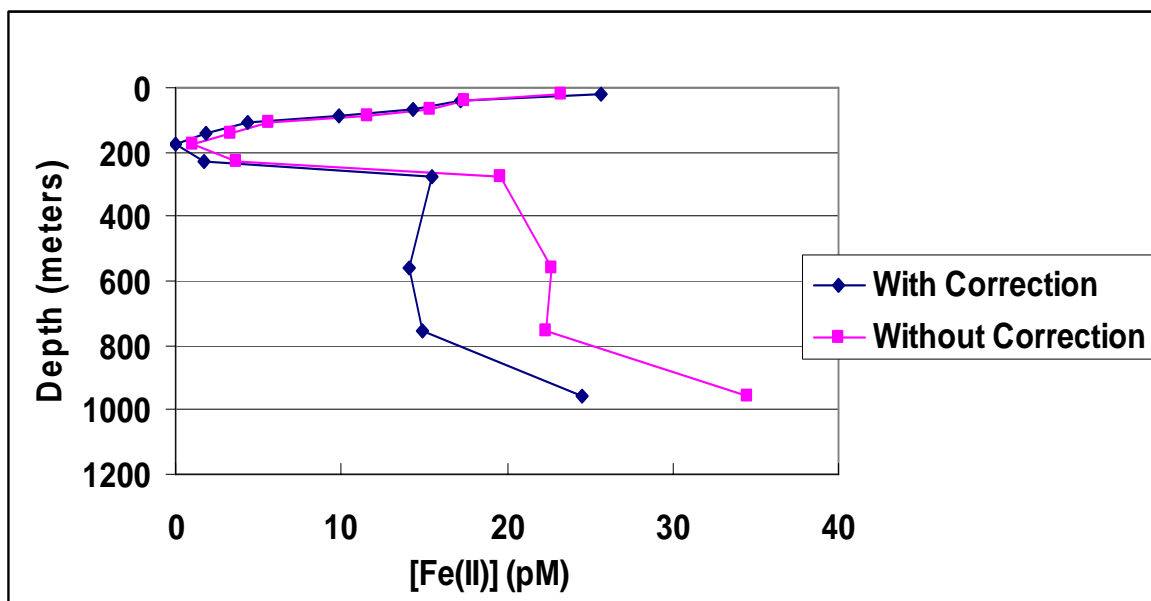


Fig. 15: Vertical profile of Fe(II) concentration for P16N/10 (8°S, 152°W) showing concentrations calculated with (blue diamonds) and without (pink squares) correction for system response changes over time. This station was chosen because it is typical of both the median concentration profile and the median sample stability behavior.

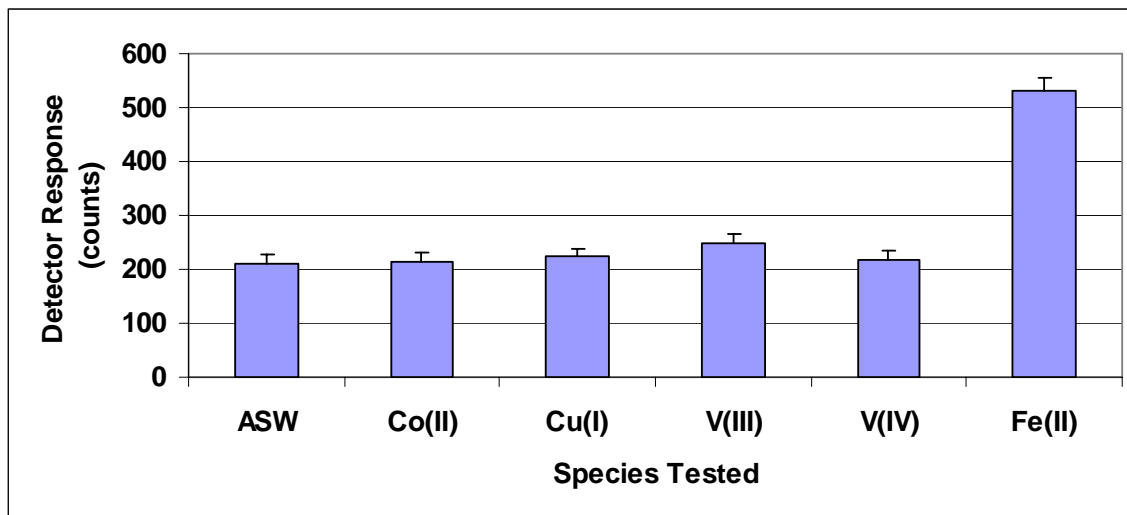


Fig. 16: Shown here are the responses of potential trace metal interferences to analytical system following addition of 50 pM to acidified seawater (pH 6). ASW (far left) is the acidified seawater control (no metal added). The V(IV) response is estimated based on the results of Hopkinson and Barbeau (2007). The counting period is 100 ms.

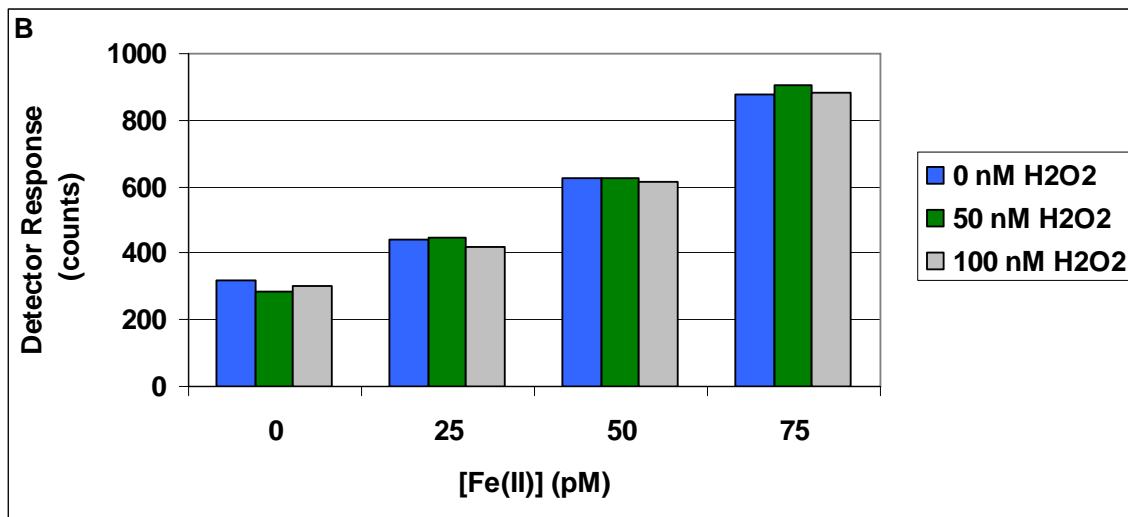
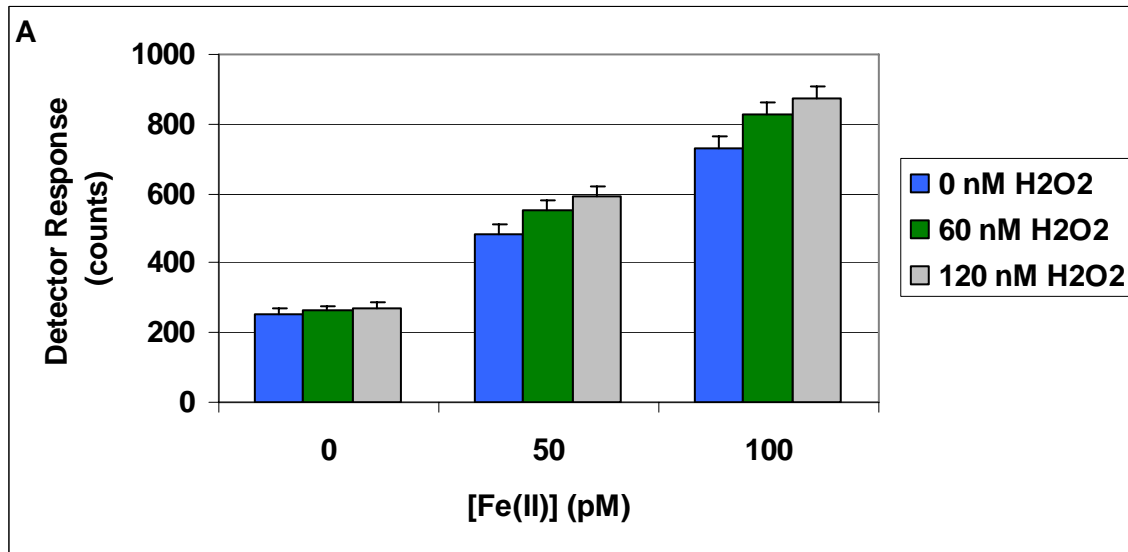


Fig. 17: These graphs show the system response to H₂O₂ added after sample acidification (**A**) and prior to acidification (**B**). The system response in counts is shown on the y-axis (counting period = 100 ms) and the Fe(II) concentration is shown categorically on the x-axis. Blue, green, and gray bars correspond to 0, 50, and 100 nM of added H₂O₂.

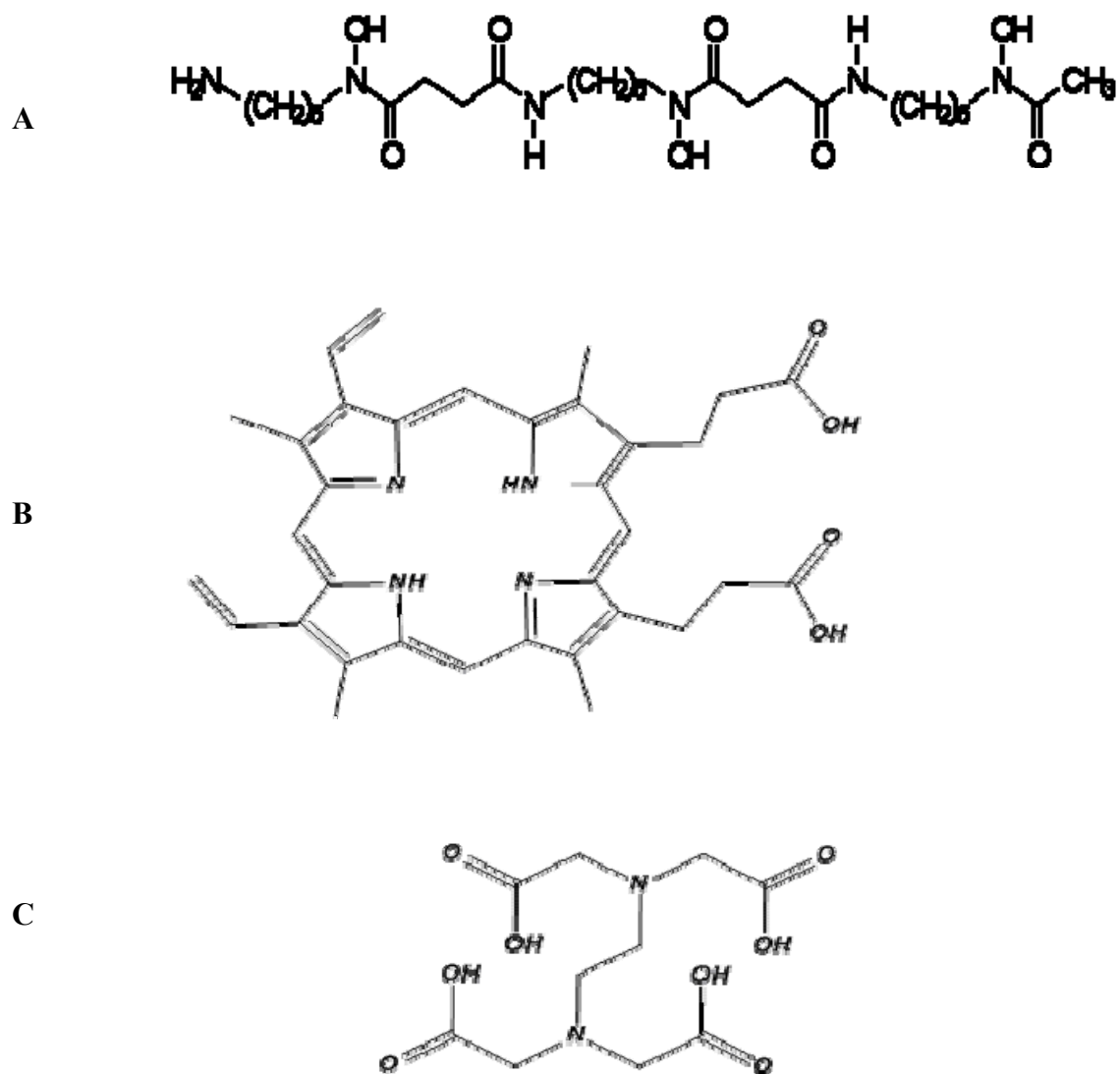


Fig. 18: Structures of ligands used in interference experiments are shown in (A) desferrioxamine, a fungal siderophore, (B) protoporphyrin IX, a heme analog, and (C) EDTA, a synthetic metal chelator.

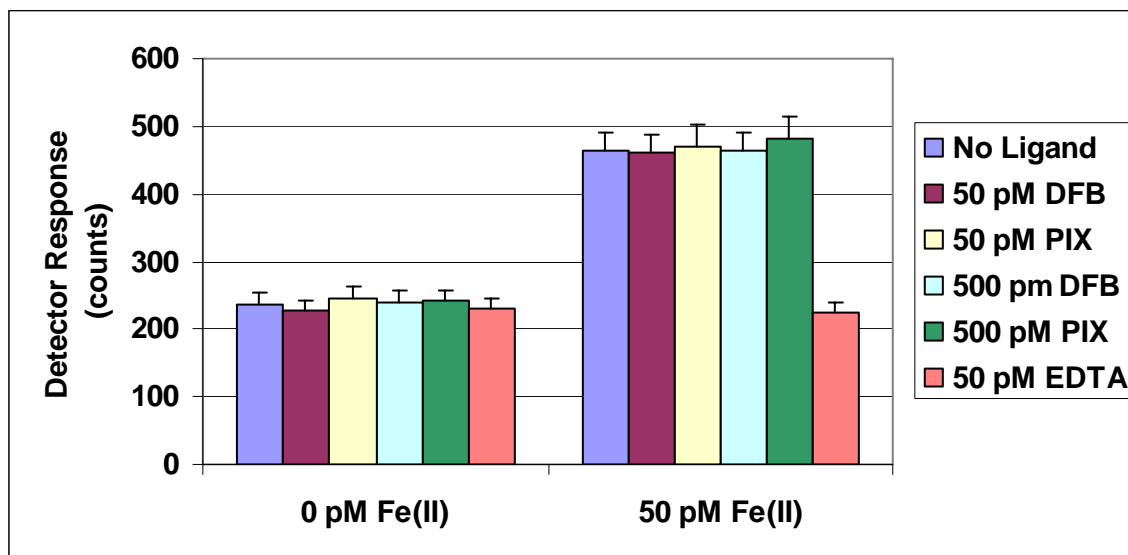


Fig. 19: The system response in counts on the y-axis is shown for organic ligands with no added Fe(II) (left) and for additions of Fe(II)-ligand complexes, pre-equilibrated in EPW at 1:1 and 1:10 iron-ligand ratios. Ligands tested were desferrioxamine B (DFB), protoporphyrin IX (PIX), and EDTA. Counting interval is 100 ms.

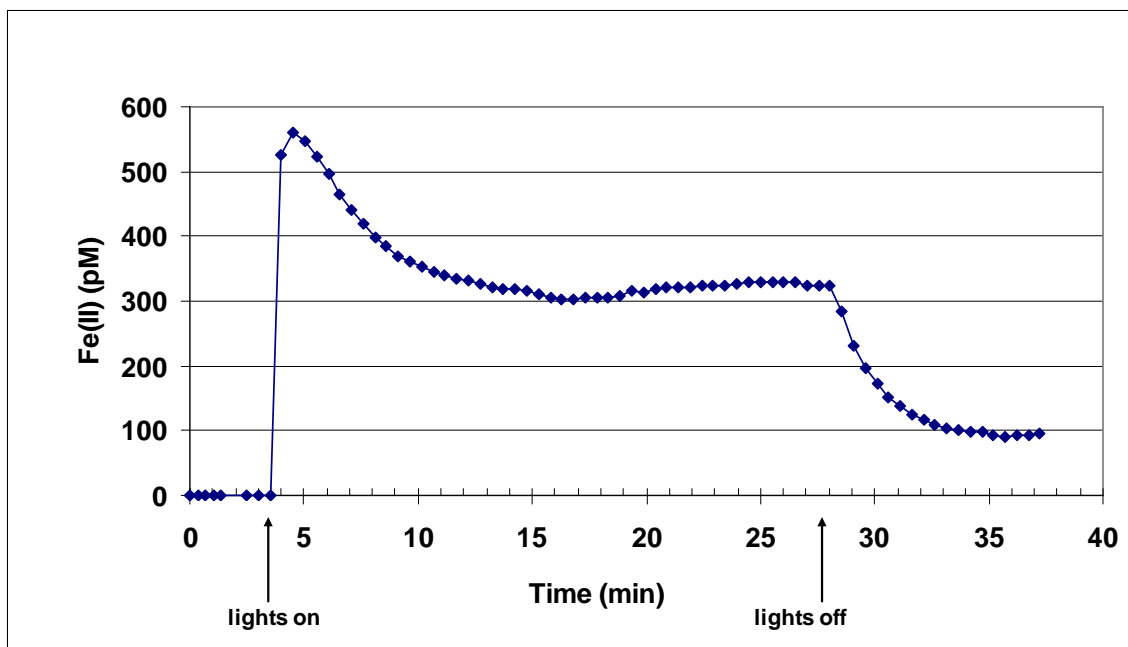


Fig. 20: System response as pM Fe(II) (y-axis) plotted against time during an irradiation experiment using filtered seawater from Station P16N/59 collected at a depth of 20 m. Sample was irradiated in 250 mL Teflon container using (4) 15 W mercury lamps (nominal wavelength of 254 nm). The initial system response was equivalent to 555 pM Fe(II), more than double the concentration of dissolved iron in the sample (270 pM). The excess system response is attributed to the generation of free radicals by UV oxidation of DOM present in the sample, and it is further hypothesized that the response attenuation observed during the 5-15 min interval represents consumption of this DOM. The plateau observed at 15-20 min approximates the concentration of dissolved iron, suggesting complete reduction of Fe(III).

Table 2: Listed below are sample collection target depths (meters) for cruises PO2 and P16N (actual sample depths vary).

Bottle	PO2			P16N	
	Scheme 1	Scheme 2	Scheme 3	Scheme 1	Scheme 2
12	<20	<20	<20	<20	<20
11	40	35	40	35	40
10	60	50	65	60	65
9	80	70	85	75	85
8	100	90	105	100	105
7	125	120	135	125	135
6	150	170	185	150	175
5	200	220	235	200	225
4	250	270	285	250	275
3	500	440	470	500	550
2	700	640	670	700	750
1	1000	900	970	1000	950

Table 3: Output from CO2SYS program for Station P16N/49 is shown below. Input variables were measured onboard ship and include P (pressure in dbar), T (temperature in degrees C), S (salinity in practical salinity units), PO₄ (total phosphate in μmol/kg), SIO₄ (total silicate in μmol/kg), TALK (total alkalinity in μmol/kg), and TCO₂ (dissolved inorganic carbon in μmol/kg). Output variables are derived from equilibrium calculations of the CO₂ system. Values at input conditions were calculated for *in situ* conditions. Values at output conditions were calculated for on-deck conditions (i.e one atm pressure assuming no temperature change). Values at pH 6 were calculated by reducing the magnitude of the total alkalinity by 1225 μmol/kg (equivalent to the addition of 21 μL of 6M q-HCl to 100 mL of seawater) and re-calculating the values for one atm. pressure assuming no temperature change and no loss of CO₂ due to gas exchange with the atmosphere.

Input Conditions							Values at Input Conditions				Values at Output Conditions				Values at pH 6			
P	T	S	PO ₄	SIO ₄	TALK	TCO ₂	pH	CO ₂	HCO ₃ ⁻	CO ₃ ⁻⁻	pH	CO ₂	HCO ₃ ⁻	CO ₃ ⁻⁻	pH	CO ₂	HCO ₃ ⁻	CO ₃ ⁻⁻
5.8	20.93	35.35	0.02	0.00	2324.60	2016.80	8.08	11.39	1782.76	222.65	8.08	11.39	1782.75	222.66	5.96	918.07	1097.68	1.05
25.1	20.93	35.35	0.02	0.00	2324.80	2017.00	8.08	11.39	1783.00	222.61	8.08	11.39	1782.94	222.67	5.96	918.07	1097.88	1.05
49.3	20.93	35.35	0.02	0.00	2330.40	2017.20	8.08	11.16	1779.75	226.29	8.09	11.16	1779.62	226.41	5.97	912.71	1103.43	1.06
74.2	20.87	35.35	0.02	0.10	2330.60	2017.50	8.08	11.15	1780.21	226.14	8.09	11.16	1780.01	226.32	5.97	912.81	1103.63	1.06
100.0	20.66	35.34	0.02	0.10	2330.20	2020.40	8.08	11.28	1785.33	223.79	8.09	11.29	1785.07	224.04	5.97	916.10	1103.25	1.06
125.7	20.60	35.34	0.02	0.00	2323.30	2020.10	8.07	11.55	1789.41	219.14	8.08	11.57	1789.09	219.44	5.96	922.65	1096.42	1.03
149.5	20.27	35.27	0.04	0.10	2318.00	2020.80	8.07	11.76	1794.19	214.85	8.07	11.78	1793.81	215.21	5.96	928.62	1091.17	1.01
199.8	16.49	34.64	0.30	2.64	2283.90	2043.50	8.04	14.21	1854.07	175.23	8.04	14.25	1853.58	175.67	5.96	985.23	1057.44	0.83
249.6	13.84	34.38	0.57	5.76	2263.90	2061.40	8.01	16.52	1895.74	149.15	8.01	16.58	1895.15	149.67	5.96	1023.10	1037.58	0.73
300.5	11.94	34.25	0.78	9.67	2266.90	2077.20	8.01	17.34	1919.84	140.03	8.02	17.42	1919.13	140.66	5.98	1035.98	1040.53	0.70
499.0	7.78	34.05	1.73	36.15	2274.20	2175.80	7.83	30.21	2061.04	84.55	7.85	30.44	2059.99	85.37	5.99	1127.53	1047.68	0.60
700.0	4.75	34.10	2.76	83.63	2321.20	2295.90	7.63	53.81	2191.93	50.16	7.66	54.24	2190.60	51.06	6.01	1201.08	1094.25	0.58
999.3	3.77	34.41	3.04	115.55	2366.40	2353.80	7.58	60.50	2247.64	45.66	7.63	61.12	2245.77	46.90	6.03	1214.03	1139.17	0.61

3. RESULTS AND DISCUSSION

3.1 Spatial Distribution of Fe(II)

3.1.1 Cruise PO2

The measured Fe(II) concentrations for PO2 samples are given in Appendix G (Table 9). Oceanographic sections of measured Fe(II) concentrations for the PO2 transect (Japan to California) are shown in Fig. 21. To adequately convey the surface detail, sections were prepared at two vertical scales, one for the upper 120 meters and one for the full 1000 meters. Sections were also made of $[\text{Fe(II)}]/[\text{Fe}_{\text{DISS}}]$, the ratio of reduced iron to total dissolved iron (Fig. 22). The ratio was determined for each sample using the concentration of Fe_{DISS} determined by shipboard spectrophotometry (data provided by C.I. Measures, University of Hawaii, pers. comm.). Bivariate plots of $[\text{Fe(II)}]$ versus $[\text{Fe}_{\text{DISS}}]$ are shown in Fig. 23. Oceanographic sections of other key variables (temperature, salinity, pH, oxygen, alkalinity, DIC, and nutrients) are presented in Appendix H.

Fe(II) concentrations for the upper PO2 section (Yokohama, Japan, to San Diego, California) are shown in Fig. 21A. Two spatially distinct concentration regimes were observed. West of 145°E latitude, concentrations of Fe(II) were relatively high (indicated by warm colors) with a median concentration of 51 pM for the upper 120 meters. East of this area, concentrations were much lower (indicated by green and dark blue colors), with a median concentration 16 pM for the upper 120 m. A concentration gradient with depth was observed throughout the section, with highest concentrations at or near the surface. East of 145°E , the concentrations decreased to undetectable levels (approximated by purple shading) usually by a depth of 60-120 meters. West of 145°E , the gradient was less steep. Concentrations declined with depth yet detectable concentrations were observed more or less throughout the water column.

The complete section (0-1000 m) is shown in Fig. 21B. Here, the area of high concentration west of 145°E is observed to occur throughout the water column, with very high values (≤ 360 pM) occurring in the deepest samples. East of this area, levels are diminished. The purple shaded area indicates samples for which Fe(II) concentrations are at or below the detection limit. Below, at depths of 800-1000 meters, detectable Fe(II) was again observed, indicated by the deep blue and cyan/green colors.

The fraction of Fe_{DISS} present as Fe(II), i.e. $[\text{Fe(II)}]/[\text{Fe}_{\text{DISS}}]$, is shown for cruise PO2 in Fig 22. As a percentage, Fe(II) varies from 0 – 54% over the entire section, with highest

percentages observed in the upper 100 meters (Fig. 22A). Below 120 meters, $[\text{Fe(II)}]/[\text{Fe}_{\text{DISS}}]$ ratios were negligible, except in the vicinity of 145°E , where percentages of 8-12% were present to a depth of 1000 meters (Fig. 22B). $[\text{Fe(II)}]$ is shown plotted against Fe_{DISS} in Fig. 23.

3.1.2 Cruise P16N

Results for P16N are given in Appendix G (Table 10). Sections of Fe(II) concentrations for P16N (Tahiti to Alaska) are shown in Fig. 24. Sections showing $[\text{Fe(II)}]/[\text{Fe}_{\text{DISS}}]$ are plotted in Fig. 25. Bivariate plots of $[\text{Fe(II)}]$ versus $[\text{Fe}_{\text{DISS}}]$ are shown in Fig. 26. Oceanographic sections of other key variables (temperature, salinity, pH, oxygen, alkalinity, DIC, and nutrients) are shown in Appendix I.

Observed concentrations for P16N (Fig. 24) were very similar to the eastern PO2 section, with Fe(II) concentrations as high as 70 pM in the uppermost samples, diminishing with depth to undetectable levels by depths of 80-120 m (Fig. 24A). Highest surface concentrations were observed in the vicinities of 5°S , 20°N , and 55°N , near the Alaskan coast. Fig. 24B shows Fe(II) concentration for the complete P16N section. The deep Fe(II) presence at 800-1000 meters was again observed (20-50 pM), with mid-depth concentrations just above the detection limit (dark blue), or undetectable (purple). Two deep samples (stations 4/2 and 6/2) that were collected at the beginning of the cruise showed very high concentrations in both Fe(II) and Fe_{DISS} (lower left area of Fig. 24B).

$[\text{Fe(II)}]/[\text{Fe}_{\text{DISS}}]$ for P16N samples is shown in Fig. 25 and plots of Fe(II) versus Fe_{DISS} are shown in Fig. 26. High percentages (20-50%) were observed in surface samples in the vicinity of the equator ($10^{\circ}\text{S} - 12^{\circ}\text{N}$). These samples were characterized by extremely low Fe_{DISS} concentrations (0.02 – 0.12 nM). At these concentrations, any detected Fe(II) would constitute a high percentage of the total dissolved iron. One sample (station 14, 4°S , 20 m) had $[\text{Fe(II)}] > [\text{Fe}_{\text{DISS}}]$, and was therefore omitted from Figs 25 and 26. The concentration of Fe_{DISS} at this station was unusually low with respect to adjacent stations. The Fe(II) concentration for this sample was more consistent with values at adjacent stations, and the anomalous percentage was likely due to low Fe_{DISS} recovery. For all other samples, including those collected on PO2, $[\text{Fe(II)}]$ was less than Fe_{DISS} .

3.1.3 Crossover Stations

The PO2 and P16N transects intersected at 30°N , 152°W . Data consistency was evaluated by examining measurements from crossover stations, defined previously as stations located within 100 km of the crossover point (Lamb et al., 2002). Stations meeting this criterion

included PO2/129, PO2/131, P16N/51, and P16N/53. Fe(II) profiles for these crossover stations are shown in Fig. 27. The shapes of the profiles are similar, although the magnitudes of the concentrations show a good deal of variance. Near the surface, concentrations were higher for the PO2 stations (31-62 pM) than for the P16N stations (25-30 pM). Samples taken near the bottom of the profile contained detectable Fe(II) at all stations. However, the concentrations measured for the P16N stations were higher (47-56 pM) than the PO2 stations (22-29 pM).

The use of crossover stations to validate analytical measurements is especially well-suited for conservative constituents that are spatially and temporally invariant. As noted by other authors (Lamb et al., 2002), crossover analysis is less well suited to validating measurements of reactive species with short residence times. This caveat would certainly apply to trace metal species such as Fe(II), whose transient concentrations depend upon other transient determinants (e.g. sunlight, dust supply, CDOM, plankton abundance, oxidation variables, etc.). Given the complexity of processes controlling trace metal abundance and redox speciation and the difficulty of accurately measuring picomolar concentrations, the similarity between the profiles is more striking than are differences in individual measurements.

3.2 Vertical Profiles and Sources of Fe(II)

Examination of vertical profiles of [Fe(II)] and [Fe(II)]/[Fe_{DISS}] can help to assess the extent to which the dataset supports or fails to support hypothetical Fe(II) production mechanisms. Although individual profiles show considerable spatial variability, a statistical or graphical approach can be used to reveal both tendency and dispersion for the entire dataset. To this end, box plots of Fe(II) concentrations were prepared, shown grouped by depth in Fig. 28 for cruises PO2 and P6N. Due to the high concentrations found in the western Pacific, for comparison purposes the PO2 transect was divided into a western segment (Fig. 28A, stations 8-30) and an eastern segment (Fig. 28B, stations 32-181). The P16N section is shown in Fig. 28C (stations 4-79).

These generalized profiles exhibit patterns that are remarkably similar, each characterized by three concentration regimes. The first regime is within the upper 120 meters and is characterized by a surface maximum which decreases with depth. The second regime is marked by low levels of Fe(II), often below the detection limit, and is located at depths between 150 – 600 meters. The third regime consists of the bottommost samples, collected at depths of 600 – 1000 meters, which often contained measurable Fe(II), though less consistently than the surface samples. Although the shapes are quite similar, it is important to note that the Fe(II) concentrations for the western PO2 segment shown in Fig. 28A are plotted on a different scale to

accommodate the higher levels observed there. However, the plots of the eastern segment of PO2 and the P16N are similar both in shape and magnitude.

Box plots of $[\text{Fe(II)}]/[\text{Fe}_{\text{DISS}}]$ grouped by depth range are shown in Fig. 29. As with the concentration plots, the overall patterns of $[\text{Fe(II)}]/[\text{Fe}_{\text{DISS}}]$ with depth are very similar. Relative to Fe_{DISS} , high concentrations of Fe(II) were present in the surface-most samples, with ratios that decline with depth, primarily as a result of declining Fe(II) concentration. At mid-depths, the fraction present as Fe(II) was very low due to very low levels of Fe(II). In the deepest part of the sections, the fraction present as Fe(II) was generally low due to the much higher concentrations of Fe_{DISS} . In addition to the similarity observed in the shapes of the plots, the plots of $[\text{Fe(II)}]/[\text{Fe}_{\text{DISS}}]$ for the eastern PO2 and P16N transects (Figs. 29B and 29C) are also quite similar in magnitude, each with median percentages of 12% in the uppermost samples. While the western segment of PO2 (Fig. 29A) shows the same general pattern as the other profiles, the percentages are distinctly higher in the upper-most depth range (< 20 m). Greater variance is also observed for discrete depth ranges (indicated by the lengths of the individual boxes).

3.2.1 Fe(II) in Surface Waters

The generalized profiles of Fe(II) concentrations and $[\text{Fe(II)}]/[\text{Fe}_{\text{DISS}}]$ appear to be consistent with a photochemical production process. They are characterized by surface maxima, an association with the upper photic zone (and in particular, the regime of UV-A light penetration), and an attenuation with depth that is also characteristic of light (Toole et al., 2003). Such a profile has been predicted in models of photoreduction of colloidal iron (Wells et al. 1991), and has been observed in studies of sunlight-related Cu(II) reduction (Moffett and Zika, 1986). H_2O_2 , a semi-stable byproduct of oxygen reduction by photochemical reactions with DOM (Cooper et al. 1983), has a similar vertical distribution. In the North Pacific, surface concentrations of H_2O_2 of 100-200 nM were found to decline with depth to low levels by 100 m (Yuan and Shiller, 2005). Identical patterns, though with slightly deeper penetration, have been observed in the Sargasso Sea (Palenik and Morel, 1988). Interestingly, the few open-ocean observations of Fe(II) made to date (discussed previously in more detail) have rarely conformed to this profile:

- At Station 72 off the Peruvian coast, Hong and Kester (1986) reported $[\text{Fe(II)}]$ of 1 nM at a depth of 21 meters ($\text{Fe}_{\text{DISS}} = 4 \text{ nM}$), with no Fe(II) detected in adjacent samples collected at 1,48, 74, and 100 meters (Fig. 30). Below this, at depths of 138-158 m, they reported concentrations of Fe(II) as high as 25 nM, about 50% of the total dissolved iron

As mentioned above, the high Fe_{DISS} concentrations observed in this study (5-165 nM) are not typical of open-ocean conditions (de Barr and de Jong, 2001).

- In the equatorial Pacific, O' Sullivan et al. (1991) obtained 7 vertical profiles of Fe(II) at 4 stations that included a mix of patterns (Fig. 31). Two of these profiles (Station 3 sampled at 1600 h and Station 7 sampled at 1000 h) showed patterns similar to the generalized profiles shown here, while two showed patterns of increasing concentration with depth (Station 3, 0600 h and Station 4, 1400 h). The others showed high Fe(II) at the surface (including one night cast), with either no Fe(II) in the subsurface, or high concentrations in the subsurface. The values for Fe(II) reported in their study are much higher than the Fe(II) concentrations reported herein for the equatorial Pacific at (152°W). As mentioned previously, they pre-concentrated Fe(II) *in situ* by pumping seawater through ferrozine-impregnated cartridges to eliminate Fe(II) oxidation during sample collection. While this could explain the much higher Fe(II) concentrations reported in their study (and the lower concentrations found in this one), they did not measure Fe_{DISS} , making interpretation of their results more difficult. Also, due to their unique sampling apparatus, they were unable to sample at depths deeper than 100 m, so no samples were collected beneath the zone of UV light penetration.
- Boye et al. (2006) reported Fe(II) concentrations in surface waters of the eastern North Atlantic of <100 – 300 pM, constituting 0-50% of the Fe_{DISS} , which they attributed to photochemical production (Fig. 32). However, the patchy vertical distribution they observed for the upper 100 m did not resemble the general profile observed in this study, possibly because the detection limit of the voltammetric method (100 pM) obscured the ambient profile.
- A vertical profile (Fig. 33) collected in the eastern tropical Pacific (15°N, 115°W) approximately 600 nautical miles off the coast of Mexico indicated no presence of Fe(II) in the upper 100 m (Hopkinson and Barbeau, 2007).
- Vertical profiles of Fe(II) were recently described for the western North Pacific (Roy and Wells, 2006, AGU conference abstract). These profiles were characterized by surface maxima (50 pM) that decayed exponentially with depth to undetectable levels by 50 m. Ratios of Fe(II) to Fe_{DISS} were as high as 50% in the surface samples, dropping to low values at depth.

In the study described by Roy and Wells, the shapes of the profiles, together with the lack of a correlation between Fe(II) and chlorophyll, were supportive of a photochemical process.

Their description of their results is consistent with those presented here, both in the shapes of the profiles and the magnitude of the concentrations and percentages. Similarly, no obvious correlation between Fe(II) and chlorophyll was observed in this study. Maximum chlorophyll concentrations typically occurred at depths of 60-100 m (Fig. 34), in contrast to the Fe(II) maximum, which nearly always occurred at depths less than or equal to 20 m. However, the evidence for photoreduction remains mostly circumstantial.

Unfortunately, the sampling design for the CLIVAR/CO₂ cruises, while very well suited for the purpose of describing vertical and horizontal trace metal distributions, was not intended to test specific hypotheses about Fe(II) source mechanisms. For example, on these cruises, the average length of time allotted for trace-metal operations was 60 minutes per station, thus, time-series measurements over diurnal cycles were not possible. However, some insight into the role of photochemical processes in generating Fe(II) might be gained by comparing [Fe(II)]/[Fe_{DISS}] from samples collected during the day versus percentages from samples collected at night.

Fig. 35 shows box plots of [Fe(II)]/[Fe_{DISS}] grouped by depth for samples collected during the day (A) and night (B). The distributions are remarkably similar, with equivalent median surface percentages of ~12%. In both plots, [Fe(II)]/[Fe_{DISS}] decreases with depth, to very low levels by 70-90 meters. Although the observed attenuation with depth is consistent with a surface photochemical production mechanism (Wells et al., 1991; Moffett and Zika, 1988), the similarity between the day and nighttime distributions is difficult to explain. Given the short Fe(II) half-life predicted for well-oxygenated, high pH surface water (0.4 min for T=25°C and 50 nM H₂O₂ – see Appendix B), it is expected that any photochemical Fe(II) presence produced in the upper water column during the day would be rapidly lost after production ceased, i.e. after sunset.

The ratio [Fe(II)]/[Fe_{DISS}] plotted against the sample collection time is shown for the uppermost sample (typically 15-20 m) of each profile measured on PO2 and P16N (Fig. 36). The dataset is biased with respect to the sample collection time (i.e. most samples were collected during the daylight and early evening hours) yet for the data shown, the fraction of Fe_{DISS} present as Fe(II) does not appear to be related to the time of sample collection. The lack of an apparent relationship may result from the mode of sample collection.

As mentioned in the methods sections, samples were collected using GO-FLO bottles that were closed via remote control as the rosette was ascending through the water column. It is assumed that any photochemical production of Fe(II) in the sampled seawater would effectively stop as bottles were shut, and that only non-photochemical production processes (if they exist) would occur in the bottles as the rosette was lifted through the water column, brought on deck,

and the bottles removed to the clean van. Oxidative processes would presumably continue uninterrupted at rates governed by the rate-controlling physical/chemical variables characteristic of the sample depth. Oxidation would not stop until the samples were collected and the pH was adjusted. The amount of Fe(II) lost to oxidation during this time can be estimated.

For the uppermost sample collected at a depth of 20 m, the time interval between sample collection and pH adjustment was typically ~11 min. Based on the half-life calculated above (0.4 min), approximately 28 half-lives would elapse before samples collected at this depth could be stabilized. Assuming even that all the Fe_{DISS} present at this depth was Fe(II), at typical Fe_{DISS} surface concentrations of 0.1-0.2 nM, the extremely rapid rate of oxidation would ensure the complete removal of all Fe(II) from the GO-FLO container well before analyses could be begun. These considerations suggest either that the source of measured Fe(II) is not photochemical, or that experimentally-determined rates of oxidation do not realistically approximate *in situ* oxidation behavior.

The oxidation rates used in this study (discussed further in [Appendix B](#)) were calculated based on rate data and rate dependencies obtained from laboratory studies involving nanomolar additions of inorganic Fe(II) to aged seawater (Millero et al., 1987; Millero and Sotolongo, 1989; King, 1998; King and Farlow, 2000; Gonzalez-Davila et al., 2005; Santana-Casiano et al., 2005). An important limitation of these half-life calculations is that they are based solely upon inorganic models of Fe(II) speciation. These models might not accurately represent Fe(II) speciation in natural waters, where the potential for organic complexation of Fe(II) exists. This subject has been poorly addressed to date, due to the analytical difficulties involved. However, laboratory studies with various model ligands have demonstrated that some organic ligands increase the rate of Fe(II) oxidation, while others, such as phthalates, retard it (Santana-Casiano et al., 2004). In the case of phthalic acid, the functional groups responsible for complexation are carboxyl groups, which are found on a variety of natural organic compounds, including humic acids and siderophores. Evidence for slower-than-predicted Fe(II) oxidation in natural waters has been suggested by several authors, including Roy and Wells (2006), Croot and Laan (2002), Boye et al. (2006) and Barbeau (2006, and references therein). These authors suggest that the disagreement between measured and predicted oxidation rates might be due to the presence of organic ligands that stabilize Fe(II) at low but detectable concentrations.

An additional limitation of experimentally-derived rate constants is that for analytical reasons, decay experiments have been based upon initial Fe(II) concentrations of 20 -200 nM. In these experiments, it has been observed that oxidation rates during the later stages of oxidation were sometimes lower than predicted (i.e. pseudo-first order kinetics could only be assumed for

the initial 1-2 half-lives of decay). This behavior was attributed to increased scavenging of superoxide by other species (including Fe(III)) as Fe(II) concentrations declined (Santana-Casiano et al., 2005). The Fe(II) concentrations observed in this study were 20-200 pM, 1000 times lower than the initial [Fe(II)] added in these experiments. Therefore, the increased importance of competing reactions at low Fe(II) levels may limit the applicability of these kinetic studies to ambient oceanic conditions.

A final limitation of the rate calculations made in this study is that the oxidation reactions by O₂ and H₂O₂ have been treated independently (i.e. additive). Recent work has shown that competition occurs between these oxidants even at ambient levels, which increases the half-life (Gonzalez-Davila et al., 2006). For O₂-saturated seawater at 25°C and pH 8 with 100 nM H₂O₂, competition between O₂ and H₂O₂ increases the predicted half-life from 0.4 min (the half-life that is calculated using methods presented here) to ~0.8 min (Gonzalez-Davila et al., 2006). Though significant, consideration of this behavior is not sufficient to overturn the conclusion that the mode of sample collection should prohibit the observation of a photochemical signature in the vertical profile of Fe(II).

3.2.2 Fe(II) in Deep Water

As shown in Fig. 21B and Fig. 24B, Fe(II) was frequently detected in deeper samples (500-1000 m). These samples were characterized by low dissolved oxygen (8-50 uM) (Fig. 45, Fig. 55), low temperatures (<4°C) (Fig. 43, Fig. 53), and low pH (~7.6) (Fig. 46, Fig. 56). These conditions predict slow oxidation rates, with half-lives on the order of 2 days. Although the long half-life alleviates logistical concerns regarding sample collection, source mechanisms are somewhat lacking. Recently, Hopkinson and Barbeau (2007) measured elevated concentrations of Fe(II) in the suboxic zone of the subtropical Pacific. At depths of 150-300 meters, concentrations of 150-175 pM were measured and represented 21-24 % of the Fe_{DISS}. They considered the possibility that this Fe(II) originated in reducing shelf sediments and was transported offshore. The likelihood of this as a source of Fe(II) to their study area was rejected, however, because their calculations showed that advective transport and horizontal diffusion would yield transport times of 2-32 years, far in excess of the predicted Fe(II) half-life. Noting that cellular iron is a mix of Fe(II) and Fe(III), they proposed that Fe(II) could arise from normal metabolic processes. Alternatively, the *in situ* remineralization of sinking biogenic particles could also account for this deep Fe(II) presence. Redox conditions within fecal pellets and marine aggregates are possibly favorable to Fe(II), with little free oxygen or sulfide present (Allredge and Cohen, 1987; Cutter, 2001).

Extremely high deep-water concentrations of Fe(II) were noted in the vicinity of 30°N, 140°E (PO2, Fig. 21) and 17°S, 152°W (P16N, Fig. 24). These high concentrations could conceivably result from very rapid subduction of Fe(II)-bearing surface water. However, two observations argue against this possibility. First, subduction of surface water should disrupt the nutrient-type profile that is typically observed for dissolved iron, leading to anomalously low Fe_{DISS} concentrations at depth. This feature that was not observed in either location (C.I. Measures, pers. comm.). Second, concentrations of CFC-11 (Fig. 37) and CFC-12 (not shown) for these sections reveal no obvious structural anomalies. For P16N, the samples showing these high concentrations were both taken from the same GO-FLO bottle (#2), which also showed unusually high Al_{DISS}. These high concentrations were attributed to inadvertent contamination of this GO-FLO bottle (C.I. Measures, pers. comm.). The extremely high iron concentrations found in the PO2 deep-water samples are discussed further in section 3.2.3.

3.2.3 Fe(II) in the Western Pacific

Most PO2 stations sampled west of 145°E had high Fe(II) concentrations near the surface (Fig. 21A and Fig. 28A). Concentrations ranged from 50-250 pM (10th and 90th percentiles, respectively) and accounted for 8-42% of the Fe_{DISS} (Fig. 22A and Fig. 29A). As with the eastern PO2 and P16N transects, concentrations and percentages decreased with depth. However, concentrations did not routinely fall below detectable levels until ~200 m. At these stations, concentrations of Fe_{DISS} and Al_{DISS} were also high, with median surface concentrations of ~0.6 nM and ~ 8 nM, respectively.

Similar high concentrations of Al_{DISS} were found in this region during the 2002 Intergovernmental Oceanographic Commission (IOC) Baseline cruise, and were attributed to high dust deposition (Brown et al., 2005; Measures et al., 2005). Surface seawater was believed to be further enriched in Al_{DISS} beyond that expected by the high dust flux, due to westward recirculation of the waters forming the Kuroshio extension, which increased the length of time these waters were exposed to the high flux (Measures et al., 2005). The high dust flux should also contribute to the concentration of Fe_{DISS}. Although several of the IOC samples in this vicinity showed high Fe_{DISS}, these high values were attributed to contamination.

On the PO2 cruise, the median flux of aerosol Fe west of 145°E was measured to be ~1000 nmol m⁻² day⁻¹, with a median flux of soluble Fe(II) of 20 nmol m⁻² day⁻¹ (Buck et al., 2006a). Given predicted oxidation rates of approximately 100 nM/day (100 pM [Fe(II)] with a pseudo first-order decay of 0.693 min⁻¹), the aerosol supply of Fe(II) to the mixed layer (~20 m) by itself should not be sufficient to produce the concentrations observed in surface seawater.

Other authors have observed slower-than-predicted Fe(II) oxidation rates in rainwater (Kieber et al. 2001), and suggested that the Fe(II) is somehow stabilized against oxidation. While this may also be the case for Fe(II) in aerosols, another possibility is that the *in situ* iron-reducing mechanisms are more effective in the presence of high concentrations of Fe_{DISS}.

East of 145°E, the dust fluxes were much lower, with median Fe_{DISS} flux of approximately 175 nmol m⁻²day⁻¹ and median flux of soluble Fe(II) equal to 4.5 nmol m⁻²day⁻¹. An area of low surface water Fe(II) concentration (10-25 pM) was found to extend from approximately 160°E to 175°E, possibly the result of minimal aerosol deposition. Further east, surface concentrations increased again to levels ranging from 20-40 pM. The effect of the wind mixed layer (WML) on controlling surface concentrations appears to be negligible, as shown in [Fig. 38](#).

Deep samples (900-100 m) taken at PO2 stations 18-28 showed very high Fe(II) and Fe_{DISS} concentrations, with [Fe(II)] ranging from 40-370 pM and [Fe_{DISS}] from 0.95-2.2 nM. These stations are located in an area of extreme bathymetric relief, with seafloor rising from a depth of 4000 m to within 1200 m of the surface ([Fig. 39](#)). This submarine ridge is part of the Izu-Bonin (Ogasawara) arc system, an intra-ocean convergent margin that is characterized by ongoing volcanic and hydrothermal activity (Stern and Arima, 1996) ([Fig. 40](#)). In hydrothermal source waters, dissolved iron can occur at high (mM) concentrations (von Damm, 1990). *In situ* observations of hydrothermal Fe(II) in plumes emanating from the Juan de Fuca ridge in the northeastern Pacific showed concentrations of 100 nM proximal to the plume (Chin et al., 1994). Concentrations were found to decrease with distance from the plume due to mixing and oxidation of Fe(II). However, plume-related Fe(II) was detected at distances of 10-15 km from the source vent.

Although a nearby hydrothermal source could account for the high concentrations of iron observed in this area, other hydrochemical data do not support this hypothesis. Hydrothermal plumes are typified by anomalously high helium isotope ratios (³He/⁴He) (Lupton and Craig, 1981). Other indicators include high concentrations of dissolved metals such as Al and Mn, low pH, low alkalinity, and high DIC (von Damm, 1990). Shipboard measurements of ³He/⁴He on cruise PO2 revealed no anomalous values (W. Jenkins, Woods Hole Oceanographic Institute, pers. comm.). Samples collected for dissolved manganese have yet to be analyzed. However, measurements of Al_{DISS} were low (<5 nM, C.I. Measures, pers. comm.) Other shipboard measurements, including pH, total alkalinity, silicate, and DIC showed no anomalous values in this vicinity ([Appendix H](#)).

An alternative source of Fe(II) and Fe_{DISS} is found in the suboxic to anoxic sediments lying atop these submerged ridges. Bacterial decomposition of organic matter in anoxic sediments can lead to the production of Fe(II). As a result, dissolved iron in sediment pore-waters has been found to reach micromolar concentrations (Elrod et al., 2004). Due to its solubility, sediment-derived Fe(II) will flux away from the sediments into the overlying water column. The half-life of Fe(II) for these waters was calculated to be ~ 7 h (Appendix B). Assuming current velocities of 1-4 cm sec⁻¹, Fe(II) produced in the sediments could be advectively transported 250-1000 m in one half-life. Transport via horizontal eddy diffusion during one half-life is expected to be ~5 km, based on a horizontal eddy diffusivity of 1000 m² sec⁻¹ (Okubo, 1971). For the trace metal casts, water depths directly below the ship at the time of sampling were between 2300 to 4200 m, resulting in a nominal minimum vertical distance between the rosette and the sediments of 1300 to 3200 m. However, continuous bathymetry data (Fig. 39) suggest that the true distance between the rosette and the ridge may have been less than this at times, especially at Stations 22 and 26, both of which had high [Fe(II)] and [Fe_{DISS}] in deep samples.

3.3 Summary of Results

The results from the two cruises suggest a relatively consistent pattern of Fe(II) occurrence and distribution in the Pacific Ocean. Surface water maxima are present in most profiles, and Fe(II) typically represents approximately 12% of the total dissolved iron. Concentrations decline with depth to undetectable levels in the upper 100 meters. The observed vertical profiles are highly suggestive of a light-related source mechanism, yet the length of time required for sampling operations relative to the short Fe(II) lifetimes predicted by kinetic models casts doubt on the ability of these surveys to detect photochemically produced Fe(II). This argument is based on kinetic models of Fe(II) oxidation that assume a purely inorganic speciation for Fe(II). The effect of organic matter on oxidation kinetics has not been fully explored, particularly at sub-nanomolar Fe(II) levels, and the limited data available leave open the possibility that Fe(II) may oxidize more slowly than currently believed.

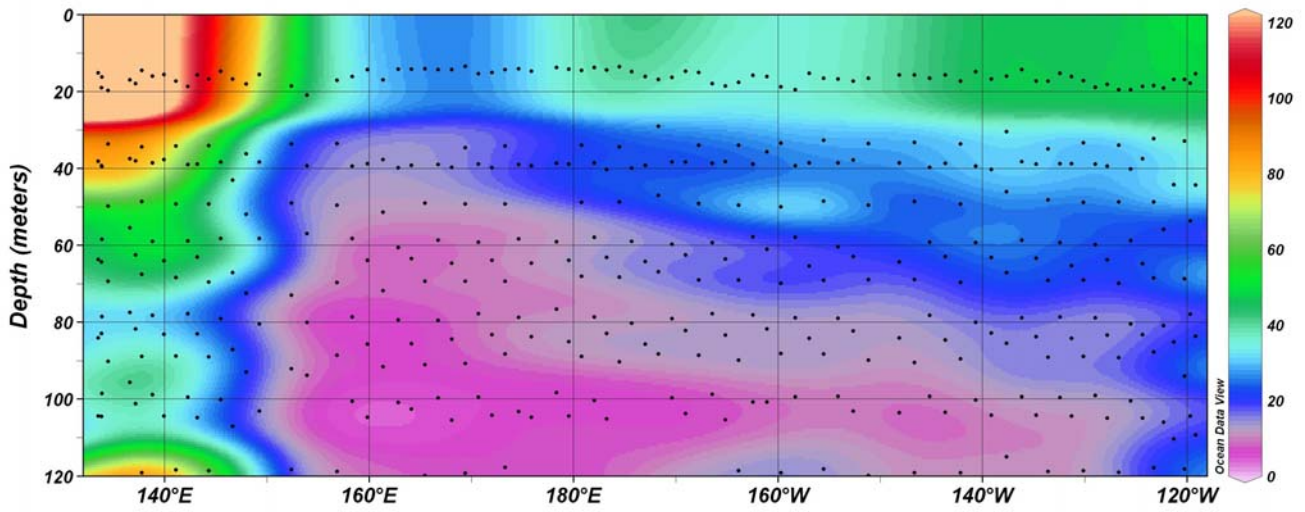
Other seawater constituents can produce a chemiluminescent response under the experimental conditions employed in this study. Though most of the metals tested are not expected to be significant interferences because of their low reactivity and low concentrations, V(IV) presents a concern. While V(V) is expected to predominate in the presence of oxygen (Wehrli and Stumm, 1989), and does not itself produce chemiluminescence, given its high concentrations in seawater a relatively modest presence of reduced V, produced perhaps by the same processes proposed for Fe(II), could interfere with Fe(II) analysis. However, due to its

lower luminol reactivity, approximately 2 nM V(IV) would be required in the flow cell to produce a system response equivalent to 50 pM Fe(II). The limited data provided by Okamura (2001) suggest that V(IV) does not occur at concentrations greater than 50 pM, while the presence of Fe(II) is supported by several studies using different analytical approaches. Though the data currently available support the case for Fe(II), more work is needed to definitively eliminate V(IV) as a potential source of analytical response.

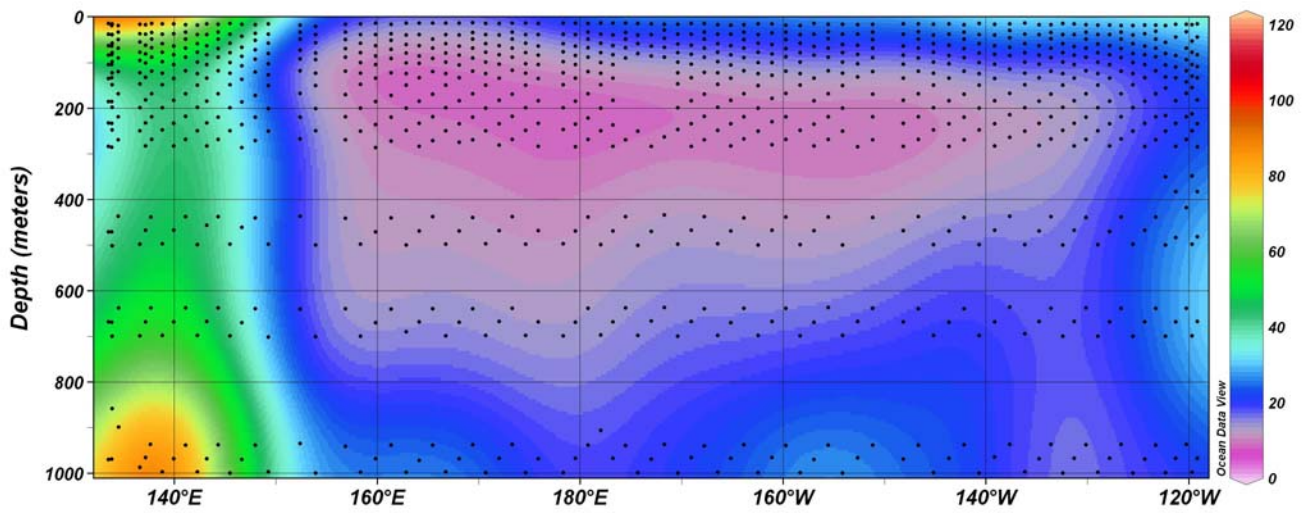
With this caveat, the implication of the findings for surface water productivity is now considered. The measurements made on PO2 and P16N show that in typical surface seawater, 10-22% (25th and 75th percentiles, respectively) of dissolved iron is present as Fe(II). For some samples (western PO2), these percentages were even higher (12-34%). It should be noted that these numbers are probably understated, due to the fact that sampling logistics likely prevented measurement of at least some photochemically-produced Fe(II). These numbers suggest that the pool of iron available for biological uptake is greater than previously believed. To date, studies of iron uptake by phytoplankton have demonstrated that only inorganic species (Fe[']) can be transported across the cell membrane. In the absence of reduction mechanisms, uptake is thus constrained by the amount of Fe(III)['] in equilibrium with Fe(III)-L, estimated to be on the order of 10⁻¹⁴ M, or about 0.03% of the total dissolved iron present (Rue and Bruland, 1995). Reduction of Fe(III)['] will produce Fe(II)['] directly, while reduction of Fe(III)-L₁, where L₁ is a strong Fe(III)-binding ligand, will produce either Fe(II)-L₁ or Fe(II)-L₂, where L₂ is an oxidized ligand photoproduct (Barbeau, 2001). The extent to which reductive iron cycling increases Fe['] depends upon the fate of these Fe(II) complexes. Complete dissociation of Fe(II) from the complex would increase Fe['] to as much as 10^{-10.6} M (the median Fe(II) concentration observed for eastern PO2 and P16N). This estimate of Fe['] is conservative because it does not consider the increased [Fe(III)[']] that will be present as an intermediate species following oxidation of Fe(II), prior to re-complexation with L₁ or L₂, an amount determined by the relative rates of Fe(II) production, oxidation, and Fe(III) complex formation. The other extreme, in which all the reduced Fe(II) remains complexed with L₁ or L₂ and no Fe(II)['] or Fe(III)['] is formed, should also enhance bioavailability to some degree due to the weaker L₁ complexes typically formed by Fe(II) and the generally weaker metal-binding capacity of the oxidized ligands (Barbeau, 2001).

Surprisingly, Fe(II) was also detected at depths of 500-1000 m at nearly half of the sampled stations. The low *in situ* temperatures, and the lower pH and oxygen levels that are typically characteristic of these depths lead to slow oxidation kinetics, with predicted half-lives on the order of hours to days. Here it is speculated that Fe(II) is derived during the remineralization of sinking particles, suboxic microenvironments within which Fe(II) might be

stabilized, or possibly from release of cellular iron, which contains a mix of Fe(II) and Fe(III). The iron speciation in these waters could be relevant to the subject of bioavailability when the water is eventually returned to the surface.

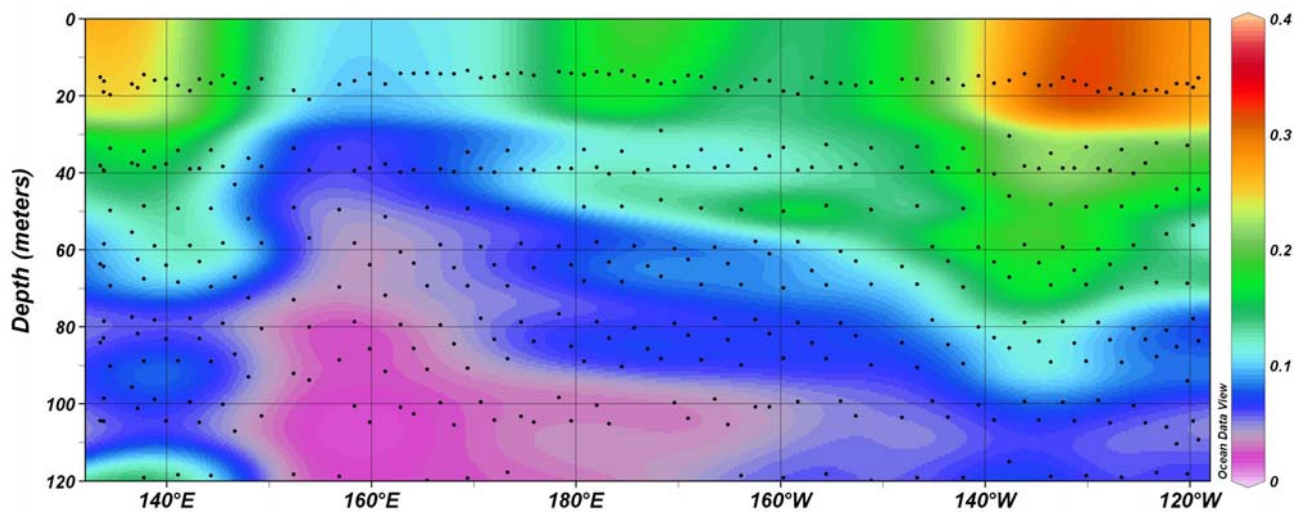


A

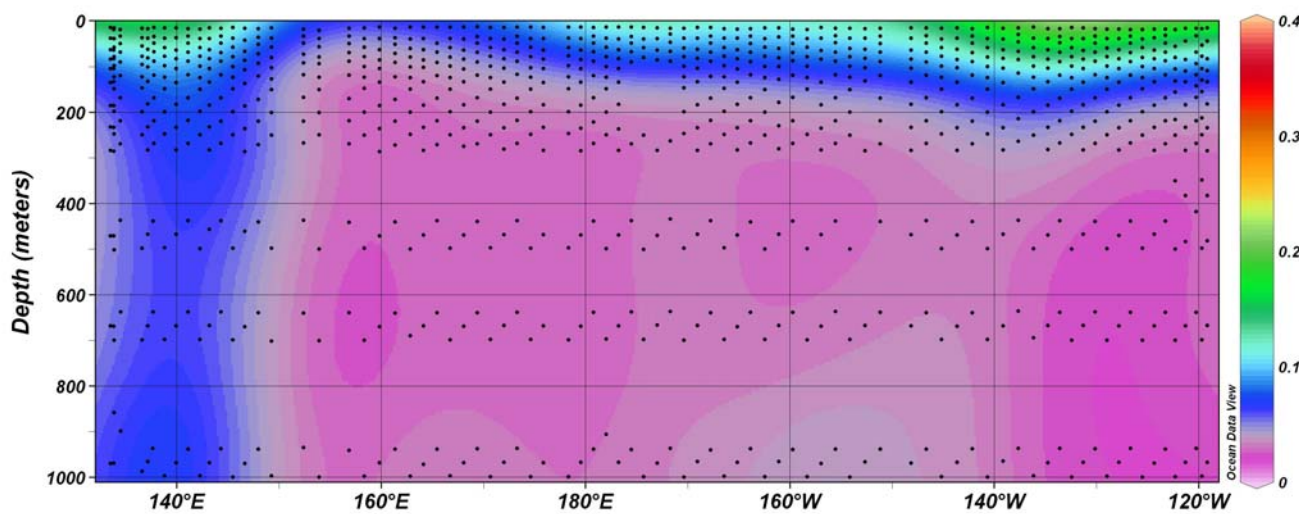


B

Fig. 21: Fe(II) concentrations for cruise PO2. An oceanographic section is shown here of Fe(II) concentrations (pM) for cruise PO2, latitudinal section from longitude 135°E (left) to 118°W (right), along 30°N latitude. Concentrations are shown from the surface to 120 meters (**A**) and from the surface to 1000 meters (**B**). The purple shade indicates values at or below the detection limit. The very light red shade represents values greater than 120 pmol/L (maximum concentration was 280 pM). All oceanographic sections were plotted using Ocean Data View software (Schlitzer, 2004).



A



B

Fig. 22: $[\text{Fe}(\text{II})]/[\text{Fe}_{\text{DISS}}]$ for cruise PO2. The ratio of reduced iron to total dissolved iron is shown here for cruise PO2, a latitudinal section along 30°N latitude, from longitude 135°E (left) to 118°W (right). Ratios are shown from the surface to 120 meters (**A**) and from the surface to 1000 meters (**B**).

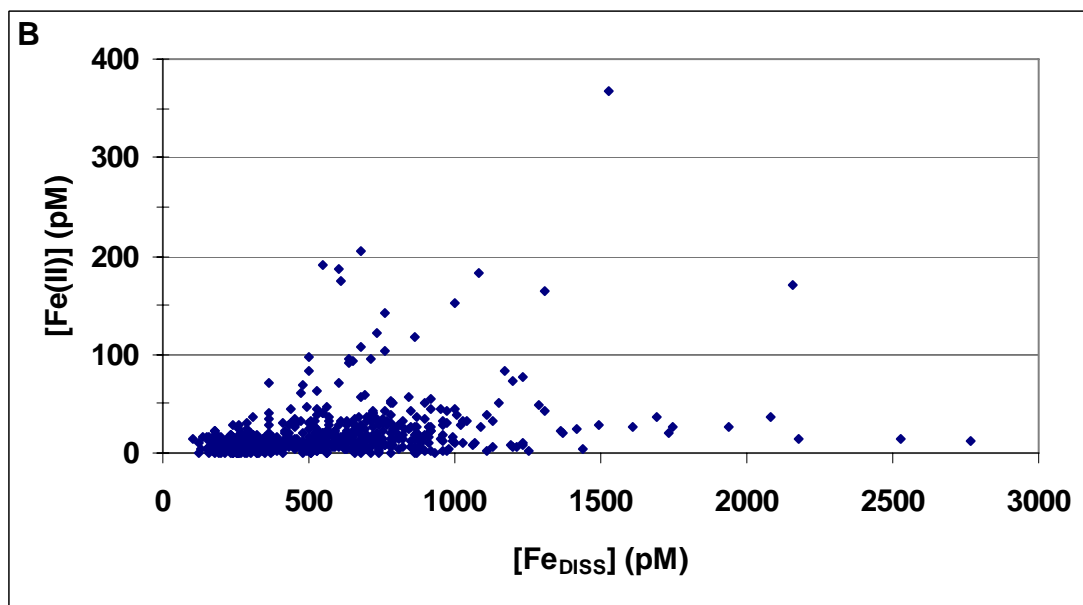
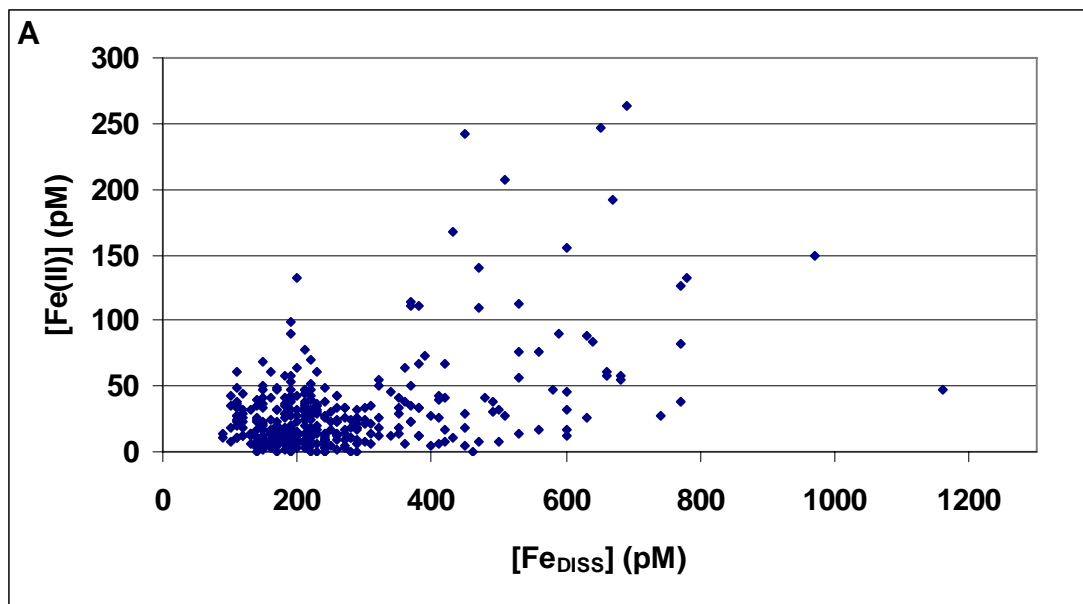
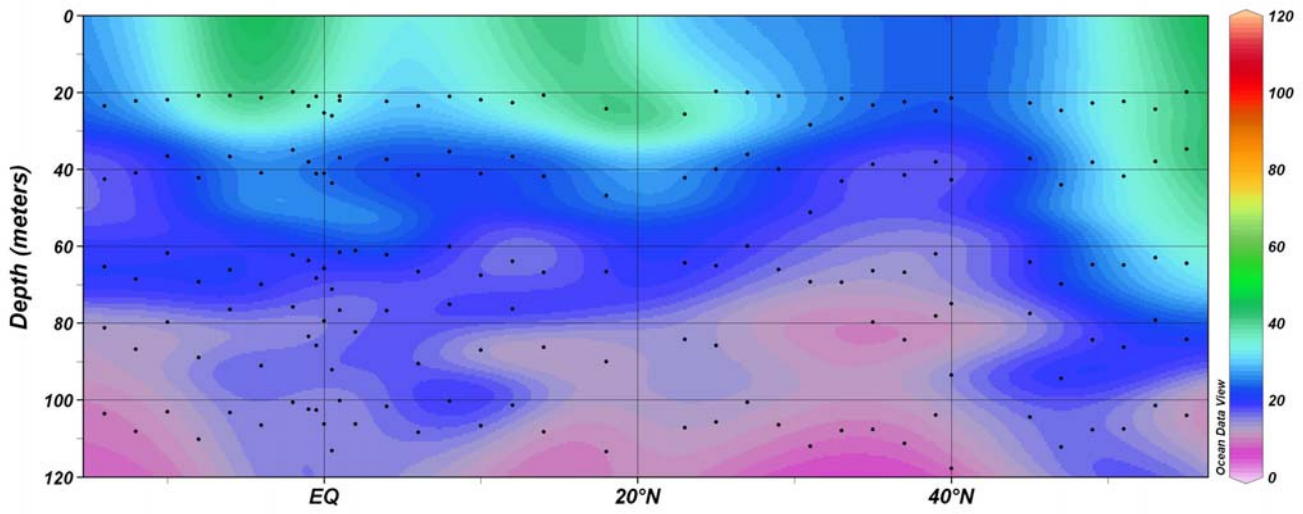
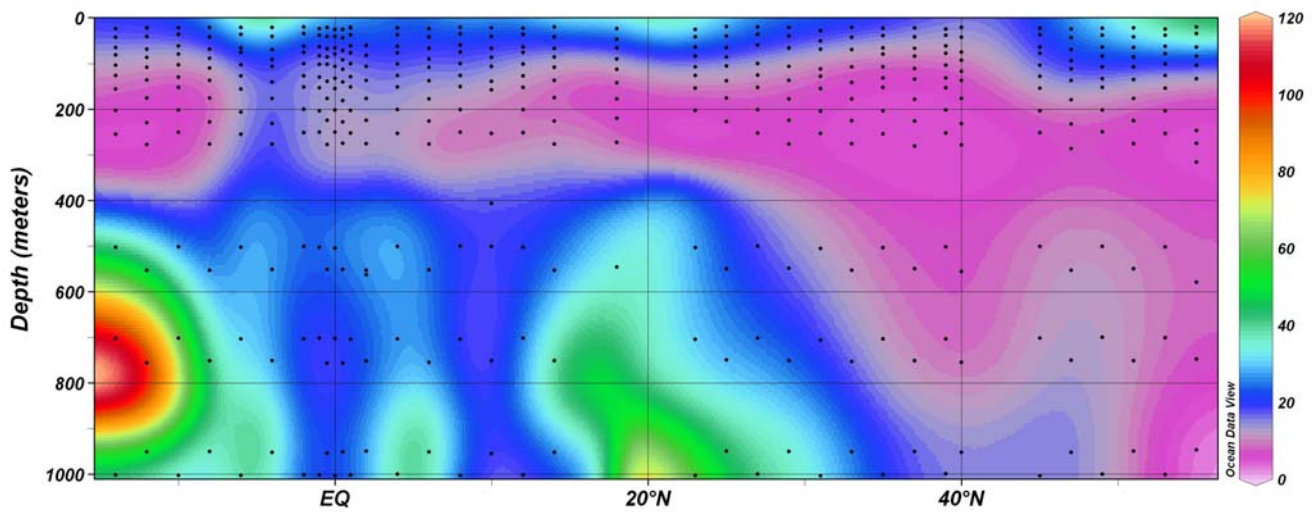


Fig. 23: Fe(II) concentrations are plotted against Fe_{DISS} concentration for PO2 samples. Samples collected at depths 0-100 m are shown in (A). Samples collected at depths of 100-1000 m are shown in (B).

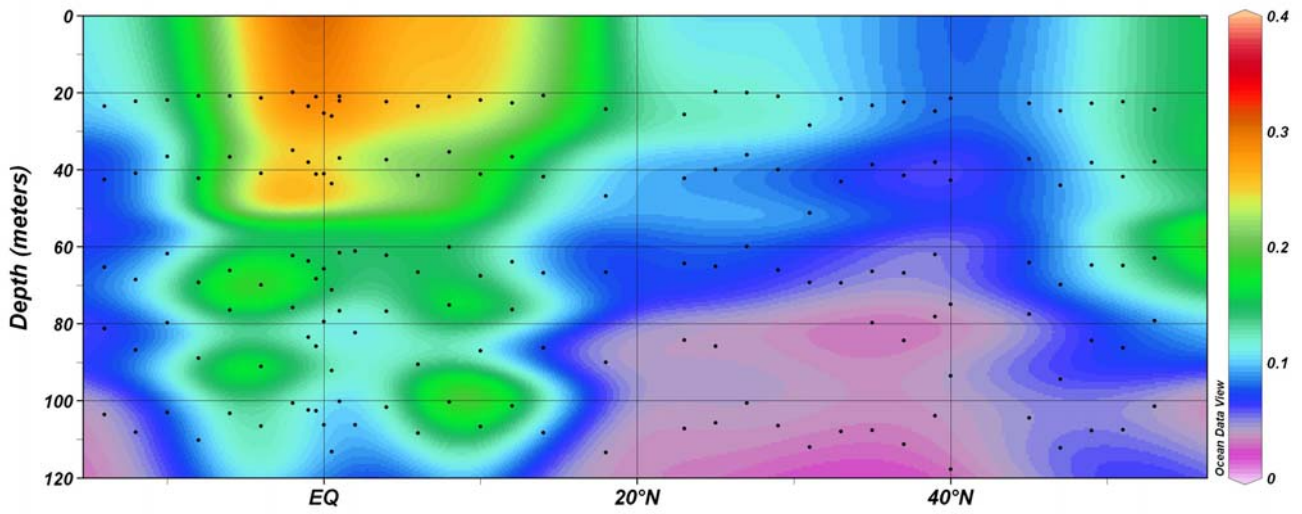


A



B

Fig. 24: Fe(II) concentrations for cruise P16N. An oceanographic section is shown here of Fe(II) concentrations (pM) for cruise P16N, meridional section along 152°W longitude, from latitude 17°S (left) to 55°N (right). Concentrations are shown from the surface to 120 meters (**A**) and from the surface to 1000 meters (**B**). The purple shade indicates values at or below the detection limit. The very light red shade represents values greater than 120 pmol/L (maximum concentration was 260 pM).



A

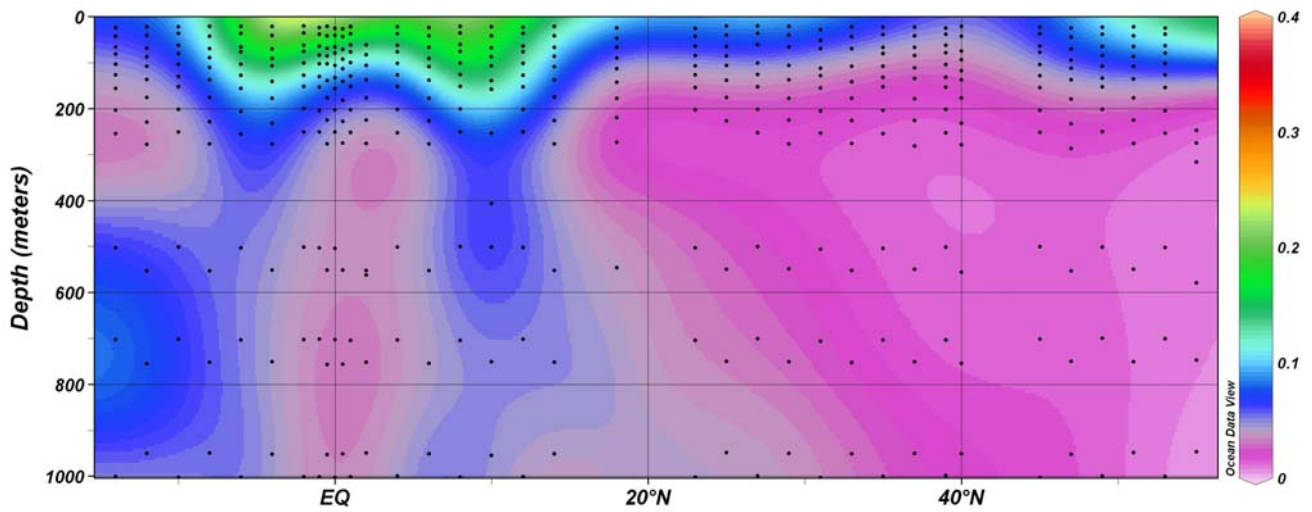


Fig. 25: $[\text{Fe(II)}]/[\text{Fe}_{\text{DISS}}]$ for cruise P16N. The ratio of reduced iron to total dissolved iron is shown here for cruise P16N, meridional section along 152°W longitude, from latitude 17°S (left) to 55°N (right). Ratios are shown from the surface to 120 meters (**A**) and from the surface to 1000 meters (**B**).

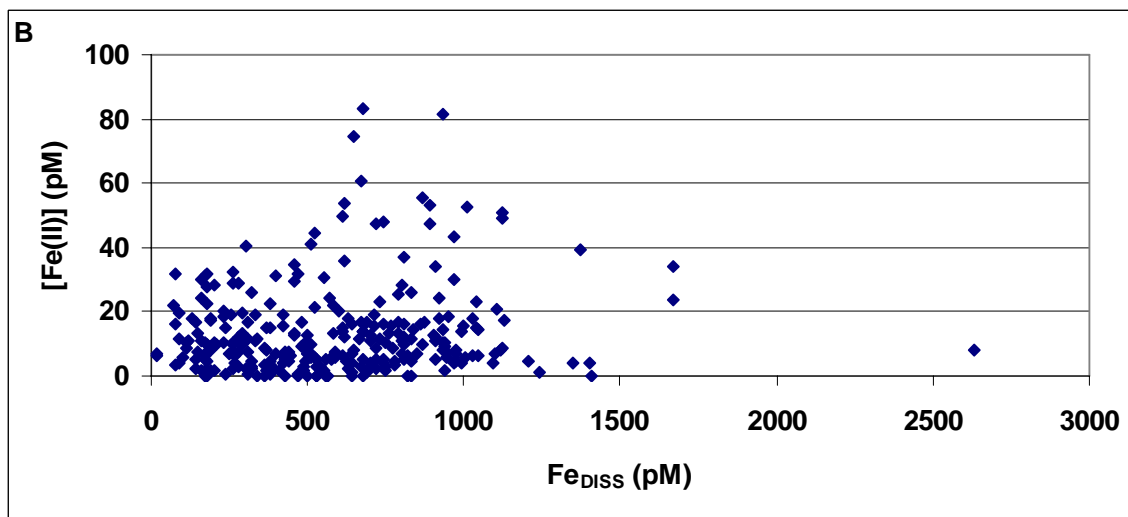
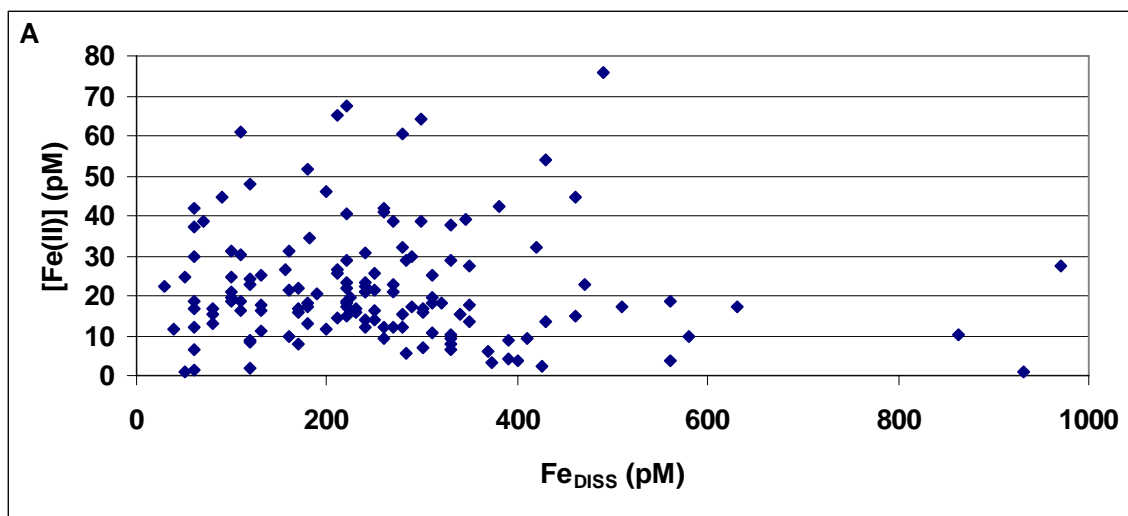


Fig. 26: Fe(II) concentrations are plotted against Fe_{DISS} concentration for P16N samples. Samples collected at depths 0-100 m are shown in (A). Samples collected at depths of 100-1000 m are shown in (B).

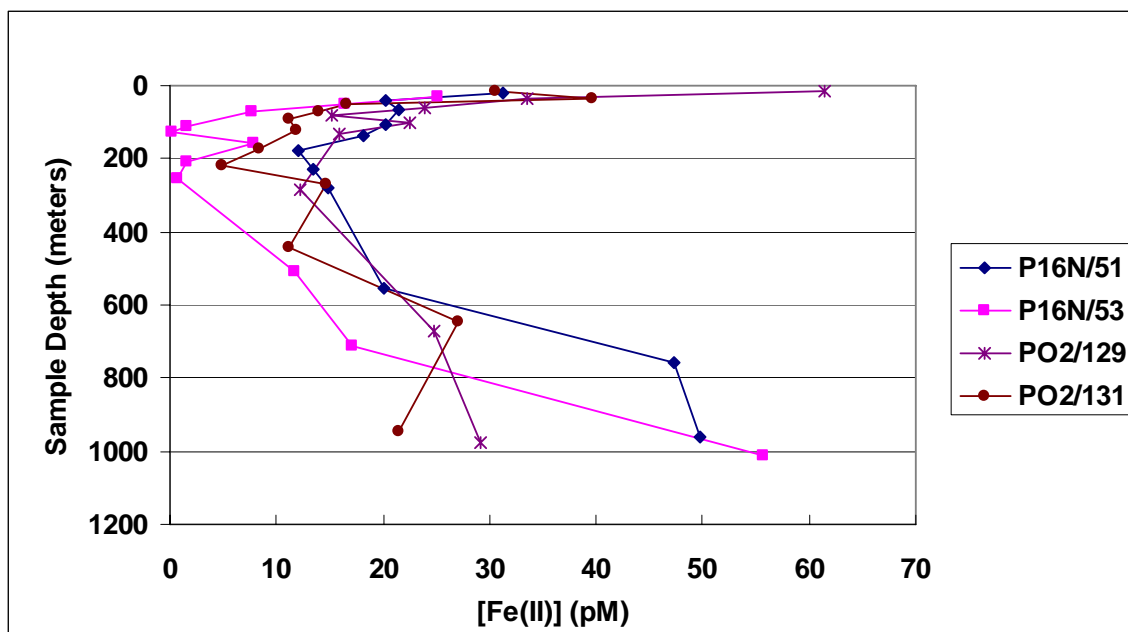


Fig. 27: Vertical profiles of Fe(II) concentration are shown plotted for PO2 and P16N crossover stations. The crossover point for the two transects was in the North Pacific (30°N,152°W). The stations shown were located within 100 km of the crossover point.

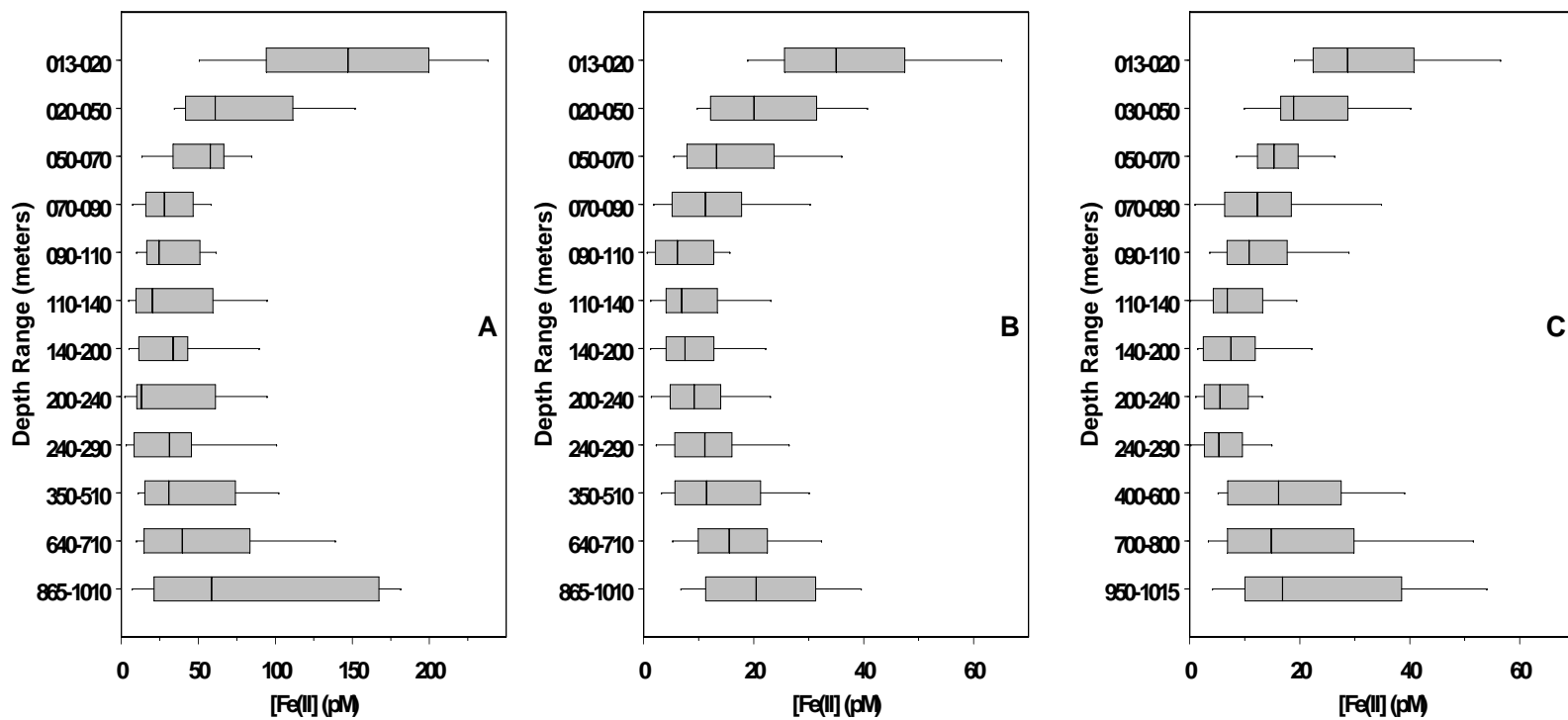


Fig. 28: Box plots of Fe(II) concentrations grouped by depth range for western PO2 (A), eastern PO2 (B), and P16N (C). The western PO2 dataset includes stations 8-30 (n=12), the eastern PO2 dataset includes stations 32-181 (n=72), and the P16N dataset includes stations 4-79 (n=34). The depth ranges correspond to individual GO-FLO bottles. The line segment bisecting each box represents the median value observed for that depth range, with the left and right sides of each box representing the lower and upper quartiles, respectively. Box whiskers indicate 10th percentile (left) and 90th percentile (right) values. Note that (A) is plotted on a different concentration scale than (B) and (C).

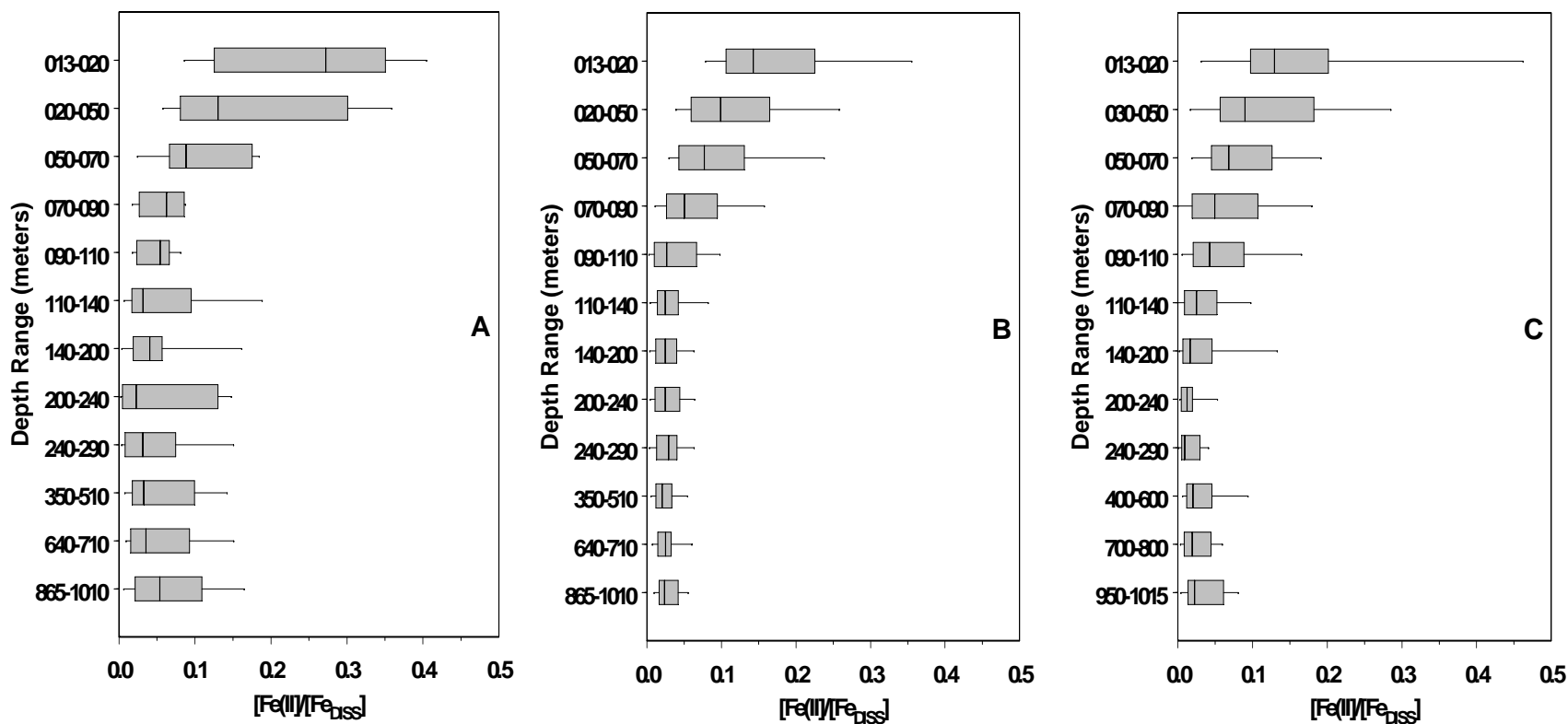


Fig. 29: Shown are box plots of Fe(II) percentages grouped by depth range for western PO2 (**A**), eastern PO2 (**B**), and P16N (**C**). The western PO2 dataset includes stations 8-30 (n=12), the eastern PO2 dataset includes stations 32-181 (n=72), and the P16N dataset includes stations 4-79 (n=34). The depth ranges correspond to individual GO-FLO bottles. The line segment bisecting each box represents the median value observed for that depth range, with the left and right sides of each box representing the lower and upper quartiles, respectively. Box whiskers indicate 10th percentile (left) and 90th percentile (right) values. These plots are all drawn to the same scale.

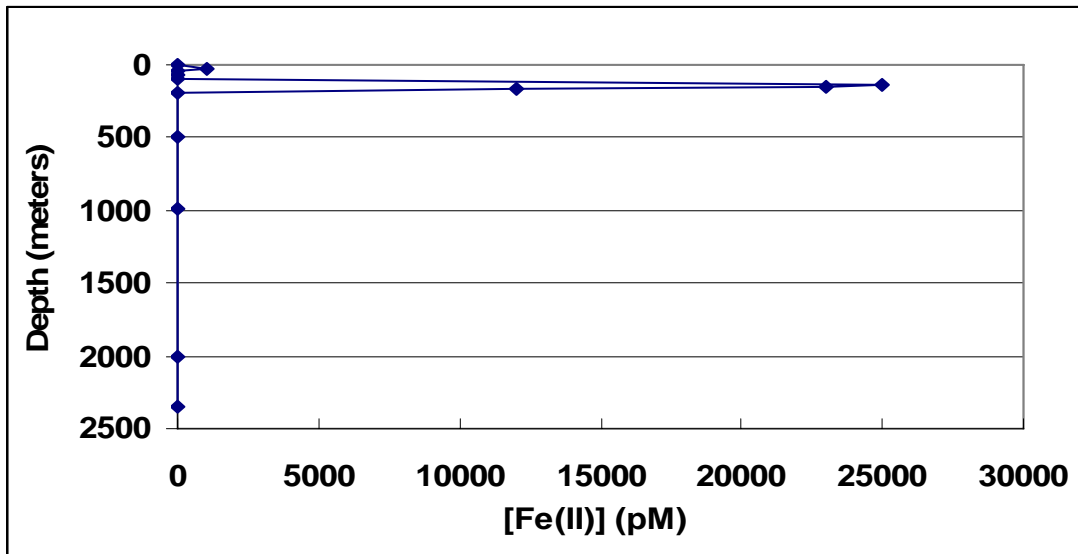


Fig. 30: Data of Hong and Kester (1986) for Station 72 (11°S, 79°W) in the eastern tropical Pacific.

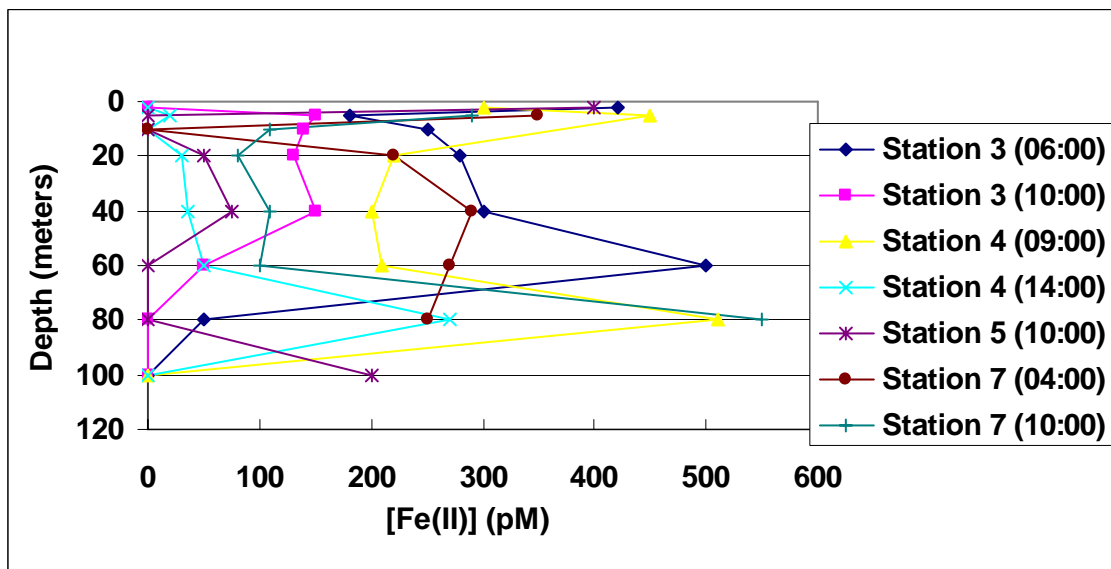


Fig. 31: Vertical profiles of O'Sullivan et al., 1991 for equatorial Pacific (vicinity 5°N, 140°W).

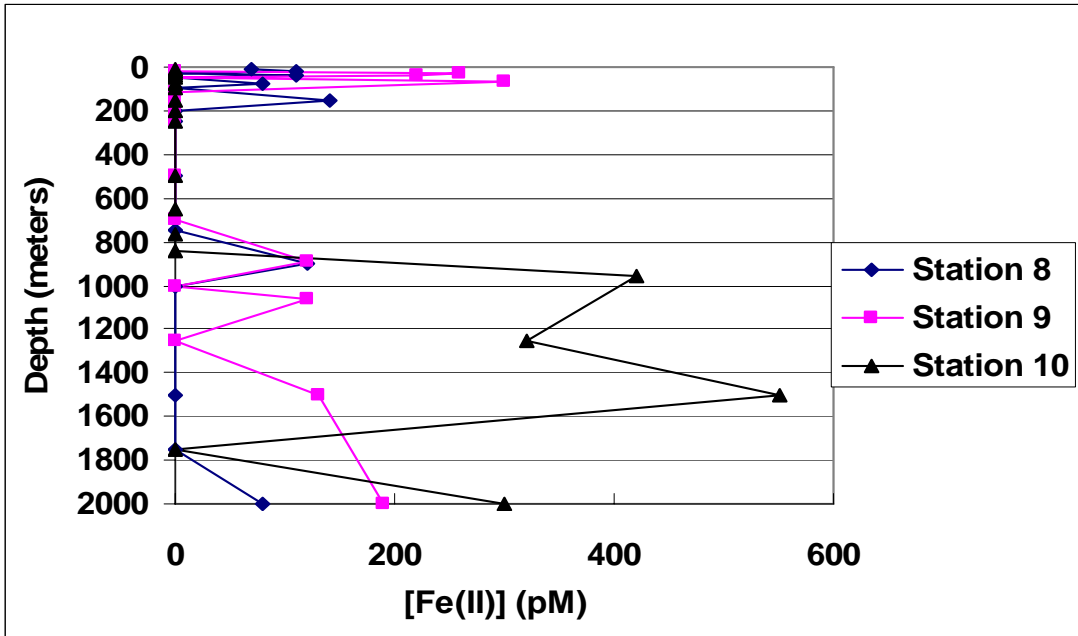


Fig. 32: Data of Boye et al. (2006) from the eastern North Atlantic.

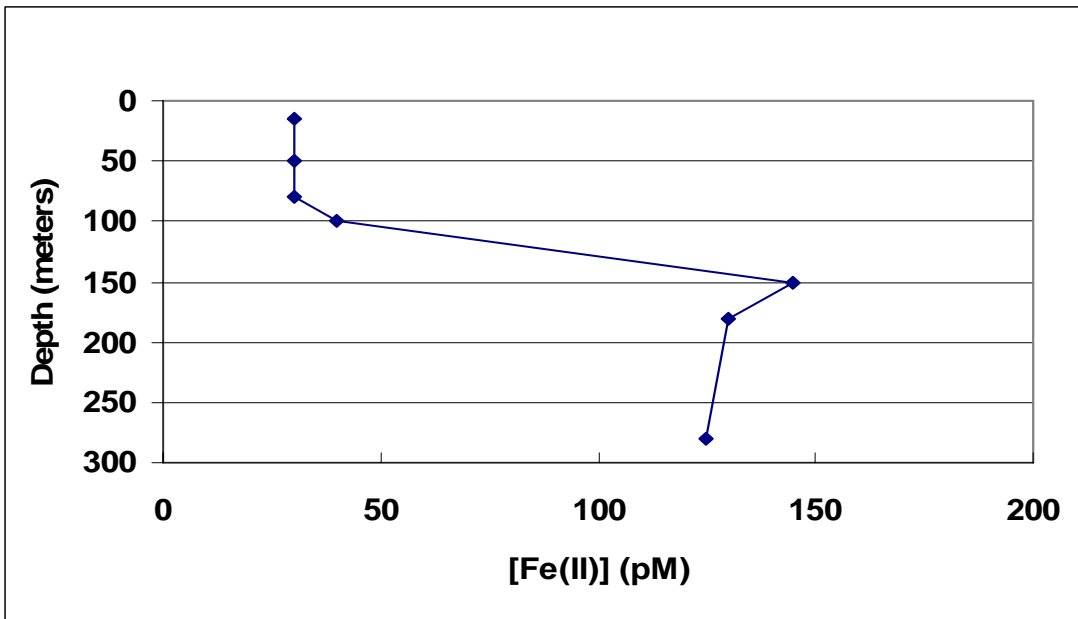


Fig. 33: Data of Hopkinson and Barbeau (2007) from the eastern tropical Pacific.

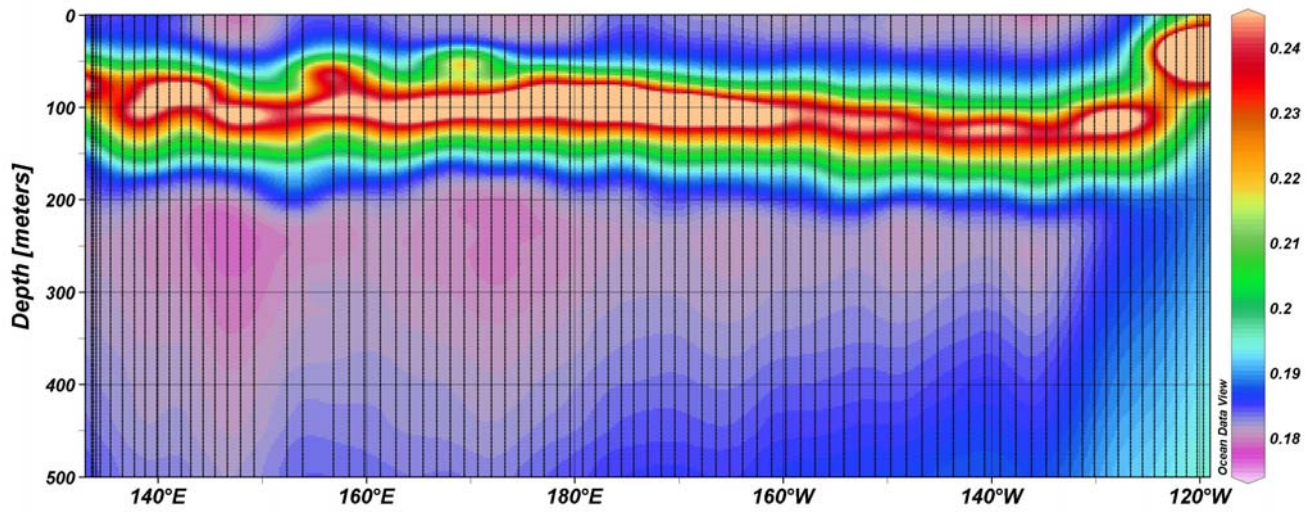


Fig. 34: Oceanographic sections of *in situ* chlorophyll fluorescence (mV) from cruise PO2, the latitudinal section along 30°N latitude, from Japan (left) to California (right). Data from P16N have not yet been made available.

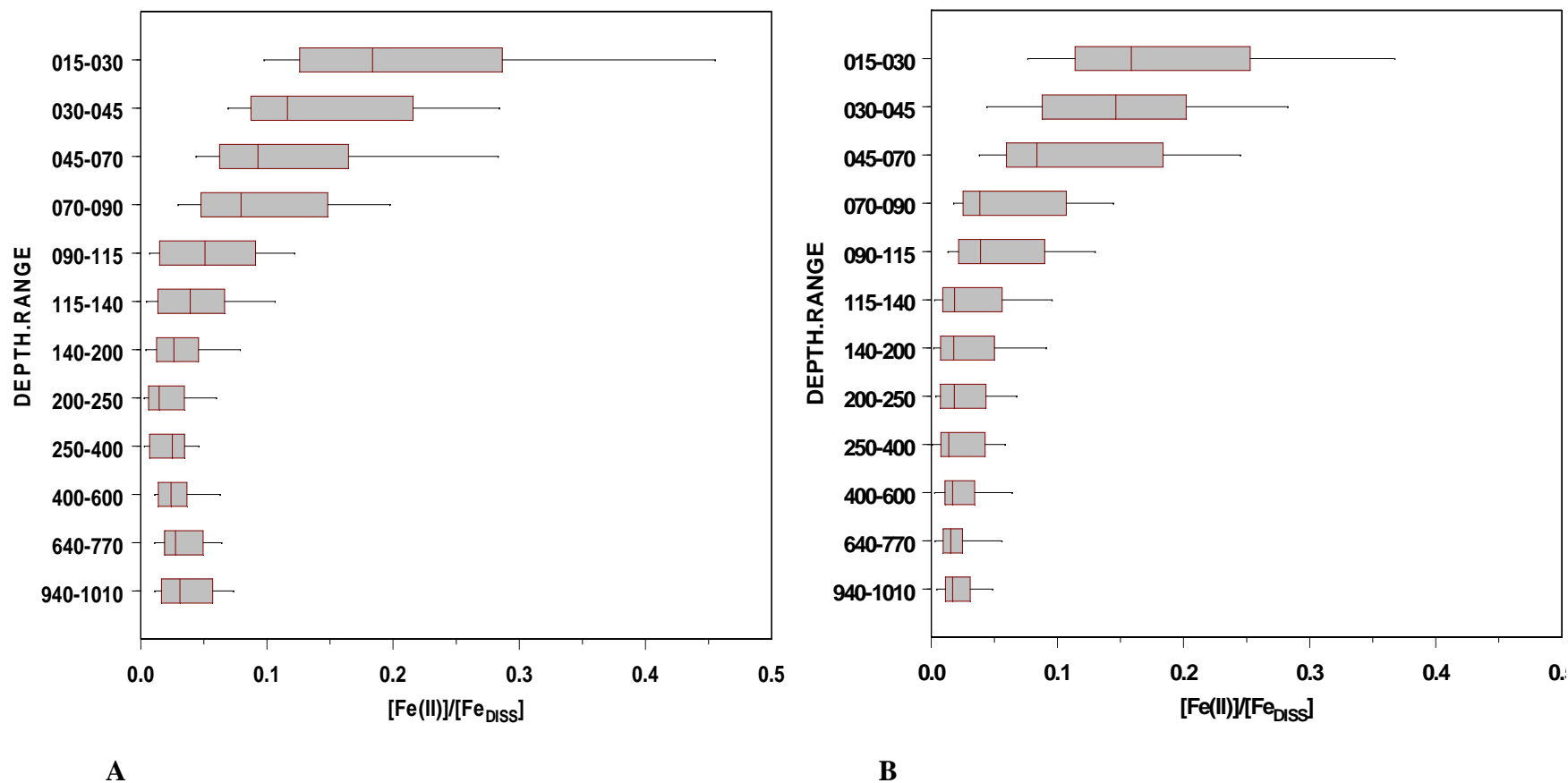


Fig. 35: Box and whisker plots of $[\text{Fe(II)}]/[\text{Fe}_{\text{DISS}}]$ grouped by depth for the PO2 and P16N samples collected during the day (**A**) and at night (**B**). Samples from the western PO2 segment (stations 8- 30) were omitted from these graphs. The line segment bisecting each box represents the median value observed for that depth range, with the left and right sides of each box representing the lower and upper quartiles, respectively. Box whiskers indicate 10th percentile (left) and 90th percentile (right) values.

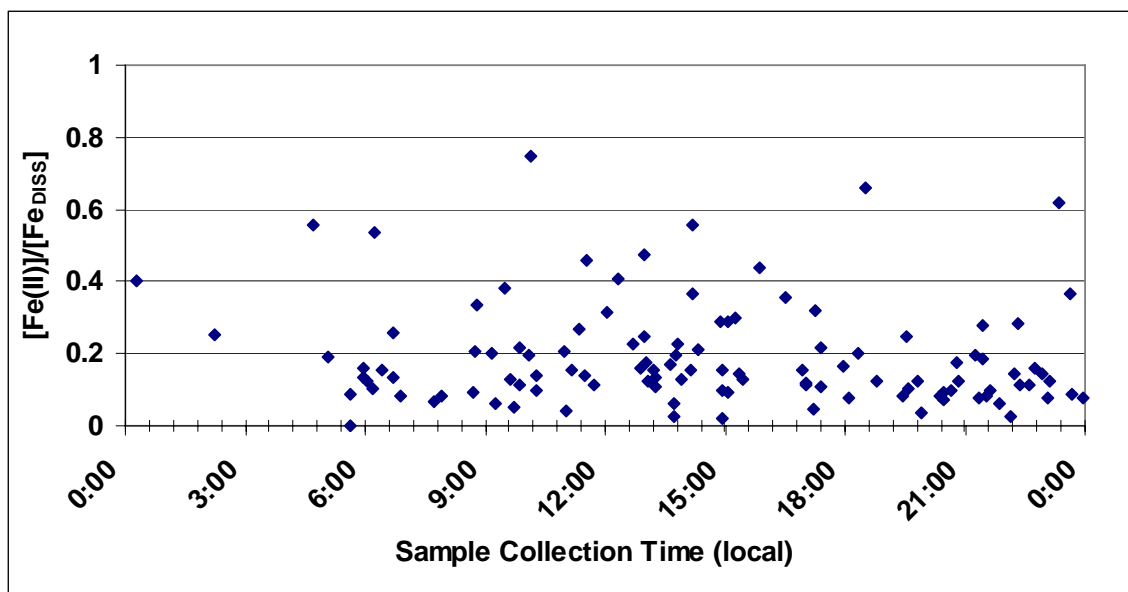
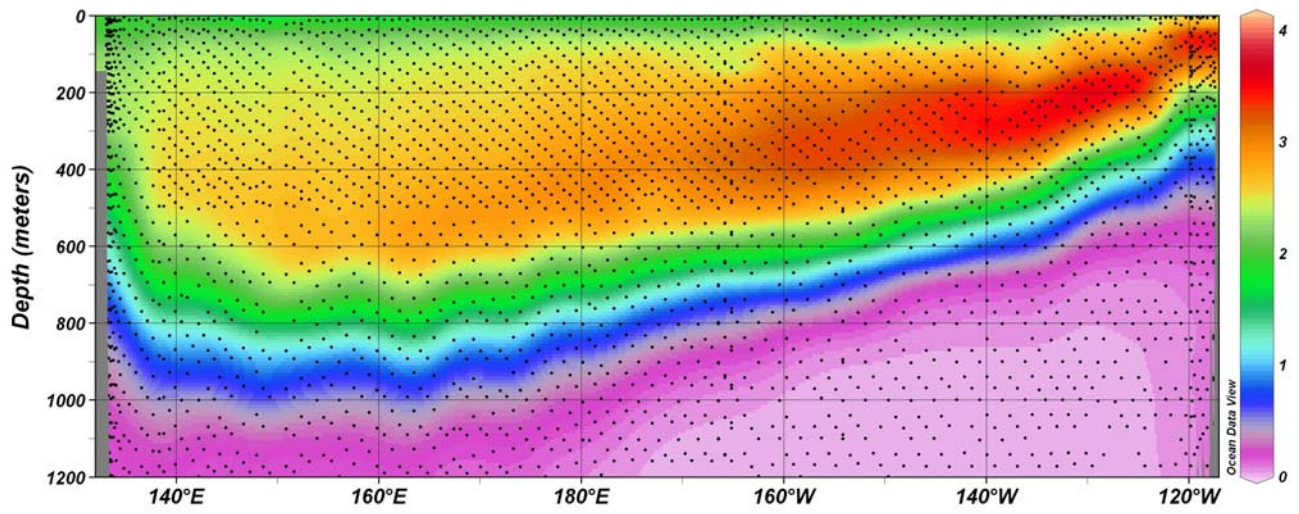
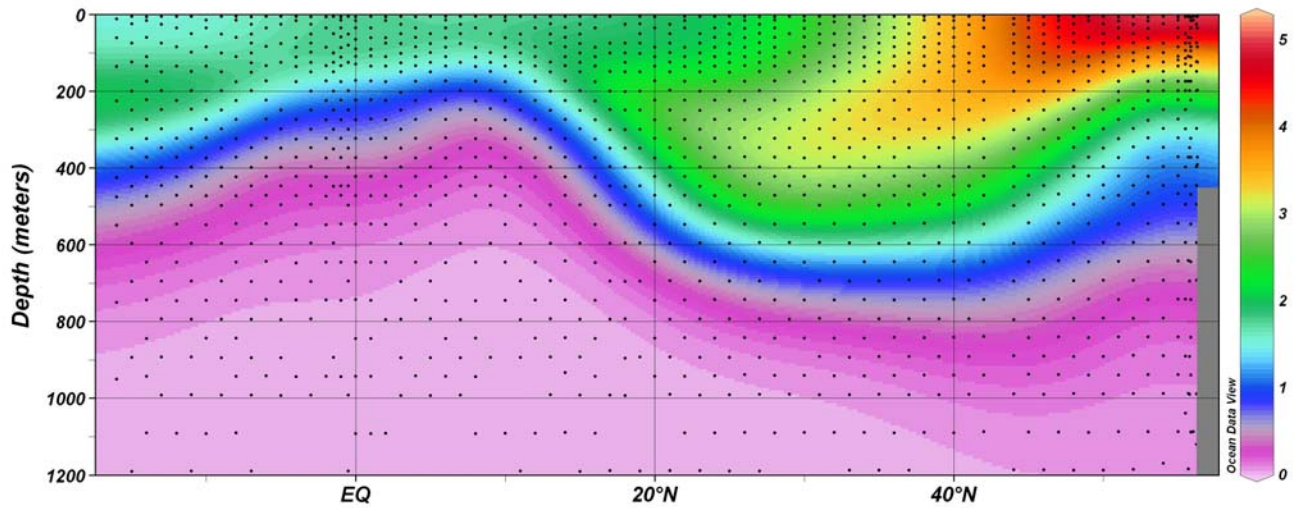


Fig. 36: Plot of $[\text{Fe(II)}]/[\text{Fe}_{\text{DISS}}]$ versus sample collection time for surface samples collected on cruises PO2 and P16N. PO2 stations west of 140°E were omitted from this plot.



A



B

Fig. 37: Oceanographic sections of CFC-11 concentration (pmol/kg) for cruise PO2 (**A**) and cruise P16N (**B**). CFC-11 is a gaseous industrial chemical used as a transient tracer of ocean circulation.

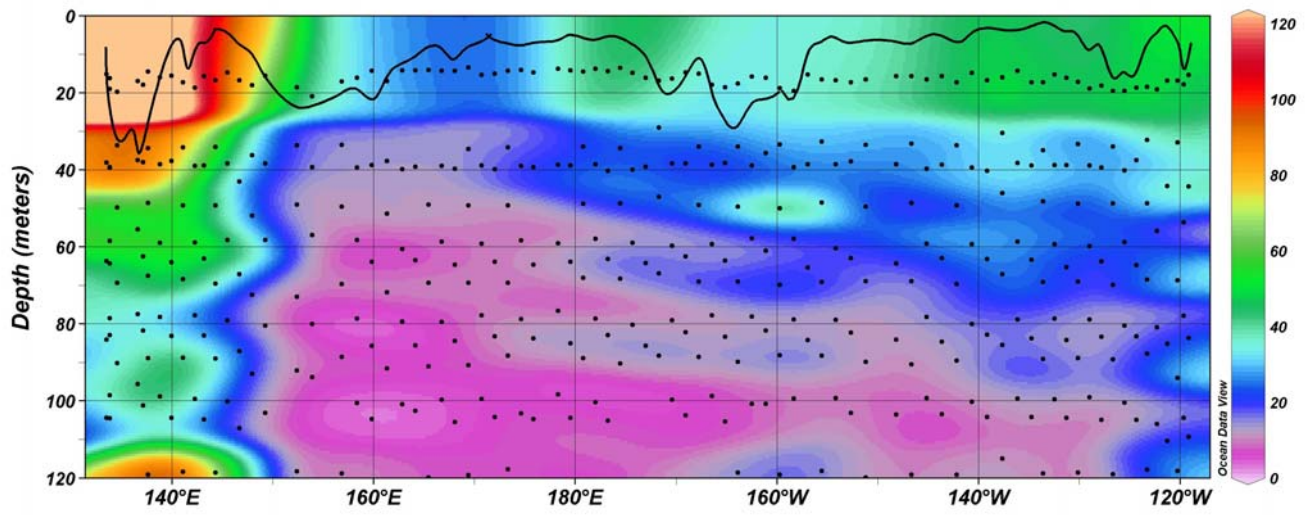


Fig. 38: Fe(II) concentrations (pM) are shown for the PO2 oceanographic section, with the depth of the wind mixed layer plotted as a solid line.

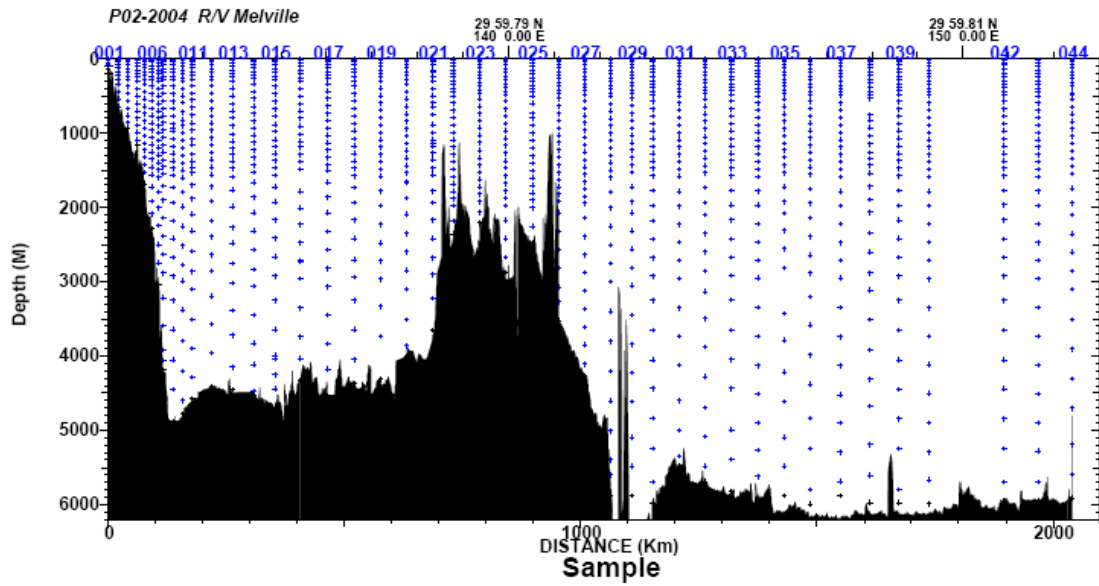


Fig. 39: Bathymetric profile of western PO2 cruise segment (Robbins, 2004). The Izu-Bonin arc system is seen centered around longitude 140°E, just left of center.

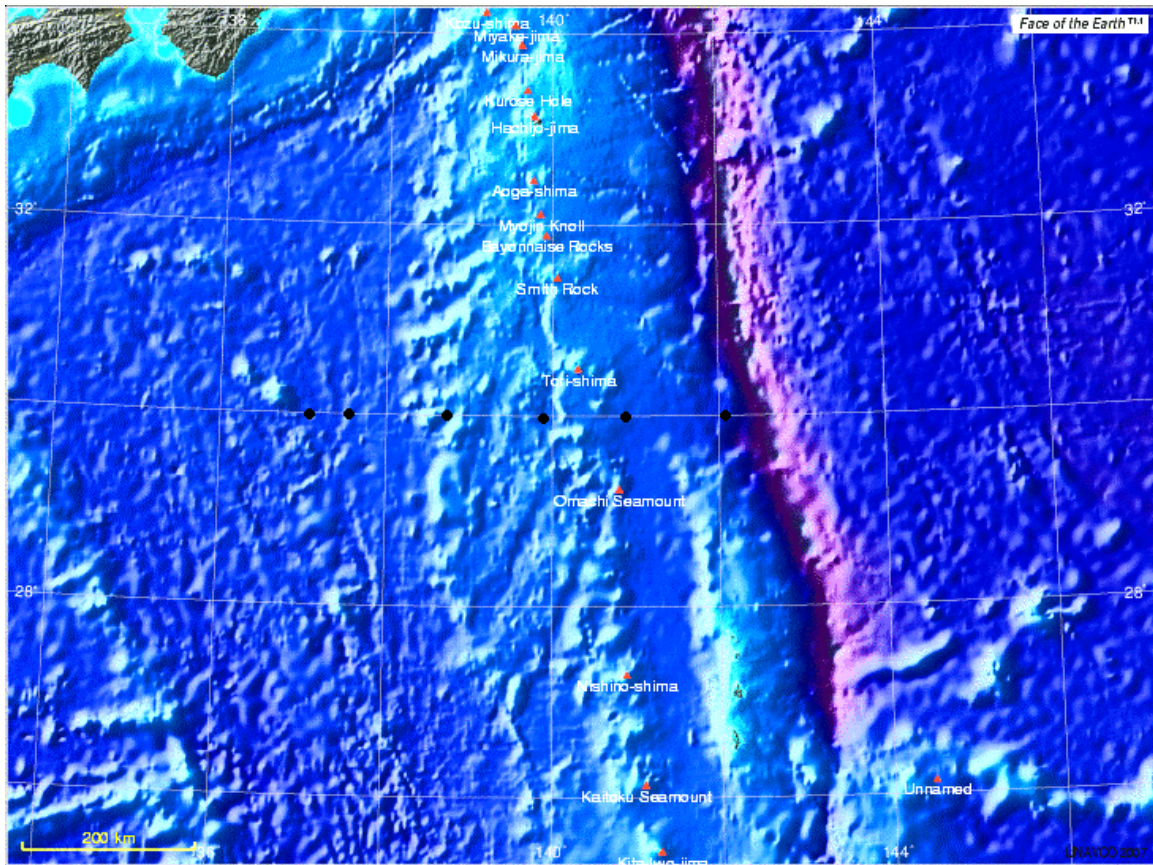


Fig. 40: Bathymetric map of western PO2 section showing locations of active volcanoes along the Izu-Bonin arc system. PO2 stations 18-28 are shown plotted from left to right as black circles. Another active volcano, Sofu-gan, is located between stations 24 and 26 at 29.8°N, 140.3°E, and is not shown on this map. It rises 99 m above sea level, and is 28 km wide at the base. [*Face of the Earth™* image courtesy of UNAVCO GMT Voyager map tool]

4. CONCLUSIONS

Iron is an essential trace element for all organisms, and its paucity in the world's oceans has been recognized as key factor controlling primary production. The manner in and extent to which iron is partitioned into various chemical species are subjects of fundamental importance, as the distribution of these species may further limit or enhance its bioavailability to marine organisms. This partitioning is to a great extent under the control of these organisms, which produce and release organic compounds with a high affinity for Fe(III). Marine organisms are also able to affect the redox speciation of iron, either by cell-surface reduction of Fe(III) or by the production of extracellular reducing agents, like superoxide. Sunlight can also provide the energy to reduce Fe(III), either directly, in the case of ligand-to-metal charge transfer, or indirectly, by reaction with CDOM to produce superoxide that reduces Fe(III). In the presence of oxygen and hydrogen peroxide, Fe(II) has a limited life-time, and will eventually oxidize to Fe(III). For a given water parcel, the overall chemical speciation is thus the result of a very dynamic and complex cycle. To date, very few measurements of iron redox speciation have been made. The goal of this study was to systematically measure the concentration of Fe(II) along two Pacific Ocean transects.

Trace metal clean sampling techniques were used to collect samples from 87 stations on the PO2 cruise and 37 stations on the P16N cruise. At each station, seawater samples were collected from 12 depths using rosette-mounted GO-FLO bottles. This approach allows for the collection of uncontaminated samples. However, due to the length of time required for rosette retrieval, it is not well-suited for the collection of transient species. In particular, if published estimates regarding the rate of Fe(II) decay are correct, measurements based on this sampling technique are likely to underestimate (or fail to detect) any direct influence of sunlight on iron speciation. This bias is likely to affect samples taken from the upper water column more than those collected at depth, since the lower temperatures, pH and oxidant concentration characteristic of deeper waters favor reduced rates of oxidation.

Because Fe(II) was expected to rapidly oxidize upon sample collection and filtration, samples were adjusted to pH 6 by immediate addition of very small amounts of 6M HCl, which delayed significant oxidative loss long enough for sample analyses to be completed. Sample acidification adds to the seawater blank response for undetermined reasons, but reported Fe(II)

concentrations were corrected for this effect. Minor time-dependent instabilities in system response, presumably associated with sample acidification, were observed and corrected for.

The luminol chemiluminescence method for Fe(II) analysis has several advantages. It is highly sensitive, and samples can be analyzed very rapidly with little alteration of the sample. It is also highly selective for Fe(II). None of the redox couples with transitions occurring under oxic conditions are believed to cause significant interference. V(III) and V(IV), which are predicted for anoxic conditions, were both found to be luminol-reactive. However, neither species has been observed in oxic seawater. Hydrogen peroxide was considered as a possible interference, yet when interference experiments were conducted in the manner that most represented field conditions, no interference by hydrogen peroxide was observed. High concentrations of organic matter in samples have been suggested to reduce analytical sensitivity. Laboratory experiments using model ligands suggest that ligands most likely to be associated with iron (i.e. siderophores) do not cause noticeable interferences. When luminol was exposed to light, an elevated baseline signal was observed, requiring light-shielding of luminol containers and tubing.

The results from the two cruises suggest a relatively consistent pattern of Fe(II) occurrence and distribution in the Pacific Ocean. Surface water maxima are present in most profiles, and Fe(II) typically represents approximately 12% of the total dissolved iron. Concentrations decline with depth to undetectable levels in the upper 100 meters. The observed vertical profiles are highly suggestive of a light-related source mechanism, yet profiles with similar patterns were detected in both day and night casts. In addition, the length of time required for sampling operations relative to the short Fe(II) lifetimes predicted by kinetic models casts doubt on the ability of these surveys to detect photochemically produced Fe(II). This latter argument is based on kinetic models of Fe(II) oxidation that assume a purely inorganic speciation for Fe(II). The effect of organic matter on oxidation kinetics has not been fully explored, particularly at sub-nanomolar Fe(II) levels, and the limited data available leave open the possibility that Fe(II) may oxidize more slowly than current models predict. Biotic reduction of Fe(III) has also been proposed to occur, either directly by membrane-bound enzymes, or indirectly, by extracellular biogenic superoxide. Either of these latter mechanisms could sustain Fe(II) production in GO-FLO bottles up until the time of sampling. However, Fe(II) maxima typically occurred at the shallowest sampling depths, and were seldom correlated with maximum chlorophyll concentration, which was generally found at greater depths.

Fe(II) was also detected at depths of 500-1000 m at nearly half of the sampled stations. The low *in situ* temperatures, and the lower pH and oxygen levels that are typically characteristic

of these depths lead to slow oxidation kinetics, with predicted half-lives on the order of hours to days. Here it is speculated that Fe(II) is derived during the remineralization of sinking particles, suboxic microenvironments within which Fe(II) might be stabilized, or possibly from release of cellular iron, which contains both Fe(II) and Fe(III). The iron speciation in these waters could be relevant to the subject of bioavailability when the water is eventually returned to the surface.

On cruise PO2, high concentrations of Fe(II) were observed throughout the water column in the area west of 145°E. In the surface waters, these high concentrations were associated with large fluxes of aerosol iron, and high concentrations of Fe_{DISS} and Al_{DISS} were also evident. A significant percentage of the iron in these aerosols was soluble Fe(II). However, *in situ* reductive processes must have contributed to the high concentrations observed, which were greater than would be expected by deposition alone. Very high concentrations of Fe(II) found in deep waters near the Izu-Bonin arc system were most likely due to sediment-derived Fe(II), as evidence of a hydrothermal source was lacking.

Studies of phytoplankton iron uptake have demonstrated that only inorganic iron species can be transported across the cell membrane. In the absence of reduction mechanisms, uptake is thus constrained by the concentration of Fe(III)' in equilibrium with ligand-bound Fe(III), estimated to be about 0.03% of the total dissolved iron present. Reduction mechanisms increase the concentration of bioavailable iron, either by producing Fe(II)' or by producing Fe(II) complexes with weaker binding constants that dissociate more readily at cell surfaces. The data presented here suggest that reduction mechanisms are active in seawater, and that Fe(II) typically accounts for 12% of the total dissolved iron in surface seawater. The results presented here indicate that the pool of iron available for biological uptake is greater than previously believed.

Future work should focus on determining the relative importance of Fe(II) production mechanisms in the open ocean, and the fate of this Fe(II) once it is produced. To overcome difficulties presented by the short half-life, measurements should ideally be made *in situ*, as in the study of Chin et al. (1994). Diel time series measurements of Fe(II) should be combined with measurements of Fe_{DISS}, O₂⁻, H₂O₂, CDOM, plankton species abundance and community composition, and downwelling irradiance so that the contributions of biogenic and photochemical processes can be separated. Finally, the rates at which picomolar levels of naturally-occurring Fe(II) species oxidize have not been elucidated, and may ultimately govern the bioavailability of iron.

APPENDIX A

STATION INFORMATION FOR CRUISES PO2 AND P16N

Table 4: Station information for cruise PO2.

STATION	DATE (UTC)	DATE (LOCAL)	LATITUDE DEC. DEG	LONGITUDE DEC. DEG	DEPTH METERS
8	6/18/04 5:26	6/18/04 14:26	32.0026	133.5137	2267
10	6/18/04 13:28	6/18/04 13:28	31.4712	133.8425	4761
12	6/19/04 4:09	6/19/04 13:09	31.4694	133.8184	4804
14	6/23/04 0:11	6/23/04 9:11	30.1888	134.5521	4574
16	6/22/04 10:43	6/22/04 19:43	29.996	136.6095	4419
18	6/22/04 0:00	6/22/04 9:00	29.9702	137.1588	4354
20	6/23/04 20:43	6/24/04 5:43	30.0026	137.6351	4178
22	6/24/04 5:48	6/24/04 14:48	30.0022	138.8016	2328
24	6/24/04 14:27	6/24/04 23:27	29.9978	139.9404	2971
26	6/25/04 2:53	6/25/04 11:53	30.0036	141.1092	3557
28	6/25/04 21:15	6/26/04 6:15	30.0052	142.2622	5990
30	6/26/04 20:29	6/27/04 5:29	30.0001	143.1773	5954
32	6/27/04 7:59	6/27/04 16:59	29.9965	144.3278	5695
34	6/28/04 8:21	6/28/04 17:21	30.0071	145.4877	5909
36	6/29/04 0:46	6/29/04 9:46	29.9871	146.6721	6152
38	6/29/04 12:00	6/29/04 21:00	30.0039	147.9579	6113
40	6/30/04 5:49	6/30/04 14:49	29.9945	149.2611	6125
44	7/1/04 22:24	7/2/04 7:24	30.0004	152.4038	5897
46	7/2/04 12:02	7/2/04 21:02	29.9948	153.9118	5811
50	7/4/04 8:29	7/4/04 17:29	29.9985	156.8488	5707
52	7/5/04 2:10	7/5/04 13:10	29.9947	158.3474	5602
54	7/5/04 19:13	7/6/04 6:13	29.9913	159.8396	5607
56	7/6/04 7:56	7/6/04 18:56	30.0033	161.352	5928
58	7/7/04 5:31	7/7/04 16:31	30.0006	162.8528	5960
60	7/7/04 21:39	7/8/04 8:39	29.9994	164.1473	5909
62	7/8/04 8:57	7/8/04 19:57	30	165.47	5798
64	7/9/04 1:20	7/9/04 12:20	29.9997	166.7641	6040
66	7/9/04 22:49	7/10/04 9:49	30.0068	168.086	5822
68	7/10/04 9:47	7/10/04 20:47	30.0008	169.4011	5651
70	7/11/04 1:45	7/11/04 12:45	30.0033	170.7014	5536
72	7/11/04 21:18	7/12/04 8:18	29.9995	172.0088	5136
74	7/12/04 8:00	7/12/04 20:00	29.9993	173.3214	4507
76	7/13/04 2:29	7/13/04 14:29	30.0059	174.6345	5388
78	7/13/04 17:09	7/14/04 5:09	29.9882	175.864	5240
82	7/14/04 22:35	7/15/04 10:35	30.001	178.3229	5233
84	7/15/04 8:20	7/15/04 20:20	30.0033	179.5495	5152
86	7/15/04 23:15	7/15/04 11:15	29.9937	-179.2175	5420

Table 4 Continued:

STATION	DATE (UTC)	DATE (LOCAL)	LATITUDE DEC. DEG	LONGITUDE DEC. DEG	DEPTH METERS
88	7/16/04 19:09	7/16/04 7:09	30.0086	-177.9822	5158
90	7/17/04 6:03	7/16/04 18:03	30.0003	-176.7542	5375
92	7/18/04 1:40	7/17/04 13:40	29.9947	-175.5156	5212
94	7/18/04 17:30	7/18/04 5:30	30.0017	-174.3042	5271
96	7/19/04 4:54	7/18/04 16:54	30.0006	-172.9828	5367
98	7/20/04 0:53	7/19/04 13:53	29.9988	-171.6769	5341
100	7/20/04 16:11	7/20/04 5:11	29.9957	-170.3706	5321
102	7/21/04 3:37	7/20/04 16:37	29.9983	-169.0571	5334
104	7/21/04 23:17	7/21/04 12:17	30.0012	-167.7524	5521
106	7/22/04 10:14	7/21/04 23:14	29.9982	-166.4453	5567
108	7/23/04 1:38	7/22/04 14:38	29.9957	-165.1287	5330
113	8/1/04 22:48	8/1/04 11:48	29.999	-163.8502	5585
115	8/2/04 19:20	8/2/04 8:20	30.0025	-162.4666	5609
117	8/3/04 8:05	8/2/04 21:05	29.9973	-161.0864	5420
119	8/4/04 0:58	8/3/04 13:58	29.9995	-159.7034	5685
121	8/7/04 22:33	8/7/04 11:33	29.9976	-158.3093	5786
123	8/8/04 14:33	8/8/04 4:33	29.9929	-156.9205	5798
125	8/9/04 3:22	8/8/04 17:22	30.0016	-155.534	5647
127	8/9/04 20:00	8/9/04 10:00	30.0004	-154.1487	5379
129	8/10/04 19:53	8/10/04 9:53	29.9974	-152.6516	5313
131	8/11/04 7:37	8/10/04 21:37	29.9978	-151.155	5622
133	8/12/04 0:06	8/11/04 14:06	30	-149.6555	5726
135	8/12/04 19:42	8/12/04 9:42	29.9993	-148.1517	4916
137	8/13/04 6:56	8/12/04 20:56	29.9982	-146.6486	4986
139	8/13/04 22:19	8/13/04 12:19	29.9997	-145.148	5223
141	8/14/04 17:30	8/14/04 7:30	30.0021	-143.643	5174
143	8/15/04 4:44	8/14/04 19:44	29.9998	-142.1387	4883
145	8/15/04 19:33	8/15/04 10:33	29.9995	-140.6388	4764
147	8/16/04 13:58	8/16/04 4:58	30.0031	-139.1377	4846
149	8/17/04 0:46	8/16/04 15:46	29.9983	-137.6356	4330
151	8/17/04 18:29	8/17/04 9:29	29.9997	-136.1378	4498
153	8/18/04 4:58	8/17/04 19:58	29.9983	-134.7399	4488
155	8/18/04 21:45	8/18/04 12:45	29.9942	-133.5804	4701
157	8/19/04 7:10	8/18/04 22:10	29.9998	-132.4308	4575
159	8/20/04 0:02	8/19/04 15:02	30.0056	-131.2731	5090
161	8/20/04 9:37	8/20/04 0:37	30.0001	-130.1186	4670
163	8/20/04 23:20	8/20/04 14:20	29.9991	-128.9586	4438
165	8/21/04 16:17	8/21/04 7:17	30.0023	-127.8033	4544
167	8/22/04 4:44	8/21/04 20:44	29.9963	-126.6565	4289
169	8/22/04 18:02	8/22/04 10:02	30.0012	-125.4932	4518
171	8/23/04 3:18	8/22/04 19:18	30.0001	-124.3392	4549
173	8/23/04 19:33	8/23/04 11:33	30.2582	-123.2647	4258
175	8/24/04 3:57	8/23/04 19:57	30.7727	-122.2747	4139
177	8/24/04 19:28	8/24/04 11:28	31.2746	-121.268	3865
179	8/25/04 4:51	8/24/04 20:51	31.7778	-120.2496	3936
182	8/25/04 21:26	8/25/04 13:26	32.0576	-119.6469	1631
184	8/26/04 5:40	8/25/04 21:40	32.3093	-119.1506	1153

Table 5: Station information for cruise P16N.

STATION	DATE (UTC)	DATE (LOCAL)	LATITUDE DEC. DEG	LONGITUDE DEC. DEG	DEPTH METERS
4	2/15/06 20:39	2/15/06 10:39	-14.000	-151.001	4286
6	2/16/06 15:49	2/16/06 5:49	-12.000	-151.000	4849
8	2/17/06 7:26	2/16/06 21:26	-10.000	-151.000	4648
10	2/18/06 5:26	2/17/06 19:26	-8.000	-151.000	4936
12	2/19/06 0:28	2/18/06 14:28	-6.000	-151.000	5031
14	2/19/06 19:42	2/19/06 9:42	-4.000	-150.999	4626
16	2/20/06 14:18	2/20/06 4:18	-2.000	-151.000	4713
18	2/21/06 5:11	2/20/06 19:11	-0.997	-150.995	4685
19	2/21/06 8:55	2/20/06 22:55	-0.500	-150.991	4303
20	2/21/06 19:42	2/21/06 9:42	0.002	-150.990	4304
21	2/22/06 2:30	2/21/06 16:30	0.500	-150.989	3462
22	2/22/06 6:13	2/21/06 20:13	0.999	-150.991	3772
24	2/22/06 22:27	2/22/06 12:27	2.000	-150.997	4351
26	2/23/06 23:30	2/23/06 13:30	4.000	-150.999	5049
28	2/24/06 18:20	2/24/06 8:20	6.000	-151.160	5037
30	2/25/06 9:51	2/24/06 23:51	8.001	-151.499	5096
32	2/26/06 5:09	2/25/06 19:09	10.000	-151.940	5143
34	2/27/06 3:52	2/26/06 17:52	12.003	-151.996	5335
36	2/27/06 19:29	2/27/06 9:29	13.999	-152.002	5661
40	3/1/06 19:15	3/1/06 9:15	18.000	-152.000	5079
45	3/12/06 22:48	3/12/06 12:48	23.001	-152.000	5393
47	3/14/06 2:49	3/13/06 16:49	25.000	-152.000	5361
49	3/15/06 0:31	3/14/06 14:31	27.000	-151.996	5304
51	3/15/06 23:24	3/15/06 13:24	28.994	-151.999	5596
53	3/16/06 19:40	3/16/06 9:40	31.000	-152.000	5299
55	3/17/06 16:33	3/17/06 6:33	33.000	-152.000	5372
57	3/18/06 8:31	3/17/06 22:31	35.001	-151.999	5652
59	3/19/06 8:31	3/18/06 22:31	37.000	-152.000	5530
61	3/20/06 7:44	3/19/06 21:44	39.000	-152.000	5779
62	3/20/06 23:20	3/20/06 13:20	40.000	-152.001	5212
66	3/24/06 0:26	3/23/06 14:26	45.002	-152.000	5281
68	3/24/06 22:42	3/24/06 12:42	46.999	-152.004	5065
70	3/25/06 19:14	3/25/06 9:14	49.000	-152.001	4976
72	3/26/06 14:38	3/26/06 4:38	51.000	-152.000	4972
74	3/27/06 8:16	3/26/06 22:16	53.000	-152.000	4430
76	3/28/06 4:37	3/27/06 18:37	54.998	-152.643	4176
79	3/29/06 5:30	3/28/06 19:30	55.770	-153.000	3882

APPENDIX B

Fe(II) OXIDATION RATES

B.1 Oxidation by Oxygen

The general rate equation for oxidation of Fe(II) by oxygen has been empirically shown to follow:

$$d[\text{Fe(II)}]/dt = -k[\text{Fe(II)}][\text{O}_2][\text{OH}^-]^2$$

where k is the overall rate constant in $\text{M}^{-3}\text{min}^{-1}$ (Millero, 1987). The strong dependence of the oxidation rate on OH^- arises from the unique rate at which individual species react with oxygen. In particular, Fe(OH)_2° and $\text{Fe(CO}_3)_2^{2-}$, which increase with increasing pH, are predicted to oxidize extremely rapidly, thus accounting for the OH^- dependency. The rate was also found to be temperature-dependent. Although the rate constant k is relatively insensitive to temperature changes, the water dissociation constant, K_w , increases with temperature. Thus, for a given pH, the OH^- concentration also increases, accounting for most of the temperature dependency.

Millero et al. (1987) made detailed studies of Fe(II) oxidation rates in seawater and found that aside from the availability of oxidants, the factors that govern the overall rate of oxidation are factors that affect the distribution of Fe(II) species in solution, and include pH, temperature, and salinity. The salinity affects the oxidation rate by leading to the formation of FeCl^+ and FeSO_4° , species which oxidize relatively slowly. For the narrow range of salinities encountered in this study (32-36 psu), changes in the predicted speciation are minimal, and salinity was therefore assumed to be constant (35 psu).

Oxygen was measured by the main hydrography groups on PO2 and P16N both by Winkler titration and by an oxygen-sensor mounted on the CTD. The reporting units for oxygen were in $\mu\text{mol/kg}$, and were converted to molar units where necessary.

The hydroxide concentration was obtained in the following manner. Shipboard measurements of total alkalinity and total dissolved inorganic carbon were used to calculate pH on the free scale, using the program CO2SYS (Lewis and Wallace, 1998), discussed further in [Appendix C](#). The hydroxide concentration on the free scale was calculated from

$$[\text{OH}^-] = K_w[\text{H}^+]^{-1}$$

with K_w corrected for T, P, and S (Millero, 1987; Millero, 1995).

The exponent in the hydroxide term of general rate equation is an approximation that works within a very limited pH range. As the pH deviates from this range, the second-order

dependency begins to deviate as well. Thus, the exponent is in fact a real function of pH. To retain the simplicity of equation 1, the empirical rate data of Santana-Casiano et al. (2005) were used to establish a relationship between $\log k$ and pH.

$$\log k = (2.616) \text{pH}^3 - (58.791) \text{pH}^2 + (438.39) \text{pH} - 1069.6$$

B.2 Oxidation by Hydrogen Peroxide

The rate equation for oxidation of Fe(II) by H₂O₂ is given by Millero et al. (1989)

$$d[\text{Fe(II)}]/dt = -k[\text{Fe(II)}][\text{H}_2\text{O}_2][\text{OH}^-]$$

Unlike the reaction with oxygen, the oxidation by H₂O₂ is approximately first-order with respect to the OH⁻, because the rate-controlling species is FeOH⁺. The H₂O₂ concentration was not measured, but estimated as a function of depth based on the results of Yuan and Shiller (2005), with surface concentrations assigned to be 100 nM attenuating to 1 nM by 200 m. The empirical rate data of Gonzalez-Davila et al. (2005, table 1) were used to define the following relationship between k , T , and pH:

$$\log k = -2.55 + (0.89) \text{pH} - (0.042) (298.15 - T_K)$$

B.3 Calculation of Fe(II) Half-Life

The overall half life time for Fe(II), considering oxidation by both O₂ and H₂O₂ can be expressed as:

$$T_{1/2} = 0.693(k'_{(\text{O}_2)} + k'_{(\text{H}_2\text{O}_2)})^{-1}$$

and is plotted for cruise PO2 in [Fig. 41](#) and for cruise P16N in [Fig. 42](#).

As described in the section 3.2.1, the half-life times calculated in this manner are likely to be underestimates for at least two reasons. First, the empirical rate data are based on first-order assumptions, which the authors acknowledge deteriorate after 1-2 half-lives. Second, treating the rates for oxygen and H₂O₂ oxidation as additive assumes there is no competition between the two oxidants for Fe(II), and assumption that has recently been invalidated. Competition lowers the effectiveness of each, and extends the half-life. In spite of these issues, the calculated half-lives should serve as good approximations of Fe(II) oxidation in seawater, to the extent that current speciation models are valid for natural waters.

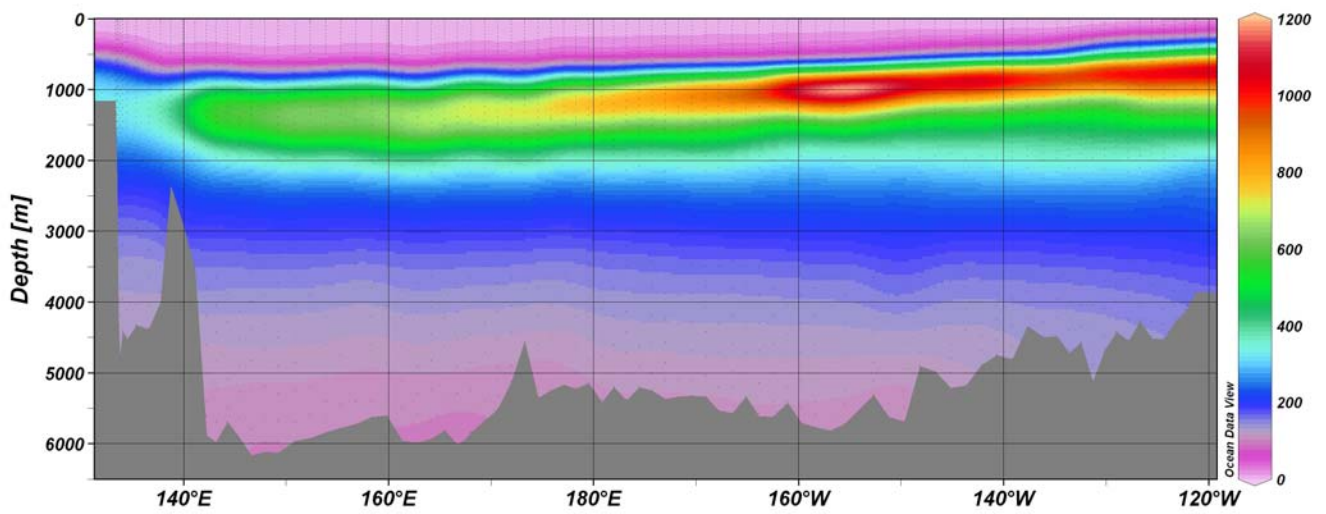


Fig. 41: Calculated half-life of Fe(II) in minutes for the PO2 section.

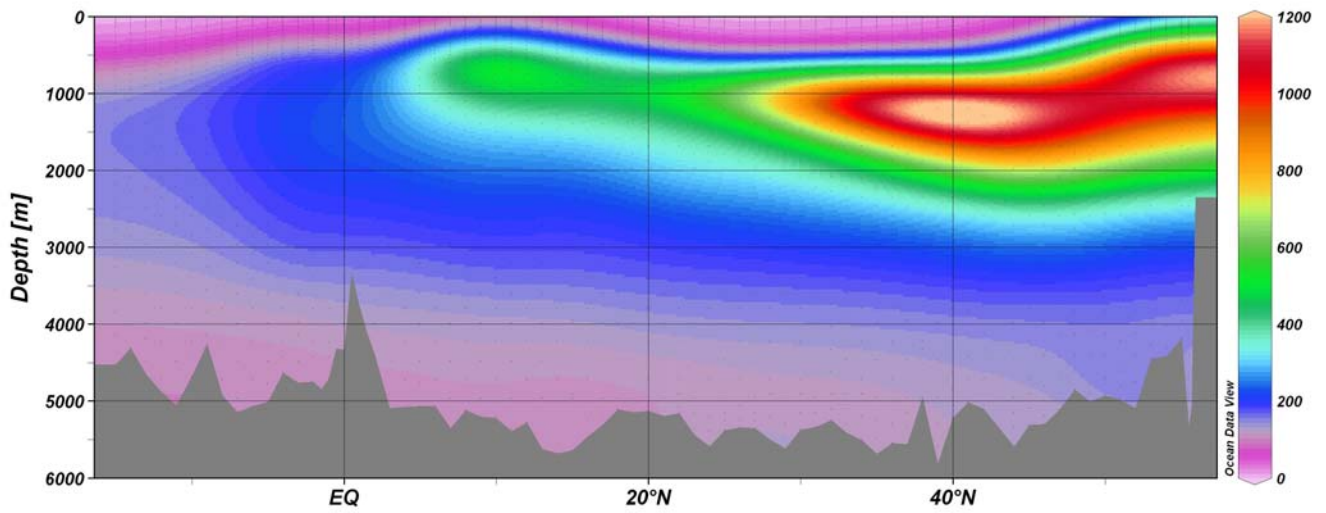


Fig. 42: Calculated half-life of Fe(II) in minutes for the P16N section.

APPENDIX C

CO₂ SYSTEM CALCULATIONS USING CO2SYS

The *in situ* pH was calculated on the free scale for each sample using the CO2SYS program (Lewis and Wallace, 1998). The program calculates the [H⁺] that minimizes the difference between the measured total alkalinity and the calculated total alkalinity, given by the equation

$$\text{TALK}_{(\text{meas})} - \text{TALK}_{(\text{calc})} = \text{TALK}_{(\text{meas})} - ([\text{HCO}_3^-] + 2[\text{CO}_3^{2-}] + [\text{B}(\text{OH})_4^-] + [\text{OH}^-] + 2[\text{PO}_4^{3-}] + [\text{HPO}_4^-] + [\text{H}_3\text{SiO}_4^-] - [\text{H}^+] - [\text{HSO}_4^-] - [\text{HF}] - [\text{H}_3\text{PO}_4]).$$

This equation is solved by expressing each concentration term in the equation as a function of its total concentration in seawater, the appropriate equilibrium constants, and the hydrogen ion concentration (Zeebe and Wolf-Gladrow, 2001). The total concentrations are determined by direct shipboard measurements of dissolved inorganic carbon, phosphate, and silicate, and by using salinity relationships to infer the total concentrations of borate, fluoride, and sulfate. The equilibrium constants are empirically derived values obtained from the literature, adjusted for temperature, salinity, and pressure. The value for the remaining variable, [H⁺], is chosen to be the concentration that minimizes the left-hand side of the equation, determined by iterative substitution.

Using the calculated pH and the corrected constants, the program then calculates the equilibrium concentrations of the individual carbon species (CO₂(aq), HCO₃⁻, and CO₃²⁻). An example showing the input and output variables is shown for Station P16N/49 (Table 3). Fig. 46 (Appendix H) and Fig. 56 (Appendix I) show the calculated pH on the free scale for the PO2 and P16N sections, respectively.

APPENDIX D

PMT CONTROL PROGRAM

D.1 Introduction

GetPMTdata is a VBA program running in the Excel macro environment. GetPMTdata communicates with the Hamamatsu HC135-11 photon-counting PMT module via MegaPipe, a commercially-available VB ActiveX control for serial communication. The software issues commands to the PMT, and in Acquire mode, the incoming data stream (photon counts for a pre-set time interval) is read directly into the GetPMTdata spreadsheet.

D.2 Requirements

- a) Windows XP.
- b) Excel 2000 or above.
- c) Hamamatsu HC135-11 photon-counting PMT module.
- d) A serial port or a serial-USB adaptor. If the latter is used, port configuration software such as Keyspan will be required.
- e) The Excel file GetPMTdata.xls.
- f) MegaPipe ActiveX control (provided).
- g) Rainin-RP1 Dynamax peristaltic pump (optional).

D.3 Software Installation

- a) Be sure Excel is installed.
- b) Install MegaPipe ActiveX control.
- c) If using a serial-USB adaptor, install adaptor software.
- d) Copy GetPMTdata.xls onto Excel default directory.

D.4 Hardware Installation

- a) Make sure PMT is *really* protected from light.
- b) Attach PMT to the serial port, or to the port adaptor. If using a port adaptor, attach the port adaptor to a USB slot on the computer, then open the port adaptor software. Check to see that the port(s) are enabled and verify virtual port numbers.
- c) Supply power to PMT.

D.5 Software Setup

- a) Open GetPMTdata.xls. If prompted, you must enable macros and allow ActiveX controls.
- b) If the Menu worksheet is not visible when the file opens, select any worksheet, and press the Menu tab at the bottom. Click "Clear Previous" button. Whenever this is done, the software restores the default settings, removes any old data, and should arrange the worksheets so that the Menu worksheet is in on the left side of the display, and the Summary and Settings worksheets are on the right.
- c) Select the Settings worksheet and set the value of pmtSetting(1) to the appropriate comport number. If PMT is directly connected to your computer, this is probably ComPort 1. Otherwise, enter the virtual comport number assigned by the adaptor software.

d) Returning to the Menu worksheet, click "Initialize PMT." A message box should appear confirming that the PMT has been initialized. If there is no response, it may be because the PMT is not powered, the PMT (or port adaptor) is not connected to the computer, or the comport is not configured properly.

D.6 Software Operation

The software acquires data in a manner dictated by the design of the Hamamatsu photon-counting PMT. In the Acquire mode, these PMTs count photons over a user-defined counting interval. When the Acquire button is clicked, GetPMTData commands the PMT to count photon pulses over that interval. The PMT then returns the number of pulses counted back to the software in hexadecimal format, via the serial connection. The software converts the response to ASCII integer format, and inserts the value into the RawData spreadsheet. Multiple readings can be acquired for a single sample; these readings will all be stored in the RawData spreadsheet. The average and standard deviation of the responses are inserted into the Summary spreadsheet when the Acquire mode is exited. These responses are also graphically presented in the Excel charts below the main menu.

D.7 Software Settings

- pmtSetting(1): This is the comport setting. Set it once as described above.
- pmtSetting(2): Not functional at this time.
- pmtSetting(3): This is the counting time, in intervals of 10 ms. The default is 10 (i.e. an interval of 100 ms). Set higher for weak signals, and lower for strong signals. Note that the PMT counter has the potential to become "saturated" – do not make this setting too high!
- pmtSetting(4): Due to signal variance inherent in the system, the user may wish to "sample" the PMT signal; that is, collect more than one reading for a particular experimental event. The default is 30 readings per sample. The counting time in the default mode is 100 ms, thus 30 readings will be made in approximately 3 seconds.
- pmtSetting(5): This setting is currently not in use.
- pmtSetting(6): The voltage to the PMT can be adjusted to accommodate weak or strong signals. This setting is currently not used.
- runSetting(1): The software can collect data for a pre-specified number of samples, set here, by setting runSetting (3) to "On."
- runSetting(2): This specifies the interval of time between auto samples.
- runSetting(4): This sets a time delay prior to data acquisition. It is useful to allow for travel time from sample to detector.
- calSetting(1): This is the number of spiked samples to be used in calibration, including the blank sample.
- calSetting(2): This is the spike increment.
- rp1Setting(1): This is the comm. port setting for the Rainin RP1 Pump.
- rp1Setting(2): This is the desired pump speed (rpm).
- rp1Setting(3): This is the On/Off setting for software pump control.

D.8 Program Code

```
' program to read data from Hamamatsu HC135-11 photon-counting photomultiplier
' serial port communication requires installation of MegaPipe VBA control (see instructions)
' program written by Paul Hansard in VBA, running under Excel
' initialize
```

```
Dim talkback As String, byt As Integer, PMTcount As Integer
Public pump_init As String
```

```
Private Sub CommandButton1_Click()
' this sub removes all previous data, and restores setting defaults
Application.Windows.Arrange ArrangeStyle:=xlArrangeStyleTiled
response = MsgBox("Clear All Data?", vbOKCancel + vbQuestion, "")
If response = 1 Then
' clear previous data
Worksheets("Rawdata").Range("B2:EZ500").ClearContents
Worksheets("Rawdata").Range("C1:EZ1").ClearContents
Worksheets("Summary").Range("A2:E200").ClearContents
Set curcell = Worksheets("Settings").Cells(6, 2)
curcell.Value = 0
End If
End Sub
```

```
Private Sub CommandButton2_Click()
' subroutine to initialize PMT
' this sub attempts to communicate with PMT, using parameter settings on page 3,
' and returns an error setting to sheet 3 if no comm established
' first initialize
Dim cm, xy, sdata As String
Dim vdata As Variant
' get number of readings per sample from Settings sheet
Set curcell = Worksheets("Settings").Cells(5, 2)
nread = curcell.Value
' assign data labels
For I = 1 To nread
Set curcell = Worksheets("RawData").Cells(I + 1, 1)
curcell.Value = I
Next I
' get commport setting
Set curcell = Worksheets("Settings").Cells(2, 2)
PortOpen = curcell.Value
pmtport = "Com" + LTrim(Str(PortOpen))
' get # periods to count
Set curcell = Worksheets("Settings").Cells(4, 2)
nperiod = curcell.Value
' this opens the port and sends the code for default PMT power to the PMT
With MegaPipeCtrl1
.Port = pmtport
.BaudRate = 9600
.Parity = pNone
.StopBits = 1
.DataBits = 8
```

```

.RThreshold = 2
.PortOpen = True
.OutputStringData = "D" + Chr(13)
End With
' The following command tells the PMT how many 10 ms periods to count
MegaPipeCtrl1.OutputStringData = "P" + Chr(nperiod) + Chr(13)
End Sub

```

```

Private Sub CommandButton3_Click()
' this is data acquisition procedure
Set curcell = Worksheets("Settings").Cells(4, 2)
fac1 = curcell.Value
Set curcell = Worksheets("Settings").Cells(5, 2)
fac2 = curcell.Value
Delay = fac1 * fac2 / 100
Set curcell = Worksheets("Settings").Cells(8, 2)
ncollect = curcell.Value
Set curcell = Worksheets("Settings").Cells(9, 2)
sampling_interval = curcell.Value
' get pump settings
Set curcell = Worksheets("Settings").Cells(17, 2)
pumpport = "Com" + LTrim(Str(curcell.Value))
Set curcell = Worksheets("Settings").Cells(18, 2)
pumpspeed = curcell.Value * 100
Set curcell = Worksheets("Settings").Cells(19, 2)
autopump = curcell.Value
Set curcell = Worksheets("Settings").Cells(2, 2)
pmpport = "Com" + LTrim(Str(curcell.Value))
' If (autopump = "On" And pump_init <> "Yes") Then
If (autopump = "On") Then
    Call initialize_pump(pumpport)
    pump_init = "Yes"
    Call start_pump(pumpspeed, pumpport)
Else
    Call start_pump(pumpspeed, pumpport)
End If
' now must see if autoacquire is activated, if not, do manual
Set curcell = Worksheets("Settings").Cells(10, 2)
autocollect = curcell.Value
Set curcell = Worksheets("Settings").Cells(11, 2)
tdelay = curcell.Value
If autopump = "On" And tdelay >= 20 Then
    Start = Timer
    Do While Timer < Start + (tdelay - 10)
    Loop
    Call prime_pump(pumpspeed)
    Start = Timer
    Do While Timer < Start + 8
    Loop
Else
    Start = Timer

```

```

    Do While Timer < Start + tdelay
    Loop
End If
If autocollect = "Off" Or ncollect = 1 Then
    Call acquire(pmtport)
Else
    Call acquire(pmtport)
    ncount = 1
    Do
        Start = Timer ' Set start time.
        Do While Timer < Start + (sampling_interval - Delay)
        Loop
        Call acquire(pmtport)
        ncount = ncount + 1
    Loop Until (ncount = ncollect)
End If
If autopump = "On" Then
    Call stop_pump(pumpport)
End If
MsgBox ("Acquire Finished")
End Sub

```

```

Private Sub CommandButton4_Click()
' this is the calibration routine
' this subroutine collects and graphs calibration data, calculates slope and detection limits
' assumes curve linearity, DLs calculated per Long and Wisefordner (1982)
' first clear previous calibration data
Set curcell = Worksheets("Settings").Cells(14, 2)
lastCdate = curcell.Value
response = MsgBox("Clear Previous Calibration Data from" + Str(lastCdate) + "?",
    vbOKCancel + vbQuestion, "")
If response = 1 Then
    ' next get settings
    Worksheets("Calibration").Range("b2:c10").ClearContents
    Set curcell = Worksheets("Settings").Cells(12, 2)
    nstds = curcell.Value
    Set curcell = Worksheets("Settings").Cells(13, 2)
    stdinc = curcell.Value
    ' then prompt user for samples
    For I = 1 To nstds
        MsgBox ("Begin Pumping +" + Str((I - 1) * stdinc) + " Standard")
        Call CommandButton3_Click
        Set myrange = Worksheets("RawData").Columns(2)
        myave = Application.WorksheetFunction.Average(myrange)
        mystdev = Application.WorksheetFunction.StDev(myrange)
        Set curcell = Worksheets("Calibration").Cells(I + 1, 2)
        curcell.Value = (I - 1) * stdinc
        Set curcell = Worksheets("Calibration").Cells(I + 1, 3)
        curcell.Value = myave
        Set curcell = Worksheets("Calibration").Cells(I + 1, 4)
        curcell.Value = mystdev
    Next I
End If

```

```

Next I
Set curcell = Worksheets("Settings").Cells(14, 2)
curcell.Value = Now()
Set curcell = Worksheets("Calibration").Cells(16, 2)
calSlope = curcell.Value
Set curcell = Worksheets("Settings").Cells(15, 2)
curcell.Value = calSlope
End If
Call CommandButton1_Click
End Sub

```

```

Private Sub MegaPipeCtrl1_OnComm(ByVal count As Long)
' if RThreshold is 0, this event is never fired.
' during file-transfer process, this event is never fired even if RThreshold > 0.
Dim vdata As Variant
Dim sdata As String
Dim I, bcount As Integer
I = MegaPipeCtrl1.AvailDataCount
MsgBox ("PMT Initialized!")
bcount = count
' convert Variant to String
vdata = MegaPipeCtrl1.Read(count)
For I = 1 To count
sdata = sdata & Chr(vdata(I - 1))
Next I
I = MegaPipeCtrl1.AvailDataCount
MegaPipeCtrl1.PortOpen = False
End Sub

```

```

Public Sub readcounts(Ingresult)
' this routine reads incoming counts from PMT in binary, converts to human format
Dim instring As Variant
Dim sdata As String
Do
dummy = DoEvents()
Loop Until (MegaPipeCtrl1.AvailDataCount >= 4)
instring = MegaPipeCtrl1.InputData
' translate into ascii
Ingresult = Val(AscB(MidB(instring, 4, 1)))
Ingresult = Ingresult + (256 * Val(AscB(MidB(instring, 3, 1))))
Ingresult = Ingresult + (65536 * Val(AscB(MidB(instring, 2, 1))))
Ingresult = Ingresult + (16777216 * Val(AscB(MidB(instring, 1, 1))))
End Sub

```

```

Public Sub acquire(pmtport)
' this sub tells the PMT to start counting
Dim myrange As Range
Dim I, j, numread As Integer
' Clear Rawdata column 2
Worksheets("Rawdata").Range("b2:b201").ClearContents
' get time interval between samples

```

```

Set curcell = Worksheets("Settings").Cells(9, 2)
autoset3 = curcell.Value
' get number of this sample
Set curcell = Worksheets("Settings").Cells(6, 2)
nthsamp = curcell.Value + 1
' get number of readings to collect
Set curcell = Worksheets("Settings").Cells(5, 2)
nread = curcell.Value
With MegaPipeCtrl1
    .Port = pmtport
    .BaudRate = 9600
    .Parity = pNone
    .StopBits = 1
    .DataBits = 8
    .RThreshold = 0
    .PortOpen = True
End With
Set curcell = Worksheets("RawData").Cells(1, nthsamp + 2)
curcell.Value = nthsamp
For I = 1 To nread
    lngresult = 0
    MegaPipeCtrl1.OutputStringData = "S" + Chr(13)
    Call readcounts(lngresult)
    Set curcell = Worksheets("RawData").Cells(I + 1, 2)
    curcell.Value = lngresult
    Set curcell = Worksheets("RawData").Cells(I + 1, nthsamp + 2)
    curcell.Value = lngresult
Next I
Set curcell = Worksheets("Settings").Cells(6, 2)
curcell.Value = nthsamp
MegaPipeCtrl1.PortOpen = False
Set myrange = Worksheets("RawData").Columns(2)
myave = Application.WorksheetFunction.Average(myrange)
mystdev = Application.WorksheetFunction.StDev(myrange)
Worksheets("Summary").Activate
Set curcell = Worksheets("Summary").Cells(nthsamp + 1, 1)
curcell.Value = Time
Set curcell = Worksheets("Summary").Cells(nthsamp + 1, 2)
curcell.Value = nthsamp
Set curcell = Worksheets("Summary").Cells(nthsamp + 1, 3)
curcell.Value = myave
Set curcell = Worksheets("Summary").Cells(nthsamp + 1, 4)
curcell.Value = mystdev
ActiveWindow.ScrollRow = 10
Worksheets("Menu").Activate
End Sub

Private Sub initialize_pump(pumpport)
' this sub establishes pump communication
With MegaPipeCtrl2
    .Port = pumpport

```

```

.FlowControl = None
.Parity = pEven
.BaudRate = 19200
.DataBits = [Eight Bits]
.StopBits = 1
.RThreshold = 1
End With
MegaPipeCtrl2.PortOpen = True
' The first command initializes the pump
MegaPipeCtrl2.OutputStringData = Chr(255) + Chr(129)
' The second command locks the pump
MegaPipeCtrl2.OutputStringData = Chr(10) + "L" + Chr(13)
MegaPipeCtrl2.PortOpen = False
End Sub

```

```

Private Sub start_pump(pumpspeed, pumpport)
' sub to start pump operation at desired speed
MegaPipeCtrl2.PortOpen = True
pumpcommand = "R" + LTrim(Str(pumpspeed))
MegaPipeCtrl2.OutputStringData = Chr(10) + pumpcommand + Chr(13)
MegaPipeCtrl2.OutputStringData = Chr(10) + "jF" + Chr(13)
MegaPipeCtrl2.PortOpen = False
End Sub

```

```

Private Sub prime_pump(pumpspeed)
' sub to jet the pump 20 s prior to count in order to remove any bubbles from flowcell
pumpcommand = "R" + LTrim(Str(pumpspeed))
MegaPipeCtrl2.PortOpen = True
MegaPipeCtrl2.OutputStringData = Chr(10) + "R4000" + Chr(13)
Start1 = Timer ' Set start time.
Do While Timer < Start1 + 1.5
Loop
MegaPipeCtrl2.OutputStringData = Chr(10) + pumpcommand + Chr(13)
MegaPipeCtrl2.PortOpen = False
End Sub

```

```

Private Sub stop_pump(pumpport)
' sub to stop pump so that samples can be switched
MegaPipeCtrl2.PortOpen = True
MegaPipeCtrl2.OutputStringData = Chr(10) + "R0000" + Chr(13)
MegaPipeCtrl2.OutputStringData = Chr(10) + "U" + Chr(13)
MegaPipeCtrl2.PortOpen = False
End Sub

```

```

Private Sub MegaPipeCtrl2_OnComm(ByVal count As Long)
' this sub waits for the pump to signal that it is on and waiting commands
instring = MegaPipeCtrl2.InputData
End Sub

```

APPENDIX E

CALIBRATION DATA

Table 6: Calibration data for cruise PO2.

Station Number	Collection Time (Local)	Cal. Points	Cal. Range pM	Cal. Slope (mV/pM)	Slope Error (mV/pM)	Intercept (mV)	Int Error (mV)	Blank (mV)	Detection Limit ^(a) (pM)
8	6/18/04 14:26	4	0-300	0.06	0.001	1.8	0.26	1.7	13
10	6/18/04 23:07	2	0-200	0.07		0.9		0.9	
12	6/19/04 13:09	5	0-200	0.06	0.061	3.7	0.30	3.9	15
14	6/22/04 9:30	2	0-200	0.06		1.7		1.7	
16	6/22/04 19:43	2	0-200	0.08		1.7		1.7	
18	6/23/04 9:42	2	0-200	0.07		1.7		1.7	
20	6/24/04 5:43	2	0-200	0.09		1.8		1.8	
22	6/24/04 15:16	2	0-300	0.07		2.1		2.1	
24	6/24/04 23:27	4	0-300	0.06	0.010	1.7	0.75	2.1	35
26	6/25/04 12:20	2	0-300	0.10		2.9		2.9	
28	6/26/04 6:15	2	0-200	0.14		2.0		2.0	
30	6/27/04 5:56	2	0-200	0.10		2.5		2.5	
32	6/27/04 16:59	2	0-200	0.08		3.0		3.0	
34	6/28/04 17:58	2	0-200	0.12		4.2		4.2	
36	6/29/04 9:46	2	0-200	0.19		4.5		4.5	
38	6/29/04 21:31	2	0-200	0.12		4.5		4.5	
40	6/30/04 14:49	2	0-200	0.14		4.9		4.9	
44	7/2/04 7:54	2	0-100	0.13		4.0		4.0	
46	7/2/04 21:02	4	0-200	0.12	0.002	1.9	0.28	2.2	7
50	7/5/04 13:10	2	0-200	0.18		2.7		2.7	

Table 6 Continued:

Station Number	Collection Time (Local)	Cal. Points	Cal. Range μM	Cal. Slope (mV/ μM)	Slope Error (mV/ μM)	Intercept (mV)	Int Error (mV)	Blank (mV)	Detection Limit ^(a) (μM)
52	7/6/04 6:42	2	0-100	0.09		3.2		3.2	
54	7/6/04 18:56	2	0-100	0.09		3.3		3.3	
56	7/6/04 17:01	2	0-100	0.15		2.2		2.2	
58	7/8/04 8:39	2	0-200	0.08		3.0		3.0	
60	7/8/04 19:57	2	0-200	0.11		2		2	
62	7/9/04 12:53	5	0-200	0.09	0.004	2.4	0.47	2.7	16
64	7/10/04 9:49	2	0-100	0.06		2.1		2.1	
66	7/10/04 21:20	2	0-100	0.11		3.7		3.7	
68	7/11/04 13:16	2	0-100	0.16		3.5		3.5	
70	7/12/04 8:18	2	0-100	0.14		2.8		2.8	
72	7/12/04 20:26	2	0-100	0.15		3.0		3.0	
74	7/13/04 14:56	2	0-100	0.13		3.1		3.1	
76	7/14/04 5:09	2	0-100	0.11		3.2		3.2	
78	7/14/04 16:08	2	0-100	0.13		4.8		4.8	
82	7/15/04 10:35	2	0-100	0.13		3.1		3.1	
84	7/15/04 20:50	2	0-100	0.10		3.7		3.7	
86	7/15/04 11:15	2	0-100	0.09		2.3		2.3	
88	7/16/04 7:44	2	0-100	0.13		4.3		4.3	
90	7/16/04 18:03	2	0-100	0.09		1.9		1.9	
92	7/17/04 14:10	2	0-100	0.09		3.6		3.6	
94	7/18/04 5:30	2	0-100	0.13		2.8		2.8	
96	7/18/04 17:25	2	0-100	0.13		2.8		2.8	
98	7/19/04 13:53	2	0-100	0.06		1.8		1.8	
100	7/20/04 5:38	2	0-100	0.11		3.2		3.2	
102	7/20/04 16:37	2	0-100	0.10		1.2		1.2	

Table 6 Continued:

Station Number	Collection Time (Local)	Cal. Points	Cal. Range pM	Cal. Slope (mV/pM)	Slope Error (mV/pM)	Intercept (mV)	Int Error (mV)	Blank (mV)	Detection Limit ^(a) (pM)
104	7/21/04 12:43	2	0-100	0.07		2.1		2.1	
106	7/21/04 23:14	2	0-100	0.09		1.6		1.6	
108	7/22/04 14:38	2	0-100	0.08		1.3		1.3	
113	8/1/04 11:48	4	0-100	0.11	0.004	2.7	0.40	2.8	11
115	8/2/04 8:20	2	0-100	0.10		1.8		1.8	
117	8/2/04 21:05	2	0-100	0.08		1.8		1.8	
119	8/3/04 13:58	2	0-100	0.07		2.2		2.2	
121	8/7/04 11:33	2	0-100	0.07		1.2		1.2	
123	8/8/04 4:33	2	0-100	0.07		1.2		1.2	
125	8/8/04 17:22	2	0-50	0.05		1.2		1.2	
127	8/9/04 10:00	2	0-50	0.05		1.1		1.1	
129	8/10/04 9:53	2	0-50	0.03		0.9		0.9	
131	8/10/04 21:37	2	0-50	0.04		0.9		0.9	
135	8/12/04 9:42	2	0-50	0.04		0.7		0.7	
137	8/12/04 20:56	5	0-200	0.04	0.002	0.6	0.26	0.8	19
139	8/13/04 12:19	2	0-50	0.03		1.3		1.3	
141	8/14/04 7:30	2	0-50	0.04		1.4		1.4	
143	8/14/04 19:44	2	0-50	0.05		1.5		1.5	
145	8/15/04 10:33	2	0-50	0.04		1.2		1.2	
147	8/16/04 4:58	2	0-50	0.06		3.1		3.1	
149	8/16/04 15:46	2	0-50	0.04		2.0		2.0	
151	8/17/04 9:29	2	0-50	0.06		2.4		2.4	
153	8/17/04 19:58	2	0-50	0.06		2.0		2.0	
155	8/18/04 12:45	2	0-50	0.02		1.2		1.2	
157	8/18/04 22:10	2	0-50	0.04		1.9		1.9	
159	8/19/04 15:02	2	0-50	0.06		2.4		2.4	
161	8/20/04 0:37	2	0-50	0.09		2.8		2.8	

Table 6 Continued:

Station Number	Collection Time (Local)	Cal. Points	Cal. Range pM	Cal. Slope (mV/pM)	Slope Error (mV/pM)	Intercept (mV)	Int Error (mV)	Blank (mV)	Detection Limit ^(a) (pM)
163	8/20/04 14:20	2	0-50	0.04		2.8		2.8	
165	8/21/04 7:17	2	0-50	0.07		3.4		3.4	
167	8/21/04 20:44	2	0-50	0.08		3.2		3.2	
169	8/22/04 10:02	4	0-150	0.08	0.002	2.7	0.21	2.8	8
171	8/22/04 19:18	2	0-50	0.05		3.2		3.2	
173	8/23/04 11:33	2	0-50	0.05		3.6		3.6	
175	8/23/04 19:57	2	0-50	0.05		4.1		4.1	
177	8/24/04 11:28	2	0-50	0.07		3.9		3.9	
179	8/24/04 20:51	2	0-50	0.07		4.2		4.2	
182	8/25/04 13:26	2	0-50	0.10		5.7		5.7	
184	8/25/04 21:40	2	0-100	0.09		3.6		3.6	

(a) Detection limit is calculated as 3 standard deviations of the intercept divided by the calibration slope.

Table 7: Calibration data for cruise P16N.

Station Number	Collection Time	Luminol Age	Stds	Range	Cal. Slope	Slope Error	Intercept	Int. Error	Blank	Detection Limit ^(a)
4	2/15/06 10:39	3	4	0-75	5.60	0.26	78.0	12.0	89.0	6.4
6	2/16/06 5:49	2	4	0-75	3.30	0.32	83.0	30.0	110.0	27.3
8	2/16/06 21:26	4	4	0-75	4.90	0.51	50.0	25.0	70.0	15.3
10	2/17/06 19:26	3	4	0-75	3.40	0.43	70.0	20.0	60.0	17.6
12	2/18/06 14:28	4	5	0-100	3.74	0.30	58.0	17.0	66.0	13.6
14	2/19/06 9:42	5	5	0-100	3.80	0.28	43.0	17.0	66.0	13.4
16	2/20/06 4:18	5	5	0-100	4.00	0.32	60.0	19.0	104.0	14.3
18	2/20/06 19:11	6	4	0-75	4.50	0.15	139.0	7.0	145.0	4.7
19	2/20/06 22:55	6			(4.5)				135.0	
20	2/21/06 9:42	7	5	0-100	5.10	0.38	206.0	23.0	236.0	13.5
21	2/21/06 16:30	5	4	0-75	4.00	0.35	124.0	15.0	124.0	11.3
22	2/21/06 20:13	6	4	0-75	4.40	0.38	111.0	18.0	111.0	12.3
24	2/22/06 12:27	6			(4.4)				124.0	
26	2/23/06 13:30	7	5	0-100	5.50	0.35	63.0	21.0	89.0	11.5
28	2/24/06 8:20	8	5	0-100	5.00	0.27	101.0	16.0	130.0	9.6
30	2/24/06 23:51	9	4	0-75	4.80	0.29	96.0	18.0	96.0	11.3
32	2/25/06 19:09	5	4	0-75	4.20	0.40	83.0	19.0	97.0	13.6
34	2/26/06 17:52	6	4	0-75	3.80	0.28	100.0	13.0	97.0	10.3
36	2/27/06 9:29	6	4	0-75	3.60	0.28	165.0	13.0	160.0	10.8
40	3/1/06 9:15	8	4	0-75	4.50	0.37	89.0	17.0	98.0	11.3
45	3/12/06 12:48	11	3	0-50	2.90	0.14	215.0	9.0	158.0	9.3
47	3/13/06 16:49	12	3	0-50	4.00	0.08	184.0	5.0	182.0	3.8
49	3/14/06 14:31	13	5	0-100	5.60	0.31	162.0	19.0	162.0	10.2
51	3/15/06 13:24	14	5	0-100	4.00	0.30	137.0	18.0	158.0	13.5
53	3/16/06 9:40	15	4	0-75	3.30	0.32	168.0	17.0	182.0	15.5
55	3/17/06 6:33	16	3	0-50	4.80	0.08	312.0	6.0	210.0	3.8
57	3/17/06 22:31	16	3	0-50	4.00	0.26	182.0	19.0	186.0	14.3

Table 7 Continued:

Station Number	Collection Time	Luminol Age	Stds	Range	Cal. Slope	Slope Error	Intercept	Int. Error	Blank	Detection Limit ^(a)
59	3/18/06 22:31	4	2	0-25	4.20		135.0		100.0	0.0
61	3/19/06 21:44	3	3	0-50	3.00	0.35	126.0	11.0	135.0	11.0
62	3/20/06 13:20	3	4	0-75	3.30	0.24	133.0	11.0	133.0	10.0
66	3/23/06 14:26	6	4	0-75	4.00	0.50	138.0	16.0	101.0	12.0
68	3/24/06 12:42	7	4	0-75	3.60	0.20	135.0	10.0	144.0	8.3
70	3/25/06 9:14	8	4	0-75	4.30	0.19	164.0	9.0	167.0	6.3
72	3/26/06 4:38	9	4	0-75	3.90	0.36	124.0	17.0	138.0	13.1
74	3/26/06 22:16	1	3	0-50	2.90	0.10	161.0	3.0	162.0	3.1
76	3/27/06 18:37	2	4	0-75	2.80	0.16	122.0	8.0	113.0	8.6
79	3/28/06 19:30	3	4	0-75	3.70	0.14	145.0	6.0	134.0	4.9

(a) Detection limit is calculated as 3 standard deviations of the intercept divided by the calibration slope.

(b) Calibration slopes from stations 18 and 22 were used to calibrate data from stations 19 and 24, respectively.

Table 8. Summary of duplicate sample results for PO2 and P16N.

Cruise	Station	Sample Date	Bottle	Sample1 pM Fe(II)	Sample2 pM Fe(II)	RSD ^(a)
PO2	50	7/5/04 13:10	1	12.6	14.8	11.3
PO2	52	7/6/04 6:42	1	45.6	38.9	11.2
PO2	54	7/6/04 18:56	1	8.5	7.3	10.2
PO2	56	7/6/04 17:01	1	21.6	19.6	7.0
PO2	58	7/8/04 8:39	12	28.4	24.5	10.3
PO2	60	7/8/04 19:57	12	21.1	18.3	9.9
PO2	62	7/9/04 12:53	12	23.5	20.1	10.9
PO2	64	7/10/04 9:49	12	32.3	19.4	35.4
PO2	66	7/10/04 21:20	12	23.6	15.5	29.6
PO2	68	7/11/04 13:16	12	15.6	16.9	5.4
PO2	72	7/12/04 20:26	1	29.5	26.8	6.7
PO2	84	7/15/04 20:50	1	10.2	10.2	0.0
PO2	90	7/16/04 18:03	1	31.9	34.1	4.7
PO2	94	7/18/04 5:30	1	24.2	27.3	8.3
PO2	98	7/19/04 13:53	12	15.9	7.9	47.1
P16N	12	2/18/06 14:28	12	53.5	42.8	15.7
P16N	14	2/19/06 9:42	12	72.4	57.1	16.7
P16N	16	2/20/06 4:18	12	45.8	29.5	30.5
P16N	22	2/21/06 20:13	7	8.2	11.8	25.7
P16N	24	2/22/06 12:27	7	20.7	14.3	25.7
P16N	26	2/23/06 13:30	7	6.9	6.4	5.8
P16N	28	2/24/06 8:20	3	38.2	36.0	4.2
P16N	30	2/24/06 23:51	12	46.7	48.5	2.8
P16N	30	2/24/06 23:51	3	10.4	8.8	12.3
P16N	32	2/25/06 19:09	2	12.4	10.7	10.2
P16N	34	2/26/06 17:52	3	13.7	15.0	6.5
P16N	36	2/27/06 9:29	12	53.9	57.2	4.2
P16N	40	3/1/06 9:15	1	26.2	22.7	10.3
P16N	45	3/12/06 12:48	1	123.4	120.7	1.6
P16N	47	3/13/06 16:49	5	1.8	0.3	106.1
P16N	47	3/13/06 16:49	1	20.8	23.5	8.8
P16N	49	3/14/06 14:31	10	22.7	19.6	10.1
P16N	49	3/14/06 14:31	1	30.0	26.4	9.0
P16N	51	3/15/06 13:24	11	21.3	21.8	1.6
P16N	51	3/15/06 13:24	1	53.3	48.5	6.6
P16N	53	3/16/06 9:40	1	76.1	77.6	1.4
P16N	55	3/17/06 6:33	10	8.3	6.9	13.6
P16N	55	3/17/06 6:33	1	27.1	30.2	7.7
P16N	57	3/17/06 22:31	1	17.8	18.8	3.9
P16N	59	3/18/06 22:31	1	23.8	22.9	2.9
P16N	61	3/19/06 21:44	4	5.0	2.7	43.0
P16N	62	3/20/06 13:20	12	16.1	13.6	11.5
P16N	62	3/20/06 13:20	4	3.6	1.8	47.1
P16N	66	3/23/06 14:26	12	13.0	13.3	1.3

Table 8 Continued:

Cruise	Station	Sample Date	Bottle	Sample1 pM Fe(II)	Sample2 pM Fe(II)	RSD ^(a)
P16N	68	3/24/06 12:42	12	49.4	43.1	9.8
P16N	68	3/24/06 12:42	8	36.9	26.1	24.3
P16N	70	3/25/06 9:14	11	24.2	21.6	7.9
P16N	70	3/25/06 9:14	8	18.8	15.6	13.4
P16N	74	3/26/06 22:16	11	62.4	60.7	2.0

(a) relative standard deviation

APPENDIX F

METHOD DETAILS

F.1 Advance Preparation

1. Prepare 10 mM Fe(II) stock solution.
 - 1.1 Fill trace-metal clean 1 L FEP container with ~800 mL EPure water.
 - 1.2 Add 16 mL 6M q-HCl and shake.
 - 1.3 Add 3.92 g of $\text{Fe}(\text{NH}_4)_2(\text{SO}_4)_2 \cdot 6\text{H}_2\text{O}$ and shake vigorously until completely dissolved. Fill to 1 L with EPure water and shake.
 - 1.4 Store at 4°C in dark. Shelf life ~ 1 month. Shake prior to use.
2. Prepare 1 mM luminol reagent.
 - 2.1 Fill clean 2 L FEP container with ~ 1700 mL EPure water.
 - 2.2 Add 150 mL concentrated NH_4OH (11 M).
 - 2.3 Add 0.354 g powdered luminol and shake vigorously. Allow to sit 24 hrs in dark to allow for complete dissolution.
 - 2.4 Add 50 mL 6M q-HCl and shake thoroughly.
 - 2.5 Heat at 60°C for 15 hours. Cool to room temperature.
 - 2.6 Adjust volume to 2L with q-HCl and EPure water so that pH is 10.25-10.3.
3. Collect seawater for calibration.
 - 3.1 Give pre-cleaned 2L opaque HDPE container to Bill Landing.
 - 3.2 Request filtered (0.2 μm) seawater from specific depth/GOFLO.
 - 3.3 Allow to sit for 24 h prior to use.
 - 3.4 Immediately prior to use in calibration, acidify to pH 6 by adding 20 μL 6M q-HCl to 100 mL seawater.
4. Prepare sample containers for sample collection.
 - 4.1 Add 500 μL q-HCl to sample containers containing either seawater or EPure water. Allow to sit for 6 h.
 - 4.2 Under clean conditions, empty containers, rinse each container 3 times with EPure water, and cap.
 - 4.3 Immediately prior to sample collection, add 29 μL 6M q-HCl to each container and cap.

F.2 Sample Collection

1. Remove filter from freezer 1 h prior to sampling.
2. Begin sample collection as soon as GOFLO bottles are secure in clean van. Samples are collected from shallowest to deepest, i.e. GOFLO 12 to 1.
 - 2.1. Loosen vent nut at top of GOFLO.
 - 2.2. Insert filter tube into GOFLO port.
 - 2.3. Prior to collecting first sample, allow seawater to flow through filter for 1 minute (~ 6 filter volumes). Subsequent samples are collected after rinsing filter for 30 seconds (3 filter volumes).
 - 2.4. Prior to collecting first sample, start watch chronometer or otherwise note exact time.
 - 2.5. Uncap sample container, taking care not to lose acid preservative.
 - 2.6. Fill container to shoulder, taking care not to shield container mouth from any water drops falling off GOFLO.

- 2.7. Cap container tightly and shake well.
3. Repeat 2.1-2.7 until all GOFLOs have been sampled.
4. Collect one duplicate sample from one GOFLO bottle.

F.3 System Preparation and Calibration

1. Rinse system and purge any air.
 - 1.1. Pump 20-30 mL 0.024 M q-HCl through luminol and sample lines.
 - 1.2. Pump 20-30 mL EPure water through luminol and sample lines.
 - 1.3. Pump acidified seawater (ASW) through sample line and luminol reagent through reagent line until low stable system response is obtained. [Baseline response may vary with luminol age but should be stable over ~12 hour periods.]
 - 1.4. Purging of air can be accomplished by manually accelerating pump speed.
 - 1.5. Pump control software will also ramp pump speed for 2 seconds approximately 20 seconds prior to analysis.
 - 1.6. Avoid introduction of air to system by removing lines from solution only when pump is off.
2. Prepare intermediate and working stock solutions immediately prior to analysis.
 - 2.1. Prepare 500 μM Fe(II) intermediate stock by adding 500 μL 10 mM stock solution to 100 mL 0.024 q-HCl in clean 125 mL HDPE container and shaking thoroughly.
 - 2.2. Prepare 500 nM Fe(II) working stock by adding 100 μL 500 μM Fe(II) intermediate stock (2.1) to 100 mL 0.024 q-HCl in clean 125 mL HDPE container and shaking thoroughly.
3. Prepare calibration standards and perform calibration.
 - 3.1. Fill pre-cleaned 125 mL HDPE containers with 100 mL aged seawater.
 - 3.2. Under the Settings worksheet, enter number of calibration points (including blank) and spike increment (nM), typically 5 and 25, respectively.
 - 3.3. Under Settings worksheet, select number of data points to acquire, and time delay prior to acquisition.
 - 3.4. Select Calibration Mode from the menu.
 - 3.5. Add 20 μL 6M q-HCl to the +0 calibration standard (i.e. the blank) and invert several times.
 - 3.6. Click Acquire. Pump will start and sample will run through system for pre-selected length of time, prior to data acquisition, after which pump will stop.
 - 3.7. Prepare next calibration standard while blank is being analyzed. Add 20 μL 6M q-HCl to next standard, and add the appropriate volume of 500 nM Fe(II) working stock (typically 50 μL for 25 nM calibration increment). Shake.
 - 3.8. Continue in this fashion until all standards are run.
 - 3.9. Software will record the date and time of the calibration, and calculate the slope and intercept of the calibration using the Excel *slope* and *intercept* functions. Linearity should be confirmed by visual inspection of the calibration data, which are graphed automatically on the calibration worksheet.
4. Detection limit calculation.
 - 4.1. Calculation based on standard deviation of the blank.
 - 4.1.1. $S_{BL} = \Sigma(y_i - y_{ave})^2/n$, where y_i are the system responses (counts) for the 50 blank readings, and y_{ave} is the average.
 - 4.1.2. Detection limit is equal to 3 times the standard deviation obtained from the blank measurement.
 - 4.2. Calculation based on error in calibration intercept.

- 4.2.1. Use the Excel data analysis tool bar to regress the system calibration responses (counts) against the calibration concentrations (pM) to obtain the standard error of the intercept, s_{INT} .
- 4.2.2. The detection limit is 3 times the standard error of the intercept, i.e. $3s_{INT}$.
- 4.3. Calculation based on a propagation-of-errors approach.
 - 4.3.1. Use the Excel data analysis tool bar to regress the system calibration responses (counts) against the calibration concentrations (pM) to obtain the the intercept y_{INT} , slope m , intercept error s_{INT} , and slope error s_m .
 - 4.3.2. The detection limit is then given by: $3(s_{BL}^2 + s_{INT}^2 + (y_{INT}/m)^2 s_m^2)^{1/2}/m$ (Long and Wisefordner, 1983).

F.4 Sample Analysis

1. Begin sample analysis immediately after sample collection.
2. Analyze samples in order of collection (usually beginning with shallowest sample, and ending with deepest).
 - 2.1. Uncap sample container, insert sample line. Select Acquire from Menu. This will start pump. After specified delay, data acquisition will begin.
 - 2.2. Visually monitor system response for stability during data acquisition.
 - 2.3. After acquisition, pump stops. Remove cap from next sample in queue. Transfer sample line to new sample. Place cap on old sample and twist clockwise until reasonably tight.
 - 2.4. Continue until all samples have been analyzed.
3. Repeat entire analysis sequence two more times.

F.5 Sample stability correction and concentration calculation.

1. Sort data by sample number (descending) and analysis time (ascending).
2. Insert sample collection time for the first sample into the appropriate space on spreadsheet.
3. Calculate the sample collection time for remaining samples by dividing the time required to complete sampling by the number of samples collected, and adding the correct multiple to the sample begin time.
4. For each sample/analysis, calculate the acidification time interval between sample collection and analysis by subtracting the sample collection time from the analysis time.
5. Calculate any trend with time by applying the slope function to the system response (y variable) and acidification time interval (x variable) for the 3 measurements made on the sample. Use the intercept function to estimate the system response at the time of acidification.
6. The estimated system response at the time of acidification (y intercept) is converted to a concentration by subtracting the system response for the acidified blank and dividing the result by the calibration slope.

APPENDIX G
DATA TABLES FOR PO2 AND P16N

Table 9: Data for cruise PO2.

Station No.	Sample No.	Pressure (db)	Temp. (degC)	Salinity (psu)	Fe _{DISS} ^a (nM)	Fe _{DISS} Flag ^b	Fe(II) Raw ^c (pM)	Fe(II) Corr. ^d (pM)	Fe(II) Flag ^b	Fe(II):Fe _{DISS} Ratio
8	12	15.2	23.7858	34.426	0.67	2	202	192	2	0.29
8	11	38.4	23.01	34.483	0.59	2	96	90	2	0.15
8	10	64.1	21.2471	34.5935	0.66	2	65	58	2	0.09
8	9	84.7	18.9374	34.6903	0.74	2	39	28	2	0.04
8	8	105.2	17.8167	34.6898	0.89	2	27	17	2	0.02
8	7	136.6	16.6389	34.6623	0.86	2	12	3	2	0.00
8	6	186.9	15.2174	34.5972	0.86	2	9	0	2	0.00
8	5	234.8	13.6162	34.5117	0.96	2	12	2	2	0.00
8	4	286.4	11.8013	34.4011	0.90	2	12	3	2	0.00
8	3	474.7	7.1119	34.2623	1.00	2	19	11	2	0.01
8	2	674.4	4.6696	34.3074	1.06	2	16	8	2	0.01
8	1	979	3.2865	34.4374	1.13	2	14	7	2	0.01
10	12	16.3	25.6692	34.4649	0.97	2	162	149	2	0.15
10	11	39.8	24.9993	34.5535	0.77	2	93	83	2	0.11
10	10	58.9	24.0926	34.6414	0.64	2	88	83	2	0.13
10	9	79.1	22.8933	34.6882	0.66	2	65	60	2	0.09
10	8	99.3	21.2255	34.6054	0.77	2	47	38	2	0.05
10	7	123.9	19.4819	34.6115	0.87	2	36	27	2	0.03
10	6	149.8	18.8693	34.8009	0.89	2	13	5	2	0.01
10	5	199.6	16.5306	34.67	0.88	2	12	4	2	0.00
10	4	250	15.0731	34.5995	0.93	2	9	0	2	0.00
10	3	505.7	7.5202	34.2853	1.23	2	17	9	2	0.01
10	2	706.1	4.753	34.3044	1.21	2	13	6	2	0.01

Table 9 Continued:

Station No.	Sample No.	Pressure (db)	Temp. (degC)	Salinity (psu)	Fe _{DISS} ^a (nM)	Fe _{DISS} Flag ^b	Fe(II) Raw ^c (pM)	Fe(II) Corr. ^d (pM)	Fe(II) Flag ^b	Fe(II):Fe _{DISS} Ratio
10	1	866	3.8261	34.3942	1.20	2	13	7	2	0.01
12	12	19.1	26.115	34.7422	0.78	2	133	132	2	0.17
12	11	39.6	25.3726	34.7619	0.68	2	55	55	2	0.08
12	10	64.8	23.2584	34.8992	0.60	2	14	12	2	0.02
12	9	83.5	21.7801	34.8522	0.60	2	17	16	2	0.03
12	8	105.3	21.039	34.8736	0.76	2	14	9	2	0.01
12	7	134.8	20.4599	34.8749	0.68	2	9	8	2	0.01
12	6	187.2	19.3729	34.8336	0.78	2	19	15	2	0.02
12	5	235.1	18.4019	34.8211	0.68	2	1	0	2	0.00
12	4	288.4	17.2678	34.7336	0.85	2	11	6	2	0.01
12	3	475.2	12.2183	34.4007	0.92	2	58	55	2	0.06
12	2	675.4	6.9949	34.1793	0.97	2	45	42	2	0.04
12	1	978.1	4.0982	34.3724	1.20	2	73	73	2	0.06
14	12	19.9	24.9269	34.5944	0.60	2	38	32	2	0.05
14	11	33.9	24.7798	34.6202	0.63	4	32	26	2	0.04
14	10	50.1	24.6284	34.6508	0.56	2	21	17	2	0.03
14	9	69.8	23.6501	34.7681	0.50	2	11	8	2	0.02
14	8	90.8	22.2061	34.8793	0.47	2	9	8	2	0.02
14	7	120.9	21.349	34.8943	0.51	2	13	10	2	0.02
14	6	170.3	20.7788	34.8991	0.52	2	11	8	2	0.02
14	5	220.7	19.9002	34.8842	0.51	2	9	7	2	0.01
14	4	271.6	18.9575	34.8509	0.65	2	9	6	2	0.01
14	3	440.9	16.4012	34.6921	0.69	2	9	6	2	0.01
14	2	643.6	11.1239	34.3392	0.81	2	22	15	2	0.02
14	1	906.6	5.6348	34.2096	0.88	2	19	12	2	0.01
16	12	17.1	25.2338	34.6283	0.58	2	52	48	2	0.08
16	11	37.7	24.5694	34.586	0.50	2	36	33	2	0.07
16	10	55.8	23.1316	34.7072	0.45	2	19	18	2	0.04
16	9	78	21.6198	34.8673	0.42	2	9	7	2	0.02
16	8	96.3	20.6251	34.8686	0.43	2	12	10	2	0.02
16	7	124.1	19.6633	34.8398	0.58	2	22	19	2	0.03

Table 9 Continued:

Station No.	Sample No.	Pressure (db)	Temp. (degC)	Salinity (psu)	Fe _{DISS} ^a (nM)	Fe _{DISS} Flag ^b	Fe(II) Raw ^c (pM)	Fe(II) Corr. ^d (pM)	Fe(II) Flag ^b	Fe(II):Fe _{DISS} Ratio
16	6	148.5	19.2124	34.8559	0.59	2	14	11	2	0.02
16	5	200.4	18.6778	34.8748	0.68	2	17	13	2	0.02
16	4	251.3	18.1473	34.8348	0.73	2	19	12	2	0.02
16	3	502.4	14.33	34.5515	0.88	2	14	7	2	0.01
16	2	705.4	8.3354	34.2009	1.07	2	17	10	2	0.01
16	1	996.2	4.5251	34.2925	1.11	2	9	2	2	0.00
18	12	18	24.2215	34.5085	0.69	2	270	264	2	0.38
18	11	38.3	23.716	34.5745	0.65	2	253	247	2	0.38
18	10	63	21.9238	34.76	0.63	2	93	88	2	0.14
18	9	82.3	20.7919	34.876	0.68	2	63	58	2	0.09
18	8	101.9	20.0633	34.8758	0.84	2	66	56	2	0.07
18	7	133.5	19.2006	34.8752	0.92	2	32	21	2	0.02
18	6	183.8	18.7184	34.8752	6.49	4	13	4	2	0.00
18	5	234	18.3705	34.8506	2.77	3	21	13	2	0.00
18	4	285.5	17.9051	34.8178	3.48	3	38	30	2	0.01
18	3	471.2	14.6649	34.5688	2.18	3	21	14	2	0.01
18	2	674	9.0595	34.2297	2.08	3	44	37	2	0.02
18	1	974.4	4.6515	34.2911	2.16	3	177	171	2	0.08
20	12	14.6	25.1248	34.7433	0.45	2	243	242	2	0.54
20	11	34.6	23.559	34.7645	0.42	2	66	67	2	0.16
20	10	49	22.006	34.8666	0.41	2	38	39	2	0.10
20	9	68	20.4758	34.8797	0.38	2	41	34	2	0.09
20	8	89.6	19.2242	34.8658	0.38	2	36	33	2	0.09
20	7	120	18.7539	34.8536	0.53	2	65	62	2	0.12
20	6	170.4	17.9586	34.8031	0.64	4	94	91	2	0.14
20	5	220.4	17.3178	34.7602	0.64	2	96	95	2	0.15
20	4	270.4	16.7162	34.7181	0.68	2	108	107	2	0.16
20	3	441.9	13.0525	34.4632	0.76	2	108	103	2	0.14
20	2	643.4	7.8802	34.1839	0.86	2	127	117	2	0.14
20	1	945.4	4.2678	34.2795	1.31	2	176	164	2	0.13
22	12	16.1	25.49	34.782	0.47	2	141	140	2	0.30
22	11	38.8	22.7963	34.8448	0.37	2	113	114	2	0.31

Table 9 Continued:

Station No.	Sample No.	Pressure (db)	Temp. (degC)	Salinity (psu)	Fe _{DISS} ^a (nM)	Fe _{DISS} Flag ^b	Fe(II) Raw ^c (pM)	Fe(II) Corr. ^d (pM)	Fe(II) Flag ^b	Fe(II):Fe _{DISS} Ratio
22	10	59.4	20.6563	34.8678	0.36	2	63	64	2	0.18
22	9	78.8	19.3846	34.86	1.16	3	54	47	2	0.04
22	8	99.6	18.7399	34.8637	0.53	2	116	113	2	0.21
22	7	124.5	18.4359	34.848	0.50	2	101	98	2	0.20
22	6	150	17.986	34.8213	0.50	2	86	83	2	0.17
22	5	201.1	17.5025	34.805	0.47	2	63	61	2	0.13
22	4	249.9	17.2412	34.8007	0.49	2	48	46	2	0.09
22	3	501.8	13.1983	34.4769	0.65	2	98	93	2	0.14
22	2	704.4	8.1722	34.1876	0.76	2	152	141	2	0.19
22	1	1006.6	4.3171	34.2912	1.08	2	194	183	2	0.17
24	12	15.7	23.8487	34.6664	0.60	2	49	46	2	0.08
24	11	38	22.5779	34.7283	0.51	2	30	28	2	0.05
24	10	64.5	20.5812	34.809	0.41	2	8	7	2	0.02
24	9	83.7	19.8639	34.824	0.45	2	7	5	2	0.01
24	8	105.2	19.3447	34.831	0.55	2	22	19	2	0.04
24	7	136.3	18.5037	34.828	0.70	2	13	4	2	0.01
24	6	184.7	17.8315	34.8039	0.90	2	29	18	2	0.02
24	5	235.4	17.2556	34.7699	0.78	2	19	10	2	0.01
24	4	285.2	16.9651	34.7611	0.74	2	11	2	2	0.00
24	3	471.8	13.7532	34.5085	0.80	2	30	19	2	0.02
24	2	674.3	8.213	34.2013	0.96	2	32	19	2	0.02
24	1	977.4	4.3303	34.2978	1.11	2	51	39	2	0.04
26	12	17.4	24.5	34.7438	0.51	2	210	208	2	0.41
26	11	34.4	22.5476	34.7329	0.43	2	169	168	2	0.39
26	10	49.6	20.8794	34.7924	0.37	2	110	111	2	0.30
26	9	68.9	19.2723	34.8442	0.38	2	110	111	2	0.29
26	8	89.5	18.3533	34.8312	0.47	2	111	110	2	0.23
26	7	119.3	17.9684	34.8167	0.61	2	179	175	2	0.29
26	6	169.6	17.3419	34.7981	0.60	2	191	186	2	0.31
26	5	220	17.093	34.7946	0.55	2	193	190	2	0.35
26	4	271	16.6257	34.7318	0.68	2	211	206	2	0.30
26	3	441.4	12.7478	34.4382	0.73	2	132	122	2	0.17

Table 9 Continued:

Station No.	Sample No.	Pressure (db)	Temp. (degC)	Salinity (psu)	Fe _{DISS} ^a (nM)	Fe _{DISS} Flag ^b	Fe(II) Raw ^c (pM)	Fe(II) Corr. ^d (pM)	Fe(II) Flag ^b	Fe(II):Fe _{DISS} Ratio
26	2	643	7.4702	34.1489	1.00	2	164	153	2	0.15
26	1	946.8	4.1792	34.262	1.53	2	378	367	2	0.24
28	12	18.8	26.5118	34.9202	0.60	2	158	155	2	0.26
28	11	39.3	22.1925	34.9259	0.41	2	44	43	2	0.11
28	10	59.3	21.0725	34.9117	0.39	2	72	73	2	0.19
28	9	78.4	19.5726	34.8615	0.37	2	22	24	2	0.06
28	8	100.2	18.7864	34.8451	0.42	2	23	22	2	0.05
28	7	125.3	18.4582	34.837	0.56	2	20	17	2	0.03
28	6	150.6	18.0449	34.815	0.73	2	42	34	2	0.05
28	5	200.3	17.3138	34.7753	0.75	2	43	34	2	0.05
28	4	251.5	16.8659	34.7486	0.72	3	49	40	2	0.06
28	3	503	11.7509	34.3759	0.79	2	60	50	2	0.06
28	2	703.7	6.3879	34.0639	0.85	2	53	42	2	0.05
28	1	1006.3	3.9427	34.2668	0.95	2	58	45	2	0.05
30	12	15.8	25.3189	34.8534	0.56	2	78	75	2	0.13
30	11	39.1	21.4189	34.8048	0.35	2	41	42	2	0.12
30	10	63.5	19.9884	34.8595	0.38	2	66	67	2	0.18
30	9	83.6	18.7563	34.8438	0.40	2	29	28	2	0.07
30	8	105.6	18.2155	34.8118	0.57	2	35	32	2	0.06
30	7	135.6	17.7859	34.7951	0.55	2	43	40	2	0.07
30	6	186.2	17.2168	34.7666	0.76	2	52	43	2	0.06
30	5	234.7	16.8753	34.7592	0.68	3	62	57	2	0.08
30	4	285.4	16.2153	34.6946	0.70	2	42	32	2	0.05
30	3	460.4	12.1121	34.3853	0.72	2	36	26	2	0.04
30	2	673.6	6.7281	34.0481	0.84	2	36	25	2	0.03
30	1	977	4.0754	34.2453	1.03	2	45	33	2	0.03
32	12	16.8	27.2779	34.9663	0.53	2	58	56	2	0.11
32	11	34.3	22.4258	34.9067	0.41	2	27	26	2	0.06
32	10	49.6	20.6358	34.9052	0.37	2	22	23	2	0.06
32	9	70.1	19.7419	34.8891	0.35	2	17	18	2	0.05
32	8	89.7	19.1177	34.8595	0.49	2	33	31	2	0.06
32	7	119.5	18.1293	34.8123	0.65	2	23	19	2	0.03

Table 9 Continued:

Station No.	Sample No.	Pressure (db)	Temp. (degC)	Salinity (psu)	Fe _{DISS} ^a (nM)	Fe _{DISS} Flag ^b	Fe(II) Raw ^c (pM)	Fe(II) Corr. ^d (pM)	Fe(II) Flag ^b	Fe(II):Fe _{DISS} Ratio
32	6	169.9	17.3642	34.7843	0.51	2	17	14	2	0.03
32	5	221.3	17.1356	34.8003	0.52	2	14	11	2	0.02
32	4	270.8	16.6588	34.7384	0.58	2	21	18	2	0.03
32	3	441.8	13.1744	34.4614	0.70	2	29	19	2	0.03
32	2	643.2	8.1012	34.1011	0.65	2	25	19	2	0.03
32	1	946.2	4.3552	34.1979	0.82	2	25	13	2	0.02
34	12	14.8	27.8651	34.9504	0.77	2	133	127	2	0.16
34	11	38.6	22.3446	34.829	0.31	2	20	21	2	0.07
34	10	58.6	20.7631	34.922	0.32	2	53	54	2	0.17
34	9	79.7	19.6952	34.9301	0.32	2	18	19	2	0.06
34	8	100.9	19.0872	34.903	0.34	2	8	9	2	0.03
34	7	124.4	18.4749	34.8545	0.41	2	11	10	2	0.02
34	6	150.1	17.9672	34.8144	0.45	2	5	4	2	0.01
34	5	201.1	17.3849	34.8099	0.58	2	10	7	2	0.01
34	4	251.7	17.0663	34.7755	0.55	2	24	21	2	0.04
34	3	502.5	12.4855	34.4057	0.61	2	22	17	2	0.03
34	2	705.1	7.1291	34.0603	0.52	3	24	20	2	0.04
34	1	1008.5	4.1019	34.2363	0.86	2	17	6	2	0.01
36	12	16.9	25.6524	34.8447	0.35	2	33	34	2	0.10
36	11	43.4	22.3953	34.8805	0.28	2	11	11	2	0.04
36	10	67.6	20.0363	34.9173	0.26	2	9	9	2	0.03
36	9	87.7	19.1428	34.8927	0.26	2	2	2	2	0.01
36	8	107.9	18.5697	34.8498	0.35	2	1	2	2	0.01
36	7	138.7	17.8441	34.8152	0.51	2	3	0	2	0.00
36	6	188.3	17.2787	34.7997	0.53	2	11	8	2	0.02
36	5	238.5	17.1159	34.8043	0.52	2	8	5	2	0.01
36	4	288.9	16.8062	34.7651	0.53	2	9	6	2	0.01
36	3	465.3	13.5834	34.5022	0.67	2	9	4	2	0.01
36	2	676.2	7.8226	34.0978	0.78	2	16	6	2	0.01
36	1	978.8	4.1111	34.2294	0.97	2	42	29	2	0.03
38	12	18.1	25.9168	35.0283	0.48	2	42	40	2	0.08
38	11	36.5	23.2815	34.9866	0.29	2	24	24	2	0.08

Table 9 Continued:

Station No.	Sample No.	Pressure (db)	Temp. (degC)	Salinity (psu)	Fe _{DISS} ^a (nM)	Fe _{DISS} Flag ^b	Fe(II) Raw ^c (pM)	Fe(II) Corr. ^d (pM)	Fe(II) Flag ^b	Fe(II):Fe _{DISS} Ratio
38	10	52.3	21.6437	34.9504	0.26	2	13	13	2	0.05
38	9	73	20.447	34.8955	0.24	2	9	9	2	0.04
38	8	93.6	19.6183	34.9043	0.28	2	19	19	2	0.07
38	7	121.8	18.9279	34.8769	0.26	2	25	25	2	0.10
38	6	173.6	18.0566	34.825	0.36	2	39	40	2	0.11
38	5	222.1	17.4213	34.785	0.36	2	70	71	2	0.20
38	4	273.4	16.9976	34.7671	0.44	2	32	30	2	0.07
38	3	443.8	14.4357	34.546	0.48	2	71	69	2	0.14
38	2	645.1	9.3438	34.1762	0.56	2	50	47	2	0.08
38	1	947.3	4.5652	34.1745	0.78	2	61	50	2	0.06
40	12	15.7	27.9377	35.0215	0.53	2	78	76	2	0.14
40	11	38.6	22.5925	34.9637	0.27	2	13	13	2	0.05
40	10	58.6	21.411	34.9506	0.26	2	13	13	2	0.05
40	9	81	19.8926	34.8251	0.24	2	3	3	2	0.01
40	8	103.9	19.077	34.8302	0.30	2	3	4	2	0.01
40	7	128.2	18.3427	34.8197	0.34	2	2	4	2	0.01
40	6	152.1	17.728	34.8032	0.34	2	0	1	2	0.00
40	5	202.4	17.2503	34.7997	0.41	2	2	1	2	0.00
40	4	252.4	17.1064	34.7958	0.44	2	46	45	2	0.10
40	3	502.3	13.2573	34.4737	0.51	2	4	0	2	0.00
40	2	708.1	8.1029	34.0932	0.53	2	5	2	2	0.00
40	1	1006.5	4.3762	34.1845	0.65	2	18	13	2	0.02
44	12	18.7	25.4864	34.8956	0.30	2	24	25	2	0.08
44	11	33.9	22.7924	35.006	0.20	2	10	10	2	0.05
44	10	49.4	21.6442	35.0942	0.21	2	6	6	2	0.03
44	9	73.5	20.3338	35.036	0.19	2	4	5	2	0.03
44	8	92.8	19.0846	34.9073	0.24	2	2	2	2	0.01
44	7	119.2	18.2363	34.8489	0.24	2	0	0	2	0.00
44	6	169.2	17.3859	34.7688	0.35	2	-1	0	2	0.00
44	5	221.9	17.069	34.7727	0.40	2	6	4	2	0.01
44	4	269.8	16.717	34.7437	0.46	2	10	9	2	0.02
44	3	440.3	13.8662	34.5059	0.55	2	7	4	2	0.01

Table 9 Continued:

Station No.	Sample No.	Pressure (db)	Temp. (degC)	Salinity (psu)	Fe _{DISS} ^a (nM)	Fe _{DISS} Flag ^b	Fe(II) Raw ^c (pM)	Fe(II) Corr. ^d (pM)	Fe(II) Flag ^b	Fe(II):Fe _{DISS} Ratio
44	2	646	8.8237	34.1372	0.62	2	10	4	2	0.01
44	1	943.6	4.4472	34.1636	0.87	2	49	37	2	0.04
46	12	21	26.2801	34.7206	0.37	2	32	36	2	0.10
46	11	39.6	22.8722	34.8625	0.24	2	10	11	2	0.05
46	10	57.3	20.815	34.8433	0.24	2	5	7	2	0.03
46	9	80.6	19.4077	34.8077	0.24	2	3	4	2	0.02
46	8	94.5	18.7588	34.8308	0.27	2	3	4	2	0.02
46	7	124.6	17.8665	34.7934	0.32	2	3	6	2	0.02
46	6	152.2	17.463	34.7874	0.47	2	5	5	2	0.01
46	5	202.6	17.1374	34.7815	0.39	2	5	7	2	0.02
46	4	251.4	16.818	34.7507	0.52	2	27	26	2	0.05
46	3	503.7	12.2184	34.3919	0.53	2	13	12	2	0.02
46	2	706.9	6.4778	33.976	0.73	2	28	20	2	0.03
46	1	1009	3.9746	34.2457	0.82	2	27	18	2	0.02
50	12	17.2	25.6544	34.6088	0.49	2	40	39	2	0.08
50	11	33.8	23.3111	34.6719	0.35	2	13	14	2	0.04
50	10	49.9	22.7095	34.7184	0.34	2	12	13	2	0.04
50	9	70.2	21.9397	34.7608	0.38	2	11	12	2	0.03
50	8	89.2	21.3473	34.7766	0.53	2	16	14	2	0.03
50	7	119.7	19.9917	34.7994	0.56	2	18	16	2	0.03
50	6	171.6	18.0154	34.7811	0.52	3	11	8	2	0.02
50	5	221	17.036	34.7549	0.67	2	12	8	2	0.01
50	4	271.5	16.2877	34.6783	0.70	2	14	5	2	0.01
50	3	445.2	13.0809	34.4644	0.71	2	10	0	2	0.00
50	2	644.7	6.5645	33.9913	0.92	2	15	3	2	0.00
50	1	949.4	4.0426	34.2306	1.09	2	37	26	2	0.02
52	12	16.2	26.7451	35.0851	0.29	2	18	18	2	0.06
52	11	39.7	19.9908	34.7956	0.24	2	9	9	2	0.04
52	10	58.6	18.8837	34.7865	0.25	2	5	5	2	0.02
52	9	79.2	18.1309	34.8009	0.46	3	2	0	2	0.00
52	8	101.3	17.7073	34.7989	0.28	2	2	2	2	0.01
52	7	124.6	17.2565	34.7822	0.38	2	7	8	2	0.02

Table 9 Continued:

Station No.	Sample No.	Pressure (db)	Temp. (degC)	Salinity (psu)	Fe _{DISS} ^a (nM)	Fe _{DISS} Flag ^b	Fe(II) Raw ^c (pM)	Fe(II) Corr. ^d (pM)	Fe(II) Flag ^b	Fe(II):Fe _{DISS} Ratio
52	6	149.5	17.0068	34.7754	0.48	2	23	21	2	0.04
52	5	201.7	16.6368	34.75	0.49	2	4	2	2	0.00
52	4	252.3	16.1291	34.6984	0.56	2	5	2	2	0.00
52	3	502.6	10.5129	34.2751	0.74	2	14	4	2	0.01
52	2	705.7	6.2769	34.0537	0.82	2	17	6	2	0.01
52	1	1007	3.976	34.2458	1.69	3	47	36	2	0.02
54	12	14.4	26.1524	34.8113	0.37	2	49	50	2	0.14
54	11	39	21.6957	34.8085	0.29	2	16	16	2	0.06
54	10	64.3	19.62	34.8184	0.27	2	3	3	2	0.01
54	9	86.3	18.6556	34.8279	0.29	2	1	1	2	0.00
54	8	105.5	18.1087	34.8157	0.36	2	5	6	2	0.02
54	7	135.2	17.6066	34.8026	0.38	2	7	9	2	0.02
54	6	187.3	17.0617	34.7753	0.45	2	8	7	2	0.02
54	5	238.2	16.6339	34.7491	0.49	2	11	9	2	0.02
54	4	289.2	16.2477	34.7203	0.56	2	11	8	2	0.01
54	3	474.6	12.5821	34.4154	0.67	2	12	7	2	0.01
54	2	676.2	6.8349	34.0078	0.85	2	16	5	2	0.01
54	1	977.1	4.0728	34.2231	0.99	2	26	13	2	0.01
56	12	17.1	26.1894	35.3303	0.35	2	28	29	2	0.08
56	11	38	23.2501	35.1059	0.28	2	25	25	2	0.09
56	10	51.7	21.4201	35.0645	0.42	3	17	16	2	0.04
56	9	72.3	20.1003	35.0204	0.19	2	13	14	2	0.08
56	8	92.2	19.033	34.9312	0.24	2	13	13	2	0.06
56	7	123.5	18.2297	34.8749	0.26	2	11	11	2	0.04
56	6	173.5	17.0769	34.7722	0.32	2	11	13	2	0.04
56	5	222.1	16.6479	34.744	0.35	2	14	15	2	0.04
56	4	274.4	16.2493	34.7085	0.36	2	13	15	2	0.04
56	3	444.4	13.602	34.4753	0.36	2	19	20	2	0.06
56	2	645.5	8.5382	34.1009	0.55	2	17	14	2	0.03
56	1	947	4.6903	34.1504	0.65	2	21	16	2	0.02
58	12	14.3	25.8896	35.1591	0.24	2	28	28	2	0.12
58	11	40.1	22.7012	35.1124	0.19	2	10	11	2	0.06

Table 9 Continued:

Station No.	Sample No.	Pressure (db)	Temp. (degC)	Salinity (psu)	Fe _{DISS} ^a (nM)	Fe _{DISS} Flag ^b	Fe(II) Raw ^c (pM)	Fe(II) Corr. ^d (pM)	Fe(II) Flag ^b	Fe(II):Fe _{DISS} Ratio
58	10	61	20.2832	34.9924	0.19	2	6	7	2	0.04
58	9	80	19.1981	34.9517	0.20	2	2	2	2	0.01
58	8	101.6	18.5716	34.9133	0.26	2	0	0	2	0.00
58	7	125.2	18.0017	34.8557	0.25	2	0	0	2	0.00
58	6	150.7	17.6932	34.8331	0.29	2	2	2	2	0.01
58	5	201.6	17.1141	34.775	0.28	2	19	19	2	0.07
58	4	250.6	16.6232	34.7271	0.33	2	11	13	2	0.04
58	3	503.9	13.0964	34.4465	0.41	2	32	30	2	0.07
58	2	696.1	8.4887	34.1052	0.52	2	36	32	2	0.06
58	1	1007	4.4298	34.1788	0.71	2	42	32	2	0.04
60	12	14.3	25.6837	35.2214	0.23	2	14	14	2	0.06
60	11	39.5	23.0289	35.1642	0.18	2	7	8	2	0.04
60	10	63.9	20.3019	34.97	0.16	2	3	4	2	0.02
60	9	86.2	19.06	34.8906	0.18	2	1	2	2	0.01
60	8	103.3	18.5121	34.8974	0.21	2	0	0	2	0.00
60	7	134.3	17.9143	34.8542	0.24	2	0	0	2	0.00
60	6	186.2	16.9423	34.7562	0.34	2	3	4	2	0.01
60	5	234.9	16.6021	34.7367	0.35	2	3	4	2	0.01
60	4	286.1	16.2069	34.7073	0.38	2	4	6	2	0.02
60	3	473.6	13.0805	34.4437	0.56	2	4	1	2	0.00
60	2	674.3	8.0482	34.0755	0.60	2	11	5	2	0.01
60	1	980.5	4.3863	34.1725	0.87	2	32	20	2	0.02
62	12	14.2	24.6578	35.18	0.29	2	25	27	2	0.09
62	11	35.2	22.9016	35.0644	0.23	4	-999	-999	2	-4.34
62	10	49.4	20.6972	34.8844	0.18	2	10	12	2	0.07
62	9	69.8	19.1398	34.856	0.19	2	6	8	2	0.04
62	8	91.7	18.2601	34.8514	0.22	2	5	5	2	0.02
62	7	120.8	17.3745	34.7936	0.27	2	4	4	2	0.02
62	6	170.6	16.7622	34.7668	0.39	2	11	13	2	0.03
62	5	221.1	16.3685	34.7309	0.41	2	11	11	2	0.03
62	4	273.5	15.8397	34.6834	0.38	2	9	11	2	0.03
62	3	441.7	12.893	34.4372	0.47	2	10	9	2	0.02

Table 9 Continued:

Station No.	Sample No.	Pressure (db)	Temp. (degC)	Salinity (psu)	Fe _{DISS} ^a (nM)	Fe _{DISS} Flag ^b	Fe(II) Raw ^c (pM)	Fe(II) Corr. ^d (pM)	Fe(II) Flag ^b	Fe(II):Fe _{DISS} Ratio
62	2	644.6	7.6663	34.0504	0.62	2	20	16	2	0.03
62	1	947.3	4.1928	34.2027	0.82	2	43	33	2	0.04
64	12	14.4	26.0014	35.2104	0.20	2	38	32	2	0.16
64	11	39.3	21.5804	34.9997	0.19	2	15	12	2	0.06
64	10	59.1	19.3908	34.9042	0.21	2	13	10	2	0.05
64	9	80.1	18.1105	34.8076	0.17	2	12	9	2	0.05
64	8	100.4	17.3265	34.7763	0.18	2	10	7	2	0.04
64	7	125.3	16.8288	34.7384	0.21	2	10	6	2	0.03
64	6	150.9	16.5171	34.7206	0.26	2	12	8	2	0.03
64	5	200.5	16.0373	34.6836	0.31	2	13	11	2	0.04
64	4	251.7	15.3718	34.6337	0.37	2	15	13	2	0.03
64	3	502.2	10.0656	34.2188	0.53	2	33	24	2	0.05
64	2	705.3	5.665	34.0231	0.73	2	29	14	2	0.02
64	1	1006.6	3.7051	34.2829	0.90	2	71	50	2	0.06
66	12	14.4	25.0952	35.0541	0.18	2	24	25	2	0.14
66	11	40	20.9865	35.0236	0.15	2	6	7	2	0.05
66	10	65.1	19.0754	34.874	0.14	2	6	7	2	0.05
66	9	85	18.3394	34.8872	0.17	2	0	0	2	0.00
66	8	106.3	17.7926	34.8172	0.33	3	2	3	2	0.01
66	7	134.3	17.3349	34.7893	0.26	2	5	5	2	0.02
66	6	185.5	16.8526	34.7576	0.32	2	7	8	2	0.03
66	5	235.8	16.469	34.7279	0.33	2	9	10	2	0.03
66	4	277.4	16.0954	34.6949	0.33	2	10	11	2	0.03
66	3	473.3	11.6551	34.3465	0.43	2	16	14	2	0.03
66	2	675.2	6.3125	34.0116	0.55	2	20	16	2	0.03
66	1	976.8	3.8832	34.248	0.72	2	54	44	2	0.06
68	12	13.5	23.5979	34.815	0.23	2	18	18	2	0.08
68	11	34.8	20.8936	34.756	0.17	2	14	15	2	0.09
68	10	49.6	19.9233	34.7944	0.19	2	10	11	2	0.06
68	9	69.8	19.0048	34.7997	0.27	3	16	16	2	0.06
68	8	91.4	18.3515	34.8489	0.22	2	10	10	2	0.05
68	7	120.2	17.6991	34.8131	0.34	2	11	12	2	0.03

Table 9 Continued:

Station No.	Sample No.	Pressure (db)	Temp. (degC)	Salinity (psu)	Fe _{DISS} ^a (nM)	Fe _{DISS} Flag ^b	Fe(II) Raw ^c (pM)	Fe(II) Corr. ^d (pM)	Fe(II) Flag ^b	Fe(II):Fe _{DISS} Ratio
68	6	169.9	16.9406	34.7751	0.35	2	10	11	2	0.03
68	5	221.7	16.3752	34.7217	0.33	2	10	11	2	0.03
68	4	271.4	15.7082	34.6631	0.38	2	10	11	2	0.03
68	3	443.5	11.5448	34.3339	0.43	2	14	12	2	0.03
68	2	644.6	6.3434	33.9879	0.69	2	18	12	2	0.02
68	1	946.1	3.8981	34.2469	0.81	2	28	16	2	0.02
70	12	15.4	24.7627	35.2533	0.17	2	18	18	2	0.11
70	11	39.1	21.7162	35.1064	0.17	2	11	12	2	0.07
70	10	59.6	19.9789	35.024	0.15	2	8	9	2	0.06
70	9	78.4	18.9249	34.9359	0.16	2	8	9	2	0.05
70	8	100.2	18.0957	34.8514	0.18	2	4	5	2	0.03
70	7	125.3	17.3218	34.7859	0.16	2	5	6	2	0.04
70	6	150.7	16.9031	34.7471	0.22	2	6	6	2	0.03
70	5	202.1	16.4977	34.7242	0.27	2	12	12	2	0.04
70	4	251.7	16.1234	34.7154	0.45	2	12	10	2	0.02
70	3	501.8	10.7757	34.268	0.54	2	18	15	2	0.03
70	2	704	6.0367	34.0157	0.62	2	21	16	2	0.03
70	1	1008	3.7906	34.2698	0.78	2	50	40	2	0.05
72	12	15.1	24.6478	35.3013	0.19	2	17	18	2	0.09
72	11	40.1	20.7255	35.0672	0.13	2	12	13	2	0.10
72	10	64.3	18.7248	34.879	0.15	2	11	12	2	0.08
72	9	83.9	18.0485	34.833	0.18	2	6	7	2	0.04
72	8	105	17.4346	34.7892	0.22	2	3	3	2	0.02
72	7	135.5	17.0471	34.7553	0.22	2	7	7	2	0.03
72	6	184.6	16.5346	34.7276	0.25	2	8	8	2	0.03
72	5	236.3	16.0696	34.6857	0.25	2	8	8	2	0.03
72	4	283.4	15.464	34.6347	0.28	2	10	10	2	0.03
72	3	472.3	11.7379	34.3513	0.40	2	12	11	2	0.03
72	2	673.3	6.5716	34.0305	0.52	2	15	11	2	0.02
72	1	975.9	4.0128	34.2208	0.66	3	30	24	2	0.04
74	12	14.4	25.153	35.0595	0.29	2	21	21	2	0.07
74	11	34.4	21.9343	35.1313	0.19	2	9	10	2	0.05

Table 9 Continued:

Station No.	Sample No.	Pressure (db)	Temp. (degC)	Salinity (psu)	Fe _{DISS} ^a (nM)	Fe _{DISS} Flag ^b	Fe(II) Raw ^c (pM)	Fe(II) Corr. ^d (pM)	Fe(II) Flag ^b	Fe(II):Fe _{DISS} Ratio
74	10	49.6	19.9614	34.9596	0.18	2	7	8	2	0.05
74	9	69.8	18.6033	34.9003	0.17	2	4	5	2	0.03
74	8	88.9	17.9854	34.8551	0.19	2	4	5	2	0.03
74	7	118.6	17.2486	34.7745	0.25	2	4	4	2	0.02
74	6	170.8	16.8304	34.7463	0.28	2	5	5	2	0.02
74	5	219.7	16.4813	34.7205	0.31	2	5	6	2	0.02
74	4	270.6	15.9482	34.6784	0.33	2	5	6	2	0.02
74	3	441.5	12.6113	34.4007	0.41	2	6	5	2	0.01
74	2	644	7.365	34.0243	0.61	2	15	10	2	0.02
74	1	945.6	4.3228	34.1716	0.78	2	11	0	2	0.00
76	12	14.2	25.8256	35.2463	0.23	2	35	35	2	0.15
76	11	39.3	21.9148	35.1197	0.18	2	17	18	2	0.10
76	10	58.8	19.3811	34.9292	0.17	2	12	13	2	0.08
76	9	79.3	18.5917	34.9155	0.17	4	12	13	2	0.08
76	8	104	17.8137	34.8432	0.16	2	12	13	2	0.08
76	7	124.6	17.3927	34.7986	0.18	2	5	6	2	0.03
76	6	151.2	16.9999	34.758	0.23	2	19	19	2	0.08
76	5	200.8	16.5286	34.7324	0.25	2	11	11	2	0.04
76	4	250.4	15.8624	34.6701	0.31	2	11	13	2	0.04
76	3	502.5	10.8211	34.2709	0.41	2	9	8	2	0.02
76	2	703.7	6.2258	33.998	0.59	2	25	22	2	0.04
76	1	1007.6	3.8371	34.2547	0.68	2	34	28	2	0.04
78	12	14.8	24.1391	35.1499	0.26	2	23	23	2	0.09
78	11	39.6	19.7538	34.9119	0.19	2	53	54	2	0.28
78	10	65.1	18.4477	34.8861	0.19	2	10	11	2	0.06
78	9	84.4	17.7058	34.8309	0.19	4	39	40	2	0.21
78	8	105.5	17.0413	34.7538	0.24	2	14	14	2	0.06
78	7	136	16.6571	34.7305	0.30	3	11	13	2	0.04
78	6	185.4	16.4345	34.7225	0.29	2	11	11	2	0.04
78	5	235	15.9004	34.6864	0.33	2	11	12	2	0.04
78	4	286.3	15.1011	34.5906	0.34	2	11	12	2	0.04
78	3	472.5	10.9902	34.2748	0.39	2	10	11	2	0.03

Table 9 Continued:

Station No.	Sample No.	Pressure (db)	Temp. (degC)	Salinity (psu)	Fe _{DISS} ^a (nM)	Fe _{DISS} Flag ^b	Fe(II) Raw ^c (pM)	Fe(II) Corr. ^d (pM)	Fe(II) Flag ^b	Fe(II):Fe _{DISS} Ratio
78	2	674	6.1185	34.0173	0.56	2	25	22	2	0.04
78	1	977.5	3.7701	34.2634	0.63	2	27	21	2	0.03
82	12	13.8	21.5056	34.8164	0.24	2	10	10	2	0.04
82	11	38.9	18.2342	34.7226	0.21	2	4	4	2	0.02
82	10	59.5	17.3492	34.7465	0.22	2	1	1	2	0.00
82	9	77.2	16.6276	34.7256	0.23	2	1	1	2	0.00
82	8	99	16.2624	34.6868	0.28	4	1	1	2	0.00
82	7	124	15.8796	34.6606	0.27	2	1	1	2	0.00
82	6	149.9	15.6609	34.6413	0.30	2	1	2	2	0.01
82	5	200.6	14.9578	34.5907	0.32	2	2	3	2	0.01
82	4	249.1	14.075	34.5223	0.32	2	1	3	2	0.01
82	3	501.7	8.7305	34.0963	0.51	2	5	2	2	0.00
82	2	704.9	5.1534	34.063	0.74	2	11	0	2	0.00
82	1	1008.2	3.4727	34.3186	0.79	4	23	12	2	0.02
84	12	14.3	25.9431	35.2385	0.27	2	33	33	2	0.12
84	11	39.2	23.0252	35.2652	0.20	2	13	13	2	0.07
84	10	64.4	21.0736	35.128	0.17	2	6	7	2	0.04
84	9	85.7	19.8512	35.0452	0.15	2	1	2	2	0.01
84	8	105.2	18.9708	34.9676	0.18	2	1	2	2	0.01
84	7	135.6	17.8809	34.8484	0.20	2	7	7	2	0.03
84	6	186.4	16.5885	34.713	0.24	2	1	1	2	0.00
84	5	236.7	15.7067	34.636	0.34	3	1	2	2	0.01
84	4	286.9	14.8326	34.5705	0.26	2	1	1	2	0.00
84	3	473.6	10.8086	34.2399	0.33	2	3	4	2	0.01
84	2	674.6	6.5183	34.0232	0.46	2	15	13	2	0.03
84	1	975.8	3.805	34.2483	0.58	2	10	6	2	0.01
86	12	14.6	24.8854	35.123	0.31	2	34	35	2	0.11
86	11	34.2	22.0833	35.1387	0.32	2	11	12	2	0.04
86	10	49.2	21.2038	35.1266	0.29	2	10	10	2	0.03
86	9	68.6	19.4546	34.9902	0.29	2	5	5	2	0.02
86	8	89.6	18.3503	34.8856	0.31	2	5	7	2	0.02
86	7	121.4	17.2643	34.7734	0.31	2	5	7	2	0.02

Table 9 Continued:

Station No.	Sample No.	Pressure (db)	Temp. (degC)	Salinity (psu)	Fe _{DISS} ^a (nM)	Fe _{DISS} Flag ^b	Fe(II) Raw ^c (pM)	Fe(II) Corr. ^d (pM)	Fe(II) Flag ^b	Fe(II):Fe _{DISS} Ratio
86	6	170.2	16.5176	34.7208	0.35	2	5	7	2	0.02
86	5	223.3	15.9013	34.6742	0.35	2	8	9	2	0.03
86	4	270.9	15.3407	34.6307	0.42	2	9	7	2	0.02
86	3	442.3	11.9483	34.3619	0.52	2	11	8	2	0.01
86	2	644.3	7.0795	34.0237	0.62	2	24	18	2	0.03
86	1	946.7	3.9967	34.2169	0.72	2	25	14	2	0.02
88	12	13.8	24.994	34.6885	0.29	2	19	19	2	0.07
88	11	38.8	18.9576	34.7574	0.30	2	6	7	2	0.02
88	10	58.3	17.622	34.7312	0.40	3	6	5	2	0.01
88	9	79.2	16.7916	34.706	0.24	2	0	0	2	0.00
88	8	101.1	16.2796	34.6784	0.25	2	0	0	2	0.00
88	7	124.8	15.9274	34.656	0.28	2	14	14	2	0.05
88	6	150.1	15.5977	34.627	0.33	2	0	0	2	0.00
88	5	201.4	14.7675	34.5668	0.31	2	9	10	2	0.03
88	4	251.3	13.8339	34.4946	0.39	2	0	1	2	0.00
88	3	502.9	9.0463	34.115	0.49	2	9	7	2	0.02
88	2	703.4	5.4081	34.0282	0.66	2	16	10	2	0.02
88	1	914.7	4.0313	34.2221	0.70	2	17	7	2	0.01
90	12	14.5	24.5518	35.1782	0.20	2	132	132	2	0.66
90	11	40.5	21.2675	35.1245	0.16	2	60	61	2	0.38
90	10	63.6	18.2949	34.8503	0.15	2	39	40	2	0.27
90	9	83.5	17.5346	34.793	0.15	2	22	23	2	0.15
90	8	105.9	16.9879	34.7513	0.18	2	14	15	2	0.09
90	7	135.1	16.4009	34.7133	0.22	2	4	4	2	0.02
90	6	184.8	15.5055	34.6211	0.28	2	2	2	2	0.01
90	5	238.7	14.6373	34.5536	0.32	2	4	6	2	0.02
90	4	286.1	13.7088	34.4814	0.33	2	4	6	2	0.02
90	3	473.5	9.7834	34.1727	0.37	2	9	10	2	0.03
90	2	674.2	5.8573	34.0038	0.56	2	6	3	2	0.01
90	1	976.5	3.691	34.2805	0.66	2	5	0	2	0.00
92	12	13.6	24.7716	34.714	0.21	2	77	77	2	0.37
92	11	34.6	20.7761	34.8487	0.21	2	35	35	2	0.17

Table 9 Continued:

Station No.	Sample No.	Pressure (db)	Temp. (degC)	Salinity (psu)	Fe _{DISS} ^a (nM)	Fe _{DISS} Flag ^b	Fe(II) Raw ^c (pM)	Fe(II) Corr. ^d (pM)	Fe(II) Flag ^b	Fe(II):Fe _{DISS} Ratio
92	10	49.1	19.0873	34.7896	0.12	2	22	23	2	0.19
92	9	68.8	17.4703	34.7186	0.13	2	4	6	2	0.04
92	8	91	16.4432	34.6821	0.14	2	0	0	2	0.00
92	7	120.2	15.9888	34.6595	-999.00	9	-999	-999	9	-999
92	6	169.6	15.5532	34.6251	-999.00	9	-999	-999	9	-999
92	5	222.1	14.5502	34.5476	-999.00	9	-999	-999	9	-999
92	4	271.2	13.5198	34.4697	0.28	2	2	2	2	0.01
92	3	441.8	10.0271	34.1854	0.34	2	1	3	2	0.01
92	2	643.2	5.8907	34.0132	0.48	2	8	6	2	0.01
92	1	947.9	3.8276	34.2669	0.50	2	35	31	2	0.06
94	12	14.9	22.8135	34.8615	0.18	2	27	28	2	0.16
94	11	40.2	18.4959	34.7812	0.18	2	17	18	2	0.10
94	10	59.4	17.0623	34.716	0.19	2	15	16	2	0.09
94	9	80.8	16.4045	34.6872	0.20	2	15	15	2	0.08
94	8	100.6	16.139	34.6769	0.24	2	-999	-999	9	-999
94	7	125.6	15.9035	34.6593	0.42	4	-999	-999	9	-999
94	6	151.2	15.6296	34.6337	0.35	4	-999	-999	9	-999
94	5	200.4	14.6625	34.5567	0.32	4	-999	-999	9	-999
94	4	252.9	13.6267	34.4789	0.31	2	17	18	2	0.06
94	3	504.7	8.6216	34.0908	0.42	2	23	21	2	0.05
94	2	704.5	5.248	34.0423	0.57	2	24	21	2	0.04
94	1	1008	3.5229	34.3311	0.59	2	24	21	2	0.04
96	12	16.2	25.3488	35.2154	0.22	2	47	47	2	0.21
96	11	39.5	20.0335	34.8764	0.18	2	40	41	2	0.23
96	10	64.7	17.8783	34.7694	0.19	2	19	20	2	0.11
96	9	86.3	17.0496	34.7445	0.17	2	22	23	2	0.14
96	8	106.2	16.6523	34.7318	0.19	2	-999	-999	2	-999
96	7	135.9	16.0979	34.6788	0.32	4	-999	-999	2	-999
96	6	186.1	14.7785	34.5707	0.38	4	-999	-999	2	-999
96	5	236.5	13.961	34.5063	0.28	2	-999	-999	2	-999
96	4	286.1	12.8827	34.423	0.29	2	24	24	2	0.08
96	3	474	9.1568	34.1277	0.36	2	27	28	2	0.08

Table 9 Continued:

Station No.	Sample No.	Pressure (db)	Temp. (degC)	Salinity (psu)	Fe _{DISS} ^a (nM)	Fe _{DISS} Flag ^b	Fe(II) Raw ^c (pM)	Fe(II) Corr. ^d (pM)	Fe(II) Flag ^b	Fe(II):Fe _{DISS} Ratio
96	2	672.3	5.7306	34.0361	0.51	2	35	32	2	0.06
96	1	978.1	3.7995	34.2818	0.60	2	34	28	2	0.05
98	12	17	25.7542	35.3475	0.21	2	19	44	2	0.21
98	11	29.2	24.6967	35.2957	0.19	2	12	37	2	0.20
98	10	47.3	22.4071	35.1628	0.18	2	8	34	2	0.19
98	9	67.4	19.9246	35.056	0.17	2	5	31	2	0.18
98	8	88.9	18.9488	34.9793	0.17	2	5	31	2	0.18
98	7	115.5	17.7476	34.839	-999.00	1	-999	-999	9	-999
98	6	166.6	16.1758	34.6884	-999.00	1	-999	-999	9	-999
98	5	217	15.1138	34.5825	-999.00	1	-999	-999	9	-999
98	4	265.5	14.2647	34.5251	0.29	2	5	30	2	0.10
98	3	437.5	10.7712	34.2417	0.36	2	8	35	2	0.10
98	2	642	6.2794	34.0278	0.53	2	23	44	2	0.08
98	1	944.9	3.912	34.259	0.69	2	40	59	2	0.09
100	12	16.4	25.0635	35.1789	0.24	2	0	0	2	0.00
100	11	38.6	21.2244	35.1149	0.20	2	7	7	2	0.03
100	10	60.1	20.2422	35.1105	0.19	2	7	8	2	0.04
100	9	79.7	18.4709	34.9146	0.17	2	4	5	2	0.03
100	8	100.4	17.5383	34.8255	0.17	2	0	1	2	0.01
100	7	124.2	16.5079	34.7182	0.19	2	0	1	2	0.01
100	6	148.3	15.7955	34.6509	0.27	4	3	3	2	0.01
100	5	201.1	14.7365	34.5604	0.26	2	1	1	2	0.00
100	4	248.5	13.7476	34.4748	0.29	2	3	3	2	0.01
100	3	502.3	8.8348	34.1092	0.40	2	7	5	2	0.01
100	2	705.8	5.3301	34.0321	0.55	2	11	8	2	0.01
100	1	1009.1	3.6965	34.3004	0.60	2	19	14	2	0.02
102	12	14.8	23.8525	34.8718	0.17	2	19	20	2	0.11
102	11	38.6	19.9152	34.926	0.17	2	9	10	2	0.06
102	10	63	17.4473	34.7896	0.15	2	6	7	2	0.05
102	9	82.8	16.7407	34.7168	0.15	2	4	5	2	0.04
102	8	104.5	16.147	34.6626	0.18	2	3	4	2	0.02
102	7	134.8	15.6233	34.6323	0.26	2	3	3	2	0.01

Table 9 Continued:

Station No.	Sample No.	Pressure (db)	Temp. (degC)	Salinity (psu)	Fe _{DISS} ^a (nM)	Fe _{DISS} Flag ^b	Fe(II) Raw ^c (pM)	Fe(II) Corr. ^d (pM)	Fe(II) Flag ^b	Fe(II):Fe _{DISS} Ratio
102	6	185.3	14.5822	34.5405	0.25	2	4	4	2	0.02
102	5	236	13.8324	34.4752	0.24	2	3	3	2	0.01
102	4	286.1	12.9412	34.4009	0.25	2	3	3	2	0.01
102	3	471.8	9.4134	34.1354	0.35	2	3	5	2	0.01
102	2	672.9	5.5223	34.0196	0.54	2	7	4	2	0.01
102	1	974.5	3.761	34.281	0.57	2	26	22	2	0.04
104	12	15.1	25.0817	35.243	0.21	2	47	47	2	0.22
104	11	34.2	20.8593	35.0944	0.26	2	23	23	2	0.09
104	10	49.5	19.3199	35.0544	0.22	2	16	16	2	0.07
104	9	69.5	18.3772	34.9514	0.28	2	10	10	2	0.04
104	8	89.2	17.3172	34.8439	0.22	2	7	7	2	0.03
104	7	122.4	16.47	34.7434	0.34	2	7	8	2	0.02
104	6	170.5	14.8502	34.5377	0.33	2	10	11	2	0.03
104	5	220.2	13.6654	34.4577	0.31	2	34	36	2	0.11
104	4	271.6	12.9003	34.4107	0.31	2	6	7	2	0.02
104	3	441.8	9.418	34.1402	0.39	2	16	17	2	0.04
104	2	644.7	5.5843	34.0232	0.67	2	27	22	2	0.03
104	1	948.4	3.8236	34.2811	0.72	2	26	15	2	0.02
106	12	18	25.1716	35.4397	0.25	2	22	22	2	0.09
106	11	38.9	21.9898	35.2014	0.20	2	12	12	2	0.06
106	10	59.7	19.5315	34.9733	0.18	2	13	14	2	0.08
106	9	78.4	18.4352	34.9311	0.18	2	10	11	2	0.06
106	8	99.5	17.4249	34.8571	0.18	2	5	6	2	0.03
106	7	124.2	16.7037	34.7684	0.21	2	5	5	2	0.02
106	6	149.3	16.2439	34.7216	0.24	2	7	7	2	0.03
106	5	200	14.8372	34.541	0.24	2	7	7	2	0.03
106	4	250.8	13.6843	34.4238	0.29	2	8	8	2	0.03
106	3	501.5	8.7377	34.1006	0.40	2	13	11	2	0.03
106	2	704.1	5.3775	34.0573	0.53	2	20	16	2	0.03
106	1	1006.8	3.8571	34.3223	0.59	2	11	7	2	0.01
108	12	18.7	24.9782	35.4134	0.26	2	25	25	2	0.10
108	11	38.5	24.1997	35.4367	0.25	2	17	17	2	0.07

Table 9 Continued:

Station No.	Sample No.	Pressure (db)	Temp. (degC)	Salinity (psu)	Fe _{DISS} ^a (nM)	Fe _{DISS} Flag ^b	Fe(II) Raw ^c (pM)	Fe(II) Corr. ^d (pM)	Fe(II) Flag ^b	Fe(II):Fe _{DISS} Ratio
108	10	64	20.1004	35.1423	0.17	2	10	11	2	0.06
108	9	84	19.0425	35.0467	0.18	2	7	9	2	0.05
108	8	106.1	18.0626	34.9255	0.19	2	5	6	2	0.03
108	7	135.4	16.8265	34.8013	0.25	2	4	4	2	0.02
108	6	184.3	15.9159	34.6931	0.27	2	5	5	2	0.02
108	5	235.9	14.8365	34.5505	0.25	3	1	1	2	0.01
108	4	284.8	13.6217	34.4286	0.30	2	3	4	2	0.01
108	3	473	9.8006	34.1501	0.36	2	5	6	2	0.02
108	2	676.1	5.9566	34.036	0.48	2	9	7	2	0.01
108	1	976.5	3.7315	34.2583	0.56	2	14	10	2	0.02
113	12	17.7	25.3355	35.3652	0.34	2	43	45.5	2	0.13
113	11	34.2	21.3603	35.1916	0.32	2	26	25.7	2	0.08
113	10	49.9	19.7169	35.0745	0.31	2	15	13.1	2	0.04
113	9	69.5	18.363	34.9368	0.30	2	21	21.1	2	0.07
113	8	90.5	17.2782	34.8401	0.36	2	7	5.4	2	0.01
113	7	119.5	16.5124	34.7562	0.41	2	7	5.8	2	0.01
113	6	170.3	15.0569	34.5543	0.43	2	7	5.4	2	0.01
113	5	220.8	14.0523	34.4557	0.46	2	9	7.5	2	0.02
113	4	269.7	12.9847	34.3861	0.47	2	7	5.7	2	0.01
113	3	443.8	9.864	34.1622	0.51	2	7	5.7	2	0.01
113	2	643.8	5.9099	34.0067	0.63	2	20	18.0	2	0.03
113	1	945.7	3.9005	34.2907	0.77	2	31	27.5	2	0.04
115	12	15.9	25.4949	35.3889	0.30	2	29	34.1	2	0.11
115	11	39.2	20.1649	35.0476	0.24	2	21	25.7	2	0.11
115	10	58.2	18.3916	34.8814	0.21	2	17	19.5	2	0.09
115	9	78.7	17.5686	34.8023	0.22	2	14	16.9	2	0.08
115	8	101.5	16.7203	34.7013	0.24	2	10	12.2	2	0.05
115	7	125.4	16.1117	34.6227	0.28	2	9	10.8	2	0.04
115	6	151.8	15.434	34.5768	0.28	2	9	10.4	2	0.04
115	5	201.6	13.8343	34.4025	0.30	2	8	9.5	2	0.03
115	4	252.5	12.6334	34.3306	0.36	2	8	9.0	2	0.03
115	3	503.7	8.0628	34.0653	0.50	2	15	16.8	2	0.03

Table 9 Continued:

Station No.	Sample No.	Pressure (db)	Temp. (degC)	Salinity (psu)	Fe _{DISS} ^a (nM)	Fe _{DISS} Flag ^b	Fe(II) Raw ^c (pM)	Fe(II) Corr. ^d (pM)	Fe(II) Flag ^b	Fe(II):Fe _{DISS} Ratio
115	2	703.9	5.018	34.0473	0.62	2	17	17.0	2	0.03
115	1	1008.4	3.5168	34.3192	0.69	2	25	24.4	2	0.04
117	12	16.2	25.2592	35.2793	0.29	2	33	32.6	2	0.11
117	11	35.9	22.2397	35.0382	0.27	2	23	26.4	2	0.10
117	10	61.4	18.966	34.89	0.24	2	12	12.6	2	0.05
117	9	82.3	17.3341	34.6926	0.26	3	12	12.6	2	0.05
117	8	101.5	16.9392	34.6637	0.24	2	6	5.2	2	0.02
117	7	128.8	16.2564	34.6587	0.28	2	6	5.2	2	0.02
117	6	180.4	14.8468	34.5332	0.28	2	6	6.3	2	0.02
117	5	231.9	12.7229	34.2883	0.31	2	6	5.2	2	0.02
117	4	282.6	12.0922	34.2774	0.35	2	8	7.6	2	0.02
117	3	471	8.6459	34.0935	0.47	2	9	7.3	2	0.02
117	2	673.6	5.2618	34.0177	0.59	2	14	11.5	2	0.02
117	1	974.2	3.5901	34.2938	0.67	2	15	11.3	2	0.02
119	12	18.9	25.4314	35.3271	0.26	2	34	33.9	2	0.13
119	11	33.7	23.7502	35.1752	0.22	2	52	51.1	2	0.23
119	10	50.4	20.607	34.9816	0.19	2	102	98.4	2	0.52
119	9	70.4	18.2856	34.8147	0.21	2	38	38.7	2	0.18
119	8	88.8	17.1707	34.7409	0.23	2	37	36.0	2	0.16
119	7	120	16.0383	34.6556	0.26	2	28	27.5	2	0.11
119	6	169.1	14.2649	34.4583	0.32	3	6	5.0	2	0.02
119	5	220.7	13.0849	34.3587	0.31	2	7	6.5	2	0.02
119	4	271	11.8797	34.2646	0.35	2	14	11.7	2	0.03
119	3	442.4	9.217	34.1233	0.44	2	14	14.3	2	0.03
119	2	643.9	5.4377	34.0112	0.61	2	14	13.2	2	0.02
119	1	948	3.6358	34.2912	0.70	2	38	36.2	2	0.05
121	12	19.6	24.6126	35.363	0.21	2	41	36.4	2	0.17
121	11	39.6	21.2747	35.263	0.19	2	35	26.8	2	0.14
121	10	58.3	19.4338	35.0608	0.19	2	25	19.4	2	0.10
121	9	79.4	18.4267	34.9408	0.20	2	18	13.0	2	0.07
121	8	100.1	17.534	34.8461	0.23	2	16	12.7	2	0.06
121	7	125.6	16.2896	34.6495	0.27	4	16	10.9	2	0.04

Table 9 Continued:

Station No.	Sample No.	Pressure (db)	Temp. (degC)	Salinity (psu)	Fe _{DISS} ^a (nM)	Fe _{DISS} Flag ^b	Fe(II) Raw ^c (pM)	Fe(II) Corr. ^d (pM)	Fe(II) Flag ^b	Fe(II):Fe _{DISS} Ratio
121	6	150.9	14.8593	34.499	0.30	4	16	12.1	2	0.04
121	5	199.6	13.8322	34.4165	0.25	2	-999	-999	9	-999
121	4	251.2	12.879	34.3438	0.27	2	25	19.9	2	0.07
121	3	503	8.369	34.0777	0.42	2	21	14.6	2	0.03
121	2	704.9	4.9625	34.0411	0.57	2	46	36.7	2	0.06
121	1	1008.3	3.5626	34.3177	0.63	2	40	32.1	2	0.05
123	12	15.3	24.5393	35.2879	0.27	2	30	33.4	2	0.12
123	11	38.8	21.1	35.0115	0.23	2	29	30.0	2	0.13
123	10	65.9	17.1537	34.5754	0.23	2	17	19.2	2	0.08
123	9	84.8	16.0688	34.5837	0.21	2	9	8.1	2	0.04
123	8	105.7	15.1657	34.4945	0.21	2	-999	-999	9	-999
123	7	135.3	14.1647	34.4087	0.26	3	11	10.3	2	0.04
123	6	185.3	13.2631	34.3661	0.26	2	9	9.3	2	0.04
123	5	236.8	12.2625	34.2905	0.28	2	12	13.5	2	0.05
123	4	285.4	11.5485	34.2528	0.31	2	11	11.5	2	0.04
123	3	472.5	8.2295	34.0643	0.44	2	15	12.7	2	0.03
123	2	674.6	5.0517	34.0302	0.58	2	18	17.2	2	0.03
123	1	978.5	3.6022	34.3249	0.71	2	108	95.6	2	0.13
125	12	16.6	24.589	35.3779	0.27	2	33	33.3	2	0.12
125	11	32.9	21.6852	35.1913	0.19	2	19	20.1	2	0.11
125	10	48.8	20.4803	35.0991	0.20	2	15	15.9	2	0.08
125	9	69.6	19.136	34.9382	0.20	2	13	12.5	2	0.06
125	8	88.9	18.4263	34.9331	0.21	2	13	13.8	2	0.07
125	7	119.1	17.1475	34.748	0.32	4	10	13.0	2	0.04
125	6	170.3	14.7445	34.482	0.27	2	6	6.3	2	0.02
125	5	220.7	13.0019	34.2661	0.29	2	6	6.3	2	0.02
125	4	271.1	12.1791	34.267	0.33	2	8	9.6	2	0.03
125	3	442.2	9.0677	34.1102	0.40	2	6	4.9	2	0.01
125	2	642.6	5.3329	34.0049	0.53	2	13	9.9	2	0.02
125	1	946.6	3.7642	34.2846	0.64	2	15	12.0	2	0.02
127	12	16.9	24.9645	35.4267	0.22	2	30	30.1	2	0.14
127	11	38.8	22.236	35.2341	0.17	2	16	12.9	2	0.08

Table 9 Continued:

Station No.	Sample No.	Pressure (db)	Temp. (degC)	Salinity (psu)	Fe _{DISS} ^a (nM)	Fe _{DISS} Flag ^b	Fe(II) Raw ^c (pM)	Fe(II) Corr. ^d (pM)	Fe(II) Flag ^b	Fe(II):Fe _{DISS} Ratio
127	10	60.8	20.4453	35.1037	0.16	2	13	16.0	2	0.10
127	9	79.5	19.4994	35.0297	0.16	2	7	7.2	2	0.04
127	8	100	18.4648	34.8904	0.19	2	3	0.4	2	0.00
127	7	124.6	17.1158	34.6915	0.20	3	1	0.9	2	0.00
127	6	151.9	15.9448	34.5452	0.19	2	1	0.9	2	0.00
127	5	201.7	13.937	34.3928	0.23	2	1	0.9	2	0.00
127	4	252.2	12.7951	34.3223	0.28	2	1	0.9	2	0.00
127	3	503.9	7.747	34.0468	0.37	2	5	5.1	2	0.01
127	2	704.3	4.7635	34.0634	0.48	2	11	11.3	2	0.02
127	1	1008.5	3.5208	34.3589	0.56	2	16	12.9	2	0.02
129	12	17.4	25.0588	35.3996	0.23	2	50	61.5	2	0.27
129	11	38.1	24.523	35.3789	0.21	2	30	33.6	2	0.16
129	10	63.4	19.2408	34.8436	0.16	2	24	24.0	2	0.15
129	9	82.9	18.0842	34.7668	0.16	2	15	15.2	2	0.09
129	8	103.9	16.7878	34.6037	0.18	2	15	22.5	2	0.13
129	7	133.2	15.8841	34.555	0.25	3	12	15.9	2	0.06
129	6	185.6	13.7254	34.3606	0.26	3	-999	-999	9	-999
129	5	235.2	12.7664	34.3009	0.21	2	-999	-999	9	-999
129	4	286.9	11.8328	34.2522	0.26	2	12	12.2	2	0.05
129	3	472	8.4673	34.0681	0.36	2	-999	-999	9	-999
129	2	673	4.9252	34.0325	0.50	2	21	24.7	2	0.05
129	1	974.8	3.6912	34.3342	0.66	2	33	29.1	2	0.04
131	12	16.6	24.559	35.1663	0.25	2	31	30.6	2	0.12
131	11	33.8	24.5298	35.2282	0.22	2	36	39.6	2	0.18
131	10	49.9	21.2958	35.0168	0.15	2	17	16.7	2	0.11
131	9	69.4	19.6649	34.9543	0.16	2	14	13.9	2	0.09
131	8	90.5	18.0488	34.7391	0.15	2	11	11.1	2	0.07
131	7	120.8	16.4611	34.5523	0.21	3	8	11.8	2	0.06
131	6	170.5	14.0151	34.3435	0.18	2	8	8.3	2	0.05
131	5	220.4	12.546	34.2196	0.21	2	8	4.9	2	0.02
131	4	271.2	11.7256	34.2125	0.23	2	11	14.6	2	0.06
131	3	443	8.8117	34.0821	0.30	2	11	11.1	2	0.04

Table 9 Continued:

Station No.	Sample No.	Pressure (db)	Temp. (degC)	Salinity (psu)	Fe _{DISS} ^a (nM)	Fe _{DISS} Flag ^b	Fe(II) Raw ^c (pM)	Fe(II) Corr. ^d (pM)	Fe(II) Flag ^b	Fe(II):Fe _{DISS} Ratio
131	2	644.3	5.0948	34.0237	0.45	2	31	27.1	2	0.06
131	1	946.6	3.7782	34.3303	0.56	2	25	21.5	2	0.04
135	12	15.8	24.9209	35.1469	0.23	2	28	35.6	2	0.15
135	11	38.8	22.8601	34.908	0.17	2	23	19.8	2	0.12
135	10	64.8	18.2035	34.4738	0.13	2	16	11.9	2	0.09
135	9	84.7	17.1112	34.4269	0.14	2	11	6.7	2	0.05
135	8	104.3	15.9672	34.3191	0.16	2	8	0.8	2	0.00
135	7	135.8	14.3511	34.2058	0.31	3	3	4.1	2	0.01
135	6	184.8	12.7657	34.1592	0.27	2	3	4.1	2	0.02
135	5	235.1	11.6833	34.1298	0.29	2	3	0.8	2	0.00
135	4	285.8	10.8544	34.1324	0.32	2	3	4.1	2	0.01
135	3	472	7.516	34.0319	0.47	2	6	6.7	2	0.01
135	2	674.5	4.7511	34.0803	0.69	2	11	11.9	2	0.02
135	1	977.9	3.6514	34.3698	0.74	2	11	17.2	2	0.02
137	12	15.8	24.056	35.0557	0.22	2	28	25.1	2	0.11
137	11	33.4	23.4466	35.0507	0.20	2	23	23.2	2	0.12
137	10	49	21.1195	34.8456	0.22	3	16	15.8	2	0.07
137	9	69.4	19.8366	34.847	0.14	2	11	10.8	2	0.08
137	8	91.2	18.9089	34.7371	0.16	2	8	5.2	2	0.03
137	7	120	17.6062	34.5807	0.16	2	3	3.3	2	0.02
137	6	170.4	13.7949	34.0699	0.18	2	3	0.2	2	0.00
137	5	220.7	11.8952	34.0004	0.21	2	3	6.4	2	0.03
137	4	270.9	10.7172	34.0529	0.30	2	3	3.3	2	0.01
137	3	441.3	7.6191	34.023	0.46	2	6	5.8	2	0.01
137	2	644.9	4.877	34.0956	0.69	2	11	7.7	2	0.01
137	1	947.1	3.8145	34.3744	0.76	2	11	7.7	2	0.01
139	12	16.6	24.4987	35.1663	0.21	2	47	47.3	2	0.23
139	11	40	23.5727	35.0999	0.18	2	30	29.6	2	0.16
139	10	59.6	19.9256	34.6665	0.15	2	30	37.0	2	0.25
139	9	78.8	19.0401	34.6976	0.16	2	18	14.2	2	0.09
139	8	100	17.7046	34.5326	0.18	2	12	12.0	2	0.07
139	7	124.5	16.4338	34.4	0.19	2	12	15.7	2	0.08

Table 9 Continued:

Station No.	Sample No.	Pressure (db)	Temp. (degC)	Salinity (psu)	Fe _{DISS} ^a (nM)	Fe _{DISS} Flag ^b	Fe(II) Raw ^c (pM)	Fe(II) Corr. ^d (pM)	Fe(II) Flag ^b	Fe(II):Fe _{DISS} Ratio
139	6	150.8	14.9434	34.2215	0.24	3	12	12.0	2	0.05
139	5	200.4	11.891	33.9494	0.22	2	12	12.0	2	0.05
139	4	250.3	10.8252	34.0353	0.26	2	15	11.3	2	0.04
139	3	503.4	6.3282	33.9932	0.46	2	30	29.6	2	0.06
139	2	704.5	4.4329	34.158	0.55	2	41	41.4	2	0.08
139	1	1007.9	3.6052	34.416	0.57	2	33	28.9	2	0.05
141	12	15.8	24.5908	35.3154	0.24	2	42	48.0	2	0.20
141	11	38.9	22.3672	35.0369	0.21	2	28	24.4	2	0.12
141	10	63.4	19.2549	34.6918	0.18	2	14	16.8	2	0.09
141	9	85.3	18.0849	34.5633	0.24	3	14	14.0	2	0.06
141	8	104.2	17.2121	34.4996	0.21	2	8	1.5	2	0.01
141	7	135.2	15.6083	34.2988	0.25	2	8	5.0	2	0.02
141	6	185.7	12.983	34.1379	0.28	2	8	5.0	2	0.02
141	5	236.5	11.5638	34.0627	0.29	2	8	1.5	2	0.01
141	4	286.2	10.3703	34.055	0.34	2	14	14.0	2	0.04
141	3	473.5	7.031	33.9991	0.48	2	17	7.1	2	0.01
141	2	675	4.6914	34.1185	0.73	2	28	14.0	2	0.02
141	1	976.2	3.754	34.3929	0.74	2	45	27.9	2	0.04
143	12	17.4	24.9226	35.3972	0.22	2	43	42.7	2	0.19
143	11	33.9	24.1135	35.2811	0.21	2	28	27.6	2	0.13
143	10	49.6	20.762	34.8032	0.15	2	20	20.1	2	0.13
143	9	70.2	19.3141	34.6698	0.15	2	16	16.3	2	0.11
143	8	90.2	18.3199	34.5659	0.16	2	14	14.4	2	0.09
143	7	120.1	16.8496	34.3598	0.17	2	16	16.3	2	0.10
143	6	170.5	13.6471	34.065	0.20	2	16	16.3	2	0.08
143	5	221.4	11.4024	34.006	0.24	2	16	16.3	2	0.07
143	4	271.6	10.5752	34.0904	0.31	2	18	18.2	2	0.06
143	3	442.8	7.4018	34.0227	0.43	2	28	27.6	2	0.06
143	2	644.6	4.753	34.0968	0.65	2	29	29.5	2	0.05
143	1	946.1	3.7588	34.3811	0.75	2	31	31.4	2	0.04
145	12	14.9	24.5511	34.8915	0.15	2	47	46.9	2	0.31
145	11	39.7	20.5928	34.5111	0.12	2	26	25.9	2	0.22

Table 9 Continued:

Station No.	Sample No.	Pressure (db)	Temp. (degC)	Salinity (psu)	Fe _{DISS} ^a (nM)	Fe _{DISS} Flag ^b	Fe(II) Raw ^c (pM)	Fe(II) Corr. ^d (pM)	Fe(II) Flag ^b	Fe(II):Fe _{DISS} Ratio
145	10	59.7	19.3684	34.5045	0.12	2	26	29.2	2	0.24
145	9	80.6	19.2573	34.6824	0.11	2	21	23.9	2	0.22
145	8	101	17.6761	34.4222	0.14	2	15	15.4	2	0.11
145	7	125.3	16.5462	34.298	0.23	3	10	13.4	2	0.06
145	6	151.1	14.8607	34.0362	0.18	2	10	13.4	2	0.07
145	5	201.7	12.3277	33.8711	0.19	2	15	15.4	2	0.08
145	4	250.3	10.6546	33.9131	0.24	2	15	15.4	2	0.06
145	3	503	5.9097	34.0012	0.43	2	23	20.0	2	0.05
145	2	704.5	4.6202	34.2094	0.66	3	42	35.1	2	0.05
145	1	1009.1	3.6584	34.4231	0.53	2	39	39.1	2	0.07
147	12	16.8	24.6507	35.1697	0.32	2	50	50.0	2	0.16
147	11	40.5	22.0291	34.7568	0.26	2	34	41.9	2	0.16
147	10	63.6	18.7171	34.501	0.23	2	15	32.7	2	0.14
147	9	83.4	17.544	34.4307	0.22	2	5	4.8	2	0.02
147	8	105	16.5014	34.3367	0.23	2	2	3.6	2	0.02
147	7	136.1	14.6679	34.1163	0.26	2	2	3.6	2	0.01
147	6	185.6	13.0034	34.1725	0.30	2	0	0.0	2	0.00
147	5	236.3	11.7407	34.1363	0.32	2	0	0.0	2	0.00
147	4	285.5	10.1374	34.0442	0.37	2	0	0.0	2	0.00
147	3	471.8	6.6437	33.9945	0.56	2	5	0.8	2	0.00
147	2	673.7	4.6093	34.1447	0.75	2	18	13.7	2	0.02
147	1	973.3	3.7366	34.4176	0.73	2	16	10.1	2	0.01
149	12	16.1	24.4089	34.8851	0.22	2	70	70.0	2	0.32
149	11	30.6	21.6997	34.3944	0.20	2	38	42.5	2	0.21
149	10	46.4	19.402	34.0994	0.22	2	25	27.5	2	0.13
149	9	67.6	18.5046	34.2423	0.21	2	23	25.0	2	0.12
149	8	86.1	17.5481	34.2249	0.22	2	13	17.5	2	0.08
149	7	115.8	16.3917	34.1923	0.23	2	10	10.0	2	0.04
149	6	169	13.7131	34.0241	0.28	2	5	7.5	2	0.03
149	5	216.2	10.9198	33.8911	0.31	2	18	17.5	2	0.06
149	4	266.5	9.7391	33.994	0.39	2	15	15.0	2	0.04
149	3	440.8	6.7463	34.0067	0.63	2	23	22.5	2	0.04

Table 9 Continued:

Station No.	Sample No.	Pressure (db)	Temp. (degC)	Salinity (psu)	Fe _{DISS} ^a (nM)	Fe _{DISS} Flag ^b	Fe(II) Raw ^c (pM)	Fe(II) Corr. ^d (pM)	Fe(II) Flag ^b	Fe(II):Fe _{DISS} Ratio
149	2	641.2	4.8964	34.1231	0.81	2	28	27.5	2	0.03
149	1	944.9	3.7965	34.3952	0.78	2	28	30.0	2	0.04
151	12	14.4	24.2603	35.2037	0.18	2	78	36.8	2	0.20
151	11	38.5	21.8049	34.8302	0.14	2	28	34.8	2	0.25
151	10	59.1	20.8662	34.7819	0.14	2	20	24.0	2	0.17
151	9	79.4	20.0878	34.8276	0.14	2	18	22.4	2	0.16
151	8	100.1	19.4634	34.7855	0.16	2	9	13.3	2	0.08
151	7	124.9	17.5124	34.4363	0.18	2	3	3.4	2	0.02
151	6	150.3	16.1512	34.1932	0.19	2	3	8.5	2	0.04
151	5	200.8	13.0062	33.8604	0.22	2	9	13.3	2	0.06
151	4	252.8	10.6997	33.83	0.33	2	9	11.0	2	0.03
151	3	503.2	5.9544	34.0148	0.52	2	11	6.1	2	0.01
151	2	700.3	4.6211	34.1932	0.68	2	25	18.8	2	0.03
151	1	1006.6	3.7315	34.4292	0.61	2	16	10.1	2	0.02
153	12	17.4	24.214	34.5483	0.17	2	41	47.5	2	0.28
153	11	39.1	23.0724	35.095	0.16	2	30	41.2	2	0.26
153	10	63.8	20.7268	34.6821	0.13	2	23	31.9	2	0.25
153	9	84.4	20.1074	34.6966	0.13	2	12	14.4	2	0.11
153	8	105	20.004	34.9031	0.15	2	14	16.2	2	0.11
153	7	134.4	19.3172	34.8461	0.23	2	12	18.9	2	0.08
153	6	185.9	14.948	34.0761	0.28	2	10	17.1	2	0.06
153	5	235.3	11.3954	33.795	0.29	2	14	14.0	2	0.05
153	4	284.4	9.7189	33.8338	0.38	2	14	16.2	2	0.04
153	3	473.1	6.6131	33.9985	0.62	2	21	18.9	2	0.03
153	2	673.1	4.6944	34.1648	0.78	2	28	19.4	2	0.02
153	1	977.1	3.8316	34.4162	0.73	2	16	9.1	2	0.01
155	12	17.4	23.1593	33.9342	0.11	2	55	61.2	2	0.56
155	11	35.2	22.5834	34.4737	0.11	2	35	35.0	2	0.32
155	10	48.5	18.4521	33.6182	0.11	2	30	36.3	2	0.33
155	9	69.6	17.4092	33.6246	0.10	2	30	42.5	2	0.43
155	8	89.8	16.4005	33.661	0.11	2	50	37.5	2	0.34
155	7	119.7	15.8447	33.7168	0.10	2	15	15.0	2	0.15

Table 9 Continued:

Station No.	Sample No.	Pressure (db)	Temp. (degC)	Salinity (psu)	Fe _{DISS} ^a (nM)	Fe _{DISS} Flag ^b	Fe(II) Raw ^c (pM)	Fe(II) Corr. ^d (pM)	Fe(II) Flag ^b	Fe(II):Fe _{DISS} Ratio
155	6	170.9	13.1451	33.7609	0.12	2	10	10.0	2	0.08
155	5	220.6	10.6445	33.7649	0.18	2	15	15.0	2	0.08
155	4	269.8	9.8603	33.9311	0.30	2	15	21.3	2	0.07
155	3	441	6.3407	33.9986	0.62	2	25	12.5	2	0.02
155	2	644.2	4.7595	34.1665	0.75	2	35	22.5	2	0.03
155	1	945.3	3.8174	34.4123	0.72	2	25	12.5	2	0.02
157	12	15.3	23.2692	34.0887	0.12	2	41	43.7	2	0.36
157	11	39	21.8293	34.5356	0.11	2	34	33.6	2	0.31
157	10	59.7	20.4267	34.4302	0.11	2	24	27.0	2	0.25
157	9	79.2	18.982	34.2901	0.11	2	19	19.3	2	0.18
157	8	100.3	18.3703	34.3332	0.18	3	19	22.3	2	0.12
157	7	125.4	17.0437	34.1876	2.53	4	15	14.5	2	0.01
157	6	150.7	15.8997	34.0898	0.16	2	15	14.5	2	0.09
157	5	200.1	10.6764	33.5006	0.20	2	15	14.5	2	0.07
157	4	250.7	9.326	33.8249	0.31	2	15	8.6	2	0.03
157	3	504.3	5.6513	34.0371	0.65	2	22	9.8	2	0.02
157	2	706	4.5984	34.2683	0.72	2	22	9.8	2	0.01
157	1	1008.6	3.7356	34.4489	0.63	2	17	11.0	2	0.02
159	12	16.2	22.561	33.6464	0.10	2	37	35.4	2	0.35
159	11	39	19.513	33.4579	0.10	2	18	19.0	2	0.19
159	10	65.7	17.7814	33.5541	0.11	2	11	10.1	2	0.09
159	9	84.8	17.2414	33.6942	0.11	2	11	10.4	2	0.09
159	8	105.2	16.4395	33.6949	0.12	2	6	0.9	2	0.01
159	7	135.4	15.4234	33.7375	0.15	2	6	3.6	2	0.02
159	6	185.2	10.6349	33.3537	0.20	2	9	7.1	2	0.04
159	5	235.2	9.1772	33.733	0.29	2	9	7.6	2	0.03
159	4	285.4	8.5467	33.9757	0.45	2	14	14.4	2	0.03
159	3	471.8	6.0263	34.0686	0.66	2	25	22.0	2	0.03
159	2	673.1	4.9248	34.2661	0.70	2	23	14.7	2	0.02
159	1	976.2	3.9321	34.4407	0.53	2	9	2.7	2	0.01
161	12	17.3	22.5689	33.4247	0.11	2	26	27.8	2	0.25
161	11	33.6	19.6284	33.6235	0.09	2	14	14.2	2	0.16

Table 9 Continued:

Station No.	Sample No.	Pressure (db)	Temp. (degC)	Salinity (psu)	Fe _{DISS} ^a (nM)	Fe _{DISS} Flag ^b	Fe(II) Raw ^c (pM)	Fe(II) Corr. ^d (pM)	Fe(II) Flag ^b	Fe(II):Fe _{DISS} Ratio
161	10	49.2	18.1572	33.5356	0.09	2	10	10.1	2	0.11
161	9	69.5	16.8595	33.5791	0.10	2	7	7.4	2	0.07
161	8	89.6	16.3483	33.695	0.14	2	5	4.8	2	0.03
161	7	119.5	14.1994	33.6348	0.17	2	4	4.2	2	0.02
161	6	170.2	10.7799	33.4587	0.38	4	3	2.9	2	0.01
161	5	221.8	9.2703	33.7891	0.32	2	3	0.2	2	0.00
161	4	271.1	8.6193	33.9856	0.48	2	4	0.4	2	0.00
161	3	442.8	6.2653	34.0637	0.67	2	10	4.6	2	0.01
161	2	643.4	4.8956	34.236	0.75	2	15	11.0	2	0.01
161	1	946	3.9741	34.4369	0.70	2	10	4.1	2	0.01
163	12	19	22.5974	33.4117	0.11	2	50	48.4	2	0.44
163	11	39.2	20.6386	33.5819	0.12	2	31	31.5	2	0.26
163	10	60.3	18.0466	33.4369	0.11	2	22	23.4	2	0.21
163	9	79.4	16.4306	33.4112	0.12	2	11	11.8	2	0.10
163	8	99.8	15.7068	33.5641	0.12	2	11	12.0	2	0.10
163	7	125.4	14.1399	33.5027	0.13	2	4	3.1	2	0.02
163	6	150.7	12.0796	33.3996	0.17	2	2	2.7	2	0.02
163	5	200.5	9.3956	33.6055	0.26	2	11	11.0	2	0.04
163	4	251.5	8.8037	33.9704	0.41	2	11	11.0	2	0.03
163	3	503	5.6867	34.1343	0.85	2	22	12.8	2	0.02
163	2	705.6	4.6194	34.3115	0.83	2	34	25.2	2	0.03
163	1	1007.3	3.8157	34.4706	0.72	2	50	41.1	2	0.06
165	12	18.2	21.9453	33.4247	0.15	2	50	50.2	2	0.33
165	11	39.7	19.3182	33.1725	0.14	2	18	17.2	2	0.12
165	10	64.2	17.2996	33.194	0.13	2	13	13.4	2	0.10
165	9	84	16.2296	33.3008	0.14	2	4	3.2	2	0.02
165	8	105.7	15.5177	33.3783	0.19	2	1	2.0	2	0.01
165	7	135.2	13.0161	33.2167	0.25	2	0	0.0	2	0.00
165	6	186.1	9.8283	33.4136	0.37	2	4	5.4	2	0.01
165	5	236	8.9485	33.8681	0.48	2	6	4.0	2	0.01
165	4	285.2	8.2129	34.0093	0.62	2	6	4.4	2	0.01
165	3	474.5	6.137	34.1318	0.86	2	21	17.4	2	0.02

Table 9 Continued:

Station No.	Sample No.	Pressure (db)	Temp. (degC)	Salinity (psu)	Fe _{DISS} ^a (nM)	Fe _{DISS} Flag ^b	Fe(II) Raw ^c (pM)	Fe(II) Corr. ^d (pM)	Fe(II) Flag ^b	Fe(II):Fe _{DISS} Ratio
165	2	674.1	4.819	34.2874	0.81	2	13	4.2	2	0.01
165	1	976.6	3.955	34.4537	0.79	2	16	8.3	2	0.01
167	12	19.6	20.9496	33.3733	0.22	2	33	32.1	2	0.15
167	11	34.2	20.1786	33.4067	0.17	2	20	17.9	2	0.11
167	10	49.1	19.9206	33.4195	0.18	2	12	10.7	2	0.06
167	9	70.4	17.4636	33.2369	0.21	2	9	7.5	2	0.04
167	8	89.9	15.9861	33.1773	0.23	2	5	5.8	2	0.03
167	7	119.9	13.4604	33.1824	0.29	2	3	2.7	2	0.01
167	6	170.3	10.073	33.5646	0.79	2	22	14.5	2	0.02
167	5	220.8	9.7002	33.9532	1.75	2	45	27.2	2	0.02
167	4	270.1	9.2172	34.1115	1.94	2	46	27.0	2	0.01
167	3	442.3	7.6291	34.2212	1.61	2	47	27.2	2	0.02
167	2	643.6	5.6829	34.2449	0.99	2	28	15.3	2	0.02
167	1	945.2	4.3521	34.4305	0.86	2	24	14.5	2	0.02
169	12	19.7	20.9744	33.4262	0.15	2	62	68.5	2	0.46
169	11	40.4	20.1842	33.5423	0.14	2	38	39.6	2	0.28
169	10	59.2	18.6937	33.5964	0.15	2	31	33.7	2	0.22
169	9	81	16.8374	33.4255	0.12	2	17	18.1	2	0.15
169	8	101.2	15.7758	33.3874	0.16	2	15	15.7	2	0.10
169	7	125.7	14.548	33.3926	0.20	2	13	13.3	2	0.07
169	6	150.2	12.2071	33.2144	0.25	2	13	12.8	2	0.05
169	5	200.6	9.4949	33.5265	0.32	2	21	18.7	2	0.06
169	4	252.8	8.8561	33.9205	0.62	2	21	18.1	2	0.03
169	3	502.6	6.1248	34.202	0.85	2	34	27.0	2	0.03
169	2	706.2	5.0657	34.3443	0.88	2	27	14.2	2	0.02
169	1	1008.7	4.0748	34.461	0.72	2	30	19.2	2	0.03
171	12	18.8	20.6721	33.2936	0.22	2	41	38.9	2	0.18
171	11	37.8	19.5914	33.336	0.20	2	26	27.0	2	0.14
171	10	65.2	17.5406	33.298	0.22	2	19	18.2	2	0.08
171	9	83.8	16.522	33.3191	0.27	2	10	9.5	2	0.04
171	8	105.7	15.354	33.3473	0.32	2	10	8.7	2	0.03
171	7	134.8	11.7532	33.1177	1.23	4	13	11.1	2	0.01

Table 9 Continued:

Station No.	Sample No.	Pressure (db)	Temp. (degC)	Salinity (psu)	Fe _{DISS} ^a (nM)	Fe _{DISS} Flag ^b	Fe(II) Raw ^c (pM)	Fe(II) Corr. ^d (pM)	Fe(II) Flag ^b	Fe(II):Fe _{DISS} Ratio
171	6	186	9.531	33.4748	0.61	2	37	32.9	2	0.05
171	5	234.9	8.8637	33.9094	0.87	2	22	18.5	2	0.02
171	4	286	8.2547	34.028	0.95	2	19	14.8	2	0.02
171	3	471.5	6.2924	34.1788	1.42	2	30	24.4	2	0.02
171	2	673.8	5.1784	34.3278	1.37	2	30	19.8	2	0.01
171	1	977.9	4.0931	34.4588	1.36	2	30	22.9	2	0.02
173	12	18.6	19.7431	33.1025	0.19	2	75	90.1	2	0.47
173	11	32.5	19.2586	33.3343	0.18	2	50	58.4	2	0.32
173	10	49.1	17.2257	33.2226	0.19	2	46	58.5	2	0.31
173	9	69	17	33.3619	0.19	2	35	42.8	2	0.23
173	8	88.4	15.1178	33.2141	0.21	2	25	29.9	2	0.14
173	7	118.8	13.5609	33.2871	0.24	2	21	27.8	2	0.12
173	6	169.9	9.6471	33.3209	0.47	2	27	31.8	2	0.07
173	5	220.7	8.9676	33.8495	0.73	2	29	33.5	2	0.05
173	4	271.4	8.2198	34.0279	1.02	2	31	29.1	2	0.03
173	3	442.1	6.3958	34.1521	1.31	2	43	41.9	2	0.03
173	2	643.7	5.2566	34.3146	1.29	2	48	49.2	2	0.04
173	1	946.7	4.0987	34.4463	1.13	2	39	33.0	2	0.03
175	12	19.2	18.241	33.0219	0.14	2	28	25.6	2	0.18
175	11	56.3	16.6854	33.0547	0.15	2	11	11.0	2	0.07
175	10	81.5	14.5566	33.0018	0.15	2	2	3.9	2	0.03
175	9	106.8	12.8934	33.2404	0.19	2	11	12.1	2	0.06
175	8	132.8	10.1099	33.2756	0.30	2	9	11.5	2	0.04
175	7	156.9	9.2887	33.5672	0.45	2	9	6.9	2	0.02
175	6	217.8	8.6098	33.9719	0.63	3	5	3.2	2	0.01
175	5	252.2	8.2413	34.0259	0.65	2	5	1.7	2	0.00
175	4	353.2	7.1445	34.088	0.91	2	15	10.1	2	0.01
175	3	504.2	5.7244	34.1685	0.97	2	9	1.6	2	0.00
175	2	705.5	4.9202	34.359	0.96	2	22	12.0	2	0.01
175	1	1007.7	4.0149	34.4718	0.98	2	17	4.4	2	0.00
177	12	17	17.7267	33.2797	0.19	2	44	46.7	2	0.25
177	11	44.5	12.4466	32.8254	0.23	2	27	28.5	2	0.12

Table 9 Continued:

Station No.	Sample No.	Pressure (db)	Temp. (degC)	Salinity (psu)	Fe _{DISS} ^a (nM)	Fe _{DISS} Flag ^b	Fe(II) Raw ^c (pM)	Fe(II) Corr. ^d (pM)	Fe(II) Flag ^b	Fe(II):Fe _{DISS} Ratio
177	10	85.8	10.5163	33.3105	0.36	2	34	38.2	2	0.11
177	9	111.2	9.5501	33.5395	0.45	2	34	33.9	2	0.08
177	8	134.8	9.209	33.7523	0.60	2	77	71.6	2	0.12
177	7	185.1	8.8276	34.0358	0.77	2	34	32.7	2	0.04
177	6	235.6	7.9437	34.0654	0.81	2	31	27.9	2	0.03
177	5	286.4	7.5079	34.1086	0.96	2	40	33.3	2	0.03
177	4	386.5	6.151	34.0931	1.04	2	37	33.4	2	0.03
177	3	487.4	5.6542	34.2036	1.01	2	43	38.8	2	0.04
177	2	674.2	4.7632	34.3263	0.91	2	31	25.7	2	0.03
177	1	976.3	3.8956	34.4741	0.87	2	28	20.6	2	0.02
179	12	17	18.0069	33.2155	0.17	2	47	48.7	2	0.29
179	11	33.1	15.715	33.2173	0.19	2	27	32.1	2	0.17
179	10	69.2	11.6053	33.1122	0.24	2	33	37.8	2	0.16
179	9	94.7	9.9537	33.5043	0.42	2	36	40.9	2	0.10
179	8	119.1	9.242	33.7943	0.67	3	36	36.7	2	0.05
179	7	144	8.8713	33.9062	0.63	2	27	27.8	2	0.04
179	6	169	8.5709	34.0088	0.79	2	28	23.5	2	0.03
179	5	220.6	7.9353	34.0794	0.86	2	28	25.7	2	0.03
179	4	270.4	7.2447	34.1145	0.91	2	21	16.1	2	0.02
179	3	421.5	6.2177	34.2175	0.92	2	27	23.1	2	0.03
179	2	644.3	5.1424	34.3621	0.96	2	31	28.0	2	0.03
179	1	945.2	4.0768	34.4694	0.89	2	18	12.1	2	0.01
182	12	17.9	17.3541	33.1932	0.15	2	16	21.3	2	0.14
182	11	54	11.029	33.1854	0.19	2	8	8.2	2	0.04
182	10	78.5	9.936	33.4541	0.38	2	10	12.6	2	0.03
182	9	105.2	9.3579	33.7342	0.54	2	7	7.9	2	0.01
182	8	131.1	9.1023	33.9094	0.71	2	7	5.5	2	0.01
182	7	156.7	8.8982	34.0483	0.87	2	3	0.4	2	0.00
182	6	214.5	8.1345	34.1259	1.03	2	10	9.4	2	0.01
182	5	251.5	7.9016	34.1745	1.25	2	7	2.3	2	0.00
182	4	351.8	7.0615	34.2274	1.44	2	7	3.1	2	0.00
182	3	502.1	6.2845	34.3087	1.73	2	25	19.8	2	0.01

Table 9 Continued:

Station No.	Sample No.	Pressure (db)	Temp. (degC)	Salinity (psu)	Fe _{DISS} ^a (nM)	Fe _{DISS} Flag ^b	Fe(II) Raw ^c (pM)	Fe(II) Corr. ^d (pM)	Fe(II) Flag ^b	Fe(II):Fe _{DISS} Ratio
182	2	704.8	5.1067	34.3971	1.49	2	34	28.2	2	0.02
182	1	1007.6	4.164	34.4619	1.19	2	11	8.2	2	0.01
184	12	15.5	17.2181	33.3598	0.20	2	87	64.7	2	0.32
184	11	44.6	12.0867	33.2094	0.26	2	50	42.1	2	0.16
184	10	84.3	9.8039	33.5374	0.45	2	38	29.2	2	0.06
184	9	110.2	9.4086	33.7544	0.59	2	32	22.6	2	0.04
184	8	134.3	9.0205	33.9163	0.78	2	52	52.3	2	0.07
184	7	183.7	8.4525	34.0969	0.92	3	37	25.6	2	0.03
184	6	236.3	7.8324	34.1599	0.90	2	43	34.8	2	0.04
184	5	287.3	7.4467	34.2037	1.00	2	50	44.9	2	0.04
184	4	386.1	6.9066	34.2603	1.15	2	64	51.7	2	0.04
184	3	486.3	6.3995	34.3111	1.23	2	92	77.2	2	0.06
184	2	673.7	5.5294	34.3682	1.17	2	104	84.0	2	0.07
184	1	976.5	4.179	34.461	0.92	2	58	44.4	2	0.05

(a) Concentration of total dissolved iron from shipboard FIA (C.I. Measures, pers. comm.).

(b) CLIVAR data quality codes: (2) no problems detected, (4) bad measurement, (9) sample not taken

(c) Concentration of dissolved Fe(II) at time of first measurement.

(d) Concentration of dissolved Fe(II) corrected to time of filtration and pH adjustment.

Table 10: Data for cruise P16N.

Station No.	Sample No.	Pressure (db)	Temp. (degC)	Salinity (psu)	Fe _{DISS} ^a (nM)	Fe _{DISS} Flag ^b	Fe(II) Raw ^c (pM)	Fe(II) Corr. ^d (pM)	Fe(II) Flag ^b	Fe(II):Fe _{DISS} Ratio
4	12	23.6	29.1665	36.1183	0.18	2	24	18	2	0.10
4	11	42.8	29.0668	36.1417	0.24	2	17	14	2	0.06
4	10	65.7	28.913	36.1597	0.31	2	22	18	2	0.06
4	9	81.7	28.6821	36.1766	0.26	2	14	12	2	0.05
4	8	104.2	27.9785	36.2407	0.29	4	12	10	2	0.03
4	7	127.1	26.7128	36.3227	0.28	2	11	7	2	0.03
4	6	157.2	24.9995	36.3531	0.34	2	11	12	2	0.03
4	5	204.7	22.6075	36.1251	0.32	2	6	4	2	0.01
4	4	256.5	19.3434	35.626	0.32	2	4	3	2	0.01
4	3	506.7	7.4187	34.4976	0.79	2	32	17	2	0.02
4	2	708.3	5.5264	34.4619	2.47	4	250	122	4	0.05
4	1	1009.3	4.1326	34.5166	1.67	4	82	34	2	0.02
6	12	22.3	29.2362	36.0426	0.29	2	32	30	2	0.10
6	11	41.1	29.137	36.0516	0.32	2	21	18	2	0.06
6	10	68.9	28.3312	36.2539	0.35	2	32	27	2	0.08
6	9	87.3	27.9297	36.2932	0.18	2	15	13	2	0.07
6	8	108.8	27.1425	36.3456	0.37	4	13	8	2	0.02
6	7	137.4	25.6265	36.3879	0.26	2	14	10	2	0.04
6	6	176.8	23.6361	36.2757	0.09	2	12	12	2	0.13
6	5	231.2	20.4615	35.7973	0.75	2	3	3	2	0.00
6	4	279.4	16.0617	35.1607	0.09	2	3	4	2	0.04
6	3	556.9	6.6595	34.5089	0.18	2	53	32	2	0.18
6	2	761	5.3088	34.505	1.2	4	461	260	4	0.22
6	1	958.3	4.5336	34.513	0.72	2	121	47	2	0.07
8	12	22	29.2148	35.9776	0.31	2	22	20	2	0.06
8	11	36.7	29.1895	35.9801	0.33	2	12	10	2	0.03
8	10	62.1	29.0664	35.9861	0.3	2	17	16	2	0.05
8	9	80.2	28.5913	36.1253	0.26	2	9	9	2	0.04
8	8	103.7	27.3231	36.3596	0.44	4	11	8	2	0.02
8	7	130.9	25.1351	36.4041	0.38	2	3	1	2	0.00
8	6	153.8	23.6486	36.2918	0.32	2	2	2	2	0.01
8	5	203.3	20.6876	35.8367	0.26	2	3	3	2	0.01
8	4	252.6	16.4869	35.2401	0.38	2	4	3	2	0.01
8	3	504.9	7.5063	34.5843	0.78	2	7	4	2	0.01
8	2	707.3	5.9203	34.5276	2.63	4	12	8	2	0.00

Table 10 Continued:

Station No.	Sample No.	Pressure (db)	Temp. (degC)	Salinity (psu)	Fe _{DISS} ^a (nM)	Fe _{DISS} Flag ^b	Fe(II) Raw ^c (pM)	Fe(II) Corr. ^d (pM)	Fe(II) Flag ^b	Fe(II):Fe _{DISS} Ratio
8	1	1010.1	4.2858	34.5396	0.71	2	22	16	2	0.02
10	12	20.9	28.8388	35.8875	0.21	2	23	26	2	0.12
10	11	42.4	28.8101	35.8857	0.22	2	17	17	2	0.08
10	10	69.7	28.7807	35.8831	0.21	2	15	14	2	0.07
10	9	89.4	28.4841	35.9001	0.16	2	12	10	2	0.06
10	8	110.9	27.899	36.1505	0.18	2	6	4	2	0.02
10	7	138.3	26.4173	36.3366	0.19	2	3	2	2	0.01
10	6	176.9	21.8121	36.0268	0.17	2	1	0	2	0.00
10	5	229.8	17.4206	35.3583	0.2	2	4	2	2	0.01
10	4	278.4	11.9869	34.8151	0.42	2	20	16	2	0.04
10	3	557	7.1205	34.5722	0.61	2	23	14	2	0.02
10	2	757.1	5.6009	34.52	0.61	2	22	15	2	0.02
10	1	957.3	4.6302	34.5328	0.57	2	35	25	2	0.04
12	12	20.9	27.9902	35.7626	0.18	2	53	52	2	0.29
12	11	36.8	27.9745	35.7597	0.33	2	29	29	2	0.09
12	10	66.5	27.5105	35.6606	0.24	2	21	21	2	0.09
12	9	76.9	27.542	35.6712	0.11	2	16	16	2	0.15
12	8	103.9	27.14	36.245	0.14	2	18	17	2	0.12
12	7	127.8	25.1143	36.2975	0.23	2	10	10	2	0.04
12	6	157.2	19.3276	35.5736	0.11	2	9	9	2	0.08
12	5	207.5	15.4185	35.1865	0.17	2	11	11	2	0.06
12	4	256.6	12.5592	34.9346	0.26	2	11	10	2	0.04
12	3	506.3	8.3303	34.6424	0.46	2	37	35	2	0.08
12	2	708.8	6.0459	34.4443	0.46	2	31	29	2	0.06
12	1	1010.1	4.3718	34.5491	0.62	2	40	36	2	0.06
14	12	21.5	26.2915	35.2901	0.04	2	72	74	4	1.85
14	11	41.1	26.2521	35.2874	0.09	2	45	45	2	0.50
14	10	70.3	26.0998	35.2742	0.06	2	43	42	2	0.70
14	9	91.6	25.6683	35.2219	0.06	2	31	30	2	0.49
14	8	107.2	25.7876	35.3659	0.08	2	34	32	2	0.40
14	7	141.7	21.7743	35.8923	0.07	2	26	22	2	0.31
14	6	178.3	15.1009	35.1383	0.16	2	26	24	2	0.15
14	5	233.2	12.2865	34.9124	0.17	2	34	31	2	0.18
14	4	278.4	10.723	34.8042	0.28	2	32	29	2	0.10
14	3	555.5	7.2156	34.5931	0.52	2	51	44	2	0.09

Table 10 Continued:

Station No.	Sample No.	Pressure (db)	Temp. (degC)	Salinity (psu)	Fe _{DISS} ^a (nM)	Fe _{DISS} Flag ^b	Fe(II) Raw ^c (pM)	Fe(II) Corr. ^d (pM)	Fe(II) Flag ^b	Fe(II):Fe _{DISS} Ratio
14	2	756.5	5.7308	34.5358	0.62	2	64	54	2	0.09
14	1	959.8	4.5781	34.5378	0.68	2	98	83	2	0.12
16	12	20	25.8834	35.2261	0.11	2	46	61	2	0.56
16	11	35.1	25.8413	35.2243	0.11	2	25	30	2	0.27
16	10	62.7	25.4682	35.2627	0.12	2	19	23	2	0.19
16	9	76.2	25.2572	35.2392	0.11	2	15	18	2	0.17
16	8	101.2	23.8733	35.5097	0.13	2	15	18	2	0.14
16	7	127.9	18.5821	35.5278	0.11	2	11	11	2	0.10
16	6	152.8	13.748	35.0059	0.16	2	28	30	2	0.19
16	5	201.5	12.7042	34.9135	0.3	2	41	40	2	0.13
16	4	252.9	12.2494	34.8792	0.38	2	24	23	2	0.06
16	3	504.6	7.6749	34.6117	0.48	2	18	17	2	0.03
16	2	708.2	5.7163	34.4811	0.8	2	13	7	2	0.01
16	1	1009.6	4.7249	34.5461	0.72	2	15	9	2	0.01
18	12	23.6	25.7973	35.2903	0.22	2	23	23	2	0.10
18	11	38.2	25.6715	35.2952	0.08	2	17	17	2	0.21
18	10	64	24.971	35.4055	0.12	2	8	8	2	0.07
18	9	84	24.3068	35.7982	0.12	2	2	2	2	0.02
18	8	103	21.0054	35.6019	0.08	2	3	3	2	0.04
18	7	131.2	17.853	35.4663	0.14	2	5	5	2	0.04
18	6	154.1	15.67	35.2601	0.14	2	2	2	2	0.02
18	5	205.3	12.9024	34.9658	0.27	2	4	4	2	0.01
18	4	252.4	12.0611	34.8757	0.44	2	5	5	2	0.01
18	3	506.2	7.2386	34.5868	0.74	2	16	16	2	0.02
18	2	707	5.907	34.5469	0.7	2	12	12	2	0.02
18	1	1009.3	4.6105	34.5506	0.75	2	10	10	2	0.01
19	12	21.1	25.6573	35.3287	0.06	2	30	37	2	0.62
19	11	41.4	25.2445	35.3927	0.05	2	16	24	2	0.49
19	10	68.7	23.5019	35.3629	0.06	2	8	12	2	0.20
19	9	86.3	21.8649	35.5779	0.12	2	6	9	2	0.07
19	8	103.2	18.509	35.4353	0.2	2	7	10	2	0.05
19	7	139.9	15.1432	35.1604	0.42	2	6	6	2	0.01
19	6	177.8	13.586	35.0499	0.31	2	2	2	2	0.01
19	5	226.4	12.2231	34.8837	0.49	2	2	2	2	0.00
19	4	279	11.5084	34.8306	0.47	2	1	0	2	0.00
19	3	555.2	7.3758	34.5933	0.64	2	3	1	2	0.00

Table 10 Continued:

Station No.	Sample No.	Pressure (db)	Temp. (degC)	Salinity (psu)	Fe _{DISS} ^a (nM)	Fe _{DISS} Flag ^b	Fe(II) Raw ^c (pM)	Fe(II) Corr. ^d (pM)	Fe(II) Flag ^b	Fe(II):Fe _{DISS} Ratio
19	2	762.6	5.8896	34.5479	0.64	2	2	0	2	0.00
19	1	961	4.9264	34.55	0.68	2	3	0	2	0.00
20	12	25.4	25.3458	35.3816	0.03	2	18	22	2	0.75
20	11	41.2	24.7784	35.363	0.04	2	7	12	2	0.29
20	10	66.1	23.2558	35.2084	0.05	2	-4	1	2	0.01
20	9	79.9	22.0289	35.18	0.06	2	-4	1	2	0.02
20	8	106.9	18.3321	35.2585	0.15	2	4	8	2	0.05
20	7	133.3	16.1101	35.1039	0.33	2	17	19	2	0.06
20	6	156.6	14.8951	35.0275	0.42	2	21	19	2	0.05
20	5	203.6	13.2225	34.9666	0.51	2	14	10	2	0.02
20	4	252.6	12.1755	34.8756	0.46	2	16	14	2	0.03
20	3	507.9	7.6981	34.6046	0.65	2	81	74	2	0.11
20	2	707.4	6.0211	34.5484	0.58	2	27	22	2	0.04
20	1	1011.7	4.6159	34.5552	0.51	2	43	41	2	0.08
21	12	26.2	25.1392	35.2793	0.26	2	35	41	2	0.16
21	11	43.8	24.3702	35.1647	0.33	2	27	38	2	0.11
21	10	71.6	23.4128	35.041	0.24	2	16	22	2	0.09
21	9	92.7	20.2519	34.992	0.27	2	15	23	2	0.08
21	8	113.9	16.8726	34.9688	0.38	2	11	15	2	0.04
21	7	142	14.2375	35.0042	0.63	2	18	18	2	0.03
21	6	182.7	12.9556	34.9322	0.9	2	14	12	2	0.01
21	5	229.2	12.3524	34.8793	0.81	2	13	12	2	0.02
21	4	276.5	11.9957	34.8578	0.77	2	9	9	2	0.01
21	3	554.9	7.5466	34.5983	0.86	2	18	16	2	0.02
21	2	761.8	5.8915	34.5492	0.92	2	21	18	2	0.02
21	1	958.7	4.5302	34.5556	0.73	2	26	23	2	0.03
22	12	22.2	25.148	35.1007	0.22	2	25	22	2	0.10
22	11	21	25.1477	35.1179	0.24	2	18	31	2	0.13
22	10	37.2	24.7784	35.0582	0.25	2	13	16	2	0.07
22	9	61.9	24.1463	35.0502	0.27	2	10	12	2	0.05
22	8	77.1	23.7659	34.9947	0.3	2	4	7	2	0.02
22	7	100.7	21.37	34.9212	0.41	2	8	9	2	0.02
22	6	129.7	15.0413	34.7108	0.74	2	7	5	2	0.01
22	5	152.3	13.2408	34.7976	0.91	2	12	11	2	0.01
22	4	204	12.4665	34.8752	0.64	2	6	7	2	0.01
22	3	253.8	12.0406	34.8461	1.12	2	15	9	2	0.01

Table 10 Continued:

Station No.	Sample No.	Pressure (db)	Temp. (degC)	Salinity (psu)	Fe _{DISS} ^a (nM)	Fe _{DISS} Flag ^b	Fe(II) Raw ^c (pM)	Fe(II) Corr. ^d (pM)	Fe(II) Flag ^b	Fe(II):Fe _{DISS} Ratio
22	2	709.2	5.8981	34.5487	1.24	2	9	1	2	0.00
22	1	1009.6	4.6046	34.5557	0.97	2	9	4	2	0.00
24	12	32	26.4041	34.8965	0.18	2	-999	-999	9	-9.99
24	11	61.5	24.5374	35.0326	0.21	2	44	65	2	0.31
24	10	82.8	23.8014	34.9816	0.2	2	29	46	2	0.23
24	9	106.9	16.3533	34.7071	0.2	2	16	28	2	0.14
24	8	138.1	13.5037	34.8427	0.26	2	17	29	2	0.11
24	7	177.5	12.5705	34.867	0.4	2	21	31	2	0.08
24	6	226	11.9177	34.8381	1.67	4	17	24	2	0.01
24	5	277.7	11.5006	34.8146	0.68	2	11	14	2	0.02
24	4	556.6	7.1675	34.5804	0.71	2	14	19	2	0.03
24	3	757.6	5.5875	34.5458	1.12	2	51	49	2	0.04
24	2	956.8	4.8527	34.5509	1.01	2	51	52	2	0.05
24	1	566.5	7.2292	34.5831	0.89	2	54	53	2	0.06
26	12	22.4	27.0191	34.8892	0.17	2	22	22	2	0.13
26	11	37.6	26.9696	34.8899	0.18	2	15	17	2	0.10
26	10	62.5	26.7127	34.8843	0.17	2	16	17	2	0.10
26	9	77.2	26.4951	34.8615	0.23	2	15	16	2	0.07
26	8	102.2	21.343	34.8572	0.24	2	15	15	2	0.06
26	7	127.1	16.5726	34.6584	0.26	2	7	7	2	0.03
26	6	152.9	12.9504	34.6101	0.27	2	6	6	2	0.02
26	5	202.8	10.4547	34.6608	0.46	2	15	13	2	0.03
26	4	254.6	9.7302	34.6629	0.62	2	14	12	2	0.02
26	3	504.7	7.3402	34.5818	0.8	2	33	28	2	0.04
26	2	708.4	5.8264	34.5495	0.79	2	17	13	2	0.02
26	1	1007.9	4.3898	34.5623	0.74	2	53	48	2	0.06
28	12	23.6	27.2106	34.83	0.1	2	18	21	2	0.21
28	11	41.7	27.1716	34.8442	0.06	2	13	17	2	0.28
28	10	67	27.1673	34.8934	0.08	2	11	13	2	0.16
28	9	91.1	24.3431	34.7989	0.13	2	8	11	2	0.08
28	8	109	18.104	34.631	0.25	2	4	7	2	0.03
28	7	139	12.8768	34.6049	0.29	2	12	13	2	0.05
28	6	178.8	10.5602	34.653	0.5	2	14	13	2	0.03
28	5	228	9.9156	34.6783	0.59	2	8	7	2	0.01
28	4	278.9	9.4601	34.6615	0.99	2	5	4	2	0.00
28	3	556.3	7.345	34.5837	0.81	2	38	37	2	0.05

Table 10 Continued:

Station No.	Sample No.	Pressure (db)	Temp. (degC)	Salinity (psu)	Fe _{DISS} ^a (nM)	Fe _{DISS} Flag ^b	Fe(II) Raw ^c (pM)	Fe(II) Corr. ^d (pM)	Fe(II) Flag ^b	Fe(II):Fe _{DISS} Ratio
28	2	760.1	5.6836	34.5481	0.97	2	46	44	2	0.04
28	1	958.6	4.7386	34.5579	0.67	2	61	61	2	0.09
30	12	21.1	27.1134	34.8264	0.12	2	47	48	2	0.40
30	11	35.5	27.0688	34.8212	0.1	2	27	31	2	0.31
30	10	60.4	22.0337	34.6944	0.1	2	12	18	2	0.18
30	9	75.6	20.4041	34.8405	0.06	2	12	19	2	0.31
30	8	100.9	14.6107	34.3119	0.07	2	20	39	2	0.55
30	7	126.8	12.2838	34.4718	0.09	2	13	20	2	0.22
30	6	152.1	11.4533	34.6938	0.12	2	7	11	2	0.09
30	5	202.5	10.5454	34.6942	0.16	2	8	11	2	0.07
30	4	252.6	9.9312	34.6758	0.17	2	6	6	2	0.04
30	3	503.6	8.0386	34.5831	0.19	2	11	9	2	0.05
30	2	709.2	5.9684	34.5399	0.16	2	6	2	2	0.01
30	1	1010.3	4.4788	34.5623	0.17	2	10	5	2	0.03
32	12	22	26.7362	34.6508	0.1	2	24	25	2	0.25
32	11	41.4	26.2071	34.5373	0.1	2	19	20	2	0.20
32	10	67.9	18.9472	34.4967	0.08	2	14	15	2	0.19
32	9	87.5	15.2718	34.3468	0.06	2	5	6	2	0.11
32	8	107.3	12.9248	34.6261	0.08	2	15	16	2	0.20
32	7	139.9	11.891	34.7016	0.02	2	6	7	2	0.34
32	6	159	11.4585	34.7131	0.02	2	5	6	2	0.32
32	5	254.8	10.5624	34.7089	0.1	2	5	6	2	0.06
32	4	408.9	9.3462	34.6512	0.18	2	26	22	2	0.12
32	3	504.8	8.3341	34.595	0.18	2	32	28	2	0.15
32	2	756.4	5.8586	34.5286	0.18	2	12	10	2	0.06
32	1	962.2	4.7577	34.5486	0.23	2	26	19	2	0.08
34	12	22.7	26.4128	34.6008	0.12	2	26	24	2	0.20
34	11	36.8	26.3689	34.6684	0.17	2	17	16	2	0.09
34	10	64.3	26.1444	34.6571	0.2	2	12	12	2	0.06
34	9	76.8	23.8986	34.5463	0.21	2	10	27	2	0.13
34	8	101.9	16.8585	34.3986	0.19	2	6	17	2	0.09
34	7	128	13.8433	34.3784	0.15	2	5	13	2	0.09
34	6	153.3	12.042	34.44	0.21	2	8	10	2	0.05
34	5	202.8	11.1209	34.6533	0.51	2	11	6	2	0.01
34	4	252.8	10.5617	34.6857	0.59	2	10	6	2	0.01
34	3	506.2	8.1045	34.5619	0.81	2	12	10	2	0.01

Table 10 Continued:

Station No.	Sample No.	Pressure (db)	Temp. (degC)	Salinity (psu)	Fe _{DISS} ^a (nM)	Fe _{DISS} Flag ^b	Fe(II) Raw ^c (pM)	Fe(II) Corr. ^d (pM)	Fe(II) Flag ^b	Fe(II):Fe _{DISS} Ratio
34	2	706.9	6.3202	34.5197	0.94	2	12	9	2	0.01
34	1	1009.7	4.6052	34.5386	0.93	2	14	8	2	0.01
36	12	20.8	25.905	34.3617	0.28	2	57	60	2	0.22
36	11	42	25.9004	34.365	0.25	2	21	25	2	0.10
36	10	67.2	25.8442	34.4287	0.34	2	11	15	2	0.04
36	9	86.8	24.1595	34.4513	0.39	2	5	9	2	0.02
36	8	109	20.3843	34.568	0.36	2	-3	0	2	0.00
36	7	138.2	16.2093	34.3885	0.41	2	-1	2	2	0.00
36	6	175.9	12.2249	34.1428	0.5	2	8	10	2	0.02
36	5	227.6	10.0324	34.3468	0.67	2	3	3	2	0.00
36	4	278.9	9.6163	34.464	0.79	2	26	25	2	0.03
36	3	556.8	6.9809	34.5198	0.83	2	25	26	2	0.03
36	2	757.4	5.5476	34.5176	0.93	2	81	81	2	0.09
36	1	959.3	4.5345	34.5347	0.97	2	27	30	2	0.03
40	10	24.4	23.7481	34.5319	0.28	2	23	32	2	0.11
40	9	47.1	23.7192	34.6042	0.24	2	14	21	2	0.09
40	8	67	23.7805	34.7941	0.29	2	11	17	2	0.06
40	7	90.6	23.6675	34.9028	0.28	2	6	12	2	0.04
40	6	114.1	23.5951	34.9536	0.28	2	6	11	2	0.04
40	5	143.6	21.4876	35.0373	0.31	2	1	1	2	0.00
40	4	179.1	19.2217	34.8762	0.3	2	3	2	2	0.01
40	3	221.2	14.9487	34.3944	0.4	2	6	7	2	0.02
40	2	275.2	14.9487	34.3731	0.48	2	9	9	2	0.02
40	1	550.2	6.3277	34.326	0.91	2	26	34	2	0.04
45	12	25.8	22.3346	35.199	0.49	4	71	76	2	0.15
45	11	42.5	22.0101	35.3256	0.46	4	40	45	2	0.10
45	10	64.8	21.9823	35.325	0.42	4	28	32	2	0.08
45	9	84.8	21.9751	35.324	0.51	4	17	17	2	0.03
45	8	107.9	21.934	35.3146	0.68	4	13	14	2	0.02
45	7	127.1	21.0824	35.2602	0.64	4	16	16	2	0.03
45	6	155.1	19.3868	34.9892	0.94	4	9	11	2	0.01
45	5	204	16.4206	34.638	0.83	4	2	0	2	0.00
45	4	256.3	13.8714	34.363	-999	1	-999	-999	9	-9.99
45	3	507.3	7.5318	34.037	1.12	4	58	51	2	0.05
45	2	710.5	4.7714	34.1823	1.37	4	47	40	2	0.03
45	1	1011	3.9025	34.4653	1.51	4	124	110	4	0.07

Table 10 Continued:

Station No.	Sample No.	Pressure (db)	Temp. (degC)	Salinity (psu)	Fe _{DISS} ^a (nM)	Fe _{DISS} Flag ^b	Fe(II) Raw ^c (pM)	Fe(II) Corr. ^d (pM)	Fe(II) Flag ^b	Fe(II):Fe _{DISS} Ratio
47	12	19.9	22.0173	35.2853	0.47	4	21	23	2	0.05
47	11	40.2	22.023	35.2847	0.23	2	16	17	2	0.07
47	10	65.5	22.0062	35.2831	0.25	2	14	14	2	0.06
47	9	86.4	22.0062	35.2848	0.24	2	12	12	2	0.05
47	8	106.4	21.9777	35.2906	0.33	4	11	11	2	0.03
47	7	138.8	21.4595	35.2311	0.42	4	5	4	2	0.01
47	6	177.4	19.2358	34.9562	0.56	4	0	0	2	0.00
47	5	228.7	16.8565	34.6948	0.38	2	2	1	2	0.00
47	4	278.1	14.0069	34.3812	-999	1	-999	-999	9	-9.99
47	3	553.6	7.0714	34.0345	0.5	2	15	7	2	0.01
47	2	756	4.6871	34.1755	0.55	2	38	30	2	0.06
47	1	957.4	4.1034	34.3907	1.04	2	23	15	2	0.01
49	12	20.1	20.9356	35.341	0.24	2	25	23	2	0.10
49	11	36.3	20.9392	35.3409	0.25	2	23	21	2	0.09
49	10	60.4	20.9127	35.3382	0.22	2	23	19	2	0.08
49	9	77.2	20.7954	35.3327	-999	1	-999	-999	9	-9.99
49	8	101.3	20.6482	35.3324	0.31	2	21	17	2	0.05
49	7	126.2	20.5035	35.3143	0.31	2	16	11	2	0.04
49	6	153.2	19.9827	35.2327	0.31	2	11	7	2	0.02
49	5	202.9	16.121	34.5897	0.64	4	10	4	2	0.01
49	4	254.2	13.8557	34.3681	0.5	2	8	0	2	0.00
49	3	504.4	8.0436	34.0509	0.7	2	18	11	2	0.02
49	2	707.1	4.8427	34.0737	0.81	2	23	16	2	0.02
49	1	1008.6	3.7662	34.4002	1.04	2	30	23	2	0.02
51	12	21	19.9297	35.2698	0.16	2	30	31	2	0.20
51	11	40.2	19.9067	35.2697	0.19	2	21	20	2	0.11
51	10	66.5	19.9006	35.2688	0.16	2	22	21	2	0.13
51	9	85.7	19.4648	35.2104	-999	1	-999	-999	9	-9.99
51	8	107.2	19.2723	35.1755	0.23	2	21	20	2	0.09
51	7	137.9	19.0609	35.139	0.19	2	18	18	2	0.10
51	6	179.3	16.7912	34.6576	0.28	2	13	12	2	0.04
51	5	226.3	14.2173	34.3915	0.58	4	13	13	2	0.02
51	4	278.5	12.2716	34.2382	0.37	2	17	15	2	0.04
51	3	553.5	6.5185	33.9976	0.6	2	23	20	2	0.03
51	2	757.3	4.4936	34.1586	0.89	4	53	47	2	0.05
51	1	959.1	3.7933	34.3497	0.61	2	54	50	2	0.08

Table 10 Continued:

Station No.	Sample No.	Pressure (db)	Temp. (degC)	Salinity (psu)	Fe _{DISS} ^a (nM)	Fe _{DISS} Flag ^b	Fe(II) Raw ^c (pM)	Fe(II) Corr. ^d (pM)	Fe(II) Flag ^b	Fe(II):Fe _{DISS} Ratio
53	12	28.6	17.4858	34.7783	0.13	2	22	25	2	0.19
53	11	51.5	17.0655	34.7112	0.13	2	14	16	2	0.13
53	10	69.7	16.9124	34.7005	0.17	2	6	8	2	0.05
53	9	85.5	16.3122	34.6047	-999	9	-999	-999	9	-9.99
53	8	112.8	14.1277	34.3706	0.18	2	0	2	2	0.01
53	7	129.6	13.4339	34.3414	0.18	2	-2	0	2	0.00
53	6	156.6	13.1502	34.3248	0.19	2	9	8	2	0.04
53	5	206.5	12.2933	34.2785	0.17	2	0	2	2	0.01
53	4	255.3	11.3887	34.2196	0.24	2	1	1	2	0.00
53	3	509.7	6.9229	33.9882	0.73	4	14	12	2	0.02
53	2	712.1	4.4984	34.0908	0.69	2	33	17	2	0.02
53	1	1013	3.5135	34.3673	0.87	2	76	56	2	0.06
55	12	21.7	17.4776	34.8586	0.31	2	25	25	2	0.08
55	11	43.4	17.0557	34.789	0.22	2	20	18	2	0.08
55	10	69.9	16.021	34.5543	0.33	2	9	9	2	0.03
55	9	90.9	15.8389	34.5199	-999	9	-999	-999	9	-9.99
55	8	108.8	15.1777	34.4619	0.36	2	2	4	2	0.01
55	7	143.1	13.0981	34.2535	0.53	4	2	3	2	0.01
55	6	178.8	12.3641	34.2394	0.47	2	2	1	2	0.00
55	5	227.3	11.4247	34.224	0.53	2	1	0	2	0.00
55	4	278.1	10.5871	34.1486	0.55	2	2	2	2	0.00
55	3	557.4	5.972	33.9822	0.72	2	10	5	2	0.01
55	2	759.8	4.1802	34.1379	0.84	2	21	15	2	0.02
55	1	960.2	3.53	34.3069	0.99	2	21	14	2	0.01
57	12	23.4	14.2972	34.1178	0.27	2	33	38	2	0.14
57	11	39	13.9842	34.1302	0.35	4	17	18	2	0.05
57	10	66.9	14.0648	34.1802	0.35	2	12	13	2	0.04
57	9	80.3	13.9621	34.1589	0.33	2	8	6	2	0.02
57	8	108.5	13.4939	34.098	0.18	2	9	8	2	0.04
57	7	133	12.1272	34.2216	0.34	2	3	0	2	0.00
57	6	154.1	11.8596	34.2231	0.28	2	4	3	2	0.01
57	5	205.1	11.0052	34.2037	0.29	2	10	11	2	0.04
57	4	256.5	10.1266	34.1482	0.56	2	8	5	2	0.01
57	3	508.2	5.9872	33.9807	0.7	2	7	4	2	0.01
57	2	709.6	4.3322	34.1014	0.61	2	10	7	2	0.01
57	1	1010.6	3.3852	34.3273	0.87	2	17	10	2	0.01

Table 10 Continued:

Station No.	Sample No.	Pressure (db)	Temp. (degC)	Salinity (psu)	Fe _{DISS} ^a (nM)	Fe _{DISS} Flag ^b	Fe(II) Raw ^c (pM)	Fe(II) Corr. ^d (pM)	Fe(II) Flag ^b	Fe(II):Fe _{DISS} Ratio
59	12	22.6	12.9459	33.8299	0.27	2	22	21	2	0.08
59	11	41.8	12.9445	33.8293	0.3	2	19	17	2	0.06
59	10	67.3	12.6495	33.8126	0.43	2	14	13	2	0.03
59	9	85	12.6778	33.8262	0.31	2	13	11	2	0.03
59	8	112.1	12.1534	33.9961	0.52	2	8	6	2	0.01
59	7	135.3	11.1192	34.1304	0.51	2	9	7	2	0.01
59	6	179.7	10.6282	34.1677	0.59	2	7	6	2	0.01
59	5	227.8	9.8849	34.117	0.49	2	10	10	2	0.02
59	4	283.2	9.107	34.0755	0.53	2	8	5	2	0.01
59	3	554.2	4.9969	34.0043	0.83	2	14	11	2	0.01
59	2	757.9	3.9926	34.1647	0.76	2	16	13	2	0.02
59	1	959.7	3.3295	34.2977	0.67	2	23	17	2	0.03
61	12	24.9	12.0157	33.6597	0.33	2	16	8	2	0.02
61	11	38.3	12.017	33.6642	0.37	2	18	6	2	0.02
61	10	62.5	11.9845	33.657	0.46	2	20	15	2	0.03
61	9	78.7	11.9779	33.6548	0.39	2	14	4	2	0.01
61	8	104.7	11.9518	33.6524	0.36	2	15	9	2	0.02
61	7	133	11.3739	33.8858	0.43	2	5	0	2	0.00
61	6	154.5	10.9078	34.0197	0.43	2	10	7	2	0.02
61	5	203.3	10.0966	34.089	0.38	2	7	5	2	0.01
61	4	254.9	9.3365	34.0623	0.41	2	5	0	2	0.00
61	3	505.9	5.8247	33.9631	0.58	2	13	6	2	0.01
61	2	709.9	4.309	34.0908	0.72	2	12	2	2	0.00
61	1	1008.7	3.2747	34.3081	0.68	2	24	14	2	0.02
62	12	21.6	10.8293	33.376	0.63	2	16	17	2	0.03
62	11	43.1	11.3465	33.5373	0.58	2	10	10	2	0.02
62	10	75.5	11.6292	33.6368	0.56	2	17	19	2	0.03
62	9	94.3	11.6958	33.663	0.56	2	4	4	2	0.01
62	8	118.7	11.1374	33.9862	0.53	2	0	0	2	0.00
62	7	138.6	10.8632	34.0741	0.51	2	6	6	2	0.01
62	6	178.5	10.1616	34.1301	0.54	2	3	3	2	0.01
62	5	233.9	9.3488	34.0777	0.68	2	5	5	2	0.01
62	4	280.9	8.7357	34.0362	0.69	2	4	1	2	0.00
62	3	560.6	5.085	33.9977	0.82	2	8	6	2	0.01
62	2	762	4.019	34.1584	1.03	2	10	6	2	0.01
62	1	961.2	3.3664	34.2887	0.93	2	19	15	2	0.02

Table 10 Continued:

Station No.	Sample No.	Pressure (db)	Temp. (degC)	Salinity (psu)	Fe _{DISS} ^a (nM)	Fe _{DISS} Flag ^b	Fe(II) Raw ^c (pM)	Fe(II) Corr. ^d (pM)	Fe(II) Flag ^b	Fe(II):Fe _{DISS} Ratio
66	12	22.9	7.0964	32.9229	0.28	2	13	6	2	0.02
66	11	37.5	7.0922	32.9221	0.40	2	8	4	2	0.01
66	10	64.7	7.0898	32.9217	0.43	2	9	2	2	0.01
66	9	78.1	7.0841	32.9214	0.37	2	9	3	2	0.01
66	8	105.3	7.0729	32.9213	0.53	2	27	21	4	0.04
66	7	129.6	7.2496	33.1091	0.43	2	9	5	2	0.01
66	6	155.7	7.7128	33.7921	0.63	2	5	2	2	0.00
66	5	205.3	6.9927	33.8563	0.56	2	2	0	2	0.00
66	4	254.2	6.3475	33.8672	0.37	2	4	2	2	0.01
66	3	505.3	4.5122	34.0284	0.98	2	11	7	2	0.01
66	2	708.7	3.7077	34.1711	0.94	2	15	8	2	0.01
66	1	1013.6	3.0835	34.3435	0.91	2	20	12	2	0.01
68	12	24.9	6.22	32.7616	0.43	2	50	54	2	0.13
68	11	44.4	6.2166	32.7617	0.35	2	33	39	2	0.11
68	10	70.4	6.212	32.762	0.22	2	34	41	2	0.18
68	9	95.2	6.2133	32.7675	0.38	2	36	42	2	0.11
68	8	113.2	6.2247	32.7835	0.26	2	26	32	2	0.12
68	7	138.4	6.3974	33.3478	0.47	2	25	32	2	0.07
68	6	181.2	5.9448	33.7395	0.32	2	16	26	2	0.08
68	5	234.9	5.2528	33.8078	0.65	2	10	8	2	0.01
68	4	289	4.9384	33.8676	0.66	2	11	12	2	0.02
68	3	558.6	3.8078	34.1139	1.03	2	16	18	2	0.02
68	2	758.2	3.4157	34.251	1.10	2	19	21	2	0.02
68	1	962.5	3.0833	34.3397	0.92	2	21	24	2	0.03
70	12	22.9	5.2194	32.6473	0.22	2	33	29	2	0.13
70	11	38.5	5.2212	32.6473	0.16	2	24	26	2	0.17
70	10	65.3	5.2229	32.648	0.22	2	18	15	2	0.07
70	9	85.1	5.2398	32.6534	0.28	2	18	15	2	0.05
70	8	108.7	5.3768	32.6875	0.26	2	19	19	2	0.07
70	7	134.8	4.8855	33.6013	0.29	2	20	19	2	0.07
70	6	153.8	4.7372	33.6828	0.38	2	4	3	2	0.01
70	5	203.6	4.3003	33.789	0.49	2	3	3	2	0.01
70	4	252.4	4.1796	33.8614	0.63	2	5	5	2	0.01
70	3	506.1	3.7282	34.1089	0.94	2	7	6	2	0.01
70	2	707.4	3.3616	34.2438	0.77	2	17	15	2	0.02
70	1	1011.1	2.8948	34.3741	1.00	2	18	16	2	0.02

Table 10 Continued:

Station No.	Sample No.	Pressure (db)	Temp. (degC)	Salinity (psu)	Fe _{DISS} ^a (nM)	Fe _{DISS} Flag ^b	Fe(II) Raw ^c (pM)	Fe(II) Corr. ^d (pM)	Fe(II) Flag ^b	Fe(II):Fe _{DISS} Ratio
72	12	22.5	4.5731	32.665	0.18	2	34	34	2	0.19
72	11	42.1	4.5638	32.6655	0.28	2	30	29	2	0.10
72	10	65.4	4.5523	32.6657	0.22	2	21	20	2	0.09
72	9	87	4.5218	32.7457	0.22	2	17	17	2	0.08
72	8	108.5	4.1743	33.5434	0.44	2	11	7	2	0.01
72	7	136.4	4.0424	33.7198	0.57	2	6	5	2	0.01
72	6	178.3	4.0571	33.8143	0.75	2	4	2	2	0.00
72	5	227.4	3.9332	33.8603	0.70	2	4	3	2	0.00
72	4	278.6	3.9739	33.9534	0.74	2	7	4	2	0.01
72	3	555	3.5262	34.1734	1.05	2	15	15	2	0.01
72	2	758.7	3.217	34.2874	1.10	2	9	7	2	0.01
72	1	959.6	2.8673	34.3764	0.97	2	8	4	2	0.00
74	12	24.6	3.4588	32.8387	0.26	2	51	42	2	0.16
74	11	38.3	3.4634	32.8393	0.30	2	63	64	2	0.21
74	10	63.5	3.4656	32.8417	0.22	2	75	67	2	0.31
74	9	79.9	3.6073	32.9567	0.30	2	42	38	2	0.13
74	8	102.4	4.4995	33.5975	0.49	2	15	5	2	0.01
74	7	127.8	4.404	33.8036	0.93	2	18	11	2	0.01
74	6	155.8	4.212	33.8632	1.04	2	16	7	2	0.01
74	5	206.1	4.0771	33.9308	1.09	2	14	4	2	0.00
74	4	255.8	3.9849	33.9938	1.12	2	19	8	2	0.01
74	3	507.1	3.5294	34.2033	1.35	2	18	4	2	0.00
74	2	708.2	3.1379	34.2976	1.21	2	14	5	2	0.00
74	1	1011.8	2.6907	34.4093	0.94	2	12	2	2	0.00
76	12	20.00	-999.00	-999.00	999.00	9	54	53	2	0.00
76	11	35.00	-999.00	-999.00	-999.00	9	43	41	2	0.00
76	10	65.00	-999.00	-999.00	-999.00	9	27	24	2	0.00
76	9	85.00	-999.00	-999.00	-999.00	9	16	14	2	0.00
76	8	105.00	-999.00	-999.00	-999.00	9	10	7	2	0.00
76	7	135.00	-999.00	-999.00	-999.00	9	10	6	2	0.00
76	6	249.8	4.086	33.9757	0.81	2	11	5	2	0.01
76	5	277.9	4.0405	33.9919	0.83	2	13	4	2	0.01
76	4	319.4	3.9823	34.0312	0.91	2	15	5	2	0.01
76	3	585.3	3.5334	34.2205	0.80	2	20	11	2	0.01
76	2	755.6	3.1982	34.3059	0.85	2	17	7	2	0.01
76	1	957.5	2.8517	34.3809	0.82	2	11	0	2	0.00

Table 10 Continued:

Station No.	Sample No.	Pressure (db)	Temp. (degC)	Salinity (psu)	Fe _{DISS} ^a (nM)	Fe _{DISS} Flag ^b	Fe(II) Raw ^c (pM)	Fe(II) Corr. ^d (pM)	Fe(II) Flag ^b	Fe(II):Fe _{DISS} Ratio
79	12	22.4	4.1566	32.5407	1.05	2	68	36	2	0.03
79	11	39.5	4.0072	32.5824	0.97	2	33	28	2	0.03
79	10	66	4.0794	32.7075	0.86	2	17	10	2	0.01
79	9	79.6	4.0739	32.8129	0.93	2	7	1	2	0.00
79	8	103.5	4.7225	33.2648	0.78	2	8	4	2	0.00
79	7	128	5.3562	33.6578	1.41	2	8	0	2	0.00
79	6	153.9	5.1212	33.7373	1.40	2	10	4	2	0.00
79	5	206.4	4.5432	33.85	1.01	2	12	6	2	0.01
79	4	253.8	4.4657	33.9162	0.97	2	17	8	2	0.01
79	3	506.9	3.7898	34.1396	1.13	2	23	17	2	0.02
79	2	707.8	3.4274	34.2581	0.95	2	28	19	2	0.02
79	1	1011.4	2.8703	34.381	0.87	2	25	17	2	0.02

(a) Concentration of total dissolved iron from shipboard FIA (C.I. Measures, pers. comm.).

(b) CLIVAR data quality codes: (2) no problems detected, (4) bad measurement, (9) sample not taken

(c) Concentration of dissolved Fe(II) at time of first measurement.

(d) Concentration of dissolved Fe(II) corrected to time of filtration and pH adjustment.

APPENDIX H

OCEANOGRAPHIC SECTIONS FOR PO2 TRANSECT

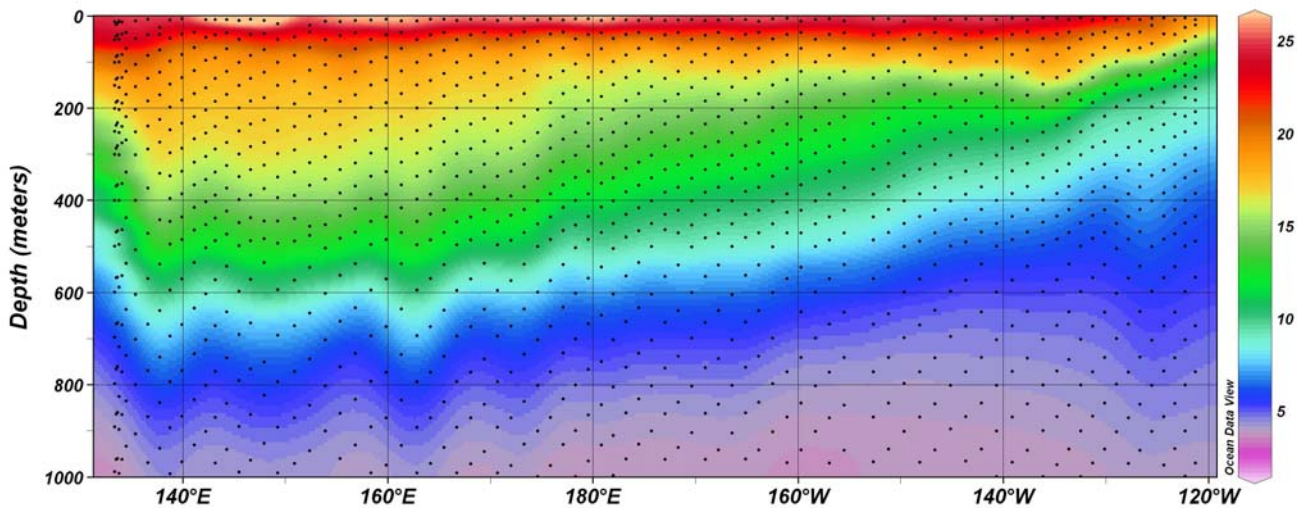


Fig. 43: Oceanographic section of temperature (deg. C) for cruise PO2, the latitudinal section along 30°N latitude, from Japan (left) to California (right).

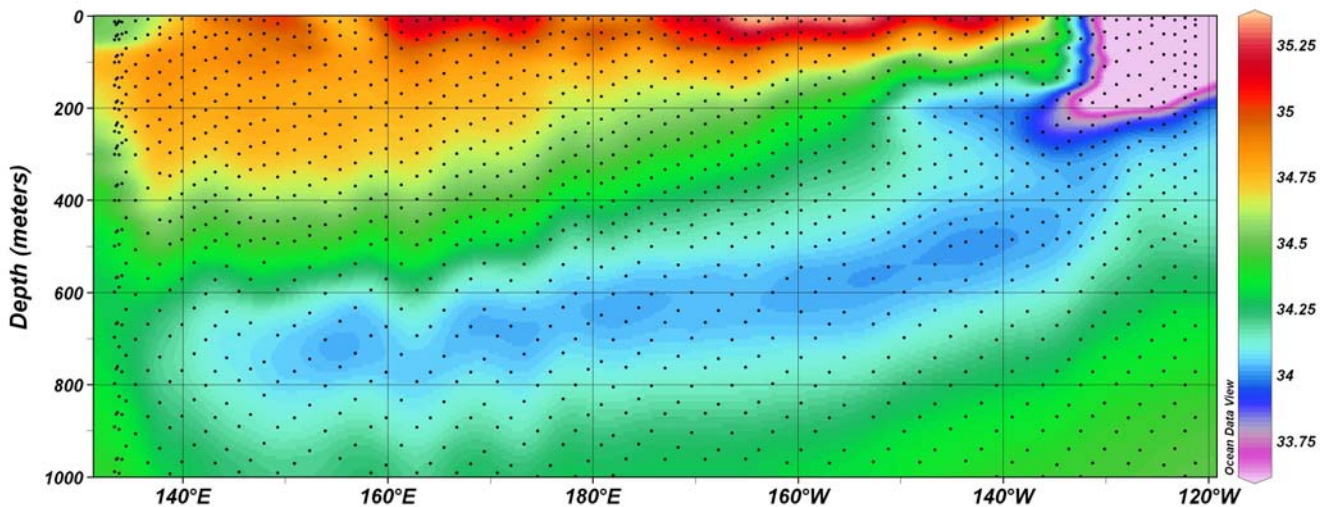


Fig. 44: Oceanographic section of salinity (psu) for cruise PO2, the latitudinal section along 30°N latitude, from Japan (left) to California (right).

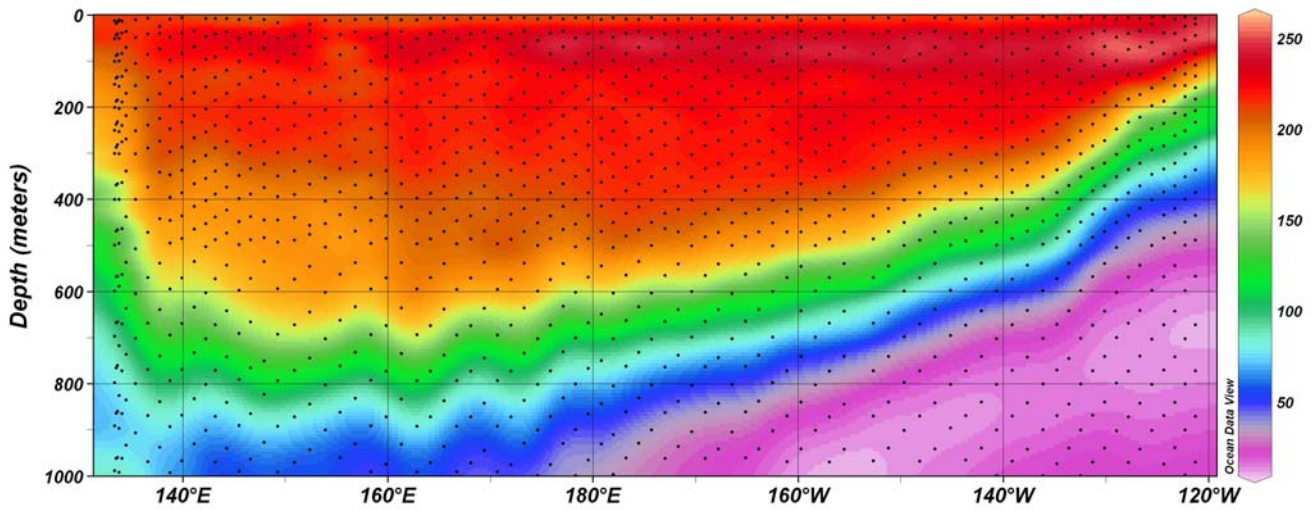


Fig. 45: Oceanographic section of dissolved oxygen ($\mu\text{mol/kg}$) for cruise PO2, the latitudinal section along 30°N latitude, from Japan (left) to California (right). [Data are from the CLIVAR and Carbon Hydrographic Data Office (<http://cchdo.ucsd.edu/>).]

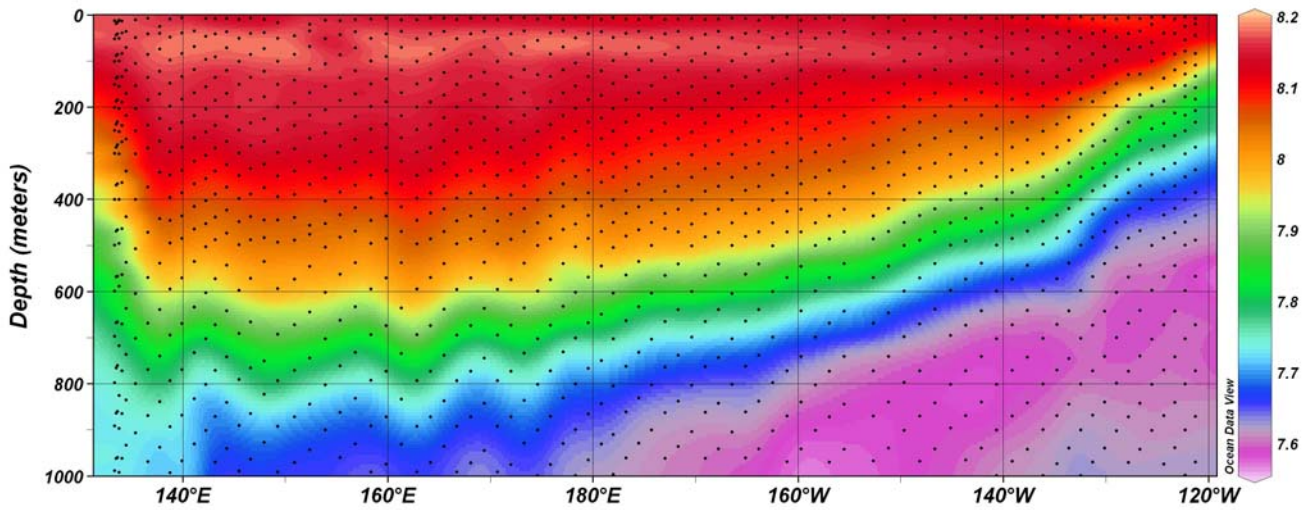


Fig. 46: Oceanographic section of pH (standard units on the free scale) for cruise PO2, the latitudinal section along 30°N latitude, from Japan (left) to California (right). Values for pH were derived as described in Appendix C.

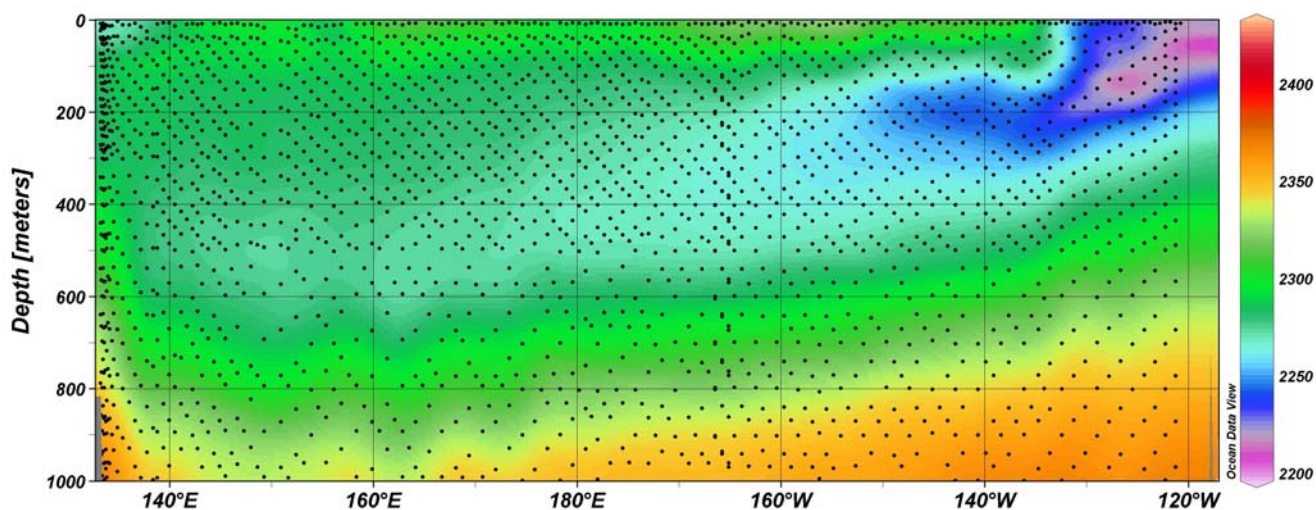


Fig. 47: Oceanographic section total alkalinity ($\mu\text{mol}/\text{kg}$) for cruise PO2, the latitudinal section along 30°N latitude, from Japan (left) to California (right). [Data are from the CLIVAR and Carbon Hydrographic Data Office (<http://cchdo.ucsd.edu/>).]

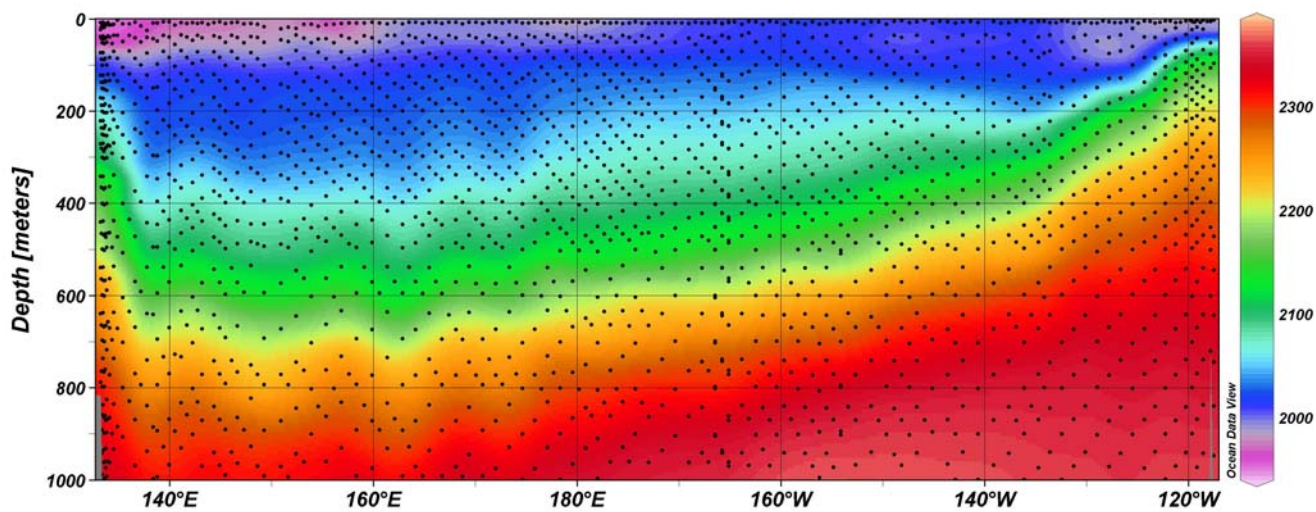


Fig. 48: Oceanographic section of dissolved inorganic carbon ($\mu\text{mol}/\text{kg}$) for cruise PO2, the latitudinal section along 30°N latitude, from Japan (left) to California (right). [Data are from the CLIVAR and Carbon Hydrographic Data Office (<http://cchdo.ucsd.edu/>).]

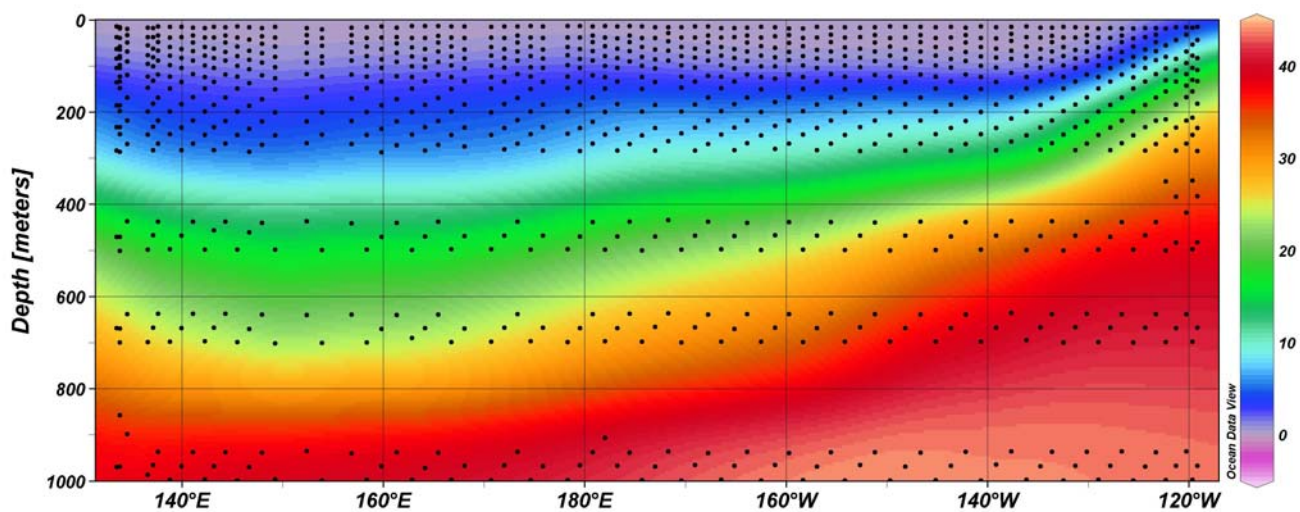


Fig. 49: Oceanographic section of nitrate ($\mu\text{mol/kg}$) for cruise PO2, the latitudinal section along 30°N latitude, from Japan (left) to California (right).

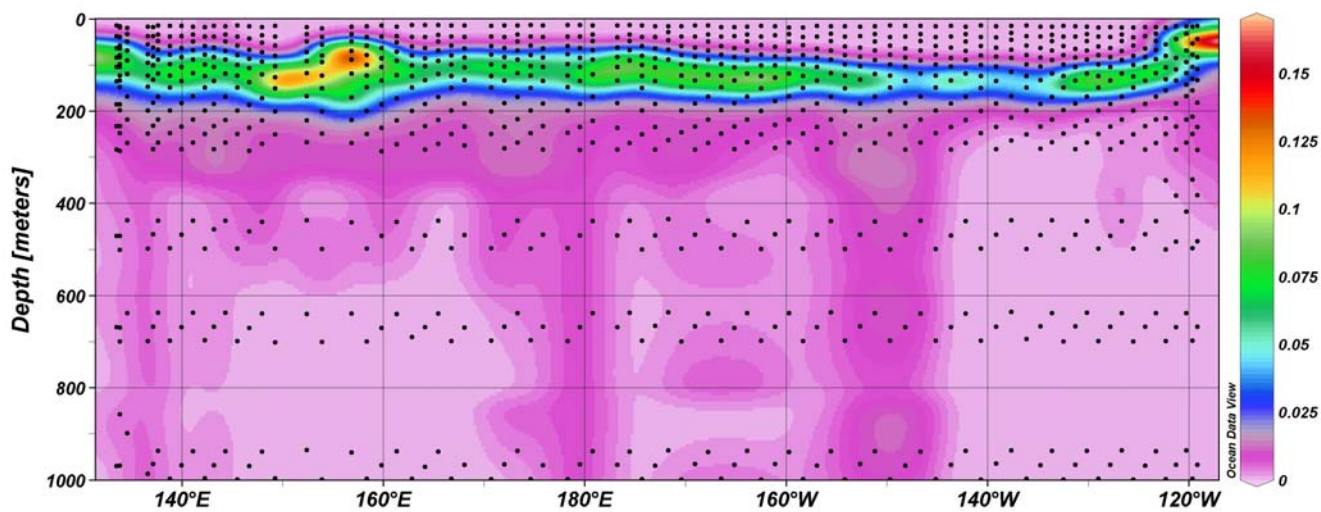


Fig. 50: Oceanographic section of nitrite ($\mu\text{mol/kg}$) for cruise PO2, the latitudinal section along 30°N latitude, from Japan (left) to California (right).

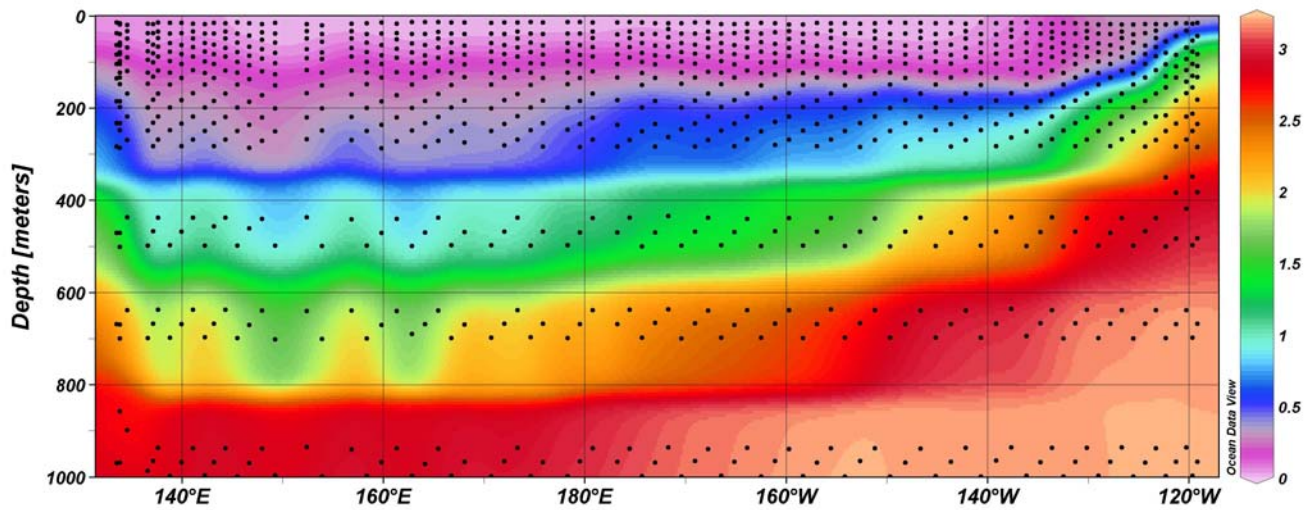


Fig. 51: Oceanographic section of phosphate ($\mu\text{mol/kg}$) for cruise PO2, the latitudinal section along 30°N latitude, from Japan (left) to California (right).

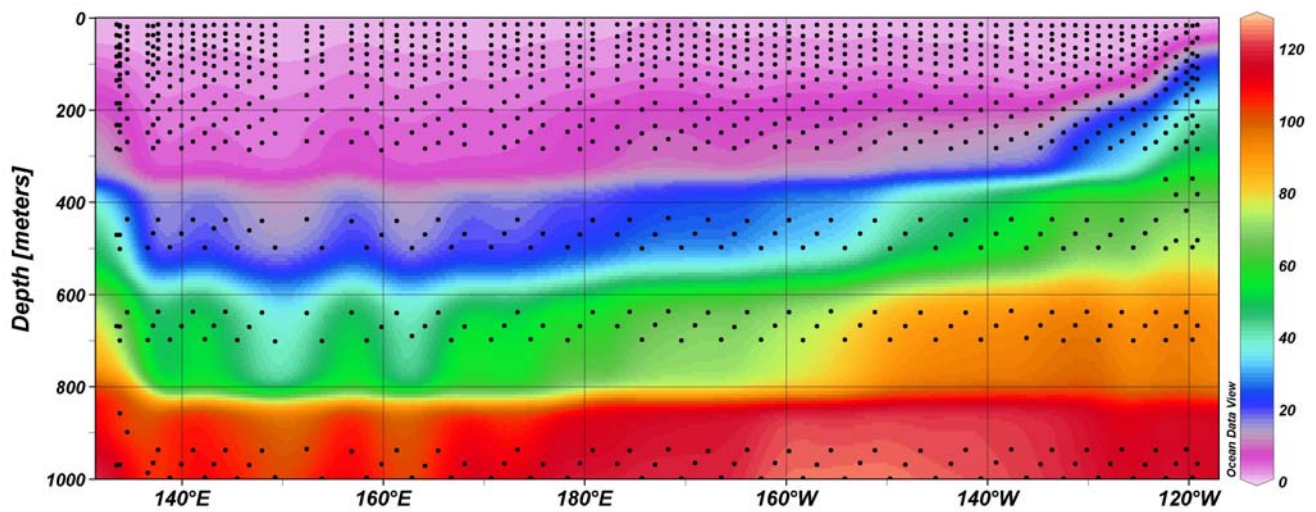


Fig. 52: Oceanographic section of silicate ($\mu\text{mol/kg}$) for cruise PO2, the latitudinal section along 30°N latitude, from Japan (left) to California (right).

APPENDIX I
OCEANOGRAPHIC SECTIONS FOR P16N TRANSECT

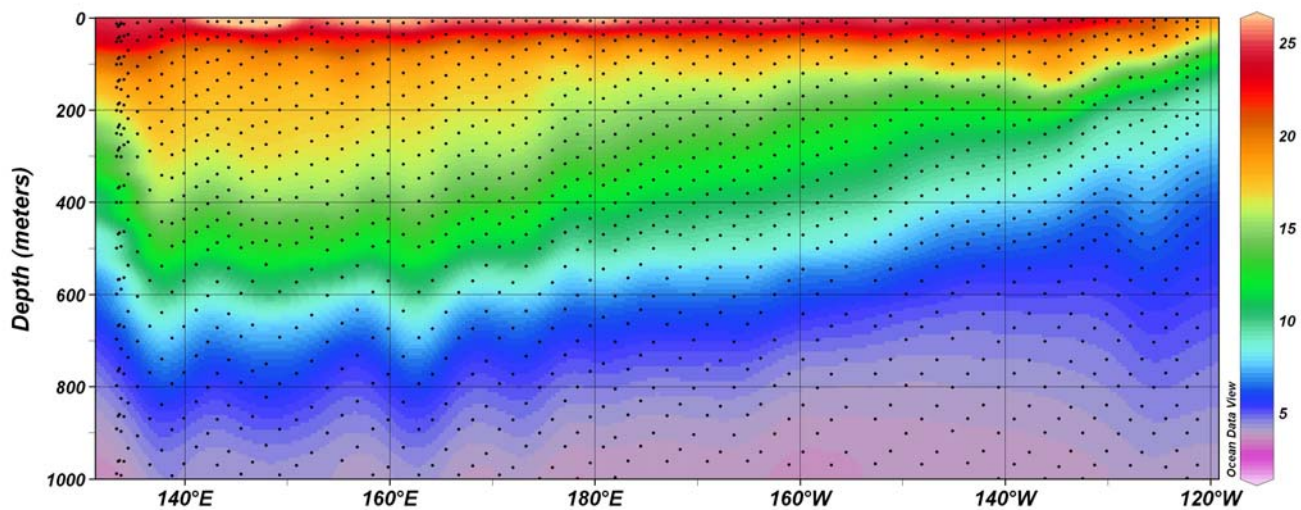


Fig. 53: Oceanographic section of temperature (deg. C) is shown here for cruise P16N, the meridional section along 152°W longitude, from Tahiti (left) to Alaska (right).

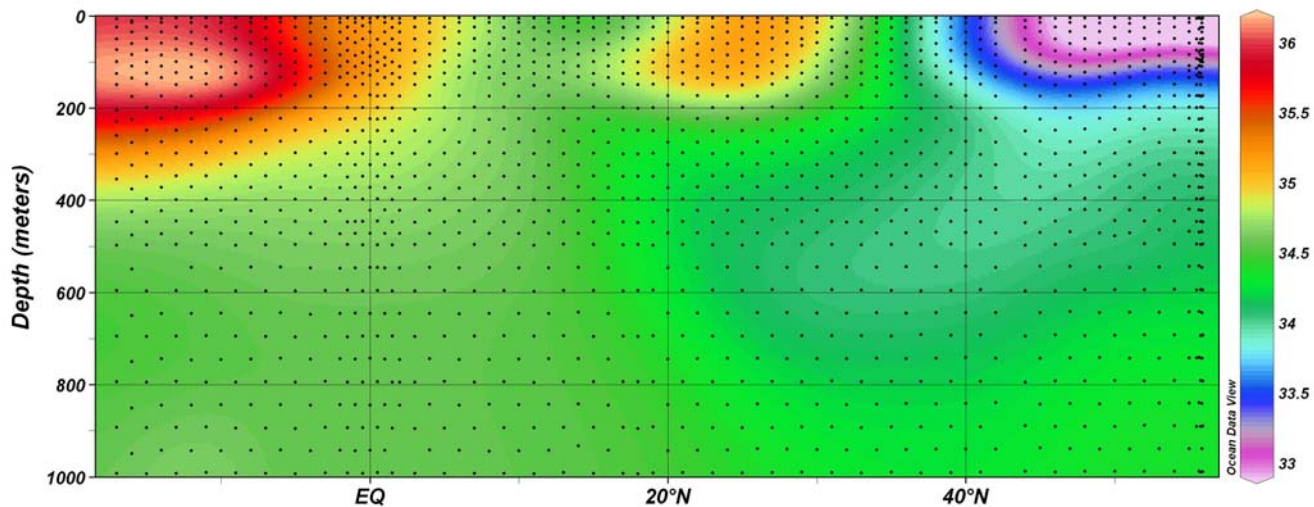


Fig. 54: Oceanographic section of salinity (psu) is shown here for cruise P16N, the meridional section along 152°W longitude, from Tahiti (left) to Alaska (right).

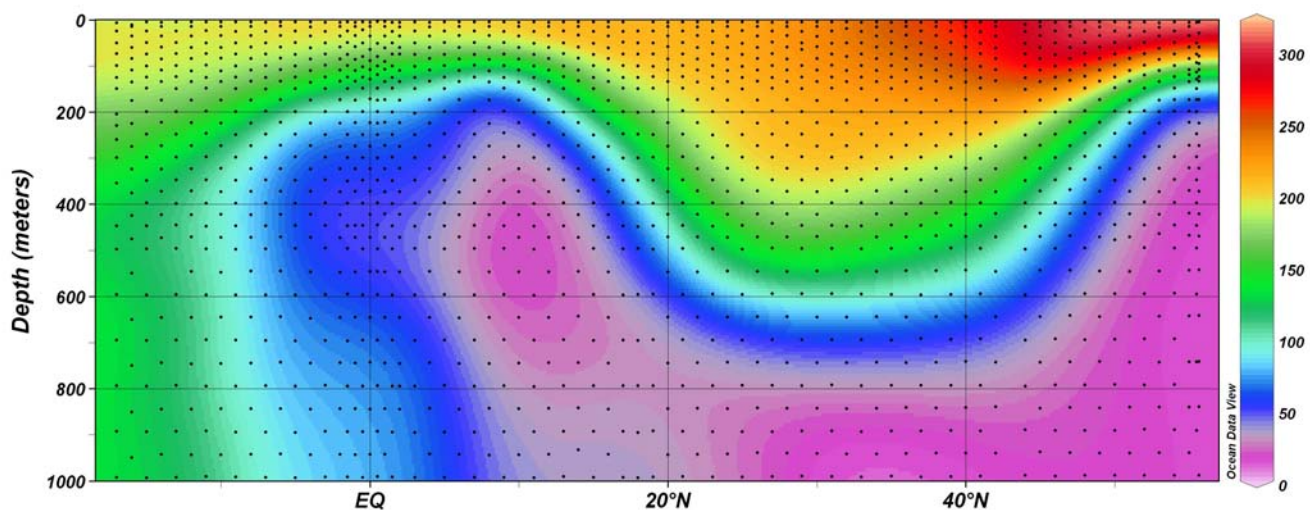


Fig. 55: Oceanographic section of dissolved oxygen ($\mu\text{mol/kg}$) is shown here for cruise P16N, the meridional section along 152°W longitude, from Tahiti (left) to Alaska (right). [Data are from the CLIVAR and Carbon Hydrographic Data Office (<http://cchdo.ucsd.edu/>).]

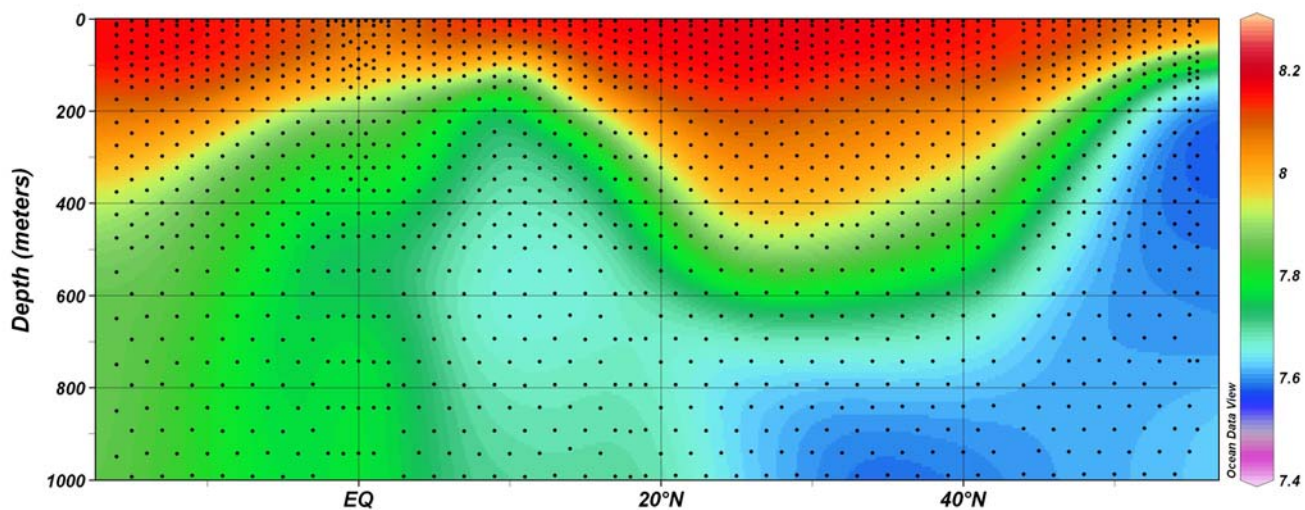


Fig. 56: Oceanographic section of pH (standard units on the free scale) is shown here for cruise P16N, the meridional section along 152°W longitude, from Tahiti (left) to Alaska (right). Appendix C describes the manner in which pH was calculated.

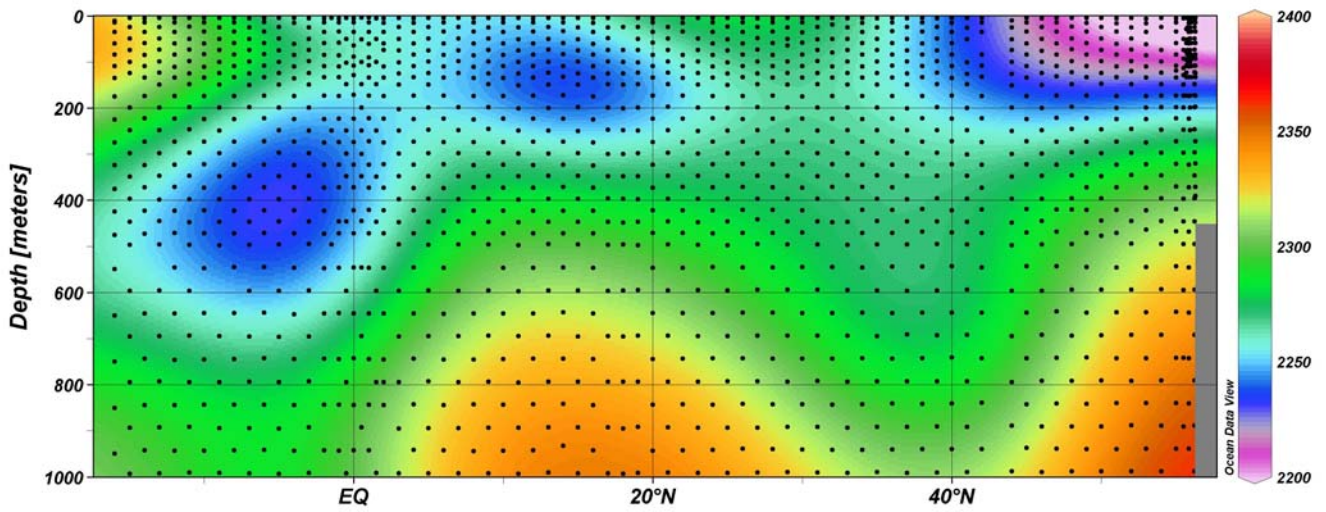


Fig. 57: Oceanographic section of total alkalinity ($\mu\text{mol}/\text{kg}$) is shown here for cruise P16N, the meridional section along 152°W longitude, from Tahiti (left) to Alaska (right). [Data are from the CLIVAR and Carbon Hydrographic Data Office (<http://cchdo.ucsd.edu/>).]

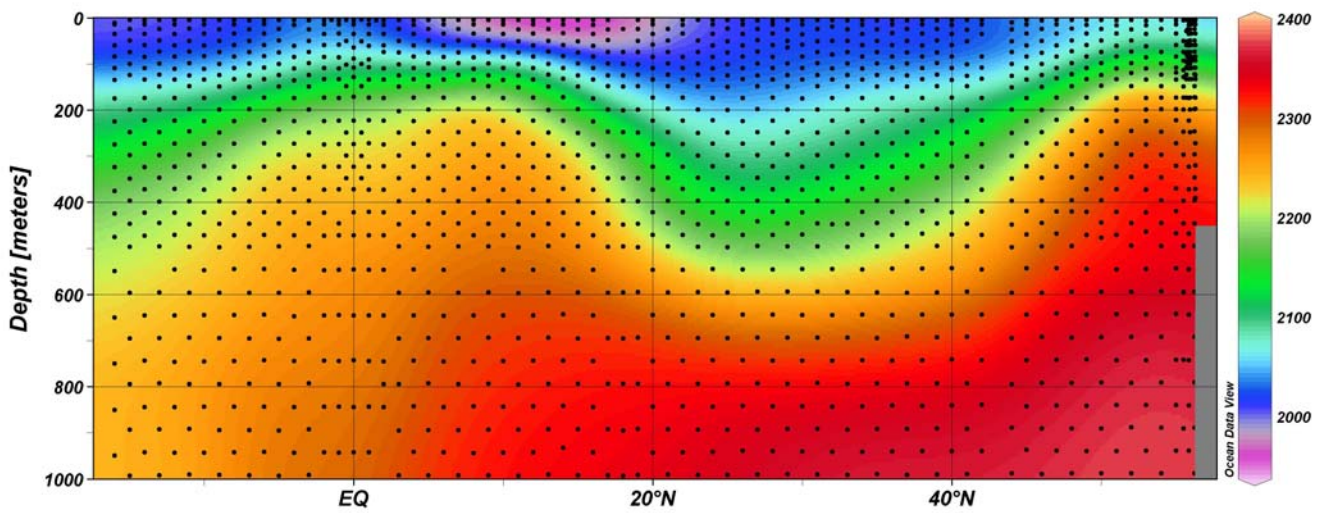


Fig. 58: Oceanographic section of dissolved inorganic carbon ($\mu\text{mol}/\text{kg}$) is shown here for cruise P16N, the meridional section along 152°W longitude, from Tahiti (left) to Alaska (right). [Data are from the CLIVAR and Carbon Hydrographic Data Office (<http://cchdo.ucsd.edu/>).]

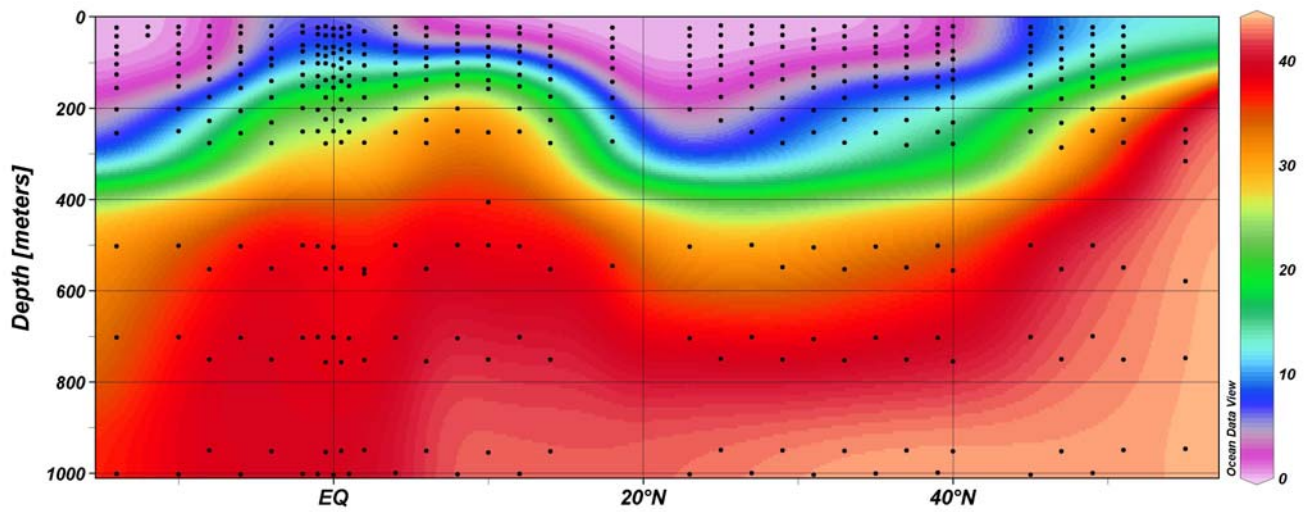


Fig. 59: Oceanographic section of nitrate ($\mu\text{mol/kg}$) is shown here for cruise P16N, the meridional section along 152°W longitude, from Tahiti (left) to Alaska (right).

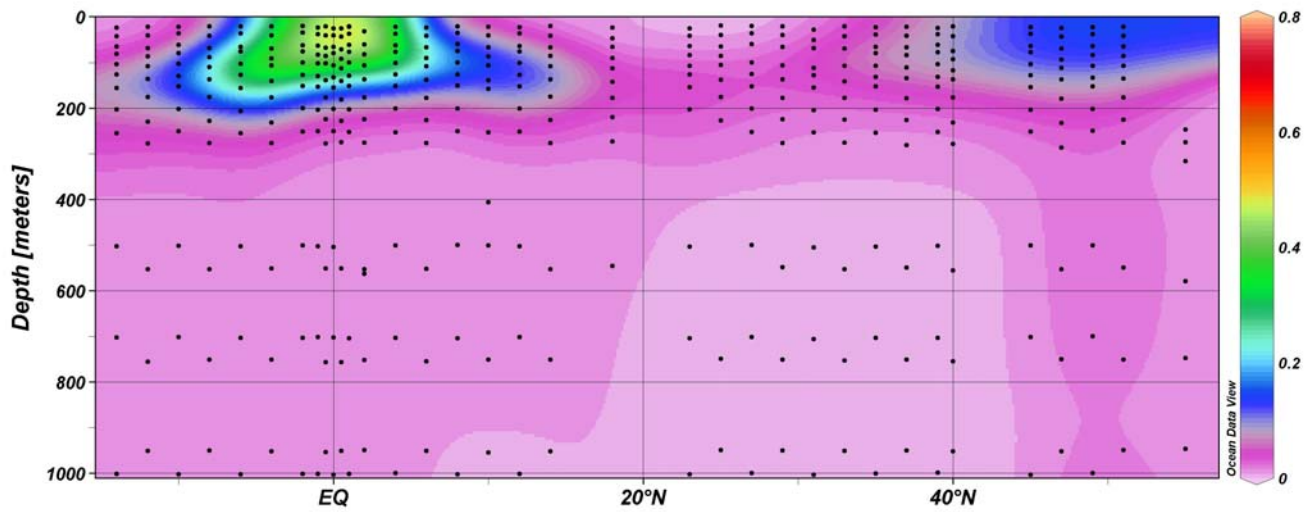


Fig. 60: Oceanographic section of nitrite ($\mu\text{mol/kg}$) is shown here for cruise P16N, the meridional section along 152°W longitude, from Tahiti (left) to Alaska (right).

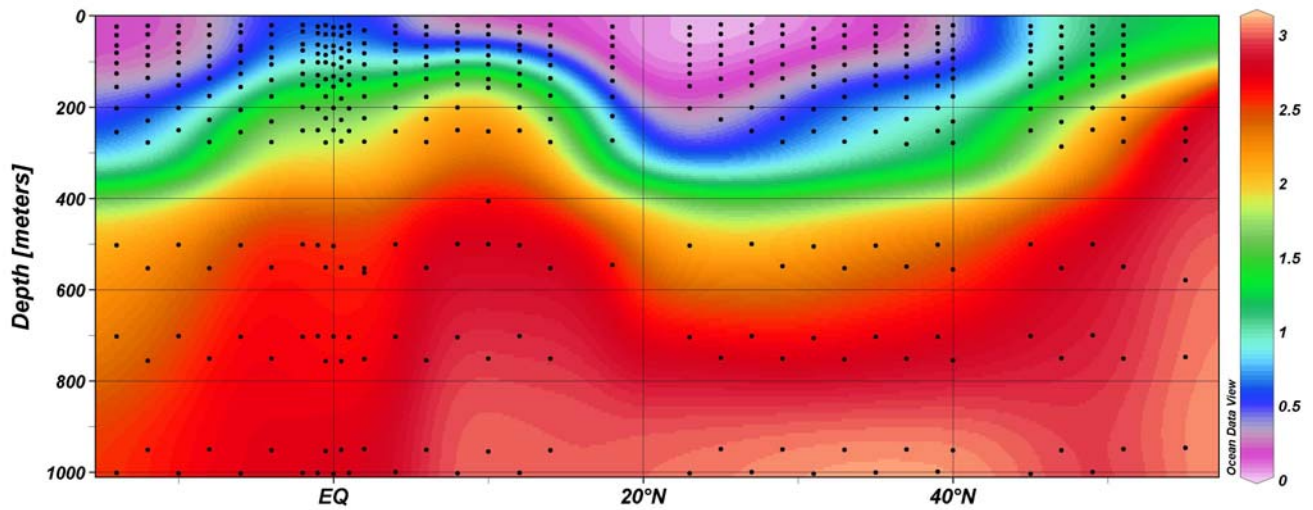


Fig. 61: Oceanographic section of phosphate ($\mu\text{mol/kg}$) is shown here for cruise P16N, the meridional section along 152°W longitude, from Tahiti (left) to Alaska (right).

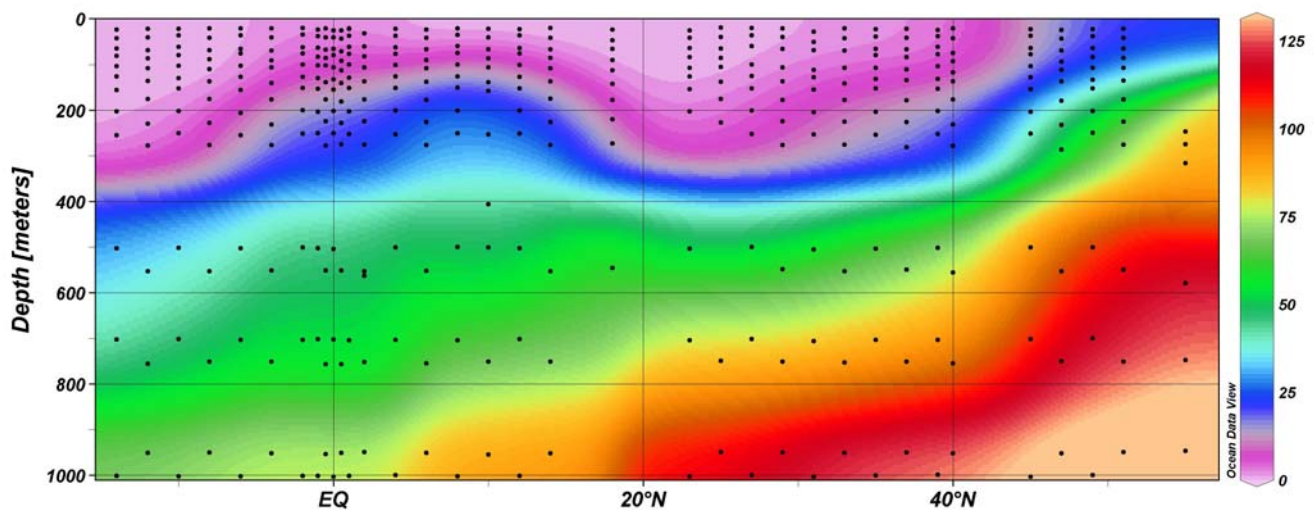


Fig. 62: Oceanographic section of silicate ($\mu\text{mol/kg}$) is shown here for cruise P16N, the meridional section along 152°W longitude, from Tahiti (left) to Alaska (right).

REFERENCES

- Allredge, A.L., and Cohen, Y., 1987, Can microscale chemical patches persist in the sea? Microelectrode study of marine snow, fecal pellets. *Science*, v. 235, p. 689-691.
- Anderson, M.A., and Morel, F.M.M., 1982, The influence of aqueous iron chemistry on the uptake of iron by coastal diatom *Thalassiosira weissflogii*: *Limnology and Oceanography*, v. 27, p. 789-813.
- Archer, D.E., and Johnson, K.S., 2000, A model of the iron cycle in the ocean: *Global Biogeochem.Cycles*, v. 14, p. 269-279.
- Barbeau, K., 2006, Photochemistry of organic iron(III) complexing ligands in oceanic systems: *Photochemistry and Photobiology*, v. 82, p. 1515-1516.
- Barbeau, K., Rue, E.L., Bruland, K.W., and Butler, A., 2001, Photochemical cycling of iron in the surface ocean mediated by microbial iron(III)-binding ligands: *Nature*, v. 413, p. 409-413.
- Bowie, A.R., Achterberg, E.P., Sedwick, P.N., Ussher, S., and Worsfold, P.J., 2002, Real-time monitoring of picomolar concentrations of iron(II) in marine waters using automated flow injection-chemiluminescence instrumentation: *Environmental Science & Technology*, v. 36, p. 4600-4607, doi: 10.1021/es020045v [doi].
- Boye, M., Aldrich, A., van den Berg, Constant M.G., de Jong, J.T.M., Nirmaier, H., Veldhuis, M., Timmermans, K.R., and de Baar, H.J.W., 2006, The chemical speciation of iron in the north-east Atlantic Ocean: *Deep Sea Research Part I: Oceanographic Research Papers*, v. 53, p. 667-683.
- Broecker, W. S., 1994, *Chemical Oceanography*, New York, Harcourt, Brace Jovanovich, Inc, 214 p.
- Brown, M.T., Landing, W.M., Measures, C.I., 2005, Dissolved and particulate Fe in the western and central North Pacific: Results from the 2002 IOC cruise: *Geochemistry, Geophysics, Geosystems*, v. 6, p. Q10001, doi:10.1029.2004GC000893.
- Bruland, K.W., and Rue, E.L., 2001, Analytical methods for the determination of concentrations and speciation of iron: *in* Turner, D.R. and Hunter, K.A., eds., *The Biogeochemistry of Iron in Seawater*: Chichester, England, John Wiley and Sons, LTD, p. 255-290.
- Bruland, K.W., 1980, Oceanographic distributions of cadmium, zinc, nickel, and copper in the North Pacific: *Earth and Planetary Science Letters*, v. 47, p. 176-
- Buck, C.S., Landing, W.M., Resing, J.A., and Lebon, G.T., 2006, Aerosol iron and aluminum solubility in the northwest Pacific Ocean: Results from the 2002 IOC cruise: *Geochemistry Geophysics Geosystems*, v. 7, p. Q04M07.
- Buck, C.S., Landing, W.M., Resing, J., and Lebon, G.T., 2006a, The solubility of aerosol iron and aluminum in the Pacific Ocean: results from the CLIVAR/CO2 Repeat Hydrography cruises: *EOS Transactions, AGU*, 87(52), Fall Meeting Supplement, Abstract A53A-0151.

- Charette, M.A. and Sholkovitz, E.R., 2003, Oxidative precipitation of groundwater-derived ferrous iron in the subterranean estuary of a coastal bay: *Geophysical Research Letters*, v. 29, p. 85-1-4.
- Chin, C. S., Coale, K.H., Elrod, V.A., and Johnson, K.S., 1994, In situ observations of dissolved iron and manganese in hydrothermal vent plumes, Juan de Fuca Ridge: *Journal of Geophysical Research*, v. 99, p. 4969-4984.
- Chisholm, S.W. and Morel, F.M.M., 1991, What controls phytoplankton production in nutrient-rich areas of the open sea?, *Limnology and Oceanography*, v. 36, preface.
- Coale, K.H., Chin, C.S., Massoth, G.J., Johnson, K.S., and Baker, E.T., 1991, In situ Chemical Mapping of Dissolved Iron and Manganese in Hydrothermal Plumes: *Nature*, v. 352, p. 325-328.
- Collienne, R.H., 1983, Photoreduction of Iron in the Epilimnion of Acidic Lakes: *Limnology and Oceanography*, v. 28, p. 83-100.
- Cooper, D.J., Watson, A.J., and Nightingale, P.D., 1996, Large decrease in ocean-surface CO₂ fugacity in response to in situ iron fertilization: *Nature*, v. 383, p. 511-513.
- Cooper, W.J., Zika, R.G., Petasne, R.G., and Plane, J.M.C., 1988, Photochemical formation of H₂O₂ in natural waters exposed to sunlight: *Environmental Science and Technology*, v.22, p. 1156-1160
- Crichton, R.R., 2001, *Inorganic Biochemistry of Iron Metabolism: From Molecular Mechanisms to Clinical Consequences*, 2nd Edition, New York, Wiley, 358 p.
- Croot, P.L. and Laan, P., 2002, Continuous shipboard determination of Fe(II) in polar waters using flow injection analysis with chemiluminescence detection: *Analytica Chimica Acta*, v. 466, p. 261-273.
- Cullen, J.J., 1991, Hypotheses to explain high-nutrient conditions in the open sea: *Limnology and Oceanography*, v. 36, p. 1578-1599.
- de Baar, H.J.W. et al., 2005, Synthesis of iron fertilization experiments: from the iron age in the age of enlightenment: *Journal of Geophysical Research*, v. 110, doi:10.1029/2004JC002601.
- de Baar, H.J.W., and de Jong, J.T.M., 2001, Distributions, sources and sinks of iron in seawater: *in* Turner, D.R. and Hunter, K.A., eds., *The Biogeochemistry of Iron in Seawater*: Chichester, England, John Wiley & Sons, LTD, p. 123-174.
- Donat, J.R. and Bruland, K.W., Trace elements in the ocean: *in* Salbu, B. and Steinnes, E., eds. *Trace Elements in Natural Waters*:, Boca Raton, Florida, CRC Press, p. 247-282.
- Elrod, V.A., Berelson, W.M., Coale, K.H., and Johnson, K.S., 2004, The flux of iron from continental shelf sediments: a missing source for global budgets: *Geophysical Research Letters*, v. 31, p. L12307, doi: doi:10.1029/2004GL020216.
- Emmenegger, L., King, D.W., Sigg, L., and Sulzberger, B., 1998, Oxidation kinetics of Fe(II) in a eutrophic Swiss lake: *Environmental Science & Technology*, v. 32, p. 2990-2996, doi: 10.1021/es980207g [doi].

- Emmenegger, L., Schonenberger, R., Sigg, L., and Sulzberger, B., 2001, Light-induced redox cycling of iron in circumneutral lakes: *Limnology and Oceanography*, v. 46, p. 49-61.
- Garrison, T., 2002, *Oceanography, An Invitation to Marine Science*: Pacific Grove, California, Wadsworth/Thompson Learning, 554p.
- Gledhill, M., and van den Berg, C.M.G., 1995, Measurement of the redox speciation of iron in seawater by catalytic cathodic stripping voltammetry: *Marine Chemistry*, v. 50, p. 51-61.
- Gledhill, M., and van den Berg, C.M.G., 1994, Determination of complexation of iron(III) with natural organic complexing ligands in seawater using cathodic stripping voltammetry: *Marine Chemistry*, v. 47, p. 41-54.
- Gobler, C.J., Hutchins, D.A., Fisher, N.S., Coper, E.M., and Sanudo-Wilhelmy, S.A., 1997, Release and bioavailability of C, N, P, Se, and Fe following viral lysis of a marine chrysophyte: *Limnology and Oceanography*, v. 42, p. 1492-1504.
- Gonzalez-Davila, M., Santana-Casiano, J.M., and Millero, F.J., 2006, Competition between O₂ and H₂O₂ in the oxidation of Fe(II) in natural waters: *Journal of Solution Chemistry*, v. 35, p. 95-111.
- Gonzalez-Davila, M., Santana-Casiano, J.M., and Millero, F.J., 2005, Oxidation of iron (II) nanomolar with H₂O₂ in seawater: *Geochimica Et Cosmochimica Acta*, v. 69, p. 83-93.
- Holland, H.D., 1984, *The Chemical Evolution of the Atmosphere and Oceans*, New Jersey, Princeton University Press, 560 p.
- Hong, H., and Kester, D.R., 1986, Redox state of iron in the offshore waters of Peru: *Limnology and Oceanography*, v. 31, p. 512-524.
- Hopkinson, B.M., and Barbeau, K.A., 2007, Organic and redox speciation of iron in the eastern tropical North Pacific suboxic zone: *Marine Chemistry*, v. In Press, Corrected Proof, .
- Hudson, R.J.M., and Morel, F.M.M., 1990, Iron transport in marine phytoplankton: kinetics of cellular and medium coordination reactions: *Limnology and Oceanography*, v. 35, p. 1002-1020.
- Hunter, K.A. et al., 2001, Summary and recommendations: *in* Turner, D.R. and Hunter, K.A., eds., *The Biogeochemistry of Iron in Seawater*: Chichester, England, John Wiley & Sons, LTD, p. 373-387.
- Hutchins, D.A., Witter, A.E., Butler, A., and Luther III, George W., 1999, Competition among marine phytoplankton for different chelated iron species. *Nature*, v. 400, p. 858-3.
- Hutchins, D.A., and Bruland, K.W., 1994, Grazer-mediated regeneration and assimilation of Fe, Zn and Mn from planktonic prey: *Marine Ecology-Progress Series*, v. 110, p. 259-269.
- Johnson, K.S. et al., 2007, Developing standards for dissolved iron in seawater: *EOS*, v. 88, p. 131-132.
- Johnson, K.S., Gordon, R.M., and Coale, K.H., 1997, What controls dissolved iron concentrations in the world ocean? *Marine Chemistry*, v. 57, p. 137-161.

- Kieber, R.J., Williams, K., Willey, J.D., Skrabal, S., Avery Jr., G.B., 2001, Iron speciation in coastal rainwater: concentration and deposition to seawater: *Marine Chemistry*, v.73, p. 83-95.
- King, D.W., 1998, Role of carbonate speciation on the oxidation rate of Fe(II) in aquatic systems: *Environmental Science & Technology*, v. 32, p. 2997-3003.
- King, D.W., and Farlow, R., 2000, Role of carbonate speciation on the oxidation of Fe(II) by H₂O₂: *Marine Chemistry*, v. 70, p. 201-209.
- King, D.W., Lounsbury, H.A., and Millero, F.J., 1995, Rates and mechanism of Fe(II) oxidation at nanomolar total iron concentrations: *Environmental Science & Technology*, v. 29, p. 818-824.
- King, D.W., Robb, A.A., and Carnecki, S.E., 1993, Photochemical redox cycling of iron in NaCl solutions: *Marine Chemistry*, v. 44, p. 105-120.
- Kuma, K., Nakabayashi, S., Suzuki, Y., Kudo, I., and Matsunaga, K., 1992, Photo-reduction of Fe(III) by dissolved organic substances and existence of Fe(II) in seawater during spring blooms: *Marine Chemistry*, v. 37, p. 15-27.
- Kustka, A.B., Shaked, Y., Milligan, A.J., King, D.W., and Morel, F.M.M., 2005, Extracellular production of superoxide by marine diatoms: Contrasting effects on iron redox chemistry and bioavailability: *Limnology and Oceanography*, v. 50, p. 1172-1180.
- Lamb, M.F. et al., 2002, Consistency and synthesis of Pacific Ocean CO₂ survey data: *Deep Sea Research II*, v. 49, p. 21-58.
- Landing, W.M., Measures, C.I., and Resing, J.A., 2003, Collaborative research: global ocean survey of dissolved iron and aluminum and aerosol iron and aluminum solubility supporting the Repeat Hydrography (CO₂) project: *Award Abstracts - National Science Foundation*, v. OCE-0223378, .
- Landing, W.M., and Bruland, K.W., 1987, The contrasting biogeochemistry of iron and manganese in the Pacific Ocean: *Geochimica Et Cosmochimica Acta*, v. 51, p. 29-43.
- Landing, W.M., Haraldsson, C., and Paxeus, N., 1986, Vinyl polymer agglomerate based transition metal cation chelating ion-exchange resin containing the 8-hydroxyquinoline functional group: *Analytical Chemistry*, v. 58, p. 3031-3035
- Lewis, E. and Wallace, D.W.R., 1998, Program developed for CO₂ system calculations: ORNL/CDIAC-105. Carbon Dioxide Information Analysis Center, Oak Ridge National Laboratory, U.S. Department of Energy, Oak Ridge, Tennessee.
- Liu, X., and Millero, F.J., 2002, The solubility of iron in seawater: *Marine Chemistry*, v. 77, p. 43-54.
- Long, G.L. and Wisefordner, J.D., 1983, Limit of detection, a closer look at the IUPAC definition: *Analytical Chemistry*, v. 55, p. 712-724.
- Maldonado, M.T., and Price, N., M., 2001, Reduction and transport of organically bound iron by *Thalassiosira oceanica* (Bacillariophyceae). *Journal of Phycology*, v. 37, p. 298-309.

- Maldonado, M.T., and Price, N., M., 1999, Utilization of iron bound to strong organic ligands by plankton communities in the subarctic Pacific Ocean. *Deep-Sea Research Part II - Topical Studies in Oceanography*, v. 46, p. 2447-26.
- Martin, J.H., Gordon, R.M., and Fitzwater, S.E., 1991, The case for iron: *Limnology and Oceanography*, v. 36, p. 1793-1802.
- Martin, J.H., 1990, Glacial-interglacial CO₂ change: The iron hypothesis: *Paleoceanography*, v. 5, p. 1-13.
- Martin, J.H. and Fitzwater, S.E., 1988, Iron deficiency limits phytoplankton growth in the north-east Pacific subarctic: *Nature*, v. 331, p. 341-343.
- Mcknight, D.M., Kimball, B.A., and Bencala, K.E., 1988, Iron photoreduction and oxidation in an acidic mountain stream: *Science*, v. 240, p. 637-640.
- McMahon, J.W., 1969, An acid-free bathophenanthroline method for measuring dissolved ferrous iron in lake water: *Water Research*, v. 3, p. 743-&.
- McMahon, J.W., 1967, The Influence of light and acid on the measurement of ferrous iron in lake water: *Limnology and Oceanography*, v. 12, p. 437-442.
- Measures, C.I. and Brown, M.T., 2005, Dust deposition to the surface waters of the western and central North Pacific inferred from surface water dissolved aluminum concentrations: *Geochemistry Geophysics Geosystems*, v. 6, Q09M03 p. 1-16.
- Measures, C.I., Yuan, J., and Resing, J.A., 1995, Determination of iron in seawater by flow injection analysis using in-line preconcentration and spectrophotometric detection: *Marine Chemistry*, v. 50, p. 3-12.
- Merchant, S. 2006, Trace Metal Utilization in Chloroplasts: *in* Wise, R.R. and Hooper, J.K., eds., *The Structure and Function of Plasmids*, the Netherlands, Springer, p. 199-218.
- Merenyi, G., Lind, J., Shen, X., and Eriksen, T.E., 1990, Oxidation potential of luminol. Is the autoxidation of singlet organic molecules and outer-sphere electron transfer?: *Journal of Physical Chemistry*, v. 94, p. 748-752.
- Miller, W.L., King, D.W., Lin, J., and Kester, D.R., 1995, Photochemical redox cycling of iron in coastal seawater: *Marine Chemistry*, v. 50, p. 63-77.
- Millero, F.J., 2002, *Chemical Oceanography*, Boca Raton, Florida, CRC Press LLC, 469 p.
- Millero, F.J., and Sotolongo, S., 1989, The oxidation of Fe(II) with H₂O₂ in seawater: *Geochimica Et Cosmochimica Acta*, v. 53, p. 1867-1873.
- Millero, F.J., Sotolongo, S., and Izaguirre, M., 1987, The oxidation kinetics of Fe(II) in seawater: *Geochimica Et Cosmochimica Acta*, v. 51, p. 793-801.
- Millero, F.J., Yao, W., and Aicher, J., 1995, The speciation of Fe(II) and Fe(III) in natural waters: *Marine Chemistry*, v. 50, p. 21-39.

- Moffett, J. and Zika, R.G., 1988, Measurement of copper(I) in surface waters of the subtropical Atlantic and Gulf of Mexico: *Geochimica and Cosmochimica Acta*, v. 52, p. 1849-1857.
- O'Sullivan, D.W., Hanson Jr., A.K., and Kester, D.R., 1995, Stopped flow luminol chemiluminescence determination of Fe(II) and reducible iron in seawater at subnanomolar levels: *Marine Chemistry*, v. 49, p. 65-77.
- O'Sullivan, D.W., and Hanson, A.K., 1991, Measurement of Fe(II) in surface water of the equatorial Pacific: *Limnology and Oceanography*, v. 36, p. 1727-1741.
- Okamura, K., Sugiyama, M., Obata, H., Maruo, M., Nakayama, E., Karatani, H., 2001, Automated determination of vanadium(IV) and (V) in natural waters based on chelating resin separation and catalytic detection with Bindschedler's green leuco base: *Analytica Chimica Acta*, v.443, p. 143-151.
- Okubo, A., 1971, Oceanic diffusion diagrams: *Deep Sea Research*, v. 18, p. 789-802.
- Palenik, B. and Morel, F.M.M., 1988, Dark production of H₂O₂ in the Sargasso Sea: *Limnology and Oceanography*, v. 33, p. 1606-1611.
- Qian, J., Mopper, K., and Kieber, D.J., 2001, Photochemical production of the hydroxyl radical in Antarctic waters: *Deep-Sea Research I*, v. 48, p. 741-759.
- Rich, H.W., and Morel, F.M.M., 1990, Availability of well-defined iron colloids to the marine diatom *Thalassiosira weissflogii*: *Limnology and Oceanography*, v. 35, p. 652-662.
- Rijkenberg, M.J.A., Gerringa, L.J.A., Carolus, V.E., Velzeboer, I., and de Baar, H.J.W., 2006, Enhancement and inhibition of iron photoreduction by individual ligands in open ocean seawater: *Geochimica et Cosmochimica Acta*, v. 70, p. 2790-2805.
- Roberts, L., 1991, "Report nixes "Geritol" fix for global warming: *Science*, v. 253, p. 1490-1491.
- Rose, A.L., Salmon, T.P., Lukondeh, T., Neilan, B.A., and Waite, T.D., 2005, Use of superoxide as an electron shuttle for iron acquisition by the marine cyanobacterium *Lyngbya majuscula*: *Environmental Science and Technology*, v. 39, p. 3708-3715.
- Rose, A.L., and Waite, T.D., 2005, Reduction of organically complexed ferric Iron by superoxide in a simulated natural water: *Environmental Science & Technology*, v. 39, p. 2645-2650.
- Rose, A.L., and Waite, T.D., 2002, Kinetic Model for Fe(II) Oxidation in seawater in the absence and presence of natural organic matter: *Environmental Science & Technology*, v. 36, p. 433-444.
- Roy, E.G. and Wells, M.L., 2006, The persistence of Fe(II) in surface waters of the iron-limited subarctic Pacific: *AGU Abstracts*
- Rue, E.L., and Bruland, K.W., 1997, The role of organic complexation on ambient iron chemistry in the equatorial Pacific Ocean and the response of a mesoscale iron addition experiment: *Limnology and Oceanography*, V. 42, p. 901-910.

- Rue, E.L., and Bruland, K.W., 1995, Complexation of iron(III) by natural organic ligands in the Central North Pacific as determined by a new competitive ligand equilibration/adsorptive cathodic stripping voltammetric method: *Marine Chemistry*, v. 50, p. 117-138.
- Santana-Casiano, J.M., Gonzalez-Davila, M., and Millero, F.J., 2005, Oxidation of nanomolar levels of Fe(II) with oxygen in natural waters: *Environmental Science & Technology*, v. 39, p. 2073-2079.
- Santana-Casiano, J.M., Gonzalez-Davila, M., and Millero, F.J., 2004, The oxidation of Fe(II) in NaCl-HCO₃⁻ and seawater solutions in the presence of phthalate and salicylate ions: a kinetic model: *Marine Chemistry*, v. 85, p. 27-40.
- Santana-Casiano, J.M., Gonzalez-Davila, M., Rodriguez, M.J., and Millero, F.J., 2000, The effect of organic compounds in the oxidation kinetics of Fe(II): *Marine Chemistry*, v. 70, p. 211-222.
- Seitz, W.R., and Hercules, D.M., 1972, Determination of trace amounts of iron(II) using chemiluminescence analysis: *Analytical Chemistry*, v. 44, p. 2143-6.
- Shapiro, J., 1966, On the measurement of ferrous iron in natural waters: *Limnology and Oceanography*, v. 11, p. 293-298.
- Shlitzer, R., 2004, Ocean Data View: <http://www.awi-bremerhaven.de/GEO/ODV>.
- Statham, P.J., German, C.R., and Connelly, D.P., 2005, Iron(II) distribution and oxidation kinetics in hydrothermal plumes at the Kairei and Edmond vent sites, Indian Ocean: *Earth and Planetary Science Letters*, v. 236, p. 588-596.
- Stern, R.J. and Arima, M., 1997, The Izu-Bonin-Marianna arc system: international efforts seek to understand convergent margins, *EOS*, v. 78, p. 85-86.
- Stumm, W. and Morgan, J.J., 1996, *Aquatic Chemistry, Chemical Equilibria and Rates in Natural Waters*, New York, Wiley, 1022 p.
- Stumm, W. and Lee, G. F., 1961, Oxygenation of ferrous iron: *Industrial and Chemical Engineering*, v. 53, p. 143.
- Sunda, W.G., 2001, Bioavailability and bioaccumulation of iron in the sea: *in* Turner, D.R. and Hunter, K.A., eds., *The Biogeochemistry of Iron in Seawater*: Chichester, England, John Wiley & Sons, LTD, p. 42-42.
- Sunda, W.G., and Huntsman, S.A., 1995, Iron uptake and growth limitation in oceanic and coastal phytoplankton: *Marine Chemistry*, v. 50, p. 189-206.
- Theiss, T.L. and Singer, P.C., 1973, Complexation of iron(II) by organic compounds in natural waters: *Environmental Science and Technology*, v. 8, 569-573.
- Ussher, S.J., Yaqoob, M., Achterberg, E.P., Nabi, A., and Worsfold, P.J., 2005, Effect of model ligands on iron redox speciation in natural waters using flow injection with luminol chemiluminescence detection: *Analytical Chemistry*, v. 77, p. 1971-1978.

- Voelker, B.M. and Sedlak, D.L., 1995, Iron reduction by photoproduced superoxide in seawater. *Marine Chemistry*, v. 50, p. 93-102.
- von Damm, K.L., 1990, Seafloor hydrothermal activity: black smoker chemistry and chimneys: *Annual Review of Earth and Planetary Science*, v. 18, p. 173-204.
- Waite, T.D., Szymczak, R., Espey, Q.I., and Furnas, M.J., 1995, Diel variations in iron speciation in northern Australian shelf waters: *Marine Chemistry*, v. 50, p. 79-91.
- Waite, T.D., 2001, Thermodynamics of the iron system in seawater. *in* Turner, D.R. and Hunter, K.A., eds., *The Biogeochemistry of Iron in Seawater*: Chichester, England, John Wiley & Sons, LTD, p. 291-51.
- Waite, T.D., and Morel, F.M.M., 1984, Coulometric study of the redox dynamics of iron in seawater: *Analytical Chemistry*, v. 56, p. 787-792.
- Watson, A., 2001, Iron limitation in the oceans, *in* Turner, D.R. and Hunter, K.A., eds., *The Biogeochemistry of Iron in Seawater*: Chichester, England, John Wiley & Sons, LTD, p. 9-39.
- Wehrli, B. and Stumm, W., 1989, Vanadyl in natural waters: absorption and hydrolysis promote oxygenation: *Geochimica and Cosmochimica Acta*, v. 53, p. 69-77.
- Weinberg, E.D., 1989, Cellular regulation of iron assimilation: *The Quarterly Review of Biology*, v. 64, p. 261-290.
- Wells, M.L., Price, N.M., and Bruland, K.W., 1995, Iron chemistry in seawater and its relationship to phytoplankton: a workshop report: *Marine Chemistry*, v. 48, p. 157-182.
- Wells, M. L., Mayer, L.M., Donard, O.F.X., de Souza Sierra, M.M., and Ackelson, S.G., 1991, The photolysis of colloidal iron in the oceans: *Nature*, v. 353, p. 248-250.
- Windom, H.L., Moore, W.S., Niencheski, L.F.H., and Jahnke, R.A., 2006, Submarine groundwater discharge: A large, previously unrecognized source of dissolved iron to the South Atlantic Ocean: *Marine Chemistry*, v. 102, p. 252-266.
- Wu, J., and Luther III, G.W., 1995, Complexation of Fe(III) by natural organic ligands in the Northwest Atlantic Ocean by a competitive ligand equilibration method and a kinetic approach: *Marine Chemistry*, v. 50, p. 159-177.
- Xiao, C., Palmer, D.A., Wesolowski, D.J., Lovitz, S.B., and King, D.W., 2002, Carbon dioxide effects on luminol and 1,10-phenanthroline chemiluminescence: *Analytical Chemistry*, v. 74, p. 2210-2216.
- Xiao, C., King, D.W., Palmer, D.A., and Wesolowski, D.J., 2000, Study of enhancement effects in the chemiluminescence method for Cr(III) in the ng l⁻¹ range: *Analytical Chemica Acta*, v. 415, p. 209-219.
- Yuan, J. and Shiller, A.M., 1999, Determination of subnanomolar levels of hydrogen peroxide in seawater by reagent-injection chemiluminescence Detection: *Analytical Chemistry*, v. 71, p. 1975-1980.

Zeebe, R.E. and Wolf-Gladrow, D., 2001, CO₂ in Seawater: Equilibrium, Kinetics, Isotopes, Amsterdam, Elsevier, 346 p.

Zerle, A.L., House, C.H., and Brantley, S.L., 2005, Biogeochemical signatures through time as inferred from whole microbial genomes: American Journal of Science, v. 305, p. 467-502.

BIOGRAPHICAL SKETCH

Education

Ph.D.	Oceanography	Florida State University (2007)
M.S.	Geology	Florida State University (1994)
B.S.	Geology	Florida State University (1986)

Employment

Colorado School of Mines Geochemistry Dept (present), Postdoctoral Researcher. I am investigating production and fate of superoxide radical in seawater.

Florida State University Oceanography Dept (2002 – 2007), Research and Teaching Assistant. I conducted low-level analyses of trace metals in seawater and assisted with collection, preparation, and analysis of open-ocean seawater samples. I was also a teaching assistant for Introductory Oceanography.

Florida Dept. Environmental Protection (1989-2007), Environmental Manager. I supervised a staff of 11 scientists and technicians involved in implementing a statewide water quality monitoring program.

Florida State University Geology Dept (1986-1989), Research and Teaching Assistant. I conducted biometric analyses of an evolving planktonic foraminiferal lineage and analyzed species abundance and diversity of deep-sea foraminiferal assemblages. I also taught undergraduate geology courses in Earth History, Physical Geology, and Invertebrate Paleontology;

Additional Related Skills and Training

- Statistics (19 graduate semester hours)
- Computer programming (Fortran, Visual Basic, PL/SQL)
- Software skills (ArcGIS, SPlus, ODV, MINEQL, Office Products)
- Monitoring Well Construction and Design, *Nielson Environmental*
- Monitoring Network Design, *University of Colorado*
- Oracle Database Design, SQL & PL/SQL programming, *Oracle Corp.*
- Certified Public Manager Training, *Florida State University*
- Advanced Open-Water Dive Certification, *PADI*

Publications/Abstracts

Hansard, S.P., Landing, W.L., and C.I. Measures 2006. Dissolved Fe(II) in the Pacific Ocean: Measurements from the P16N Clivar/CO₂ Repeat Hydrography Cruise. *Eos Trans. AGU*, 87(52), Fall Meet. Suppl., Abstract OS21C-1605.

Hansard, S.P., Landing, W.L., and C.I. Measures 2006. Dissolved Fe(II) Measurements Along a North Pacific Transect. *Eos Trans. AGU*, 87(36), Ocean Sci. Meet. Suppl., Abstract OS16M-20.

Katz, B.G., Berndt, M.P, Bullen, and S.P. Hansard 1999. Factors Controlling Elevated Lead Concentrations in Water Samples from Aquifer Systems in Florida. U.S. Geological Survey Water-Resources Investigations Report 99-4020, 22p.

Arnold, A.J., Parker, W.C., and S.P. Hansard 1995. Aspects of the post-Cretaceous Recovery of the Planktonic Foraminifera. *Marine Micropaleontology*, 26: 319-327.

Arnold, A.J., Parker, W.C., and S.P. Hansard 1994. Survivorship in the Cenozoic Planktonic Foraminifera: Comparing Exponential and Weibull Models. *Paleobios*, v. 16, suppl. no 2, Museum of paleontology, University of California, Berkeley. International meeting.

Hansard, S.P. 1994. Geographic Patterns in the Evolution of *Orbulina universa* d'Orbigny. M.S. Thesis, Florida State University, 113 p.

Furbish, D.J., Arnold, A.J., and S. P. Hansard 1990. The Species Censorship Problem: a General Solution. *Jour. Math. Geology*, 22(1): 95-106.

Arnold, A.J., Kelly, D.C., Hansard, P.C., and Parker, W.C.1990. Macro-evolutionary aspects of the Post-Cretaceous recovery in planktonic foraminifera. *Geological Society of America Abstracts*. p. a200. National meeting.

Furbish, D.J., Arnold, A.J., and S. P. Hansard 1988. The Species Censorship Problem: a General Solution. *Geological Society of America Abstracts* p.A104 National Meeting

Oceanographic Cruises

2007	R.V. Thompson	Gulf of Alaska	37 days scheduled
2006	R.V. Thompson	South-North Pacific	40 days
2004	R.V. Melville	North Pacific	72 days
2002	R.V. Pelican	Gulf of Mexico	21 days
2000	R.V. Suncoaster	Gulf of Mexico	4 days

Awards

2002	Davis Productivity Award	Florida TaxWatch
1999	Perry Williams Sportsmanship Award	Shell Point Sailboard Club
1996	Distinguished Service Award	Florida Dept Env. Protection
1988	FSU Banks Award for Research	FSU Geology Dept.